OAK RIDGE NATIONAL LABORATORY
operated by
UNION CARBIDE CORPORATION
for the
U.S. ATOMIC ENERGY COMMISSION

ORNL-TM-757
July
15

WASTE TREATMENT AND DISPOSAL PROGRESS REPORT

MAY-OCTOBER 1963

F. L. Parker
R. E. Blanco

ORNL-TM-757

HEALTH PHYSICS DIVISION

CHEMICAL TECHNOLOGY DIVISION

WASTE TREATMENT AND DISPOSAL PROGRESS REPORT

MAY-OCTOBER 1963

F. L. Parker R. E. Blanco

APRIL 1964

OAK RIDGE NATIONAL LABORATORY
Oak Ridge, Tennessee
operated by
UNION CARBIDE CORPORATION
for the
U. S. ATOMIC ENERGY COMMISSION

ABSTRACT

High-Level-Waste Calcination. Two rising-level glass-making tests were made in the vertical 8-in.-diam calciner, using TBP-25 waste to which monosodium phosphate and lead nitrate were added to form the glass mix. The average feed rate was about 5 to 6 liters/hr. Accumulation of dust in the off-gas line required frequent flushing with nitric acid to prevent plugging.

A scouting test for continuous glass making in a horizontal vessel (8 in. in diameter and 40 in. long) heated with a 25-kw furnace was successful. The aqueous waste solution containing phosphate and lead was evaporated on the surface of a shallow pool of molten glass that flowed continuously from the vessel through a jack leg to maintain a fixed pool depth. The maximum feed rate was 20 liters/hr.

High-Level-Waste Disposal - Vapor-liquid equilibria and solution densities of FTW-65 waste solutions were determined for concentrations up to 9 times normal concentration. Ceramic solids for fixation of this waste type were developed; they melted in the range 700 to 800°C and lost 5% or less of their sulfate when heated 100°C above their melting temperatures. The one chosen for demonstration of semi-engineering scale, semi-continuous fixation was satisfactorily stable with respect to sulfate loss and was noncorrosive under the usual fixation conditions but produced a large amount of dust high in iron which tended to plug the off-gas line. Sparging with nitrogen during fixation resulted in loss of about 23% of the sulfate and in catastrophic container corrosion.

A series of solid products were made from fixation of non-sulfate Purex waste. Some of these melted as low as 500 to 600°C. Two of the series were glasses.

Calcination of sulfate-deficient Purex waste (essentially $NaNO_3$ with minor amounts of SO_4^{2-} and Fe^{3+}) was shown to be practical on addition of aluminum. In the absence of any additive there was gross displacement of solids from the fixation container and volatilization of both Na^+ and SO_4^{2-}.

A column packed with copper shot removed 99.4% of the mercury from 510 bed volumes of FTW-65 (low acid) waste solution. A column packed with

aluminum turnings removed 99% of the mercury and 30 to 35% of the ruthenium from 162 bed volumes of FTW-65 waste concentrated by a factor of 3. Both copper and aluminum were attacked too rapidly by Purex 1WW waste to be effective in removing mercury from this (high acid) waste.

Type 304L stainless steel corroded at rates ≤ 0.3 mil/month in FTW-65 evaporator environments both in the presence and absence of expected additives; corrosion rates of titanium were negligible. Coupling the two metals had no appreciable effect on the corrosion of either. Tests on 304L stainless steel during calcination and fixation (melt-down) cycles for FTW-65 wastes resulted in total penetrations of about 10 and 15.3 mils/month, respectively. Maximum rates for 304L stainless steel in salt (simulating waste storage) at 300°C were about 0.03 to 0.04 mil/month.

Low-Level Waste Treatment: Scavenging-Precipitation - Ion Exchange. Pilot plant equipment and piping changes were completed. When the weak-acid strong-acid fixed-bed ion exchange system was operated for a week with waste from the ORNL equilization basin as feed, algae passed through the anthracite filter and the ion exchange beds. Further tests in the system were stopped pending completion of radiochemical analysis of stream samples. Tests with tap water feed were started in the modified scavenging-precipitation equipment.

In the laboratory-scale tests, cesium eluted from the cation exchange column with nitric acid in the Scavenging-Precipitation Ion-Exchange process was sorbed on grundite clay and the slurry recycled to the process feed stream, thus eliminating the need for an evaporation step. The optimum pH range for sorption of cesium on grundite was quite narrow, about 11.8. Sorption is essentially independent of the particle size of the grundite over the range from about 50 mesh to < 200. Addition of grundite prior to pH adjustment favors higher sorption. An alumina column removed about half the phosphate from 10,000 bed volumes of raw ORNL waste. Addition of a column of Dowex 21-K anion exchange resin following the Scavenging-Precipitation Ion-Exchange process resulted in removal of about half of the gross activity but was ineffective in removing all the ruthenium.

Foam Separation: Laboratory Development - The foam separation process to remove cesium, strontium, and other radioactive nuclides from low-radioactivity-level process waste water consists in a scavenging precipitation

by caustic-carbonate followed by countercurrent foam separation. By making the waste 5 to 10 ppm in Fe^{3+}, a coagulant, before adding caustic-carbonate, the deleterious effects of high concentrations (5 to 15 ppm) of phosphates in the water on the extent of precipitation of calcium carbonate are greatly reduced, provided that these high concentrations are only of a few hours' duration. Removal of cesium in the precipitation chamber (sludge column) by sorption on grundite clay (at approximately 0.5 lb/1000 gal water) is increased (from a DF of 8 to a DF of 15) if the clay is first baked at 600°C for 20 min. Operating conditions of the foam column, including concentrations of surfactant in inlet and exit streams, were determined with sodium dodecylbenzene sulfonate as surfactant for linear foam flow rates of 32 to 46 cm/min and at gas-to-liquid flow-rate ratios of about 10. Cesium removal in the foam column was poor when either dodecylbenzene sulfonate or any of three surfactants (RWA-100, dichlorophene, and hexachlorophene) containing an active phenolic group were used.

Foam Separation: Engineering Development - Experimental results show that foams are easily condensed while passing through an orifice with upstream/downstream pressure ratios of two or greater. The 0.015-, 0.100-, and 0.250-cm-diam orifices all gave residual foam volumes of about 0.001 the inlet volumes for foams of 0.05 to 0.08 cm mean diameters. As compared to impingement on a Teflon sheet 2 to 3 in. from the orifice, the amount of uncondensed foam was slightly decreased by placing the sheet 24 in. from the orifice, and it was slightly increased by use of a glass wall in place of the Teflon sheet. The 24-in.-diam foam column (the proposed LLW pilot plant column diameter) was operated at flows up to 80 liters/min of foam and 13 liters/min of liquid. The amount of channeling appeared acceptable when an improved liquid feed distributor was used. From foam-stability tests, it appears that the low-level-waste column should have a stable foam with 25 ppm DBS in the liquid. A proposed design and equipment flow sheet for the Foam Pilot Plant is presented.

Engineering, Economics, and Safety Evaluation. Costs of permanent storage of calcined radioactive wastes in concrete vaults and in rooms mined out of granite formations were estimated. In comparison with previously estimated costs of storage in salt mines, costs of storage in concrete vaults were five to seven times as much, and costs of storage in

granite were about twice as much. This economic advantage, as well as the greater safety it is believed to offer, makes salt the preferred choice.

Vaults for the storage of calcined solid wastes would be similar in their gross features to many of the concrete secondary containments used for tanks built for storage of liquid radioactive wastes, in that they would be underground structures of reinforced concrete with about 10 ft of earth cover and a floor-to-ceiling height of about 15 ft. For maximum safety, they would be sealed completely from the surface; space requirements were calculated by assuming dissipation of the heat of radioactive decay by conduction through the earth cover. Two types of concrete were considered: ordinary concrete, capable of withstanding 400 to 500°F, and "high-temperature concrete," capable of withstanding 1000°F.

Space requirements for the storage of calcined wastes in rooms in granite formations are about the same as those for storage in salt formations. However, excavating costs are higher for granite because heavier equipment is required, drilling is more difficult and slower, and costs of explosives are higher.

Estimations were made of the movement of Sr^{90}, Ru^{106}, and Cs^{137} in Conasauga shale following a hypothetical release of reactor fuel-processing waste from a tank. Computations were based on hydrologic and exchange characteristics of the local formation that had been obtained previously. Although the absolute values for radionuclide movement that have been calculated and presented should not be considered to be precise, since the estimates were based on a rather inadequate description of the site, the procedure used in making these calculations could be applied for any proposed site. The reliability of the estimates could be improved by improving the quantitative description of the geological formation involved.

In Conasauga shale, Sr^{90} would apparently move quite rapidly in an acid waste system, even upon neutralization of the acid by calcite ($CaCO_3$) in the formation. Movement of Sr^{90} in an alkaline waste solution would be much slower due to the formation of insoluble compounds, in addition to holdup due to ion exchange. Ruthenium-106 would be expected to move rapidly in either acid or neutralized waste systems, but it presents little long-term hazard due to its relatively short half-life. The movement of

Cs^{137} would be expected to be slow because of its fixation by the illite of the Conasauga shale (ion exchange).

Disposal in Deep Wells. Detailed logging of wells 1 and 2, before and after the casings were installed, showed that (1) the dip of the beds between the wells is unexpectedly low, (2) that there are zones of sheared or broken rock in the approximately 50 ft of shale immediately above the Rome sandstone, and (3) that there may be a few faults filled with tight clay gouge up to as high as 860 ft in the red shale into which waste mixtures are to be injected.

Four water injections, with and without fluid-loss additives, were made into slots in the injection well (well 1) at 986 ft and 966 ft, respectively. Although the recovery from the last injection is still continuing, there appears to be sufficient similarity between the injections, with and without fluid-loss additives, to suggest that there is little incentive to use such additives in setting or nonsetting mixes. The results obtained from the slotting operations that were performed for the water injection tests indicate that the well casing was not completely severed by the normal operating technique. Some modification of this method will be necessary.

The main emphasis on mix development during this period was on cheap mixes that, although not as strong as previously developed mixes, would be pumpable, would set, and would have no phase separation. The mineral attapulgite 150 is far superior to bentonite as a suspending agent for solutions with a high ionic content. Several retarders have been investigated and glucono-d-lactone (CFR-1) seems particularly effective. The density of these "low solids" mixes is greatly affected by entrained air. This phenomenon is of concern because, during an injection, the relative amounts of solids and liquids fed to the mixer will be controlled by the density of the slurry. Some means of eliminating air entrainment must be found.

A hazards analysis of the fracturing experiments was completed. It was concluded that the waste solution to be used in the first series of injections will be so low in specific activity that no significant hazard would result from its use. The other principal hazard involved in the experiments - that of working with high-pressure equipment - has been

minimized where possible by installing the pumping and mixing equipment in cells.

The experimental program for the first series of injections will consist of four injections, each of 40,000 gal.

1. An injection of a synthetic concentrated waste solution mixed with attapulgite to form a nonsetting slurry.

2. An injection of the same synthetic waste solution mixed with a cheap setting mix.

3. An injection of actual waste solution mixed with additional chemicals to increase the concentration to the same value as that in injections 1 and 2. This will be mixed with sufficient cement to form a strong setting mix.

4. An injection of actual waste solution mixed with a strong setting mix.

An estimate of the probable operating cost of the shale fracturing plant shows that the cost of the mix and the well life are the significant variables. The well life can be significantly extended by making the batch size large. For this reason it seems probable that the direction of future work will be toward larger batch sizes than it is currently planned to inject.

Construction is proceeding on phase 2 of the surface plant. The bulk storage tanks have been erected; the majority of underground lines have been installed; and foundations for the cells have been poured.

Disposal in Natural Salt Formations. Operation of the heated model room continues, and the closure rates are now less than ten times higher than the closure rates before heating. At this time it is not known if the closure rate during heating will remain above the ambient temperature rate, approach it asymptotically, or fall below it.

Design and construction of the Lyons demonstration experiment continues. A contract was let to replace the headframe, foundations, and cages to allow lowering of 7-ton loads into the mine. New power cable and hoisting cables were delivered to the Lyons site. A critical path schedule of the over-all experiment was prepared as an aid to expediting and scheduling all phases of the experiment. A contract was let for the fabrication of the trailer for the waste disposal transporter. The prime

mover (Caterpillar model 619C) for this unit was purchased. Design of other experimental components is underway.

Tentative conclusions on the radiolytic production of chlorine from irradiated rock salt indicate that the amount of oxidizing power created within the salt is independent of the size and surface area of the crystals per unit weight, but the oxidizing power can be increased by stresses and strains in the salt.

Clinch River Studies. The expected summer pulsed releases of water from Melton Hill Dam were simulated by flow through the gates during August 1963. The purpose of the experiment was to determine the dilution in the Clinch River under the changed flow regime. Rhodamine B dye was used to simulate radioactive releases. The minimum dilution was 50, in comparison with the previous median dilution of 570.

Cores taken from the bottom sediments of the Clinch River in 1962 were analyzed and showed that the major portion of the contaminated sediments has been deposited on the sides of the original stream channel.

Desorption of the nuclides from bottom sediments showed that acidified water is more effective in removing Sr^{90} from the sediments than highly salted solutions.

Analyses of fish taken from the Clinch River show that a maximum of 2.5% of the maximum permissible intake (MPI) will be received from eating 37 lb of fish per year from East Tennessee rivers. Radiation levels near filter beds in water plants upstream and downstream of the point of entry of White Oak Creek into the Clinch River are at background.

Fundamental Studies of Minerals. Cesium was desorbed from six representative clay minerals containing trace levels of Cs^{137}. The cesium on both kaolinite and montmorillonite was completely desorbed by 1 M sodium acetate after contact for 1 hr. When 1 M HNO_3 was used, the hydrobiotite and biotite released all their cesium; both illite and muscovite retained 75% and 85% of the cesium even after 24 hr of contact with the nitric acid. Since acids decompose the clay minerals, the difference in release by the minerals reflects the ease of their decomposition.

Three possible types of cesium sorption response are illustrated by the vermiculite, depending on the original cation on the exchanger. With increasing cesium concentration, the K_d for cesium can increase due to

collapse induced by the cesium replacing the magnesium ion, can decrease if the vermiculite is presaturated with potassium ion, which precollapse the layers, or can remain relatively constant if the cesium isotopically exchanges with other cesium ions. One of these three types of responses described responses observed by the other clay minerals, including montmorillonite, kaolinite, and illite.

White Oak Creek Basin Study. A series of preliminary core samples were taken in and around two of the earlier "open" type of intermediate-level waste seepage pits that were recently abandoned and filled. Radiochemical analyses of segmented sections of these cores indicate that most of the activity is associated with the sludges and precipitates that have accumulated in the pits and on the first few inches of weathered shale that comprises the side walls and bottoms of the pits. On a dry-weight basis, concentrations of Cs^{137} and Sr^{90} were observed to be as high as 96 μc/g and 17 μc/g, respectively, in the sludge, and 3 μc/g and 0.2 μc/g in the weathered shale on the side walls and bottoms of the pits. The sludge in the pits was also quite variable in thickness and distribution.

CONTENTS

CONTENTS (contd)

1. INTRODUCTION

This report is the twelveth of a series* of reports on progress in the ORNL development program, the objective of which is to develop and demonstrate on a pilot plant scale integrated processes for treatment and ultimate disposal of radioactive wastes resulting from reactor operations and reactor fuel processing in the forthcoming nuclear power industry. The wastes include those of high, intermediate, and low levels of radioactivity in liquid, solid, or gaseous states.

Principal current emphasis is on high- and low-activity liquid wastes. Under the integrated plan, low-activity wastes, consisting of very dilute salt solutions, such as cooling water and canal water, would be treated by scavenging and ion exchange processes or foam separation to remove radioactive constituents and the water would be discharged to the environment. The retained waste solids or slurries would be combined with the high-activity wastes. Alternatively, the retained solids or the untreated waste could be discharged to the environment in deep geologic formations. The high-activity wastes would be stored at their sites of origin for economic periods to allow for radioactive decay and artificial cooling.

Methods being investigated for permanent disposal of high-activity wastes include conversion of the waste liquids to solids by high-temperature "pot" calcination or fixation in the final storage container (pot) and formation of a glass or ceramic in a continuous melter. The solids would be stored in a permanently dry place such as a salt mine. This is undoubtedly the safest method because complete control of radioactivity can be ensured within present technology during treatment, shipping, and storage. Another approach is the disposal of the liquid directly into sealed or vented salt cavities. Research and development work is planned to determine the relative feasibility, safety, and economics of these methods, although the major effort will be placed on conversion to and final storage as solids.

---

*ORNL-CF-61-7-3, ORNL-TM-15, ORNL-TM-49, ORNL-TM-133, ORNL-TM-169, ORNL-TM-252, ORNL-TM-376, ORNL-TM-396, ORNL-TM-482, ORNL-TM-516, and ORNL-TM-603; see also annual reports for 1962-1963, ORNL-3492 and ORNL-3452, from the Health Physics and Chemical Technology Divisions, respectively, for more extensive discussion of progress during May through July 1963.

Tank storage or high-temperature calcination of intermediate-activity wastes may be unattractive because of their large volumes, and other disposal methods will be studied. One method, for example, the addition of solidifying agents prior to direct disposal into impermeable shale by hydrofracturing, is under investigation. Particular attention is being given to the engineering design and construction of an experimental fracturing plant to dispose of ORNL intermediate-activity wastes by this method if proved workable.

Environmental research on the Clinch River, motivated by the need for safe and realistic permissible limits of waste releases, is included in this program. The objective is to obtain a detailed characterization of fission product distribution, transport, and accumulation in the physical, chemical, and biological segments of the environment.

2. HIGH-LEVEL-WASTE CALCINATION

The pot-calcination process for converting high-activity-level wastes to solids is being studied on both a laboratory and engineering scale to provide design information for the construction of a pilot plant. Development work has been with synthetic Purex, Darex, and TBP-25 wastes. The first phase of the program is concerned with direct calcination processes where melting does not occur and little or no additives are combined with the wastes. In the second phase, enough additives are used to induce melting to form a glass-like material in which the fission products are fixed. Development of the "pot" calcination process is complete, with the exception of demonstrations in a 16-in.-diam pot, scheduled for 1964. Current emphasis is on the development of glasses that have low melting points, low solubilities, and low corrosivities; and the development of an engineering technique to convert the wastes to glasses. The methods being studied are: (1) rising level in a disposable pot and (2) a continuous melter.

2.1 Engineering Development

J. C. Suddath C. W. Hancher

Two rising-level glass tests, R-79-80 and R-81, were successfully completed. Simulated TBP-25 waste was used, to which monosodium phosphate (2 M) and lead nitrate (0.25 M) were added. The resulting solution had a density of 1.4 g/cc and could not be further concentrated in the evaporator. In fact, for the greater part of the tests it was diluted to a density of about 1.3 g/cc in the evaporator before feeding to the calciner. During both tests, a dusting problem occurred in the main off-gas line, restricting the flow. Plugging was prevented by flushing the line with water and 6 M HNO_3 acid at fairly frequent intervals. The average feed rate for test R-79-80 was about 6 liters/hr, and for test R-81 about 5 liters/hr. The resulting solid had a glassy appearance, a density of about 2.2 g/cc, and a residual nitrate composition of about 400 ppm.

	Feed (M)	Calcined Glass "Product" (Wt %)	
		Run R-79-80	Run R-81
Al	1.7	15.1	15.6
Na	2.1	13.6	13.9
Pb	0.25	6.7	---
NO_3	6.5	0.05	0.037
PO_4	2.0	55.5	56.3
Density, g/cc	1.4	---	2.24

2.1.1 Rising-Level Operating Conditions and Results

The purpose of the two rising-level TBP-25 glass tests was to try to establish the maximum rate. A control limit for the operation was that not over 1 ft of liquid was to be present in the calciner at any one time. The feed composition for the two tests was 1.3 M HNO_3, 1.7 M $Al(NO_3)_3$, 0.1 M $NaNO_3$, 0.003 M $FeNO_3$. The TBP-25 glass mix consists of TBP-25 waste to which 2-g moles of monosodium phosphate (NaH_2PO_4) and 0.25 M $Pb(NO_3)_2$ had been added per liter of original feed. The resulting glass mix has the following composition: nitrate, 6 M; aluminum, 1.7 M; sodium, 2.1 M; phosphate, 2 M; lead, 0.25 M. This feed at room temperature has a density of 1.43 g/cc and is thick and viscous. The procedure for evaporator operation in this test was similar to that for previous calcination tests. The glass mix was fed to the evaporator in the normal fashion. However, in this case it was diluted in the evaporator to about 1.35 g/cc density rather than being concentrated.

The diluted feed was fed to the calciner at a constant rate. During the first part of the test (R-79) the feed rate to the calciner was about 10 to 12 liters/hr. The rate was maintained at a level so that, as the glass formed, only two thermocouples (about 13 in. apart) would be covered with either aqueous liquid or calcined solids. After 13 hr of operation, the off-gas line was so severely plugged that the secondary off-gas line relieved the system to atmospheric pressure. The run was temporarily shut down, and the off-gas line was cleaned. At this time, 132 liters of feed had been fed to the system (Table 1). Also, 193 liters of water had been

Table 1. Hourly System Variables and Parameters

UNCLASSIFIED
ORNL DWG. 63-3541

TEST R- 79 FEED TYPE - TBP25 (GLASS). OPERATION MODE - CONTINUOUS

RUN TIME	SYSTEM FEED	SYSTEM WATER	CALCINER ADDITIVE	EVAPORATOR CONDENSATE	CALCINER FURNACE	CALCINER CONDENSATE	EVAPORATOR CONDENSATE	SYSTEM OFF-GAS	EVAPORATOR DENSITY	CALCINER CONDENSATE
HOURS	LITERS	LITERS	LITERS	LITERS	(HUNDRED-THOUSANDS OF BTUS)			CU FT	GM/CC	LITERS
1	55	31		64	1.16	.09	2.13	9	1.52	4
2	60	57		98	2.08	.36	2.87	19	1.35	14
3	60	83		129	2.96	.63	3.62	28	1.38	23
4	72	83		139	3.83	.88	4.52	38	1.36	32
5	88	110		180	4.68	1.15	5.42	48	1.39	41
6	102	110		188	5.58	1.44	6.30	57	1.38	51
7	114	141		238	6.50	1.79	7.51	67	1.33	64
8	120	141		242	7.32	1.90	8.25	77	1.38	68
9	122	140		244	7.87	1.92	9.08	88	1.36	69
10	121	167		271	8.25	1.92	9.86	99	1.37	69
11	124	167		273	8.60	1.94	10.64	109	1.37	69
12	121	193		297	8.97	1.94	11.48	119	1.37	69
13	132	193		309	9.42	1.96	2.55	129	1.37	70

added to the evaporator to steam strip the nitric acid so that the evaporator nitrate composition would be constant at about 6 M. While the off-gas line was being cleaned, the calciner pot was probed, and it was determined that there was about 9 in. of solid, thought to be glass, in the bottom of the calciner vessel.

When the off-gas line had been cleaned, the second filling of the calciner pot was started. The average feed rate for this portion of the test was between 6 and 7 liters/hr (358 liters in 55 hr) (Table 2). The combined over-all average feed rate for the test was 7.3 liters/hr (490 liters in 67 hr). During the second phase of the test, 1100 liters of water was added to remove the nitrate from the evaporator. The over-all water-to-feed ratio for this test was 2.9. During the test, the off-gas line started to plug six to eight times. The restrictions were removed by back-flushing the off-gas line with nitric acid. However, when the off-gas line was removed at the end of the test, it contained a brown, calcined substance that appeared to be calcined foam. The material balance for test R-79-80 was good except for the nitrate balance, which was only 62%. The nitrate in the evaporator condensate was unexplainably low (Table 3).

Table 3. Material Balance for Tests R-79-80

	Ionic Constituents (g)			
	NO_3	Al	Na	PO_4
Feed (490 liters)	185,220	19,012	22,834	79,380
Evaporator (25 liters)	10,025	1,105	1,117	4,400
Evaporator condensate (1405 liters)	105,675	---	---	---
Solids (129 kg)	64	19,350	17,544	71,543
Total	115,700	20,455	18,661	75,943
Percent of balance	62.5	107.6	81.7	95.7

The resulting glassy solid had the following weight percent compositions: nitrate, 0.05; aluminum, 15.1; sodium, 13.6; phosphate, 55.5; and

Table 2. Hourly System Variable and Parameters

UNCLASSIFIED
ORNL DWG. 63-3490

TEST R- 80 FEED TYPE - TBP25 (GLASS). OPERATION MODE - CONTINUOUS

RUN	SYSTEM	SYSTEM	CALCINER	EVAPORATOR	CALCINER	CALCINER	EVAPORATOR

HOURS	LITERS	LITERS	LITERS	LITERS	(HUNDRED-THOUSANDS OF BTUS)			CU FT	GM/CC	LITERS
1	26	-		10	.93	.16	.79	12	1.26	7
2	29	27		39	1.79	.41	1.69	21	1.32	16
3	35	28		46	2.59	.69	2.54	31	1.31	26
4	36	58		78	3.42	.99	3.42	42	1.31	36
5	42	58		84	4.25	1.27	4.42	52	1.32	46
6	65	84		132	4.95	1.50	5.45	63	1.33	55
7	62	84		130	5.64	1.72	6.25	74	1.31	63
8	63	115		162	6.39	1.98	7.01	84	1.33	72
9	63	116		162	7.08	2.19	7.75	95	1.31	80
10	65	142		193	7.75	2.41	8.44	108	1.30	88
11	83	172	-	240	8.44	2.62	9.52	122	1.31	96
12	85	172	-	241	9.14	2.83	10.28	133	1.32	103
13	98	198		279	9.85	3.07	11.25	144	1.33	112
14	100	226		303	10.53	3.33	12.12	154	1.35	122
15	107	257		346	11.26	3.61	13.27	165	1.31	132
16	112	257		353	11.97	3.88	14.50	176	1.32	141
17	139	283		401	12.68	4.14	15.28	187	1.33	151
18	143	313		441	13.42	4.42	16.32	198	1.30	161
19	150	314		447	14.10	4.69	17.31	209	1.31	170
20	167	340		491	14.73	4.96	18.12	219	1.31	180
21	176	340		500	15.35	5.25	18.91	230	1.31	191
22	189	340		512	15.95	5.52	19.80	240	1.31	201
23	188	371		541	16.54	5.72	20.58	251	1.31	209
24	193	371	-	547	17.19	5.94	21.69	263	1.30	217
25	199	397		577	17.85	6.06	22.41	275	1.32	221
26	200	424		608	18.56	6.33	23.74	287	1.32	231
27	202	425		610	19.17	6.63	24.81	297	1.32	243
28	203	455		642	19.65	6.69	25.66	309	1.38	245
29	215	482		680	20.28	6.87	26.84	319	1.37	252
30	219	482		683	20.98	7.19	27.70	329	1.32	263
31	236	507		728	21.62	7.49	28.59	340	1.32	274
32	247	508		739	22.27	7.80	29.49	351	1.32	285
33	269	509		762	22.91	8.10	30.39	361	1.31	295
34	277	509		770	23.49	8.38	31.28	372	1.31	306
35	277	566		827	23.99	8.45	32.46	386	1.34	309
36	277	596		854	24.35	8.47	33.12	396	1.36	309
37	293	596		873	24.86	8.70	34.08	407	1.29	318
38	296	595		875	25.48	8.98	34.98	417	1.32	328
39	302	625		909	25.99	9.16	35.89	429	1.32	334
40	308	625		918	26.46	9.31	37.18	441	1.28	340
41	306	652		933	26.85	9.41	37.80	453	1.30	344
42	306	652		938	27.25	9.50	38.68	464	1.28	347
43	309	707		999	27.63	9.57	40.37	475	1.26	350
44	309	734		1026	27.98	9.64	41.50	487	1.30	352
45	321	734		1038	28.32	9.70	42.33	497	1.29	355
46	326	734		1041	28.66	9.75	43.24	508	1.29	356
47	325	760		1068	28.96	9.75	44.18	519	1.32	356
48	323	762		1068	29.26	9.75	45.01	531	1.16	356
49	333	790		1106	29.79	10.02	46.13	542	1.27	366
50	335	791		1108	30.33	10.25	46.93	552	1.30	375
51	342	818		1144	30.76	10.38	47.80	564	1.32	380
52	349	848		1177	31.14	10.45	49.28	575	1.37	382
53	353	879		1214	31.75	10.85	50.66	585	1.35	398
54	358	936		1278	32.25	11.01	52.05	596	1.33	404
55	358	1100		1433	32.65	11.12	12.82	608	1.21	408

lead, 6.7. The glass (Fig. 1) had a number of areas that were nonhomogeneous. The bottom area contained a large number of lead globules. Other areas had nonmelted, calcined solids inclusions (white portion of Fig. 2). About 90% of the solid was a very hard, green-colored glassy substance.

After the solid had been removed from the calcined pot, the pot was sand blasted and examined. The initial wall thickness was 350 mils. Figure 3 shows one of the highly pitted areas. Some pits are 150 mils deep. The bottom 2 ft of the thermocouple well and thermocouples were completely disintegrated.

The feed for test R-81 was the standard TBP-25 feed made 2 M NaH_2PO_4 and 0.25 M in $Pb(NO_3)_2$ in order to form a glass mix. Four-hundred-eighty-two liters were fed to the system and diluted to 819 liters of feed for the calciner (Table 4). This feed was also diluted in the evaporator for operational ease in pumping into the calciner. Again, water (2455 liters) was added to the system during the course of the run to steam strip the nitric acid from the evaporator.

The operating limit for this test was that only one zone in the furnace (1 ft) could be filled with aqueous feed at one time. Therefore, the feed rate to the calciner had to be maintained at about 10 liters/hr. As the melt zones neared the top of the furnace, the rate was decreased.

The material balances for this test (Table 5) were satisfactory. The low nitrate balance (76.5%) and the high aluminum balance (120%) apparently represent errors in analysis because the sodium and phosphate balances, 97.9 and 97.1%, respectively, indicate that the sampling and measurement of volume was fairly accurate. The loss of sodium phosphate and aluminum from the calciner system was about 2.5%, probably due to entrainment (dusting).

The final glass had a residual nitrate content of 370 ppm and was fairly homogeneous in appearance but had areas of included calcined solid and metallic lead. The bulk density of the glass was 2.24 g/cc.

2.1.2 Continuous-Melter Tests

Initial tests on a horizontal continuous melting system were successful. The purpose of a continuous melt system for the fixation of high-level waste is to convert the waste to a molten glass that can flow

UNCLASSIFIED
ORNL-PHOTO 61998

Fig. 1. General View of Glass Prepared from TBP-25 Aluminum Waste.

UNCLASSIFIED
ORNL-PHOTO 61999

Fig. 2. Close-up View of Glass Prepared from TBP-25 Aluminum Waste.

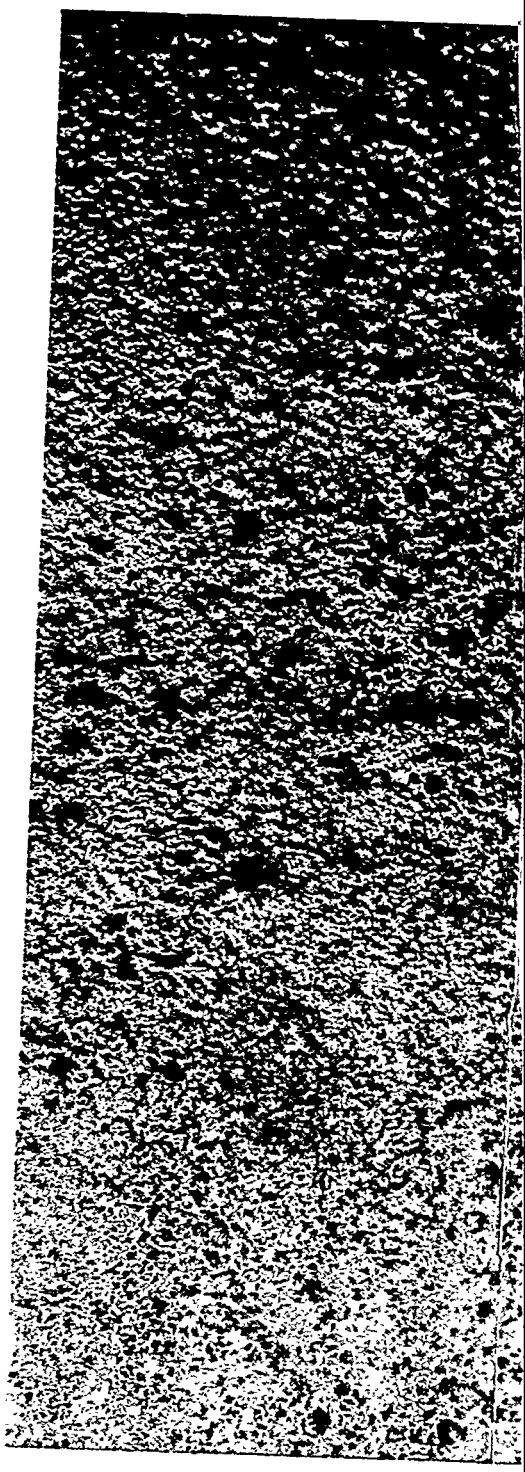

Fi
Surface

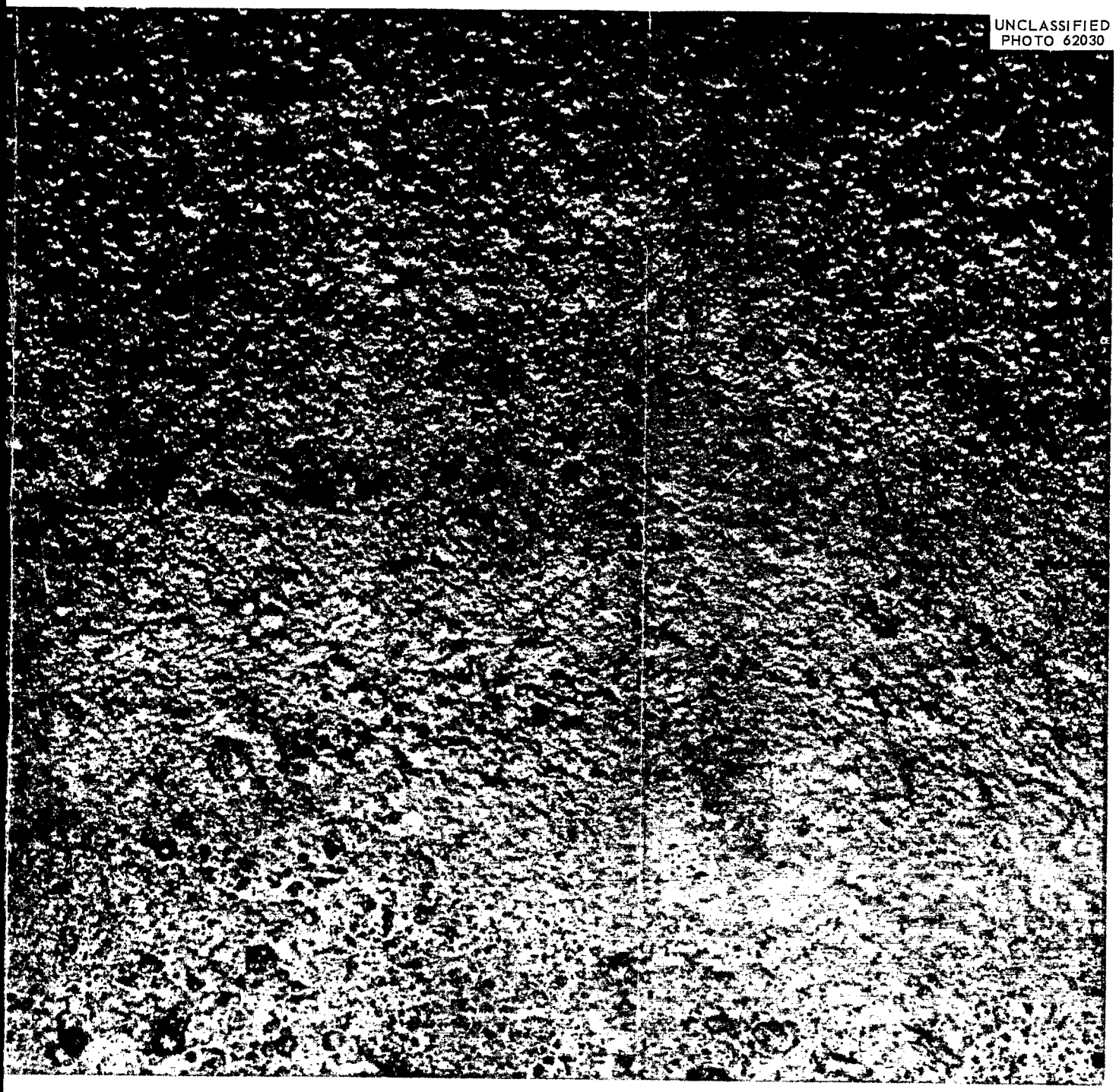

Fig. 3. Inside of Melting Pot, Showing Corrosion Pitting. The ace was sand blasted.

Table 4. Hourly System Variables and Parameters

UNCLASSIFIED
ORNL DWG. 63-5581

TEST R- 81 FEED TYPE - TBP-25 GLASS, OPERATION MODE - CONTINUOUS

RUN TIME	SYSTEM FEED	SYSTEM WATER	CALCINER ADDITIVE	EVAPORATOR CONDENSATE	CALCINER FURNACE	CALCINER CONDENSATE	EVAPORATOR CONDENSATE	SYSTEM OFF-GAS	EVAPORATOR DENSITY	CALCINER CONDENSATE
HOURS	LITERS	LITERS	LITERS	LITERS	(HUNDRED-THOUSANDS OF BTUS)			CU FT	GM/CC	LITERS
1	43	30		25	1.37	.36	.84	7	1.19	16
2	41	31		23	2.37	.70	1.72	13	1.23	29
3	49	30		30	3.38	1.15	2.60	20	1.24	46
4	52	57		60	4.59	1.74	3.57	27	1.24	67
5	61	57		71	5.85	2.38	4.51	34	1.27	89
6	73	92		117	7.06	3.04	6.36	43	1.27	113
7	83	118		153	8.30	3.67	7.46	53	1.28	136
8	104	149		205	9.47	4.25	9.52	63	1.27	156
9	113	209		274	10.71	4.76	11.35	73	1.29	174
10	121	236		308	11.84	5.20	12.92	81	1.29	190
11	121	270		334	12.71	5.49	14.11	91	1.29	201
12	142	323		417	13.80	5.94	15.98	101	1.26	218
13	143	354		449	14.77	6.26	17.40	110	1.29	230
14	144	380		475	15.69	6.53	18.73	120	1.29	240
15	145	410		509	16.58	6.74	20.09	129	1.27	249
16	154	467		573	17.36	7.04	21.53	138	1.29	260
17	153	493		598	18.17	7.32	22.81	147	1.29	271
18	153	519		624	19.07	7.57	24.04	156	1.28	281
19	154	550		655	19.90	7.82	25.31	165	1.29	292
20	155	580		667	20.83	8.11	26.58	174	1.29	303
21	156	607		715	21.75	8.42	27.87	182	1.29	315
22	164	636		753	22.57	8.71	29.11	191	1.28	327
23	169	663		785	23.49	8.96	30.41	200	1.29	337
24	171	690		813	24.19	9.23	31.59	208	1.29	348
25	180	719		844	25.01	9.55	32.55	215	1.31	361
26	184	719		854	26.00	9.93	34.02	224	1.20	376
27	209	746		907	26.97	10.27	35.35	232	1.27	389
28	223	777		951	28.00	10.61	36.73	240	1.28	402
29	235	803		989	28.91	10.92	37.98	248	1.34	415
30	240	833		1024	29.85	11.26	39.26	258	1.25	428
31	243	864		1059	30.78	11.53	40.56	268	1.25	439
32	244	894		1090	31.65	11.75	41.81	277	1.25	448
33	244	920		1116	33.19	11.98	43.07	287	1.25	457
34	253	951		1149	34.13	12.31	43.93	297	1.24	470
35	262	977		1192	35.02	12.63	45.50	305	1.25	483
36	264	1008		1224	35.93	12.93	46.71	313	1.26	495
37	272	1034		1257	36.73	13.19	47.87	319	1.26	506
38	274	1064		1290	37.53	13.45	49.10	325	1.25	517
39	279	1065		1295	38.29	13.70	50.28	332	1.25	527
40	299	1092		1343	39.04	13.95	51.46	340	1.25	538
41	302	1123		1380	39.72	14.23	52.64	347	1.25	550
									1.25	561

45	322	1233	1506	43.04	15.26	57.24	379	1.26	593
46	324	1263	1539	44.41	15.51	58.51	387	1.25	604
47	333	1288	1573	45.26	15.71	59.81	395	1.25	613
48	335	1319	1606	46.05	16.00	60.99	403	1.25	624
49	343	1319	1613	46.69	16.22	62.14	411	1.25	633
50	344	1345	1642	47.34	16.35	63.21	420	1.25	639
51	350	1376	1677	47.94	16.51	64.35	427	1.26	645
52	350	1402	1704	48.64	16.68	65.58	434	1.27	652
53	350	1433	1734	49.26	16.85	66.79	442	1.27	659
54	376	1457	1765	49.93	17.01	67.88	448	1.27	665
55	380	1488	1820	50.55	17.17	69.06	454	1.27	672
56	380	1514	1846	51.82	17.31	70.14	460	1.27	678
57	381	1541	1874	52.37	17.44	71.27	467	1.27	683
58	386	1572	1909	52.93	17.58	72.35	473	1.27	689
59	386	1597	1935	53.64	17.73	73.50	480	1.27	695
60	387	1628	1967	54.20	17.87	74.59	485	1.28	701
61	404	1628	1983	54.83	18.01	75.66	492	1.27	707
62	411	1654	2017	55.43	18.11	76.79	498	1.28	711
63	412	1681	2044	56.03	18.18	77.89	503	1.28	714
64	422	1711	2077	56.49	18.23	79.20	509	1.35	717
65	421	1741	2105	57.07	18.29	80.16	516	1.29	719
66	421	1772	2141	57.63	18.35	81.27	522	1.28	722
67	422	1798	2172	58.11	18.42	82.38	529	1.29	725
68	421	1828	2203	58.61	18.50	83.46	536	1.28	728
69	424	1854	2229	59.12	18.59	84.53	543	1.26	732
70	429	1881	2261	59.67	18.69	85.63	549	1.26	736
71	431	1911	2293	60.25	18.85	86.68	557	1.26	743
72	433	1909	2293	60.79	18.99	87.78	564	1.26	749
73	435	1937	2324	61.34	19.14	88.91	572	1.26	755
74	436	1968	2356	61.89	19.26	90.00	579	1.26	760
75	439	1999	2390	62.45	19.36	91.12	587	1.26	764
76	440	2029	2421	62.96	19.47	92.15	595	1.26	769
77	446	2059	2457	63.54	19.61	93.23	602	1.25	775
78	453	2086	2490	64.05	19.72	94.40	612	1.25	780
79	452	2117	2518	64.53	19.84	95.59	621	1.26	785
80	457	2116	2524	65.04	19.94	96.70	631	1.25	789
81	458	2146	2554	65.50	20.04	97.80	641	1.25	794
82	458	2173	2581	65.97	20.12	98.81	650	1.25	797
83	476	2202	2627	66.47	20.21	99.87	659	1.25	801
84	477	2227	2653	66.92	20.29	100.97	667	1.25	805
85	477	2254	2680	67.36	20.36	102.20	674	1.26	808
86	478	2284	2703	67.82	20.41	103.26	682	1.28	810
87	480	2310	2735	68.25	20.49	104.47	689	1.23	814
88	482	2310	2746	68.69	20.55	105.56	698	1.36	816
89	480	2337	2770	69.09	20.55	106.54	707	1.52	816
90	480	2337	2770	69.44	20.55	107.47	717	1.40	817
91	482	2367	2799	69.83	20.55	108.23	727	1.35	817
92	479	2367	2798	70.16	20.55	109.11	737	1.31	817
93	482	2393	2827	70.56	20.56	109.98	747	1.31	817
94	482	2394	2828	70.90	20.56	110.83	755	1.31	817
95	481	2393	2827	71.30	20.56	111.66	764	1.31	817
96	480	2423	2853	71.73	20.61	112.40	774	1.29	819
97	482	2454	2871	72.16	20.61	112.63	782	1.02	819
98	481	2454	2870	72.48	20.61	112.82	792	1.00	819
99	481	2454	2870	72.84	20.61	113.02	803	1.00	819

to and solidify in the final storage vessel without an intermediate calcination step. The aqueous waste solution was fed directly into a vessel that had an inventory of molten glass and enough heating capacity to evaporate water, decompose nitrate, and melt the residue. The outstanding advantage of this process is that it is a one-step continuous operation from liquid waste to the final pot receiver. A horizontal melting vessel

Table 5. Test R-81: Material Balance

	Ionic Constituents (g)			
	NO_3	Al	Na	PO_4
Feed (482 liters)	181,714	18,123	19,762	80,976
Evap. holdup	9,875	742	720	3,150
Evap. condensate	129,150	114	3	29
Solids	53	20,904	18,626	75,442
Total	139,078	21,760	19,349	78,621
Percent of balance	76.5	120	97.9	97.1
Calciner condensate (819 liters)	236,691	597	467	2,154
	130%	2.7%	2.4%	2.7%

(8 in. in diameter and 40 in. long) has been tested with simulated TBP-25 waste at rates up to 20 liters/hr. The melt vessel is heated by a resistance furnace that has four temperature-controlled zones and a total power of 25 kw. The molten glass product is withdrawn through a freeze-trap valve (Fig. 4).

Melt Vessel.-- The melt vessel is constructed of 304L stainless steel (350 mils thick). The melt vessel is 40-in. long, with a 36-in. feeding zone. A baffle 4 in. from one end extends 2 in. under the normal melt level acting as a skimmer to remove floating solids and allowing only melt to enter into the overflow line. Along the bottom of the melt vessel are five 1/4-in.-diam stainless steel lines placed at equal intervals so that nitrogen can be used for sparging the melting glass; however, very little use has been made of these sparging lines.

UNCLASSIFIED
ORNL-DWG 63-6219

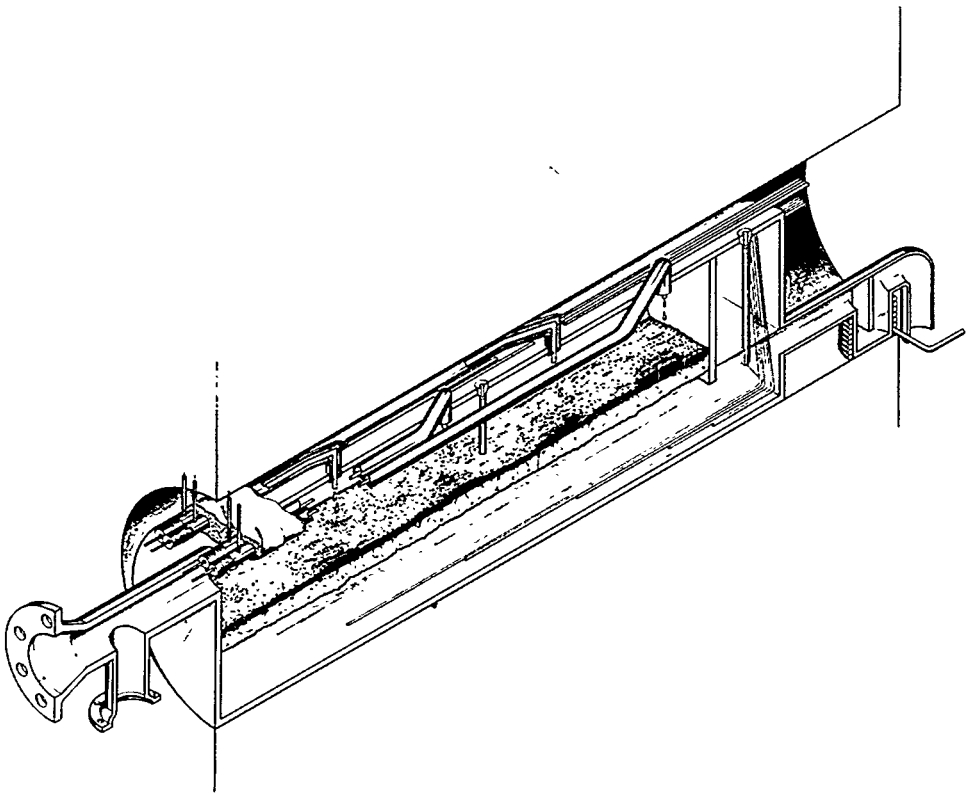

Fig. 4. High Level Waste Continuous Melter.

Feeding System.-- Four water cooled feed lines (Fig. 5) were located at equal intervals along the top of the 36-in. feeding zone. The feed lines are equipped for water flushing to calibrate flow rates and to remove all traces of feed from these lines at the termination of a feeding period. The feed is pumped from the feed hold tank with a Sigma motor pump at a rate governed by visual observation. Rates up to 20 liters/hr were acceptable during the initial start-up of the system. However, once the melt pot got a layer of deposited solids on the wall, the maximum feed rate dropped to about 10 liters/hr. The feed rate is governed by watching the amount of solids building up in the vessel, the rate being adjusted so that the solids do not build up to the feed inlet nozzles.

Off-Gas.-- The off-gas is removed through a 2-in.-diam line (Fig. 6) which is also equipped with a Pyrex view port for viewing the feed nozzles and the solids in the melt zone. The vapor flows through the off-gas line and then down through a 22-ft^2 heat exchanger into a liquid-gas separator, where the volumes of noncondensable off-gas and condensate are measured. At high feed rates, solids collecting in the off-gas line must be removed periodically by washing. These solids would be recirculated to the evaporator and returned with the feed to the melt pot in an actual plant operation.

Melt Removal.-- The molten glass exits from the rear section of the melt pot (after the calcined solids have been skimmed) through a 3/4-in. line flowing to a baffled freeze trap (Fig. 7). The volume of the freeze trap is 250 ml. The freeze trap is located inside the resistance furnace. Consequently, to freeze the contents, it must be cooled below the melting temperature of the molten glass (700 to 800°C). Cooling is attained by flowing either air or steam through the exterior cooling coils. Cooling usually takes from 10 to 15 min.

The freeze-trap discharge line is a 3/4-in. stainless steel line, autoresistance heated. This 13-in.-long line is heated easily to 800°C by using 4 to 6 v and about 400 amp of current. The melt discharged from this line in an actual plant would go to a permanent storage vessel (pot). This pot should be contained in a furnace so that the melt could be slowly cooled and annealed to prevent stresses caused by quick cooling. However, in this scouting experiment the glass is allowed to flow through into a stainless steel tray.

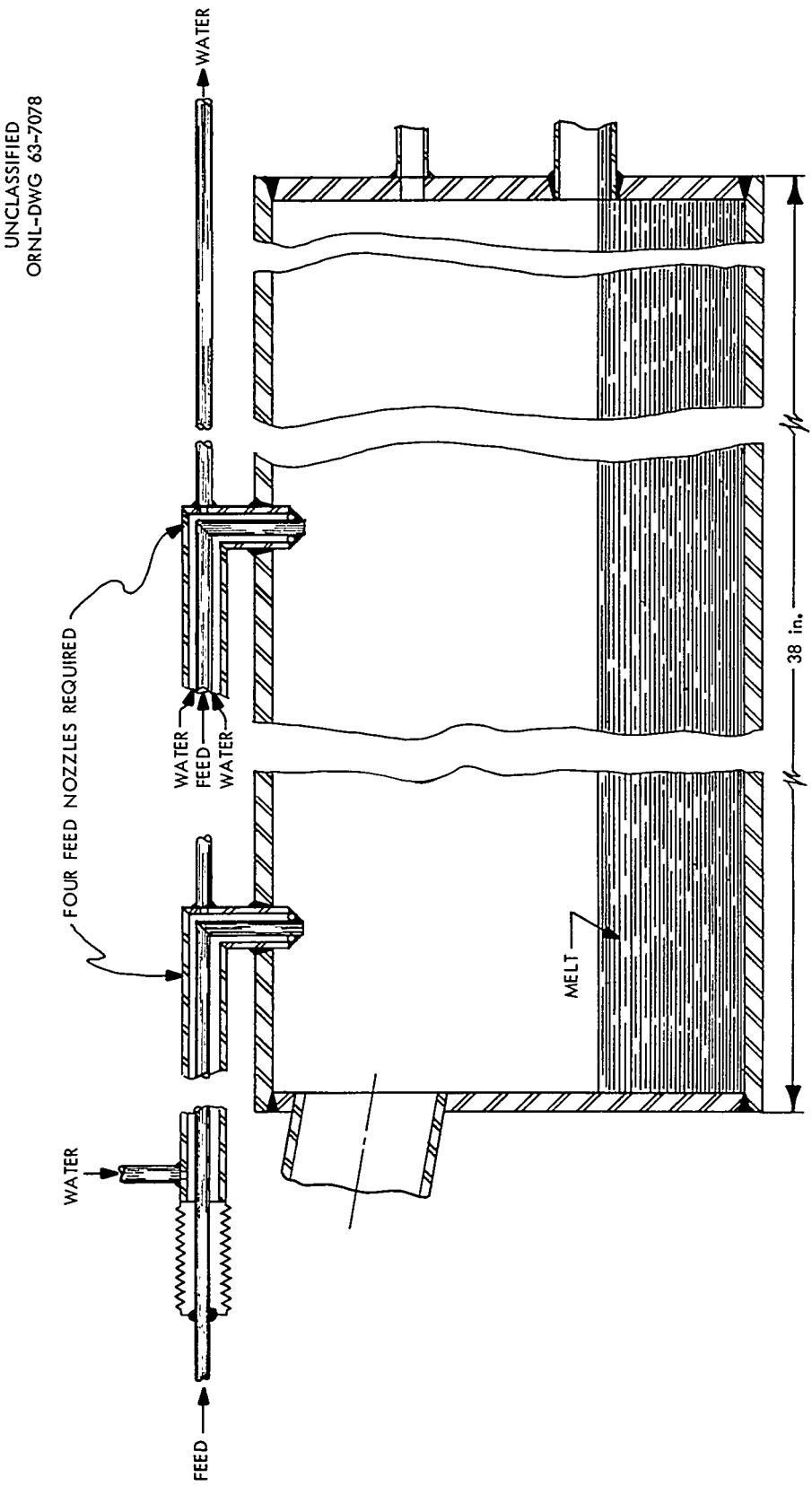

Fig. 5. Water-Jacketed Feed Line.

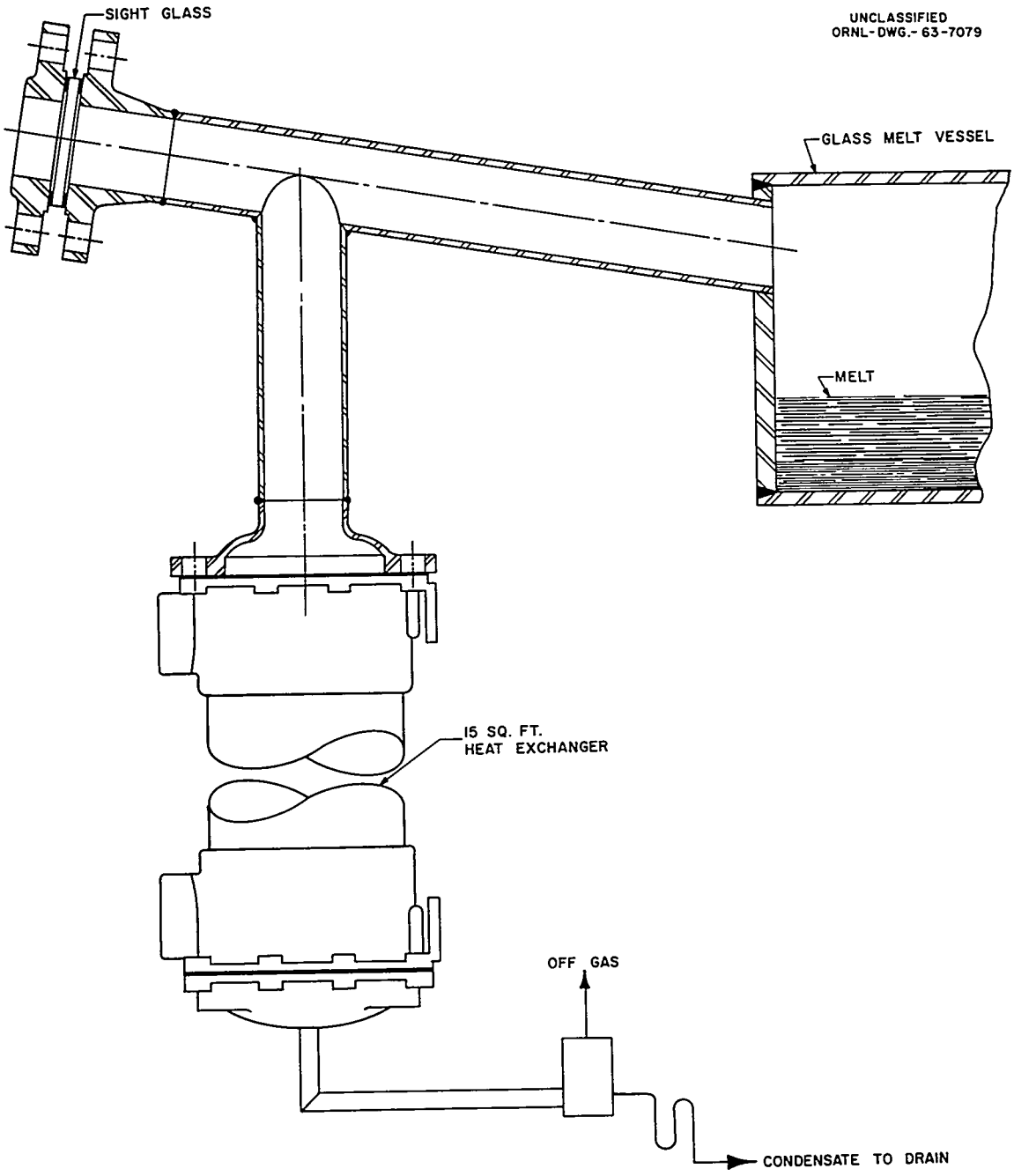

Fig. 6. Off-Gas Removal System.

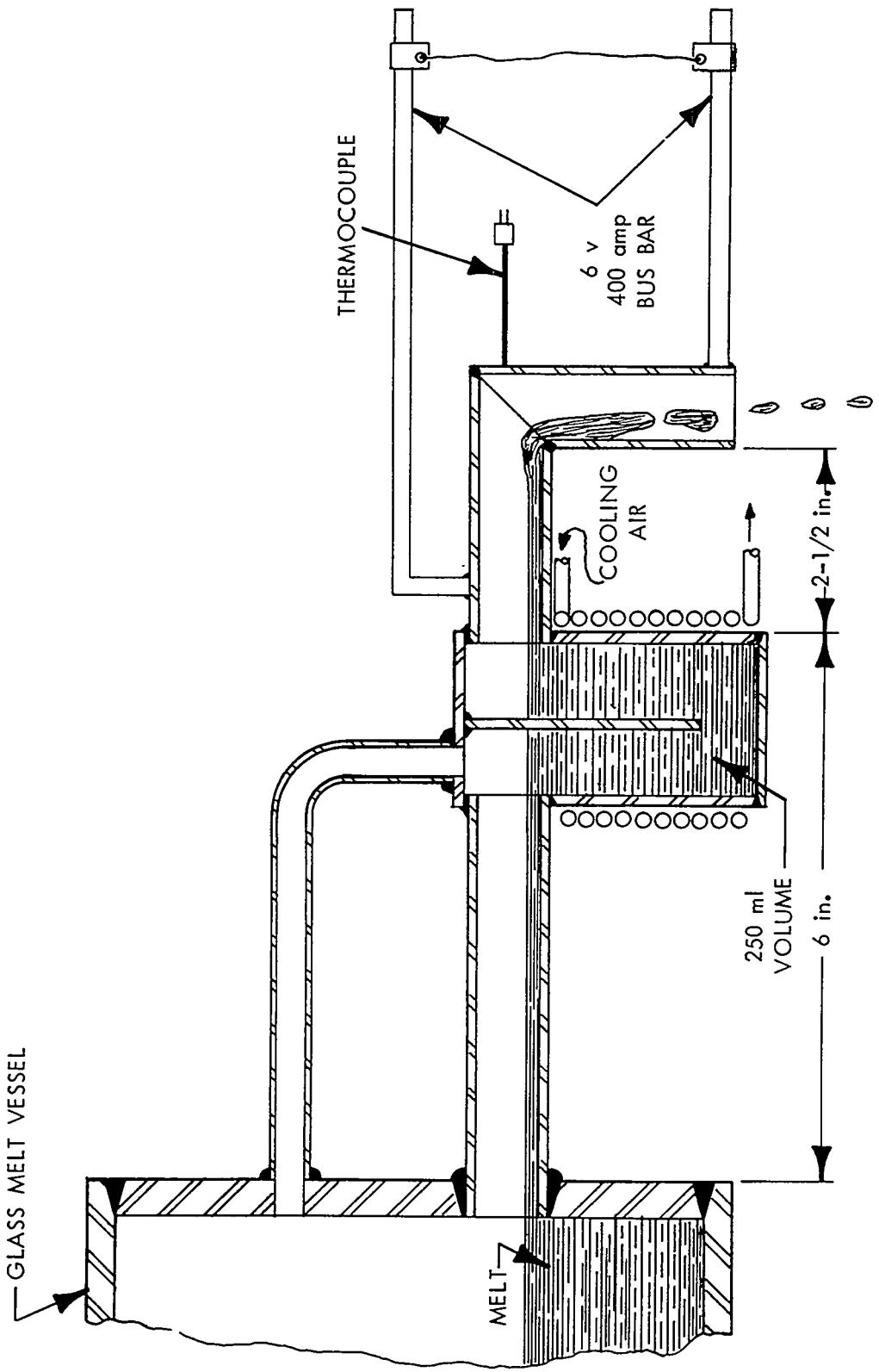

Fig. 7. Trap Freeze Valve.

2.1.3 Results

TBP-25 waste with additives of 2 moles of dibasic sodium phosphate per liter plus either lead nitrate or sodium borate (quarter mole of lead or boron) was the melt mixture tested. This mixture forms a calcined solid between 400 and 600°C and melts at about 750 to 800°C. At 850 to 900°C it is fluid enough to be removed from the melt pot by gravity flow. FTW-65 (formaldehyde-treated waste, 1965) Purex waste with lithium additives (Sec 2.2.2) has been melted in a vertical melting pot experiment and will be tested at a later date in this system.

Throughput rates of up to 20 liters/hr have been attained with TBP-25 waste with phosphate-lead additives with a furnace of 25 kw and a melt pot exterior temperature of 1000°C. There was no evidence of severe corrosion in the horizontal melt pot although it had been operated for about 15 days at temperatures varying from 600 to 1000°C. During preliminary experiments with a vertical pot, extreme corrosion was experienced with both TBP-25 glass mix and FTW-65 glass mix, especially in the area where lines were brought into the vessel beneath the melt level. In designing this horizontal melt pot, there are no lines which penetrate the vessel below the melt level. A platinum-lined vessel would probably be required for plant operations, however.

2.1.4 Future Program

The future program for the continuous, horizontal-pot melting system with various types of waste will be to determine processing-rate data, corrosion properties, and the off-gas difficulties (including solids entrainment) encountered with various types of waste. With this data, a new design of the continuous-melt vessel can be made. The vessel would be made of a material that would be compatible with the waste to be used (probably platinum lined). Later, the horizontal melt vessel could be located over the present 8-in.-diam waste calciner furnace and integrated into the system to use the continuous evaporator as a feed preparation step. The molten glass from the melt vessel would flow into one of the present 8-in.-diam vertical waste-calcining vessels where it would be suitably annealed. The off-gas and condensate from the system would be recycled to the evaporator.

2.2 Laboratory Development

W. E. Clark H. W. Godbee

During the past quarter, work was continued on the characterization and fixation of FTW-65 (Formaldehyde-treated 1965 Purex waste solution) waste and on corrosion of materials of construction. In addition, work was done on the fixation of non-sulfate and sulfate-deficient waste types.

2.2.1 Characterization of Purex FTW-65 Waste Solution

Studies were made on Purex FTW-65 waste solution (Table 6) to obtain data for use in the design of pilot-plant facilities at Hanford. The waste could be concentrated by a factor of 4 before solids began to appear in the cooled solution, and concentrations of the waste up to a factor of 9 were made. Samples of various concentrations were used to determine vapor-liquid equilibria with a Gillespie recycling still (Table 7, Fig. 8). A Westphal balance mounted over a constant temperature bath was used to determine solution densities. Densities of the FTW-65 at room temperature ranged from 1.064 g/cc for unconcentrated waste to 1.441 g/cc for the waste concentrated by a factor of 9 (Table 7, Fig. 9). Densities of the more concentrated solutions at the lower temperatures are probably lower than they should be because of crystallization of solids from the solution.

2.2.2 Fixation of Wastes

FTW-65 Waste.-- Efforts were directed toward finding mixtures which yield solid products having:

1. good sulfate retention,
2. good physical properties (glassy, insoluble, etc.),
3. low softening and melting temperatures, and
4. low corrosivity.

All these virtues are not easily combined in a single simple mixture. While special emphasis has been given at various times to low-melting products and noncorrosive products, sulfate retention was given special attention in these experiments.

Mixtures were found which have melting temperatures below 700°C. Some were quite glassy, and some lost less than 5% of their sulfate (Table 8). The current "best" FTW-65 product (No. 1, Table 8) was devised

Table 6. Compositions of Purex Waste Types Studied

Constituent (g-moles/liter waste)	FTW-65 Single Con'c	FTW-65 x 3[a]	High Sulfate Purex "1WW"	Future Acid Purex "FAP"	Non-Sulfate Purex "NSP"
H^+	0.5	1.5	5.6	0.5	3.0
Na^+	0.30	0.9	0.6	1.2	0.6
Al^{3+}	0.05	0.15	0.1	c	0.2
Fe^{3+}	0.10	0.30	0.5	0.1	0.05
Cr^{3+}	0.02	0.06	0.01	c	0.006
Ni^{2+}	0.01	0.03	0.01	c	0.006
Hg^{2+}	0.0035[d]	0.0105[d]	c	c	c
Ru	0.002	0.006	0.002	c	c
SO_4^{2-}	0.15	0.45	1.0	0.2	c
PO_4^{3-}	0.005	0.015	c	c	0.02
SiO_3^{2-}	0.01	0.03	c	c	c
F^-	0.0005	0.0015	c	c	c
NO_3	to balance	to balance	to balance	to balance	to balance

[a]The FTW x3 represents the highest concentration of this waste type that can be conveniently simulated by direct make-up from laboratory reagents without application of heat to the solution vessel.

[b]Estimated from consideration of various Savannah River plant flow-sheet wastes.

[c]Content not specified.

[d]Maximum.

Table 7. Vapor-Liquid Equilibrium and Density Data for 1965 FTW Waste Solutions

Solution	H^+ Analyzed (M)	Fe Analyzed (mg/ml)	Equilibrium Boiling Point (°C)	Density (g/ml) 23.5°C	50.0°C	75.0°C	100.0°C
FTW- Conc. x 1 *	0.55	5.40	101	1.064	1.056	1.043	1.018
Pot	0.56						
Distillate	<0.02						
FTW- Conc. x 2	1.07		102				
Pot	1.08						
Distillate	<0.02						
FTW- Conc. x 3	1.65	16.40		1.194	1.181	1.165	1.135
Pot							
Distillate							
FTW- Conc. x 4	1.87		105				
Pot	2.09						
Distillate	0.17						
FTW- Conc. x 5	2.68	23.6	108	1.317	1.301	1.273	1.265
Pot	2.91	29.0					
Distillate	0.55	<0.005					
FTW- Conc. x 7	3.44	36.0	114	1.413	1.395	1.373	1.354
Pot	3.76	42.0					
Distillate	1.40	< 0.005					
FTW- Conc. x 9	3.70	47.3	115	1.441	1.423	1.397	1.386
Pot	3.85	54.5					
Distillate	2.53	< 0.005					

*Composition, g-moles/liter: H^+-0.5, Na^+-0.3, Al^{3+}-0.05, Fe^{3+}-0.1, Cr^{3+}-0.02, Ni^{2+}-0.01, Hg^{2+}-0.0035, SO_4^{2-}-0.15, PO_4^{3-}-0.005, SiO_3^{2-}-0.01, F^--0.002, NO_3^- to balance.

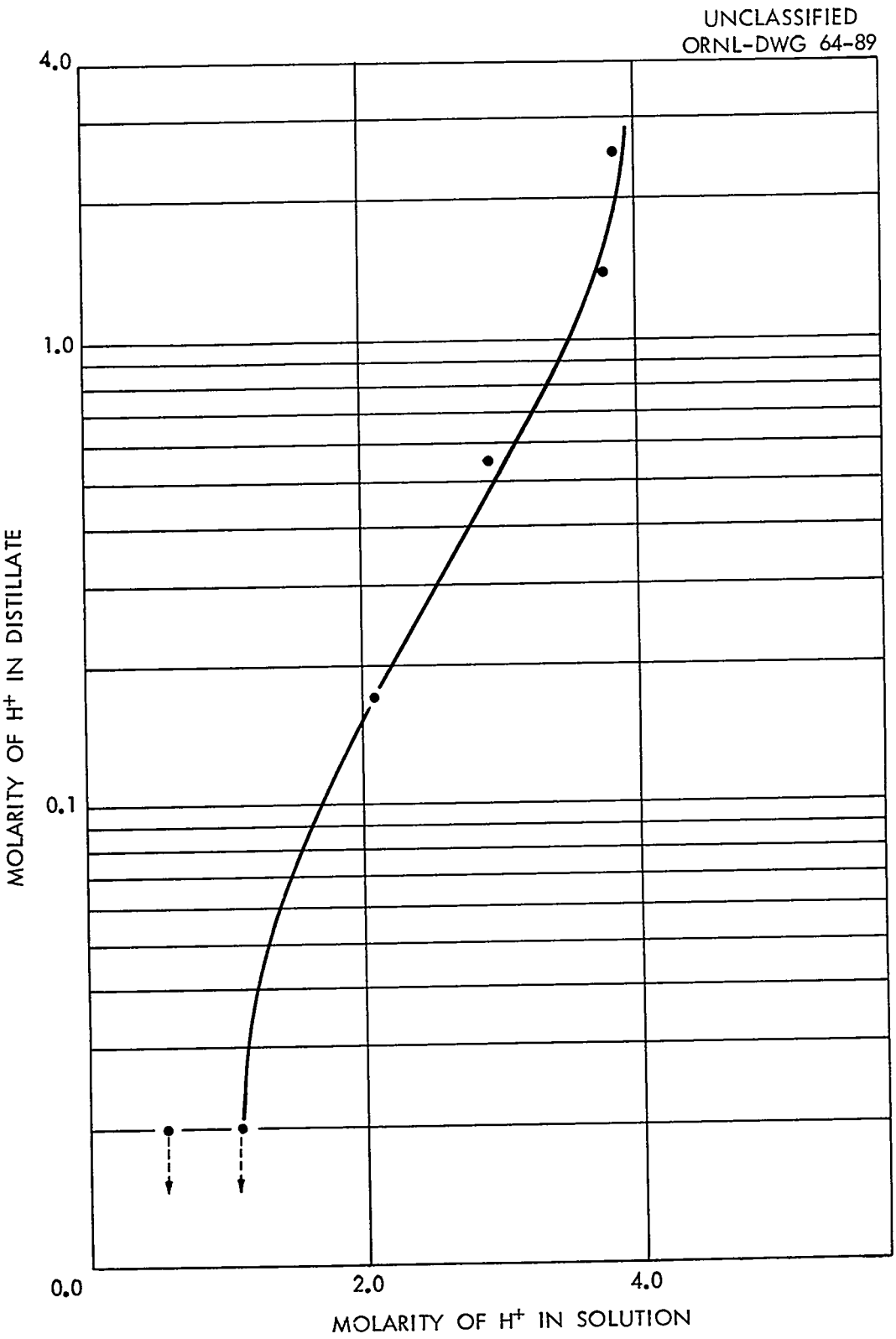

Fig. 8. Vapor-Liquid Equilibrium in FTW-65 Waste Solutions.

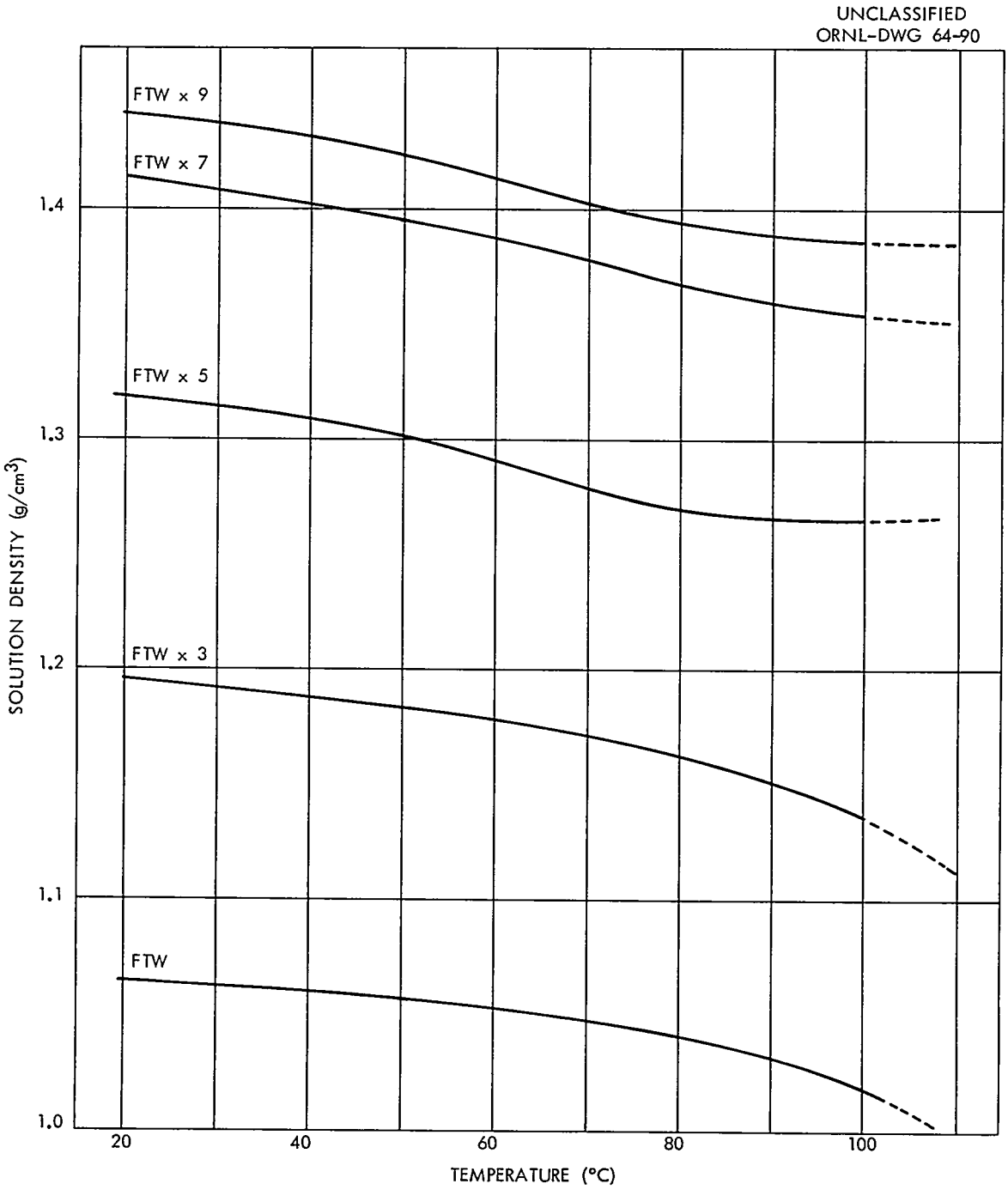

Fig. 9. Densities of FTW-65 Waste Solution at Various Concentrations.

Table 8. Fixation Experiments

Additives (gm moles/liter)	1	2	3	4	5	6	7
H_3PO_3 or H_3PO_4 [b]	1.0	1.175	1.175	1.175	1.175	1.175	1.175
LiOH	1.14	1.75	2.0	1.25	1.25	1.25	1.25
$Al(NO_3)_3$	0.5	0.153	0.153	0.153	0.153	0.153	0.153
$Na_2B_4O_7$	--	0.25	0.25	--	--	--	--
$Ca(OH)_2$	0.2	0.144	0.144	0.144	0.144	0.144	0.144
B_2O_3	--	--	--	--	0.123	0.25	--
$Pb(NO_3)_2$	--	--	--	--	--	--	0.13
MgO	--	--	--	--	--	--	--
$Ba(NO_3)_2$	--	--	--	--	--	--	--
Waste Oxides (Wt. % of theoretical)	44.5	39.9	47.0	38.6	45.8	42.4	42.2
Mole % Theoretical Oxides							
Al_2O_3	11.8	4.4	4.3	5.66	5.41	5.18	5.40
CaO	7.2	4.2	4.1	5.38	5.14	4.92	5.13
Na_2O	16.3	13.2	12.7	16.81	16.07	15.38	16.03
Li_2O	20.6	25.6	28.1	23.35	22.33	21.36	22.27
Fe_2O_3	5.4	4.4	4.2	5.60	5.36	5.13	5.34
Cr_2O_3	1.1	0.8	0.8	1.12	1.07	1.03	1.07
NiO	1.1	0.8	0.8	1.12	1.07	1.03	1.07
RuO_2	0.2	0.2	0.2	0.22	0.21	0.21	0.21
PbO	--	--	--	--	--	--	4.63
SO_3	16.3	13.2	12.7	16.81	16.07	15.38	16.03
P_2O_5	18.4	17.4	16.8	22.23	21.25	20.33	21.20
B_2O_3	--	14.5	14.1	--	4.39	8.54	--
SiO_2	1.1	0.8	0.8	1.12	1.07	1.03	1.07
F^-	0.5	0.4	0.4	0.56	0.54	0.51	0.53
BaO	--	--	--	--	--	--	--
MgO	--	--	--	--	--	--	--
Approximate Softening Temp. (°C)	700	775	750	700	700	700	700
Approximate Melting Temp. (°C)	800	825	800	750	750	750	750
% SO_3 Lost (100 min at temp. indicated)	0.7 (900)	--	--	--	--	6.0 (810)	6.2 (800)
Ratio: $\frac{\text{Chem. eqs } (Na^+ + Li^+ + M^{2+})^c}{\text{Chem. eqs } (SO_4^{2-} + PO_3^- + BO_2^- + SiO_3^{2-})}$	1.2	1.09	1.17	1.13	1.02	0.92	1.25
Description	Shiny brown rock. Insoluble, non-corrosive.	Corrosive	Corrosive	Shiny, green, soluble.	Hard gray rock, some voids. Soluble.	Very hard, dense black rock. Insoluble.	Very hard dense, gray-green rock, surface segregation. Insoluble.

[a] See Table 6 for composition.

[b] Use of H_3PO_3 for H_3PO_4 should result in little if any difference in the final product so long as there is excess NO_3^- present. Use of H_3P

[c] Where M^{2+} represents the sum of Ca^{2+}, Ba^{2+}, Mg^{2+}, and Pb^{2+}.

th FTW-65 Waste (Concentrated x 3)[a]

8	9	10	11	12	13	14	15	16	17	18
.175	1.0	1.0	1.0	1.0	1.0	1.0	1.0	1.0	1.0	1.0
.25	1.14	1.14	1.14	1.14	1.14	1.14	1.14	1.14	1.14	1.14
.153	0.5	0.5	0.5	0.5	0.5	0.5	0.5	0.5	0.5	0.5
--	--	--	--	--	--	--	--	--	--	--
.144	--	0.1	0.2	0.4	--	--	--	--	--	--
.123	--	--	--	--	--	--	--	--	--	--
.13	--	--	--	--	--	--	--	--	--	--
--	--	--	--	--	--	--	--	0.1	0.2	0.4
--	--	--	--	--	0.1	0.2	0.4	--	--	--
.9	57.0	55.8	54.7	52.5	53.9	51.0	46.2	56.1	55.3	53.7
.17	12.7	12.2	11.8	11.0	12.2	11.8	11.0	12.2	11.8	11.0
.92	--	3.8	7.2	13.5	--	--	--	--	--	--
.36	17.6	16.9	16.3	15.2	16.9	16.3	15.2	16.9	16.3	15.2
.33	22.2	21.4	20.6	19.2	21.4	20.6	19.2	21.4	20.6	19.2
.12	5.9	5.6	5.4	5.1	5.6	5.4	5.1	5.6	5.4	5.1
.02	1.2	1.1	1.1	1.0	1.1	1.1	1.0	1.1	1.1	1.0
.02	1.2	1.1	1.1	1.0	1.1	1.1	1.0	1.1	1.1	1.0
.20	0.2	0.2	0.2	0.2	0.2	0.2	0.2	0.2	0.2	0.2
.44	--	--	--	--	--	--	--	--	--	--
.36	17.6	16.9	16.3	15.2	16.9	16.3	15.2	16.9	16.3	15.2
.31	19.8	19.1	18.4	17.1	19.1	18.4	17.1	19.1	18.4	17.1
.20	--	--	--	--	--	--	--	--	--	--
.02	1.2	1.1	1.1	1.0	1.1	1.1	1.0	1.1	1.1	1.0
.51	0.6	0.6	0.5	0.5	0.6	0.5	0.5	0.6	0.5	0.5
--	--	--	--	--	3.8	7.2	13.5	--	--	--
--	--	--	--	--	--	--	--	3.8	7.2	13.5
<700	750	750	750	800	750	750	800	800	850	900
<700	850	850	800	900	800	800	900	900	900	950
1 (850)	4.9 (900)	5.5 (900)	4.8 (900)	5.3 (900)	7.5 (900)	6.4 (900)	9.7 (900)	4.6 (900)	5.6 (900)	5.1 (1000)
.13	1.03	1.13	1.24	1.44	1.13	1.24	1.44	1.13	1.24	1.44
ny, gray-en rock, face regation. oluble.	Dark brown, voids.	Dark brown, voids.	Brown, glassy voids.	Brown, glassy voids.	Brown, voids.	Brown, voids.	Brown, voids.	Dark brown, dense.	Dark brown, voids.	Dark brown, voids.

eliminates bumping during evaporation.

after experiments revealed that replacement of sodium by potassium or lithium usually resulted in products with lower melting temperatures. Potassium was eliminated from further consideration primarily because it yielded products more soluble than did either lithium or sodium. The addition of relatively large amounts of aluminum increased sulfate retention above the softening temperature and decreased the corrosivity of the melt. The addition of both lithium and aluminum* resulted in a low-melting product with a softening temperature of about 750°C which lost only 5% of its sulfate after 3 hr at 900°C and only slightly over one-third of the sulfate after 100 min at 1100°C (No. 1, Table 8). The melt was for all practical purposes completely noncorrosive in semicontinuous operations, and the leach rate was about the same as that of the corresponding Purex 1WW product tested (Fig. 10).

In establishing the range of waste oxide concentrations that may be used with this combination of additives, it was found that the final product from FTW-65 waste was changed very little by increasing the fixation additives by as much as a factor of 4 (Table 9). A single set of additives that would yield a Purex 1WW product similar to the Purex FTW-65 product and that would at the same time be applicable to the FTW-65 itself is desirable. Using both sodium and lithium as additives, products with sulfate loss in the range of 5 to 7%, no apparent solubility, and good appearance were made (FTW No. 3, 1WW-3, Table 9).** The 1WW product contained 32% waste oxides, and the FTW-65 product contained 26% waste oxides.

Non-Sulfate Purex Waste.-- Relatively little difficulty was experienced in incorporating Purex waste of the non-sulfate type into a phosphate glass. This ease may be due to the fact that the major constituents of the waste - sodium, aluminum, and iron - are all easily contained in a true glass. With only phosphoric acid and lead nitrate as additives, two true glasses were made*** (Nos. 4 and 7, Table 10). One of these (No. 4) had

---

*Additives, g-moles/liter waste: Al^{3+}- 0.5, Li^{+}- 1.14, Ca^{2+}- 0.2, PO_4^{3-}- 1.0.

**Additives: 1.0 M Al^{3+}, 2.53 M Li^{+}, 1.4 M Na^{+}, 0.16 M Fe^{3+}, and 2.27 M PO_4^{3-}.

***Additives: 0.3 M Pb^{2+} and 1.5 M PO_4^{3-}, 0.2 M Pb^{2+} and 1.5 M PO_4^{-3}, respectively.

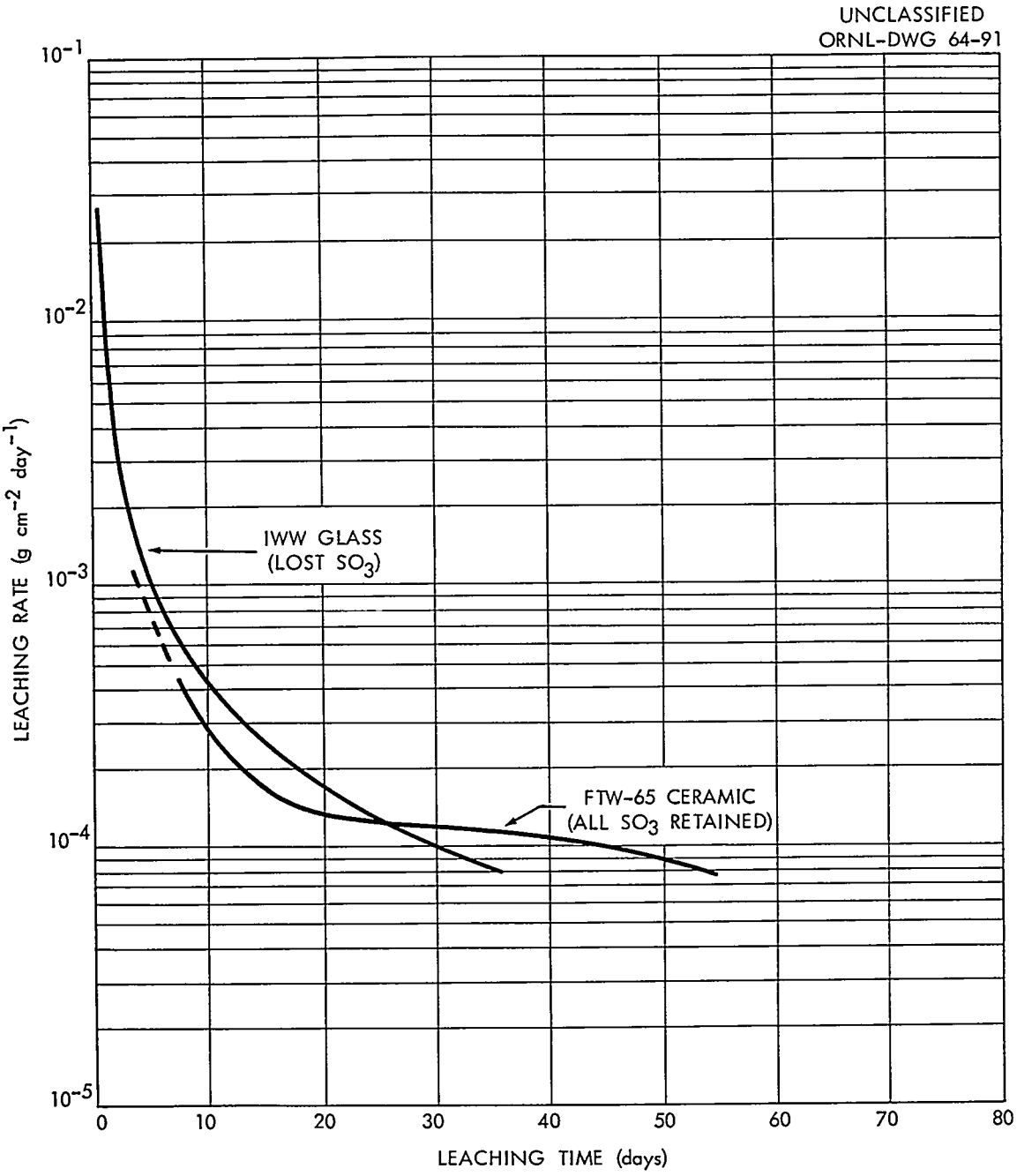

Fig. 10. Leaching Rates of lWW and FTW-65 Purex Solid Fixation Products.

Table 9. Products from Candi
for Sulfate-Bea

Additives g moles/liter waste	Additive Composition No. 1	FTW-1[b]	FTW-1/2	FTW-1/3	FTW-1/4
H_3PO_3 or H_3PO_4	4.08	1.02	2.04	3.06	4.08
$Al(NO_3)_3$	2.0	0.5	1.0	1.5	2.0
LiOH	4.6	1.14	2.3	3.4	4.6
$Ca(NO_3)_2$	0.8	0.2	0.4	0.6	0.8
NaOH	---	---	---	---	---
$Fe(NO_3)_2$	---	---	---	---	---
Waste Type	Blank- no waste	FTW-65(X3)	FTW-65(X3)	FTW-65(X3)	FTW-65(X3)
Wt % Waste Oxides, Theo.	0	44.5	29.8	22.0	17.5
Composition, mole % Oxides, Theo.					
Al_2O_3	16.29	11.8	13.33	14.17	14.56
CaO	13.03	7.2	9.27	10.30	10.83
Na_2O	---	16.3	10.43	7.73	6.09
Li_2O	37.46	20.6	26.66	29.19	31.15
Fe_2O_3	---	5.4	3.48	2.58	2.03
Cr_2O_3	---	1.1	0.7	0.52	0.41
NiO	---	1.1	0.7	0.52	0.41
RuO_2	---	0.2	0.14	0.10	0.08
SO_3	---	16.3	10.43	7.73	6.09
P_2O_5	33.22	18.4	23.82	26.40	27.73
SiO_2	---	1.1	0.7	0.52	0.41
F^-	---	0.5	0.35	0.26	0.20
Approx. Incipient Melt Temp (°C)	1000	700	750	800	800
Approx. Melt Temp (°C)	---	750	900	900	900
Approx. Pouring Temp (°C)	<1100	800	1000	1000	1000
Ratio: $\frac{\text{Chem Eq } (Na^+ + Li^+ + Ca^{2+})}{\text{Chem Eq } (SO_4^{2-} + PO_3^- + SiO_3^{2-} + F^-)}$	---	1.22	1.33	1.36	1.17
Percent SO_3 Loss	---	0.7	3.4	5.3	5.1
Description	White, Insoluble. Too viscous to pour at 1100°C.	Brown rock. Insoluble.	Brown rock. Insoluble.	Brown rock. Insoluble.	Brown rock. Insoluble.

[a] See Table 6 for waste compositions.

[b] Same as Melt 1, Table 8.

e "Universal" Additive Composition
g Purex Wastes[a]

WW -1	1WW -1/2	1WW -1/3	1WW -1/4	Additive Composition No. 2	FTW-#2	1WW #2	Additive Composition No. 3	FTW-#3	1WW -#3
1.02	2.04	3.06	4.08	2.27	2.27	2.27	2.27	2.27	2.27
0.5	1.0	1.5	2.0	1.0	1.0	1.0	1.0	1.0	1.0
1.14	2.3	3.4	4.6	2.53	2.53	2.53	2.53	2.53	2.53
0.2	0.4	0.6	0.8	---	---	---	---	---	---
---	---	---	---	1.4	1.4	1.4	1.4	1.4	1.4
	---	---	---	---	---	---	0.16	0.16	0.16
1WW	1WW	1WW	1WW	None	FTW-65(X3)	1WW	None	FTW-65(X3)	1WW
53.5	36.5	27.7	22.3	0	26.6	32.9	0	25.8	32.2
9.55	11.75	12.92	13.54	13.89	11.87	10.55	13.59	11.68	10.39
6.37	8.54	9.60	10.32	---	---	---	---	---	---
9.55	6.41	4.84	3.87	19.44	23.74	19.19	19.02	23.36	18.90
18.14	24.56	27.45	29.67	35.14	26.12	24.27	34.38	25.69	23.90
7.96	5.34	4.04	3.22	---	3.10	4.80	2.17	4.67	6.24
0.16	0.11	0.08	0.06	---	0.62	0.10	---	0.61	0.09
0.16	0.11	0.08	0.06	---	0.62	0.10	---	0.61	0.09
0.06	0.04	0.03	0.03	---	0.12	0.04	---	0.12	0.04
31.83	21.35	16.15	12.90	---	9.29	19.19	---	9.14	18.90
16.23	21.78	24.71	26.32	31.53	23.59	21.78	30.84	23.21	21.45
---	---	---	---	---	0.62	---	---	0.61	---
---	---	---	---	---	0.31	---	---	0.30	---
800	825	900	>1000		825	725		825	750
850	900	950	>>1000		900	800		900	800
.71	.92	1.03	1.12	---	1.49	1.06	---	1.49	1.06
33.5	22.9	43.1	40.0		---	2.2		5.2	6.2
Hard, black rock. Voids.	Hard gray-green rock; few voids.	Hard, gray-green rock, voids.	Hard, black, unmelted.		Brown, hard micro-crystalline. Many voids. Soluble.	Hard, dense, brown, micro-crystalline. Insoluble.		Brown, hard, micro-crystalline. Few voids. Insoluble.	Very hard, brown, micro-crystalline. Insoluble.

Table 10. Solid Products from the Fixation of Simulated Non-Sulfate Purex Waste

Additives g moles/liter waste	1	2	3	4	5	6	7	8	9	10	11	12	13	14
H_3PO_4	0.75	1.0	1.25	1.5	1.0	1.5	1.5	1.5	1.5	1.5	1.0	1.25	1.5	1.5
$Pb(NO_3)_2$	0.2	0.2	0.3	0.3	---	---	0.2	0.3	0.3	---	---	---	0.4	0.5
$Al(NO_3)_3$	---	---	---	---	---	---	---	0.1	0.2	0.3	0.3	0.2	---	---
Wt % Waste Oxides Theo.	26.5	23.4	18.5	16.9	33.3	24.9	19	16.5	16.2	22.5	29.1	26.3	15.3	14
Mole % Theoretical Oxides														
Al_2O_3	9.8	8.7	7.3	6.7	10.6	8.4	7.2	12.5	17.7	26.8	32.2	23.6	6.3	5.9
Cr_2O_3	0.3	0.3	0.2	0.2	0.3	0.3	0.2	0.2	0.2	0.2	0.2	0.2	0.2	0.2
Fe_2O_3	2.5	2.2	1.8	1.7	2.6	2.1	1.8	1.6	1.5	1.7	2.0	2.1	1.6	1.5
Na_2O	29.4	26.2	21.9	20.1	31.8	25.1	21.5	18.8	17.7	20.1	24.1	23.6	18.8	17.7
NiO	0.6	0.5	0.4	0.4	0.6	0.5	0.4	0.4	0.4	0.4	0.5	0.5	0.4	0.4
P_2O_5	37.8	44.6	46.4	50.9	54.0	63.7	54.5	47.7	44.9	50.9	41.0	50.0	47.7	44.9
PbO	19.6	17.5	21.9	20.1	---	---	14.3	18.8	17.7	---	---	---	25.1	29.5
Approximate Softening Temp (°C)	700	750	700	<650	800	<500	500	750	800	900	775	900	600	600
Approximate Melting Temp (°C)	800	850	750 (viscous)	<650	850 (viscous)	500	600	850 (viscous)	900 (viscous)	950 (viscous)	875 (viscous)	---	700 (viscous)	700 (viscous)
Description	Dark green, very hard. Near glass. Insoluble.	Pale green rock, crumbly. Soluble.	Pale green rock Soluble.	Clear green glass. Insoluble.	Two phase; some green glass, some rock. Insoluble.	Two phase; green glass and rock. Insoluble.	Green glass. Insoluble.	Green rock.	Green rock, voids.	Very hard, dense, some segregation.	Coarse green rock. Voids.	Coarse green rock. Voids.	Fine-grained green rock.	Fine-grained green rock.

very low corrosivity, contained 19% waste oxides, and melted below 650°C. Attempts to raise the melting point of this glass by addition of aluminum and at the same time retain the glassy nature did not succeed (Table 10).

2.2.3 Calcination of Non-Sulfate and Sulfate-Deficient Purex Wastes

Attempted calcination of wastes consisting of sodium nitrate with only minor amounts of other constituents resulted in the volatilization of gross amounts of solid material. Catastrophic corrosion of stainless steel and volatilization of cesium have been reported when calcination of alkaline wastes (i.e., $NaNO_3$ + NaOH) was attempted.[1] The addition of sulfuric or phosphoric acid in amounts equivalent to the excess sodium is an obvious remedy but has the disadvantage of producing calcines of relatively high leachability. There is also a possibility of obtaining partial melting, which is undesirable in a calcination process. Furthermore, addition of slightly more than an equivalent amount of acid may result in volatilization of sulfate if any is present and/or the onset of acid corrosion of the container.

The addition of an amphoteric oxide such as alumina should not only prevent the volatilization of any alkali (e.g., Na^+, Cs^+) but should make possible a relatively noncorrosive calcination process regardless of any excess of alumina employed. Furthermore, the product obtained on calcination should be relatively insoluble, compared with either sodium sulfate or sodium phosphate, and would doubtless become more insoluble the larger the relative amount of aluminum added.

To confirm this prediction, a solution consisting primarily of $NaNO_3$ and Na_2SO_4* in the mole ratio of 5:1 was evaporated to dryness, and the resulting solid residue was calcined to 900°C in a quartz cup that was in turn contained in a quartz tube fitted with an off-gas line, a condenser, and a solids trap (Fig. 11). The equipment was then disassembled, the off-gas line and condenser washed out, and the washings analyzed for Na^+ and SO_4^{2-}. This procedure was repeated with solutions to which aluminum nitrate had been added to give mole ratios of 1:3, 2:3, and 1 for $Al/NaNO_3$. The presence of sufficient aluminum to fulfill the 1:3 mole

*See composition of "Future Acid Waste," Table 6.

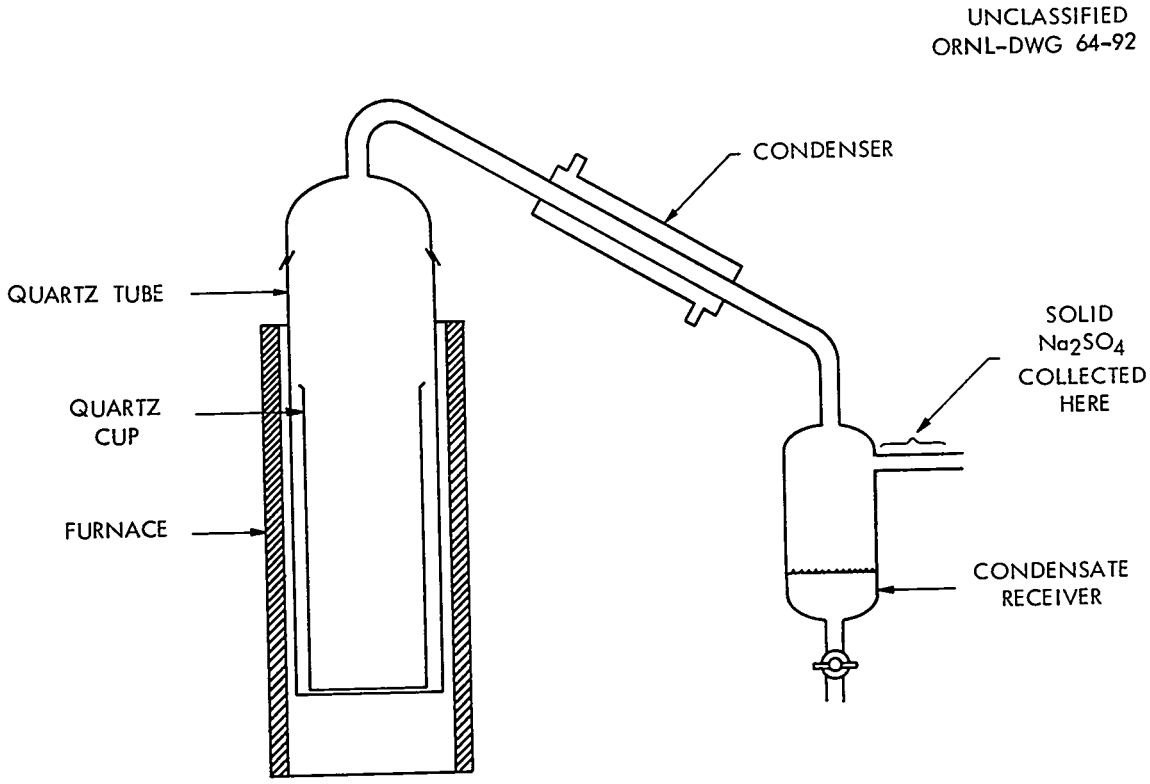

Fig. 11. Apparatus for Studying Volatility from Sulfate-Deficient Purex Waste During Fixation.

ratio prevented the gross volatilization of solids but still permitted volatilization of fairly large amounts of both sodium and sulfate (Table 11). Increasing this ratio to 2:3 or to 1 practically eliminated the volatility of both sodium and sulfate; the amounts found in the condensate were between 0.001 and 0.02 M, which are in the range of probable entrainment.

The attempted calcination of the waste without additives resulted in melting. The addition of aluminum resulted in the formation of calcines, none of which melted at 900°C. Though the production of a glass was not an objective of this particular set of experiments, the addition of aluminum is compatible with phosphate glasses should glass formation appear attractive at a later date.

2.2.4 Semiengineering-Scale Fixation Studies (FTW-65 Waste)

Five semiengineering-scale fixation experiments were run, all using lithium as an additive. The experiments were run in a stainless steel pot (4 in. in diameter and 24 in. high) with the rising-level type operation. The first one employed a mixture (No. 6, Table 8) that gave a product of superior appearance and physical properties but which lost sulfate under fixation conditions and was consequently very corrosive. The last four employed the best mix developed to date (No. 1, Table 8), which proved to be practically noncorrosive under the conditions usually employed in pot fixation (Fig. 12). However, when the melt was agitated by sparging with nitrogen gas, pot failure eventually occurred even with this melt (Table 12). It appears probable that the excessive corrosion caused by sparging was due to the inclusion of small amounts of water in the turbulent melt. This would presumably produce magnetite on the pot walls, which would then be removed by erosion and/or reaction with the flowing melt. The pot wall next to the point of failure was quite clean on the inside and was nonmagnetic, in sharp contrast to the pot corrosion that was observed previously.

Operation with the production of the "noncorrosive" melt was smooth except for problems resulting from the presence of gross amounts of solids deposited in the off-gas line in the form of fine dust. This deposition was apparently more or less continuous and and was not associated with

Table 11. Suppression of the Volatility of Sodium and Sulfate During Calcination of Sulfate-Deficient Purex Waste[a] by Aluminum Addition

	Experiment No.			
	1	2	3	4
$Al(NO_3)_3$ added g-moles/liter waste	0	0.27	0.54	0.80
Mole ratios: $Al/NaNO_3$[b]	0	0.34	0.675	1.0
Al/total Na	0	0.225	0.45	0.566
Volatility and entrainment (% of total)				
Na^+				
In off-gas line and condenser	0.25	0.13	0.005	Negligible
In condensate receiver	0.15	0.12	0.004	0.018
Total	0.45	0.25	0.009	0.018
SO_4^{2-}				
In off-gas line and condenser	0.29	0.12	< 0.003	Negligible
In condensate receiver	0.17	0.10	0.004	0.014
Total	0.46	0.22	< 0.007	0.014
Observations (See Fig. 4.)	Gross displacement of solids took place from inner cup to cooler parts of ignition tube; some white solid in exit tube from condenser receiver	No gross displacement of solids; some white in off-gas system	No gross displacement of solids; solids just visible in off-gas system	No solids visible in off-gas system

[a] Future acid purex waste. Composition (g-moles/liter): H^+, 0.5; Na^+, 1.2; Fe^{3+}, 0.1; SO_4^{2-}, 0.2; NO_3^-, ~ 1.6 (to balance).

[b] More precisely Al/(total Na - 2 x SO_4^{2-}).

UNCLASSIFIED
ORNL-PHOTO 62044

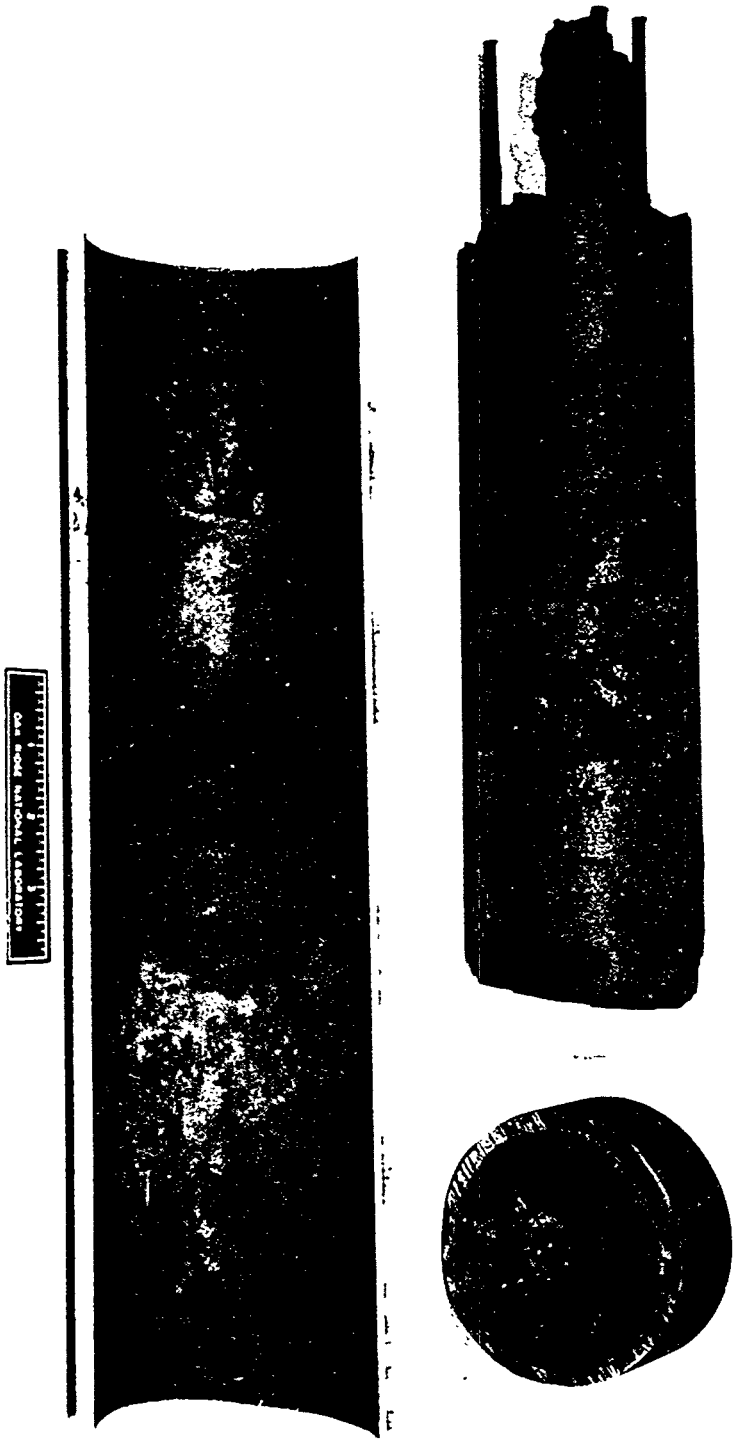

Fig. 12. Lithium-Aluminum Phosphate Ceramic from Fixation of Simulated FTW-65 Waste.

Table 12. Summary of Semiengineering-Scale Waste-Fixation Experiments: FTW-65-Lithium Ceramics FTW-65 Waste Concentrated x3 Was Used in All Cases

Additives	Experiment Designations and Amounts of Additives (g moles/liter waste)				
	5-13-63[a]	6-4-63[b]	6-19-63[b]	7-11-63[b]	8-22-63[b,d]
H_3PO_3	1.175	1.0	---	1.0[c]	---
H_3PO_4	---	---	1.0	---	1.0
LiOH	1.25	1.14	1.14	1.14	1.14
$Al(NO_3)_3$	0.153	0.5	0.5	0.5	0.5
$Ca(NO_3)_2$	0.144	0.2	0.2	0.2	0.2
$Na_2B_4O_7$	0.25	---	---	---	---
Ratio: $\frac{\text{Chem Eqs } (Na^+ + Li^+ + Ca^{2+})}{\text{Chem Eqs } (SO_4^{2-} + PO_3^- + SiO_3^{2-} + F^- + BO_2^-)}$	0.86	1.2	1.2	1.2	1.2
Wt % Waste Oxides, Theo.	42.4	44.5	44.5	44.5	44.5
Volatility & Entrainment (% of total present)					
SO_4^{2-}	40.3	6.1	1.1	0.5	22.5
Ru	26.6	20.7	37.1	29.7	22.3
Fe	5.76	6.4	14.9	6.8	3.1
PO_4^{3-}	0.23	0.4	0.4	0.4	0.18
Average Feed Rate (ml/min)	35.5	36.9	41.8	38.0	38.4
Apparent Volume Reduction (Vol unconc'd waste/vol solid)	---	~36	~36	~36	~36
Corrosion	Excessive	Neg.	Neg.	Neg.	Excessive

[a] No. 6, Table 8.

[b] No. 1, Table 8

[c] 0.1 M H_3PO_3 was added just before startup to compare Ru volatility with that from an aged solution.

[d] Operated with a sparge of N_2 at the bottom of the fixation pot.

pressure surges. Only relatively small pressure surges occurred. As might be expected, ruthenium volatility was higher than was normally observed in the absence of dusting; the highest percentage reported was 37.1% (Table 12). The most peculiar part of the phenomenon was the relatively large amount of iron in the condensate. The percentage of iron volatilized or entrained varied from about 3 to 15% of that present, while the corresponding percentage of phosphate was only 0.4%. This implies the possible formation of a volatile iron compound that decomposes to form an aerosol.

Thermocouples used in the determination of the levels of solution, calcine, and melt represent a large potential expenditure for each fixation pot since the thermocouples will not be recoverable from a radioactively "hot" fixation run. Consequently, experiments were run to further test the performance of the electrical resistance probe used for determining levels of solution, calcine, and melt.[2] Representative changes in resistance observed during fixation experiments are indicated in Table 13. Resistance increases to a maximum as calcine is formed and is dried. Melting of the calcine causes a sudden drop in resistance. Practical use of the method would probably require a background of experience, as has been found to be true even with thermocouple probes.

2.2.5 Mercury Removal

A stainless-steel column packed with commercial (unsized) copper shot and gently agitated by a small electrical buzzer removed 99.4% of the mercury from 510 bed volumes of FTW-65 waste solution. Residence time in the column was 26.5 min. The effluent contained 3.77 mg of copper per ml (about 0.06 M). No ruthenium was removed by the copper.

An unagitated glass column packed with aluminum turnings of miscellaneous shapes and sizes removed 99% of the mercury from 162 bed volumes of FTW-65 waste concentrated by a factor of 3 (Table 6). Residence time of solution in the bed was 21 min. There was a gradual mercury breakthrough with increasing operating time. After passage of 300 bed volumes only 90% of the mercury was still being removed. About 30 to 35% of the ruthenium was also removed by the aluminum column concurrently with mercury removal. Effluent from the aluminum column contained approximately 0.09 M more aluminum than the feed to the column.

Table 13. Representative Readings of an Electrical Resistance Probe in Various Phases of a Waste-Fixation Cycle

Condition	Approximate Resistance (ohms)
Empty	
Tap water (room temperature)	37,000
TBP-25 glass mix solution	
1. Room temperature	4,000
2. Boiling	2,400
3. Wet calcine (hot)	4,800
4. Dry calcine (hot)	20,000
5. Dry calcine (cold)	∞
6. Softening and melting calcine ("glass")	
a. at 820°C	5,000
b. at 940°C	200
c. at 1020°C	16

Neither aluminum nor copper was effective in removing mercury from Purex 1WW waste. Both metals were attacked rapidly by the relatively concentrated (5.6 M) nitric acid in the waste, and the resulting gas rendered the columns practically inoperable. Such a waste would require dilution to about the FTW-65 acidity prior to mercury removal.

Amalgam was drained periodically from the bottom of both the copper and aluminum columns. This indicates the possibility of operating a mercury removal column continuously with addition of the active metal (copper and aluminum) at the top and withdrawal of mercury or liquid amalgam at the bottom (Fig. 13).

2.3 Corrosion Studies

W. E. Clark

(Work performed by members of the Reactor Chemistry Division)

Welded specimens of type 304L stainless steel, titanium 45A, and Hastelloy F were exposed in and above refluxing FTW-65 waste solutions for periods of 504 to 1008 hr. Couples of 304L stainless and titanium 45A were also exposed to determine whether or not there would be galvanic corrosion between the proposed titanium condenser and the stainless steel pot head.

Maximum corrosion rates were ≤ 0.3 mil/month in all cases, including those in which the refluxing solution contained fluxing additives (e.g., H_3PO_4, $Al(NO_3)_3$, and LiOH; Table 14). These results indicate that corrosion of the overhead system should present no real problem provided that the waste composition approximates that tested. The possible effect of ruthenium as a corrosion accelerator should, however, be tested.

Specimens of mild steel (ASTM A-108) were exposed in vapor, interface solution and melt from the "noncorrosive" FTW-65 lithium mix (No. 1, Table 8). As expected, corrosion rates were catastrophic, particularly on the interface specimen which was completely severed after 2 hr of exposure. Weight losses of specimens exposed in the solution for 7 hr varied from about 50% to about 15% of the total for the solution-phase specimens, depending upon whether phosphite or phosphate was present. Weight lost by the vapor-phase specimen was about 12%. The specimen exposed in the melt was held in contact with the melt at 900°C for 4 hr, after which the furnace power was cut

UNCLASSIFIED
ORNL-DWG 64-93

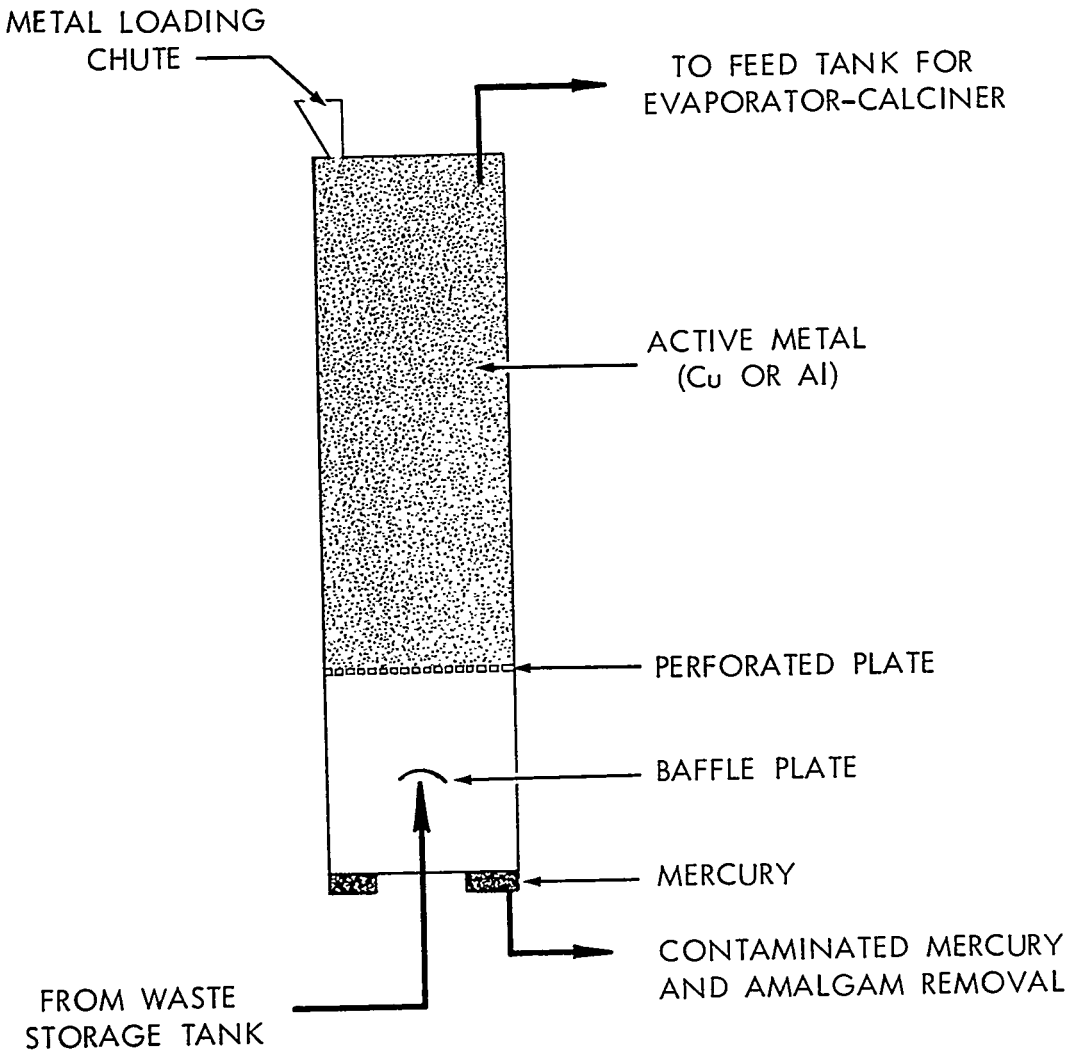

Fig. 13. Schematic Diagram of Proposed Column for Continuous Removal of Mercury from Acid Waste Solutions.

Table 14. Summary of Corrosion Tests in FTW-65 Waste Environments

Test Conditions	Exposure Time (hr)	Maximum Corrosion Rate (mils/month except as indicated) in Vapor (V), Interface (I), or Solution (S)					
				Coupled			
		304L	Ti-45A	304L	Ti-45A	Hastelloy F	Ti-0.2% Pd
Evaporator Tests							
FTW-65 ("Initial") solution; reflux	1300-1600	a	a	0.3(V)	a	a	---
FTW-65 conc'd X3 ("Final") sol'n; reflux	1008	≦ 0.1	a	≦ 0.1	a	≦ 0.1	---
FTW-65 solution plus additives;[b] reflux	1008	0.19(s)	< 0.01	0.19(s)	< 0.01	0.09(V)	---
FTW-65 conc'd X3 plus additives;[c] reflux	504	0.3(V)	a	0.2(V)	a	0.02(V)	---
Calcination-Fixation Tests							
FTW-65, + 0.0135 M $Ca(NO_3)_2$; evaporate and calcine to 1050°C	168	10 mils (total penet.)	Failed	---	---	---	Failed
FTW-65 conc'd X3 plus additives;[d] evaporate, calcine, melt and heat to 1050°C	29 (at 1050°C)	3.7(V) 283 (melt) 15.4 mils total penet.	---	---	---	---	---

[a] Indicates a slight weight gain.

[b] g-moles/liter waste sol'n; H_3PO_4 - 1.0, $Al(NO_3)_3$ - 0.5, LiOH - 1.4.

[c] g-moles/liter waste sol'n; H_3PO_4 - 4.0, $Al(NO_3)_3$ - 2.0, LiOH - 5.6.

[d] g-moles/liter waste sol'n; H_3PO_4 - 1.33, NaOH - 1.52, $Ca(OH)_2$ - 0.27, $Al(NO_3)_3$ - 0.67. This mix was developed before the lower melting and less corrosive lithium formulations.

off and the experiment was left in the furnace while it slowly cooled overnight. The weight lost by this specimen was about 4%.

Specimens of type 304L stainless steel, titanium-45A, and titanium-0.2% palladium were exposed to a calcination test in FTW-65 waste solution that contained $Ca(OH)_2$ as an additive. The specimens were held in contact with the solid calcine at 1050°C for 168 hr (1 week). The stainless steel specimen suffered fairly uniform exfoliation, which amounted to a loss of about 10 mils of metal. Both the titanium and the titanium-0.2% palladium were almost completely converted to nonmetallic substances. This was also true of specimens of the titanium alloys in FTW-65 waste calcined without additives. These tests confirm the prediction that titanium is a completely unsatisfactory material for construction of the calciner pot and confirm the suitability of type 304L stainless steel.

A specimen of type 304L stainless steel was exposed in a non-sulfate Purex waste plus additives (No. 4, Table 10) in an evaporation-fixation cycle during which it was held at 950°C in contact with the melt in air for 24 hr. There was no indication of localized attack, though the specimen had lost about a third of its weight. Note that the exposure temperature was at least 300°C above the melting temperature of the glass.

Exposure of type 304L stainless steel in salt (NaCl) of varying degrees of purity at 300°C indicate that a corrosion rate of about 0.04 mil/month can be expected during salt mine storage under these conditions (Table 15). Some incipient pitting was observed, but it apparently did not continue on longer exposure. A second set of exposures at 200, 300, and 500°C under somewhat different conditions* (Table 16) indicated higher rates ($\leq$ 0.8 mil/month) and a greater tendency toward a random pitting attack. Both the corrosion rate and the tendency toward pitting tended to decrease with increased temperature, indicating the probability that moisture in the salt was largely responsible for the attack. During salt-mine storage, the corrosion rate should, therefore, be almost negligible after the salt next to a stored pot has become dehydrated.

---

*These tests were performed for the Health Physics Division under the supervision of J. L. English of the Reactor Chemistry Division.

Table 15. Corrosion of Welded Type 304L Stainless Steel in Simulated Salt Mine Storage at 300°C

Successive 30-day exposures in fresh salt; pits starting in one cycle did not propagate in the next

	Corrosion Rate (mils/month)			
	30 day	60 day	90 day	150 day (3600 hr)
Reagent grade NaCl	< 0.01	< 0.01	< 0.01	All in range 0.01-0.03
98% NaCl -- 2% H_2O	wt gain[a]	< 0.01	< 0.01	All in range 0.01-0.03
95% NaCl -- 5% $CaSO_4$	< 0.01	< 0.01	< 0.01	All in range 0.01-0.03
92.75% NaCl -- 2% H_2O - 5% $CaSO_4$ -- 0.25% $MgCl_2$	0.03	0.04[b]	0.04[b]	All in range 0.01-0.03
99.75% NaCl -- 0.25% $MgCl_2$	0.01	0.03	0.03	All in range 0.01-0.03

[a] Weight gain approximately 0.1 mg/cm^2.

[b] Or 0.48 mil/hr.

Table 16. Corrosion of Variou
Mine Storag

Exposure time = 720 hr except as indicated. All
Numbers in parentheses indicate maxim

	Type 304L Stainless Steel			Type 310 Stainless Steel		
	200°C	300°C	500°C	200	300	5
Natural NaCl	0.6 (1.2)	0.4	0.5	0.4	0.2 (1.6)	0.1
Reagent Grade NaCl	0.1	0.2	0.3	<0.1	0.1	0.5
99.5% NaCl-0.5% H_2O	0.2 (0.4)	0.5 (2.2)	0.6	0.2 (2.9)	0.3 (1.8)	0.4
99.75% NaCl-0.25% $MgCl_2$	0.7 (2.0)	0.8	0.5	0.6 (2.1)	0.4 (1.5)	0.4
95% NaCl-5% $CaSO_4$	0.1	0.6 (2.3)	0.4	<0.1 (1.5)	0.2 (2.2)	0.3
94.5% NaCl-0.5% H_2O-0.25% $MgCl_2$-5% $CaSO_4$	0.8	0.4	0.7	0.4 (1.8)	0.3	0.2

	Inconel		INOR-8		Monel	
	200	300	200	300	200	3
Natural NaCl	0.1 0.1	0.1	0.1	0.1	0.3	0
Reagent Grade NaCl	<0.1 0.1	<0.1	0	0.1	0.1	0
99.5% NaCl-0.5% H_2O	0.1 (3.2) 0.1	<0.1 (3.7)	0.1 (2.4)	0.1 (3.0)	1.0 (7.1)	0.
99.75% NaCl-0.25% $MgCl_2$	0.2 (5.6) 0.1 (2.1)	0.2	0.2 (4.9)	0.9	0.9	0
95% NaCl-5% $CaSO_4$	0.1 0.1 (1.9)	0.1	0	0.1 (3.2)	0.1 (3.5)	0
94.5% NaCl-0.5% H_2O-0.25% $MgCl_2$-5% $CaSO_4$	0.2 (2.8) 0.2 (2.6)	0.3 (2.5)	0.2 (3.7)	0.3 (2.3)	1.2 (2.7)	0.

Metals Under Conditions Simulating Salt
of Fixed Wastes

cimens were welded except as indicated. Rates in mils/yr
pitting attack observed (total penetration in mils)

	Hastelloy C			Haynes 25			Titanium 45A		Carbon Steel ASTM: A 108 Unwelded	
	200	300	500	200	300	500	200	300	200	300
.8)	0.1	0.1	0.1	<0.1	0.1	0.2	0.2	0	2.0 (1.6)	2.0 (1.8)
.8)	<0.1	<0.1	0.1	0.1	0.1	0.1	0.1	0	1.1 (1.4)	1.6 (2.6)
.6)	0.1	0.1	0.	0.4	0.1 (3.2)	0.1	0.1	0.1	1.3 (1.8)	1.5 (2.6)
.4)	0.1	0.1	0.5	0.2(2.7)	0.2	0.3	0.2	0.1	2.7 (etch)	3.5 (1.2)
.6)	0.1	0.1	<0.1	0	0.1(3.2)	0.1	0.2	0	1.0 (2.2)	1.9 (2.2)
	0.2 (2.7)	0.1	0.1	0.1	0.1(1.5)	0.1	0.1	0.1	3.3 (etch)	3.8 (2.2)

	Nickel		Ni-o-nel		Type 347 Stainless Steel		Unwelded Type 1100 Aluminum (200 Hr)	
	200	300	200	300	200	300	200	300
	0.3	0.3	0.1	0.1 (5.8)	0.7	0.4 (2.3)	gain	gain (5.6)
(5.8)	0.2	0.1	0.1 (3.9)	0.1 (2.3)	0.1 (3.8)	0.4 (8.0)	0.6 (2.4)	0.7 (3.3)
(3.0)	0.1	0.1	0.6	0.3 (3.0)	0.5	0.7 (5.8)	0.2 (2.1)	gain (3.3)
	0.3	0.6	0.9 (3.3)	0.3 (1.6)	0.7 (1.9)	1.0	gain	gain (3.6)
(3.2)	0.1	0.1	<0.1	0.1 (3.7)	0.1 (2.2)	0.7 (2.3)	0.4 (3.0)	0.2 (2.7)
(2.0)	0.4	0.3 (6.0)	0.5 (3.0)	0.5 (4.2)	0.6 (3.0)	0.8	8.9 (4.0)	gain (4.8)

2.4 Design Studies

E. J. Frederick J. M. Holmes

2.4.1 Hanford Pilot Plant

Cooperation on the design of the Hanford Waste Calcination Pilot plant was continued, including work on the design of the pot calciner and its associated off-gas equipment and furnace.

Since an induction furnace will be used for the pot-calcination demonstration in the pilot plant, it was necessary to determine an optimum thickness of insulation between the furnace coils and the susceptor. The latter will be heated to 900 to 1000°C. An optimal insulation thickness would permit rapid cooling of the pot upon completion of calcination, yet maintain heat losses during the calcination period at a reasonable level. If no insulation were used, the heat losses to the coil would be about equal to the maximum power input, so it is doubtful if a 900°C pot wall temperature could be achieved. Air cooling of the furnace will be required as a supplement to the water coils in order to provide for emergencies such as loss of cooling water or localized cooling loads in excess of those predicted.

Transient-state cooling-rate calculations for pots filled with solids initially at 900°C were performed at Hanford, using average heat transfer coefficients between the pot and the cooling media as determined by steady-state calculations. Table 17 shows the results of these calculations as the maximum temperature of the centerline of an 8-in.-diam pot with an internal heat generation rate of 5000 Btu hr^{-1} ft^{-3} and a solids thermal conductivity of 0.2 Btu hr^{-1} ft^{-1} $°F^{-1}$. The effect of insulation thickness, the addition of a susceptor, and the use of cooling air on the maximum temperature were studied. An insulation thickness of 0.75 in. of Fiberfrax was recommended, based on these calculations. The normal heat loss through this thickness of Fiberfrax during calcination would be about 10.3 kw for the entire pot, which is not excessive.

Similar calculations for pots containing glassy solids with a thermal conductivity of at least 1.0 Btu hr^{-1} ft^{-1} $°F^{-1}$ indicated that cooling following melt formation would be easier to control. The maximum center-line

Table 17. Maximum Center-line Temperatures for Cooling of Eight-Inch Diameter Pots in an Induction Furnace

Conditions	Average Heat Transfer Coefficient Outside of Pot+	Maximum Pot Center-line Temp. For Calcine**- ^{o}F	Maximum Pot Center-line Temp. For Glassy Solids***- ^{o}F
1.5-in. insulation* and susceptor	0.83	1922	1697
0.75-in. insulation* and susceptor	1.49	1853	1685
0.75-in. insulation*; no susceptor	1.70	1844	1684
1.5-in. insulation* and susceptor + 155 cfm cooling air	2.13	1831	1682
0.75-in. insulation and susceptor + 155 cfm cooling air	2.44	1825	1682
1.5-in. insulation; no susceptor	0.87	1918	1698

*"Fiberfrax" insulation, product of the Carborundum Company.

+ Btu hr^{-1} $^{o}F^{-1}$ per square foot of area on pot calciner wall.

** Q = 5000 Btu hr^{-1} ft^{-3}, K = 0.2 Btu hr^{-1} ft^{-1} $^{o}F^{-1}$.

*** Q = 5000 Btu hr^{-1} ft^{-3}, K = Bru hr^{-1} ft^{-1} $^{o}F^{-1}$.

temperatures would be at least 143°F less than those for calcined solids (See Table 17.). The heat of crystallization of the glassy solids is taken into account in these calculations by including an allowance in the specific-heat term for the heat of crystallization.

2.4.2 Continuous Melter

The program for the fixation of high-activity-level wastes in glassy solids includes the development of a vessel for the continuous evaporation, calcination, and melting of aqueous wastes containing the glass-making additives. An horizontal agitated melter (8 in. in diameter and 36 in. long) is being built for testing on simulated Purex and TBP-25 wastes (See Fig. 14). The agitator was added to improve heat transfer to the evaporating wastes by preventing the build-up of cake on the walls above the liquid level.

Features of the vessel include the following:

1. Feed nozzles - four water-jacketed nozzles positioned on top of the vessel and evenly spaced between the vapor line and outlet baffle.
2. Agitator - slotted, low-speed agitator (1 to 10 rpm), with internal bearing and external packing gland.
3. Packing gland and bearing - internal bearing is made of high-temperature Graphalloy, externally cooled and protected from the furnace by Inconel-asbestos packing. The packing gland also utilizes this type of packing.
4. Vapor line and sight glass - vapor line is 2-in. pipe that includes a quartz sight glass for viewing the surface of the molten glass.
5. Outlet freeze valve - a baffled trap made in 2-in. pipe wound with a cooling coil is used as a freeze valve on the outlet molten-glass stream.

2.4.3 Sixteen-Inch-Diameter Pot Calciner

A 16-in.-diam pot calciner unit is being designed for installation in the test cells to study the effect of scale-up on process variables and process economics.

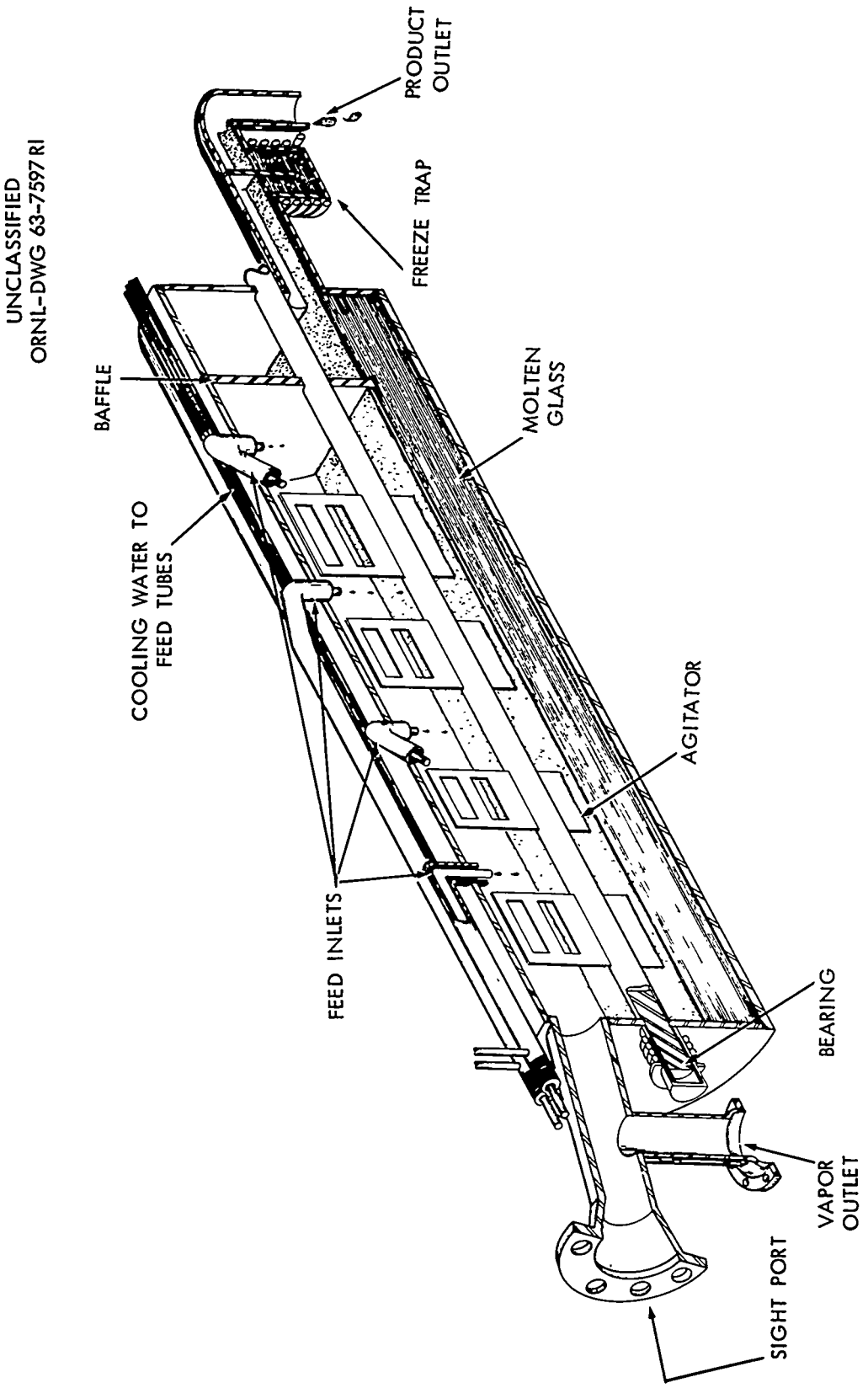

Fig. 14. Waste Fixation Vessel.

The unit will consist of a surge tank from which preconcentrated feed will be discharged through a bottom drawoff into a 5- to 10-gpm pump circulation loop and emptied back into the tank through a nozzle located in the tank head. A side stream from the loop will be fed into a 16-in.-diam stainless steel calcination pot upon demand from a liquid-level signal that actuates a control valve located in the feed line. Final evaporation and calcination of the waste to the oxides will be carried out by induction heating. The pot vapor will be condensed, sampled, and discharged to the cell-drain system. Noncondensable off-gas will be discharged to the laboratory off-gas system with no additional cleanup. A secondary off-gas line from the calciner pot connected to an intermediate liquid-seal pot, which requires 15 ft of water pressure to vent, is used as a safety valve in case of plugging in the primary off-gas line.

The induction furnace is being procured from Ajax Magnethermic Corporation, Warren, Ohio. The power supply will be a 150-kw, 3000-cycle, vertical-mounted motor-generator set. The furnace will have six 1-ft-long separate induction coils wired in parallel, with each coil controlled by an individual temperature controller. The guaranteed heat capacity of the furnace is 80 kw, supplied continuously to the pot wall at 1200°C. The maximum heat capacity of each coil is 50 kw.

3. LOW-LEVEL WASTE TREATMENT

Processes involving scavenging precipitation and ion exchange, and foam separation processes, are being developed in both laboratory and pilot-plant programs for decontaminating the large volumes of slightly contaminated water produced in nuclear installations. Oak Ridge National Laboratory low-activity waste is used for this study. The ion exchange process uses phenolic resins, as opposed to polystyrene resins, since the phenolic resins are much more selective for cesium in the presence of sodium at high pH; the cesium-sodium separation factor is 160 for phenolic groups and 1.5 for sulfonic groups. Other cations, for example, strontium and the rare earths, are also sorbed efficiently. Other ion exchangers, such as alumina, vermiculite, clinoptilolite, and organic anion resins are being studied as alternatives. The waste solution must be clarified prior to ion exchange because the resins do not remove colloids efficiently. Foam separation is being studied as an alternative to ion exchange after the clarification step and also as a method for both clarification and decontamination.

3.1 Waste Pilot-Plant Tests

L. J. King

Plant equipment and piping changes for demonstration of the fixed-bed and continuous contactor ion exchange processes proposed by I. R. Higgins[3,4] were completed, and an agitated clarifier was installed in the scavenging-precipitation portion of the plant.[5,6]

The pilot-plant program proposed for the next year includes (1) demonstration of the weak-acid strong-acid fixed-bed ion exchange process; (2) testing of the new clarifier in the scavenging-precipitation head-end equipment; (3) testing of two proposals (use of an alumina bed and split addition of ferrous ion and caustic) for overcoming the deleterious effect of phosphate on calcium removal in the scavenging-precipitation equipment; (4) demonstration of a scavenging-precipitation ion exchange process in which grundite clay is added to the ion exchange column regenerant, which is then recycled to the scavenging-precipitation portion of the plant;

(5) demonstration of the compatibility with the acid-resin flow sheets of a sodium-free head-end for removal of radiocolloids; and (6) demonstration of a foam separation process for treatment of low-activity-level waste.

Initial tests were made in the fixed-bed ion exchange system. This system was operated for a week with waste from the ORNL equilization basin as feed, using the anthracite filter to clarify the water prior to ion exchange. However, a large amount of the algae in the basin water passed through the filter and ion exchange units. In fact the effluent from the column was green. The system was shut down pending completion of radiochemical analyses that will allow complete evaluation of the test. This confirms the premise that the feed to the ion exchange column must be clarified to prevent the solids from carrying radioactivity through the system.

Tests with tap water feed were started to determine the operating characteristics of the agitated clarifier and to evaluate the need for using a flocculator with the new clarifier.

3.2 Scavenging-Precipitation Ion-Exchange Process: Laboratory Development

W. E. Clark R. R. Holcomb

Work continued on variations of the Scavenging-Precipitation Ion-Exchange process for decontaminating low-level waste. The retention of cesium in the sludge by sorption on grundite clay, the removal of phosphate from the waste by alumina, and the use of an anion exchange column to remove residual activity from the effluent from the process were investigated.

3.2.1 Removal of Anionic Activities by Ion Exchange

Passage of the effluent from the Scavenging-Precipitation Ion-Exchange process through a column of Dowex 21-K anion exchanger resulted in removal of about half the residual gross activity from the stream. Activity, including some ruthenium, began to leak through the column almost immediately.

3.2.2 Removal of Cesium in Sludge

The retention of major fractions of cesium and other activities in the head-end sludge of the Scavenging-Precipitation Ion-Exchange process would eliminate the need for evaporation of the eluate from the cation exchange column. This would decrease capital costs by eliminating the need for the evaporator and auxiliary equipment, and would decrease operating costs by eliminating the extra power and labor required for operation of the evaporator. Accordingly an experiment was run in which 1900 resin-bed volumes were processed according to the Scavenging-Precipitation Ion-Exchange flow sheet.* The eluate was then adjusted to pH 3 by addition of NaOH, mixed with grundite clay, and then metered into the low-level feed stream through the flash mixer, in which the stream was adjusted to the flow sheet - recommended pH of 11.8. The effluent from the column after passage of 1900 bed volumes of waste (containing recycled eluate) contained 1.3% of the cesium and less than 0.31% of the strontium.

Batch experiments showed that there is a narrow optimal pH range at about 11.8 for the sorption of cesium on grundite clay and that sorption is greater when the grundite is added before pH adjustment than when the procedure is reversed (Fig. 15). One gram of grundite per liter of column effluent** removed 55% of the cesium at pH 11.8. Increasing the amount of grundite to 2, 4, and 8 g/liter resulted in the removal of 83, 94, and 97%, respectively, of the cesium from the solution. The size of the grundite particles was not important; there was no detectable difference

---

*Flow-sheet outline: Sodium hydroxide and copperas were added to the waste stream in a flash mixer to give a pH of 11.8 and an iron content of 5 ppm. Flocculation and clarification were accomplished in a single vessel employing a sludge blanket. The clarified stream was filtered through anthracite and the filtrate was passed through a CS-100 cation exchange resin to remove about 99% of the cesium and the strontium that had not been removed in the scavenging-precipitation step. The resin was eluted with 10 bed volumes of 0.5 M HNO_3, rinsed with water, and regenerated with 20 bed volumes of 0.1 M NaOH. Further details as well as variations in this flow sheet are covered more fully in ORNL-3322 and ORNL-3349.

**This corresponds to 1 g per 77 liters or to 0.11 lb per 1000 gal of fresh low-level waste. Cost of grundite is $0.685 per 100-lb bag in carload lots.

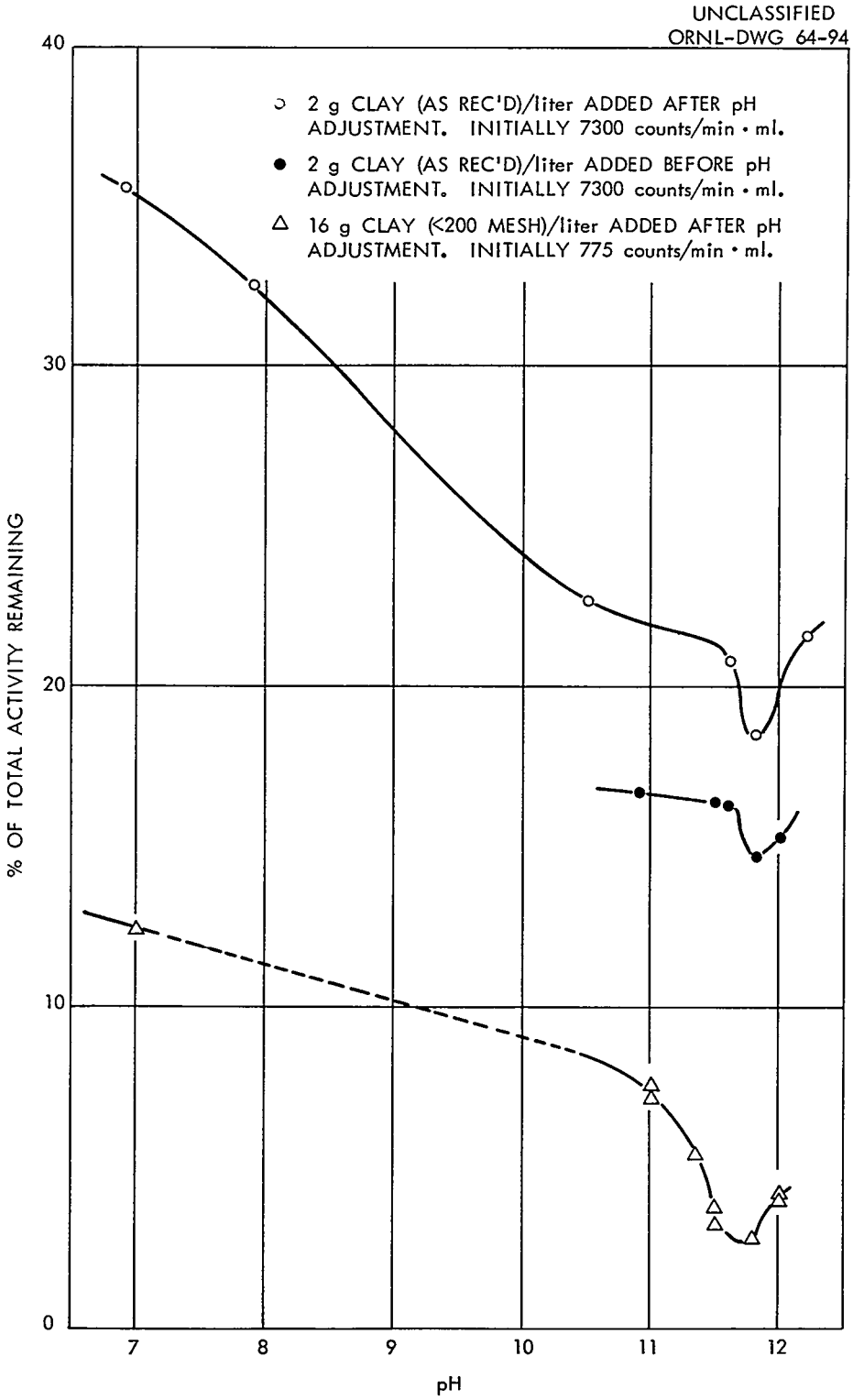

Fig. 15. The Sorption of Cesium on Grundite Clay as a Function of pH, Weight of Clay/liter of Solution, and Sequence of Addition.

in the performance of the material as purchased* and material of various classified sizes down to < 200 mesh. Use of sized material is, therefore, unnecessary for cesium removal, though use of smaller sizes may be desirable because of ease of handling in a slurry.

3.2.2 Phosphate Removal by Alumina

An upflow fluidized alumina column containing 400 g of alumina (80-200 mesh, F-20 grade) has continued to remove about half of the phosphate after passage of a total of 10,000 bed volumes of untreated low-level waste. Total phosphate in the feed varied from 0.46 to 1.6 ppm; the effluent from the alumina column varied from 0.25 to 0.77 ppm; and the fraction removed varied from 0.24 to 0.71 (Table 18). It is not yet clear whether the variations observed are due to the presence of different species of phosphate in the waste, or to normal analytical scatter in determining such small amounts of phosphate, or is characteristic of the performance of the alumina column.

3.3 Foam Separation

The Foam Separation process for decontaminating ORNL low-radioactivity-level process waste water consists of two steps: (1) a head-end, caustic-carbonate precipitation with clarification in an upflow sludge-bed filter to remove macro-quantity impurities (e.g., calcium carbonate, magnesium hydroxide, and algae), followed by (2) a countercurrent foam separation column for removing remaining trace-quantity impurities having deleterious biological effects, especially Sr^{90}.

3.3.1 Laboratory Development (E. Schonfeld, A. H. Kibbey, W. Davis, Jr.)

Sludge Bed Studies.-- Beaker tests were performed to determine the effects of aging time, pH and method of adding caustic-carbonate on the completeness of phosphate precipitation from ORNL process waste water.

---

*Grundite bond clay supplied by the Illinois Clay Products Company. Mineralogical analysis: illite 65-75%, kaolite 10-20%, quartz 5-15%. Screen analysis: > 30-trace, 40-2.2%, 50-5.8%, 70-7.6%, 100-10.6%, 140-10.5%, 200-9.7%, 270-5.6%, pan-48.0%.

Table 18. Removal of Phosphate from ORNL Low-Level Waste Solution by Upflow Through a Fluidized Alumina Column[a]

Total Phosphate in Feed[b] (ppm)	Total Phosphate in Column Effluent (ppm)	Fraction of Phosphate Removed
1.5	0.61	0.59
1.0	0.60	0.40
1.0	0.76	0.24
1.2	0.35	0.71
0.92	0.40	0.56
0.46	0.25	0.46
0.76	0.35	0.54
1.5	0.56	0.63
1.6	0.77	0.52

[a]400 g of F-20 grade Al_2O_3, 80 to 200 mesh, in a bed 2 in. in diameter.

[b]The three groups of data were obtained during three different Scavenging-Precipitation Ion-Exchange runs.

These tests were performed because previous studies[7,8] showed that the precipitation of calcium carbonate is inhibited by phosphate ion.

In beaker tests on the 400- to 500-ml scale, the addition of about 10 ppm of Fe^{3+}, as ferric chloride in 0.01 M HCl, to process waste water containing 4.6 ppm of phosphorus (measured as PO_4^{-3}) reduced the total soluble phosphorus to a minimum (0.04 ppm) at pH 7 when a 4-min stirring time was used (Fig. 16). At the higher pH value of 11.3 used in sludge-bed precipitation of calcium carbonate, the solubility of phosphorus (as PO_4^{3-}) was 0.2 to 0.3 ppm. At pH 7.2 and 11.4, phosphate precipitation almost attains its final value in 1 to 4 min (Fig. 17). After phosphate is precipitated at pH 7.2 and the pH of the water then increased to 11.4 by caustic-carbonate, the soluble phosphate concentration increases, corresponding to ferric phosphate slowly redissolving, with eventual reprecipitation of the ferric ion as a hydrous oxide. The rate at which the ferric phosphate is dissolved controls the rate at which ferric oxide can precipitate and, hence, the rate at which phosphate ion is liberated. Thus, the precipitated ferric phosphate temporarily removes phosphate ion from solution, thereby allowing calcium carbonate precipitation to be more complete. One feature of the data in Fig. 17 may be summarized by saying that when Fe^{3+} is added to practically neutral water, the subsequent deleterious effects of 4 to 5 ppm of phosphate on calcium carbonate precipitation at pH 11.4 are less than would be observed if the Fe^{3+} and caustic-carbonate were added at the same point. This mechanism makes it possible for the caustic-carbonate process to compensate for unusually large amounts (up to 10 to 15 ppm) of phosphate which occasionally appear in ORNL waste water for brief intervals. Ordinarily the soluble phosphorus concentration in the waste is in the range of 1 to 3 ppm (as PO_4^{3-}).

Demonstration sludge-bed column runs on laboratory scale at a water processing rate of 20 gal ft^{-2} hr^{-1} confirmed the findings of the beaker tests. In these runs, tap water containing 5 ppm of phosphorus as sodium orthophosphate reagent was used as feed. The Fe^{3+} (in 0.01 M HCl) was added in a premixer in which there was an approximately 4-min holdup of the water. Then 0.3 M each NaOH-Na_2CO_3 solution was introduced into the premixer exit stream, upstream from the sludge bed. Final concentration

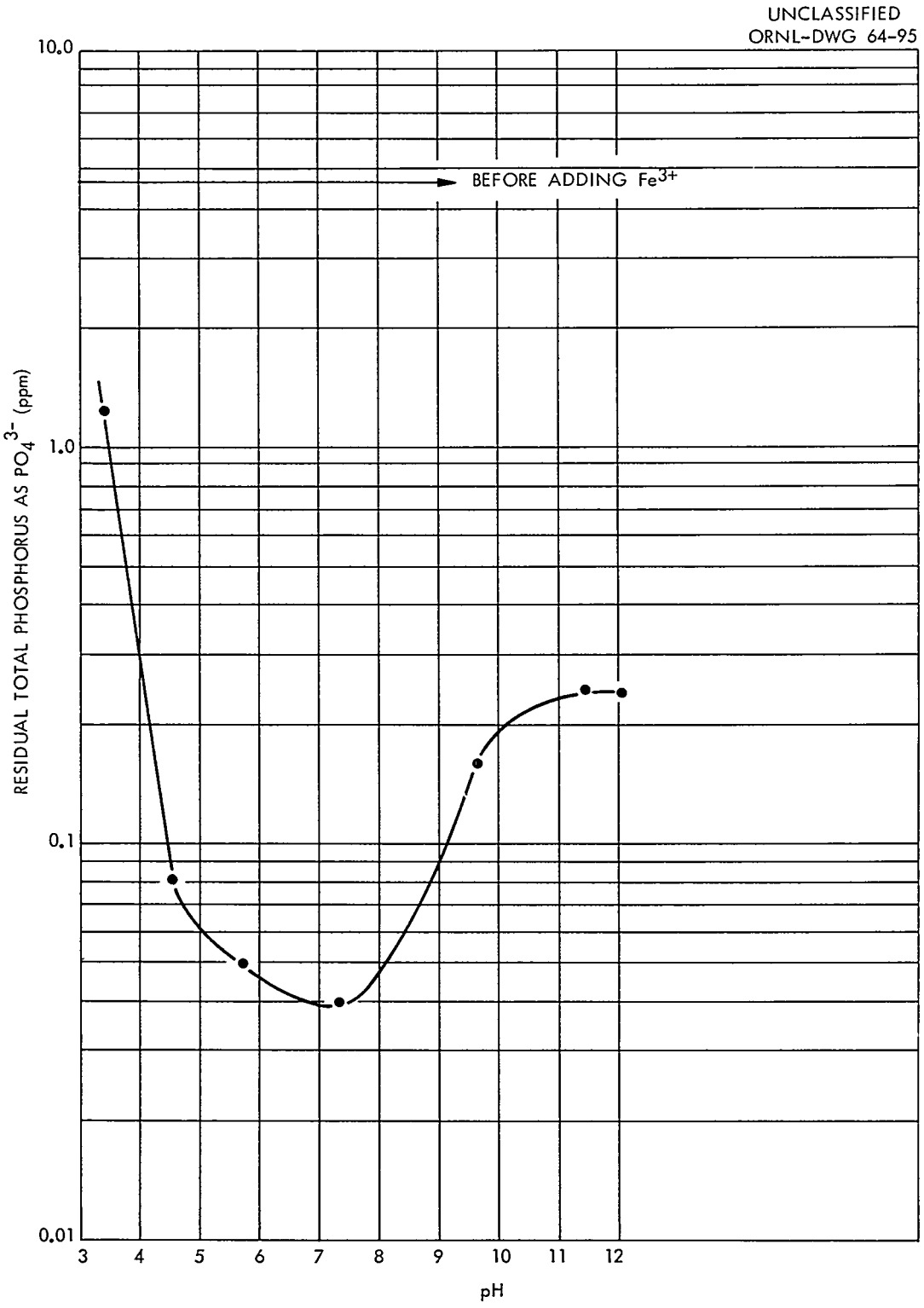

Fig. 16. Residual Phosphate in Beaker Test. Low-Activity Waste. Conditions: 4-min mixing time; ferric ion concentration, 10 ppm.

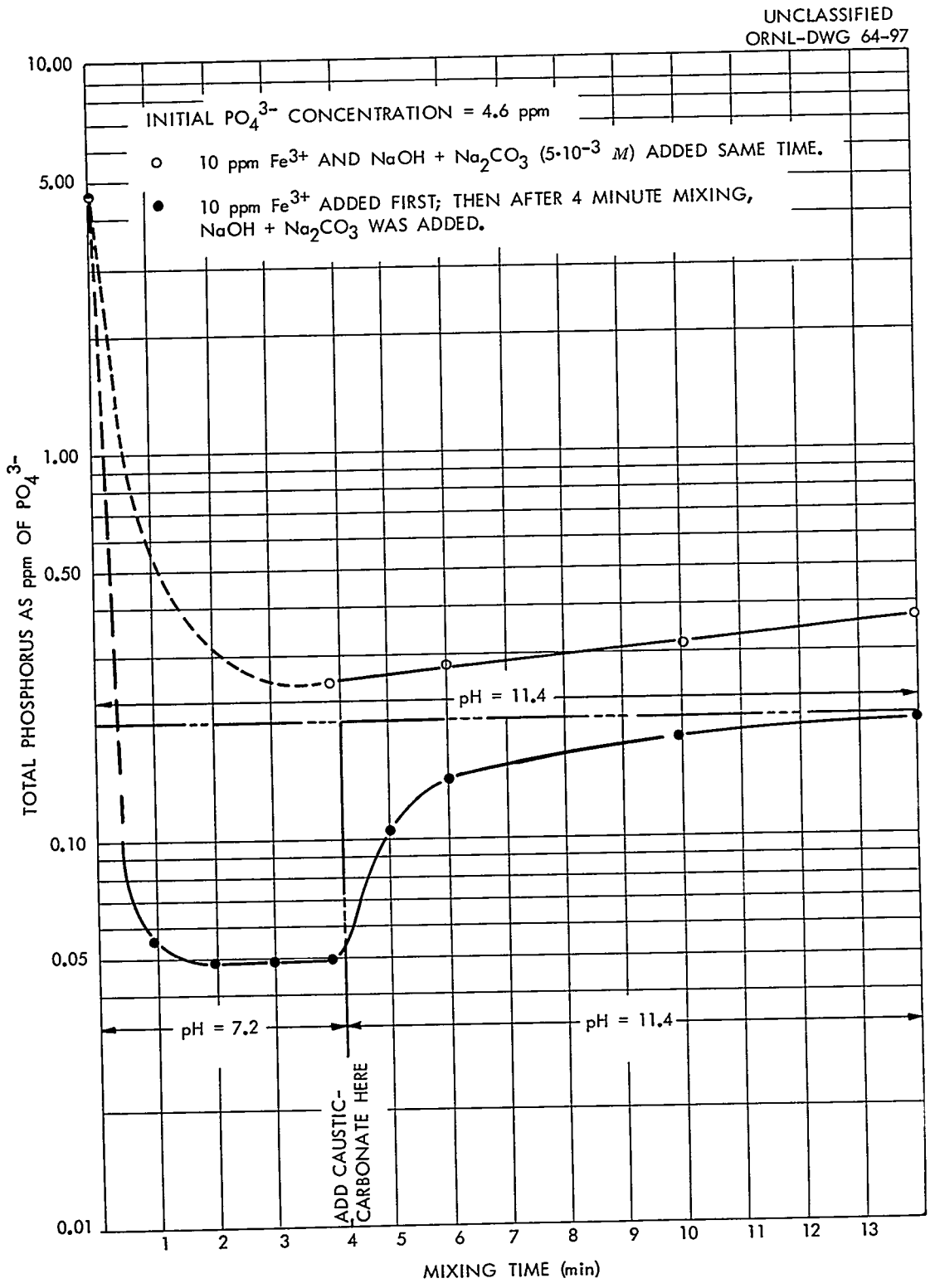

Fig. 17. Effect of pH and Mixing Time on the Phosphate Removal.

of the caustic and carbonate in the sludge-bed feed was 0.005 M each. The relatively low total hardness in the sludge-bed effluent stream under these conditions, as compared to that obtained in a similar run in which the Fe^{3+}, NaOH, and Na_2CO_3 were added together in the premixer, is shown in Fig. 18. Here the lag in phosphate build-up owing to preliminary ferric phosphate precipitation is evidenced by the lowered total hardness (as $CaCO_3$) of the sludge effluent stream even after 7 hr. Apparently, a prolonged high phosphate content in the waste water would lead to little difference in the results of separate or simultaneous ferric and caustic-carbonate addition procedures, since an equilibrium between precipitated ferric phosphate and hydrous ferric oxide would eventually be reached. However, for high phosphate concentrations of short duration, adding the reagents separately is of value.

Increasing the ferric ion concentration when phosphorus concentration in the feed increased also tended to reduce effluent total hardness.[9] In two runs, made with actual process waste water containing from 6 to 14 ppm of phosphorus (measured as PO_4^{3-}), increasing the ferric concentration from 8 to about 20 ppm decreased the total hardness in the sludge effluent to less than 2.5 ppm. The discrepancy between this hardness value and those obtained with the tap water feed (in Fig. 18) is probably the result of a difference in the form in which the phosphorus existed in the waste water and tap water solutions. The tap water contained orthophosphate, whereas the waste water contained some phosphate as algae and may have contained hexametaphosphates and tripolyphosphates from cleaning compounds such as Fab and Turco 4324. Earlier beaker tests[8] showed the orthophosphate inhibition of calcium carbonate precipitation to be more persistent than were inhibitions by other phosphates under the same conditions.

Cesium Removal.-- Previous studies showed that grundite clay (used as the -230 mesh material) removes about 90% of the cesium from ORNL process waste water when used at a concentration of about 0.5 lb of clay per 1000 gal of water in the continuous caustic-carbonate process. Two other materials have been tested as possible cesium scavengers; these are magnesium ammonium phosphate powder and a refined asbestos, Asbestos CMS, obtained from Union Carbide Corporation.

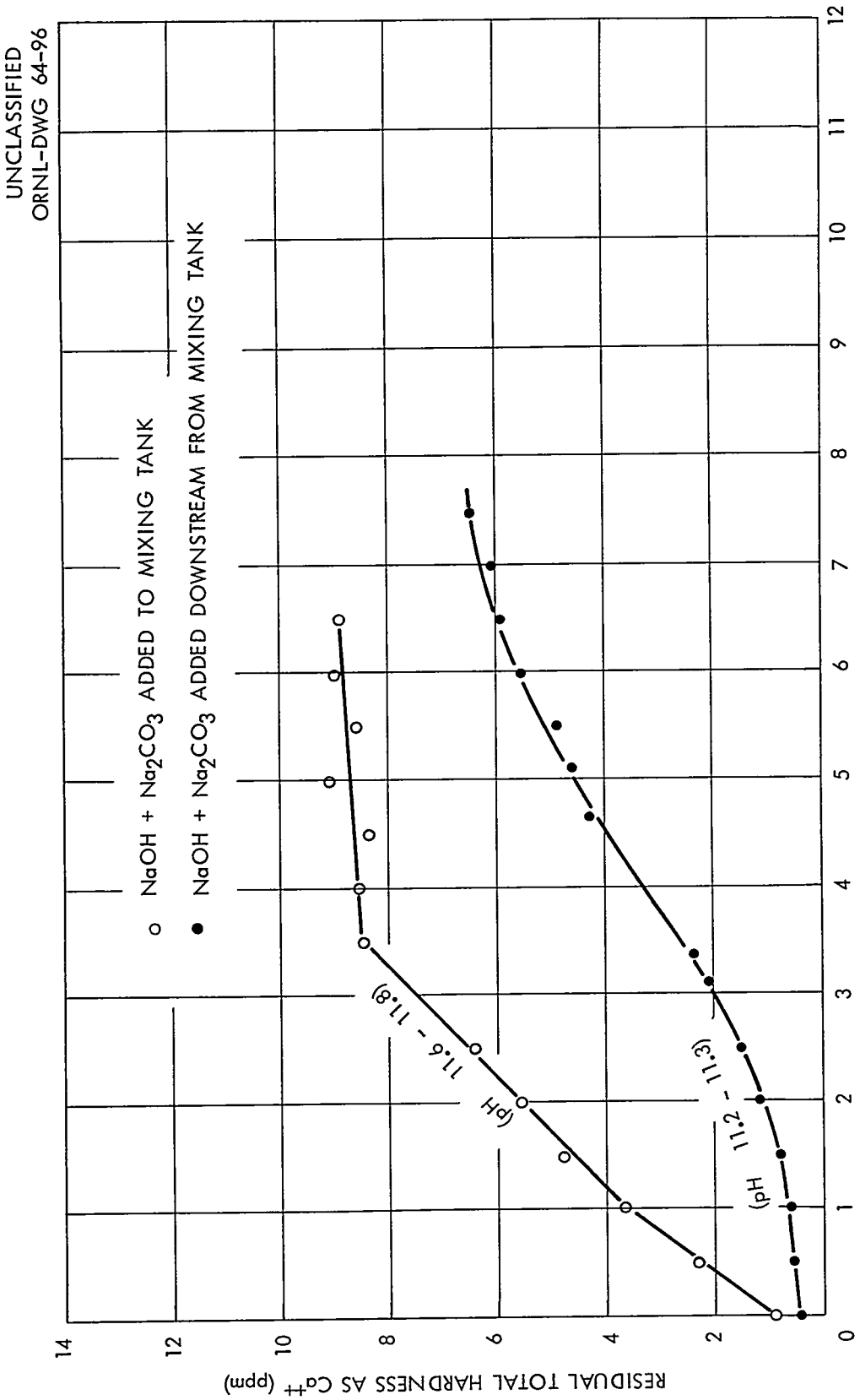

Fig. 18. Changing the Caustic-Carbonate Addition Point Can Reduce the Deleterious Effects of Phosphate on Hardness Removal.

The ability of each of these two materials, and of grundite for control purposes, to sorb cesium was tested at two concentration levels; namely, 0.5 and 5 lb per 1000 gal, or 60 and 600 ppm in beaker tests. A test consisted in adding a sample of solid to caustic-carbonate water that had been spiked with Cs^{137}, stirring for 30 min at 25 ± 1°C, filtering, and measuring the Cs^{137} content of the filtrate. In all tests the total hardness in the water was 3 ppm as $CaCO_3$.

Neither the magnesium ammonium phosphate nor the asbestos was very effective in removing cesium. The former removed 6% at the two solids-concentration values of 0.5 and 5 lb per 1000 gal; the asbestos removed 5 and 11.4%, respectively. For comparison, even a large-particle-size fraction of grundite (larger than 50 mesh) removed 54.4 and 76.5% of the cesium, while a small-particle-size fraction (-325 mesh) removed 72 and 92%, respectively.

The effect of a prebaking* for 20 min at 600°C on the efficiency of cesium removal by -230 mesh grundite was tested in continuous column operations. The baking increased the cesium decontamination factor from 8 at a concentration of 0.6 lb of clay per 1000 gal to 15 at a concentration of 0.38 lb per 1000 gal. In the absence of grundite clay, the sludge-bed decontamination factor (DF) for cesium is only 1.2 to 1.6.

Foam-Column Studies.-- Experiments were performed to evaluate foam-column performance with respect to strontium and cesium removal, both with and without recycle of foam condensate to the sludge column, with dodecylbenzene sulfonate (DBS) as a surfactant and with respect to cesium removal when other surfactants, containing "active" phenolic groups, were used.

Recycle of foam condensate was tested because such recycle is more economic with respect to surfactant usage, and also reduces the number of waste stream withdrawal points to one, namely, the sludge. With DBS as surfactant, recycle was performed without significant changes in the mechanical operations of sludge or foam columns during six runs of 8 hr to 4 days' duration.

---

*This procedure has previously been tested by T. Tamura, ORNL, Health Physics Division.

The parameter group V/LD is being correlated with strontium decontamination factors in the foam column because the numerical value of this group can be rapidly estimated. The term V is the foam flow rate in cc/min, L is the liquid feed rate in cc/min, and D is the average bubble diameter according to the equation

$$D = \sum_{i=1}^{n} D_i^3 / \sum_{i=1}^{n} D_i^2 .$$

where the subscript i refers to an individual bubble and n is the number of bubbles whose diameter is measured (from Polaroid camera photographs). Since previous sludge-bed foam-column runs using Sr^{85}-spiked tap water or waste water as feed always gave satisfactory decontamination factors (i.e., about 100 or greater) for strontium when V/LD was equal to or greater than 150, operating conditions necessary to produce at least this value[10] were determined as a function of surfactant concentration and gas flow rate. V/LD values in the range 150 to 190 were obtained at linear-foam velocities of 32 to 37 cm/min and 41 to 46 cm/min when surfactant concentrations in the foam column effluent were maintained at 9.2 to 38.8 and 10.3 to 27.8, respectively, by continuous addition of concentrated DBS solution. The corresponding sludge-column effluents (foam-column feeds) contained 10.3 to 21.9 and 21.7 to 32.5 ppm of DBS. At the lower linear foam velocity, DBS concentration in the foam condensate, whose volume was 2.8 to 3.8% of the feed volume, ranged from 1625 to 2027 ppm. At the higher foam velocity, DBS in the condensate was in the range 1175 to 1375 ppm, while the condensed volume was 6.1 to 8.6% of that of the feed. Bubble diameters obtained at the lower gas rate were 0.56 to 0.66 mm and were 0.68 to 0.82 mm at the higher gas rate. Dodecylbenzene sulfonate material balances were good in 9 of the 10 experiments on which the above numbers are based. Specifically, the influent DBS/effluent DBS ratio varied from 0.93 to 1.25 except for one value of 0.62.

Because decontamination factors for removal of strontium in a foam column from low-calcium water are expected to be in the range 100 or more, no experiments have been performed just for the purpose of maximizing this factor. However, even in a short column of over-all length 21 in. and

active foam height of only about 10 in., an Sr^{90} decontamination factor in excess of 400 was achieved with sodium dodecylbenzene sulfonate as surfactant. The accuracy of this factor was limited by the very low counting rate of the product water from the foam column.

Cesium removal by foaming is not very good. The best Cs^{137} DF values achieved to date with dodecylbenzene sulfonate are about 1.6. By contrast, cesium decontamination factors of about 15 are achieved across the sludge bed by adding 0.5 lb of baked grundite clay (baked at 600°C for 20 min) to each 1000 gal of water. Because of their usefulness in ion exchange and solvent extraction, three surfactants containing phenolic groups were tested for their ability to separate cesium from the large (0.015 M) quantities of sodium ion in the water from the sludge column that is used as feed to the foam column. These three surfactants were RWA-100 (a sodium phenyl phenol sulfonate), dichlorophene, and hexachlorophene. The column experiments were made without recycle of foam condensate.

The foaming properties of RWA-100 were inferior to those of DBS, and a stable foam was not produced under column-operating conditions unless some DBS was added. Smooth column operation was achieved at a weight ratio of RWA-100/DBS = 4/1 when RWA-100 concentration was 225 ppm and the gas/liquid flow rate ratio was equal to 26.5 to 31.9 at liquid flow rates of 28 to 34 gal ft^{-2} min^{-1}. Although the V/LD values were in the range 250 to 350 under these conditions, the cesium decontamination factors were only 1.2 to 1.5. For comparison, the DBS system, V/LD values $\geq$ 150 always gave strontium decontamination factors in the range 10 to 100. Possible reasons for the poor cesium separation are: (1) high ratio of DBS/RWA-100 or (2) pH not high enough to produce significant ionization of the phenolic group.

After screening ten additional phenolic compounds for solubility and foamability, two (hexachlorophene and dichlorophene) were chosen for testing for cesium removal in single-stage foam column runs. The test solution was made by adding Cs^{137} tracer to caustic-carbonate water from the head-end precipitation step. Since the foam generated in a solution containing up to 500 ppm of either of these phenolic surfactants was unstable, the solution was made 20 ppm in DBS. The single-stage foam column results showed no significant enrichment of Cs^{137} in the foam phase.

3.3.2 Engineering Development (P.A. Haas, D. A. McWhirter)

Engineering studies for design and application of foam separation columns were continued with the emphasis on the scaleup of components for the 24-in.-diam column proposed for a low-level-waste pilot plant. The 6- and 24-in.-diam columns were operated with orifices as simple and easily scaled-up foam breakers.

Orifice Foam Breakers.-- The idea of an orifice as a foam breaker was developed from consideration of the foam-breaking mechanism in the sonic, cyclonic, and centrifugal foam breakers. The sonic foam-breaking mechanism is ascribed to pressure cycling effects.[11] The 2-to-1 inlet-to-outlet pressure ratio found necessary to make a cyclone an effective foam breaker would produce a very rapid pressure change. Foam flowing through either a stationary fine-mesh screen or a coarse-screen centrifuge bowl is broken very poorly as compared to a fine-screen centrifuge bowl. This could be attributed to a pressure change as the foam leaves the centrifugal field in the bowl. Since sharp pressure changes and even pressure discontinuities are possible in an orifice, the performance of orifices as foam breakers was tested.

Experimental data was collected for four orifice diameters using foam from extra-coarse-porosity fritted-glass-disk gas spargers. Foam generated from 200- to 275-ppm Trepolate F-95 solution was drawn through the orifice by vacuum, with the top of the column vented to the atmosphere (Fig. 19). The amount of uncondensed foam was measured by operating the orifice for 2 to 5 min and then venting the vacuum pot and discharging the liquid and foam into a graduate. The orifice diameter, the foam rate, the pressure drop across theorifice, the foam density, the distance from the orifice to the vacuum chamber wall, and the wall material were varied.

The results show that foams are easily condensed by an orifice with residual foam volumes of about 0.001, the inlet volumes for the well-drained foams (Table 19). Pressure drops from atmospheric for the inlet foam to one-half atmosphere in the vacuum pot were adequate. The same pressure ratio would probably apply at other pressures; that is to say, an upstream to downstream pressure ratio of 2 is probably adequate. With the inlet foam at atmospheric pressure, condensation was less complete for 30 or 25 cm of Hg pressure drop as compared to 50 or 65 cm Hg and become very poor for lower pressure drops.

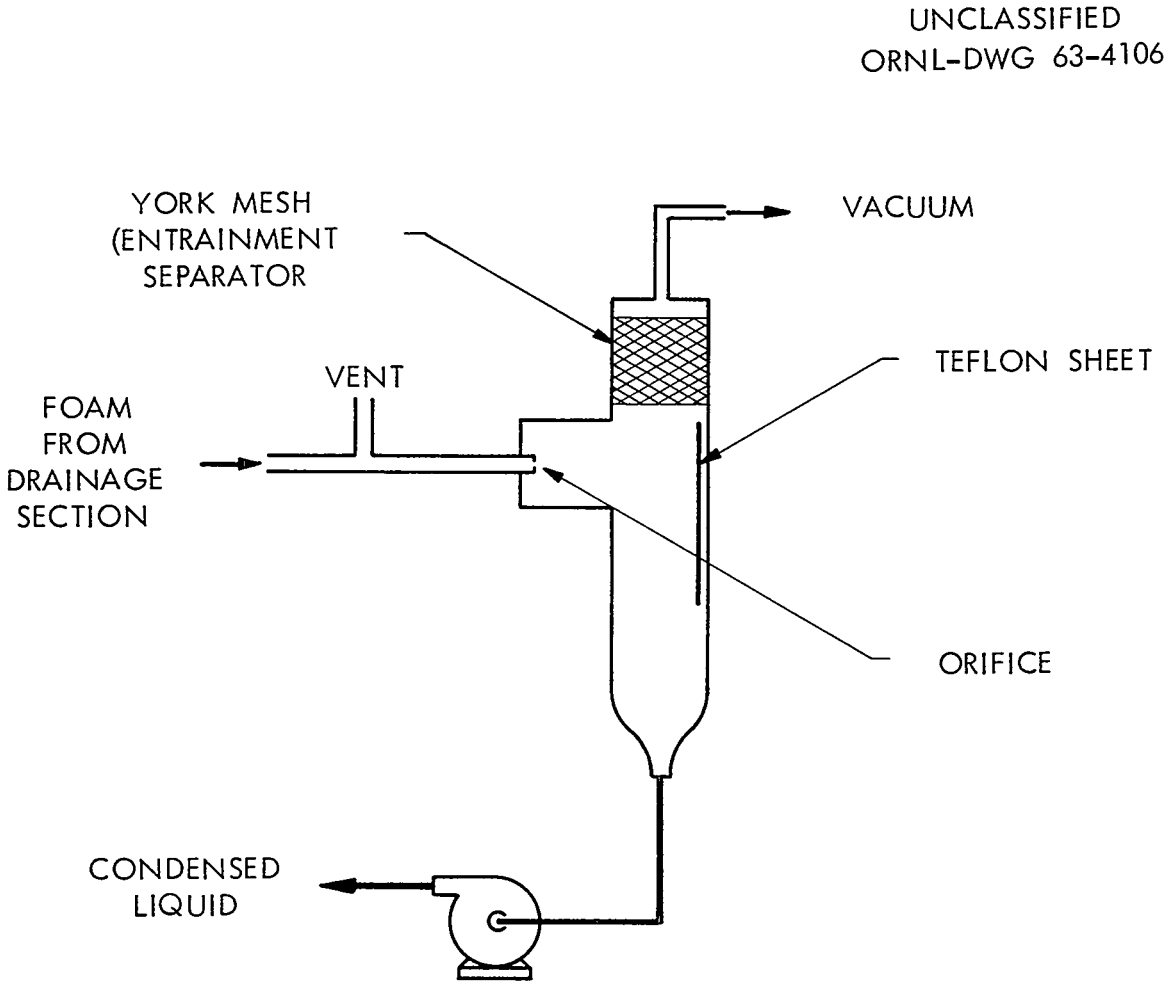

Fig. 19. An Orifice Foam-Breaker System.

The results indicate that the condensation occurs as the bubbles pass through the orifice and that orifices smaller than the bubble and impingement of the bubbles on a surface are not necessary. The condensation of foam was about equally efficient for 0.015-, 0.100-, and 0.250-cm-diam orifices. The 0.015-cm diameter would be smaller than nearly all the bubbles, while the 0.250-cm diameter would be larger than nearly all the bubbles (mean bubble diameters of 0.05 to 0.08 cm). For most of the tests, the stream from the orifices impinged on a Teflon sheet placed 2 to 3 in. from the orifice. The amount of uncondensed foam was slightly decreased by placing the orifice 24 in. from the Teflon sheet. The amount of uncondensed foam was slightly greater for a glass surface in place of the Teflon sheet. It appeared that the foam bubbles broke before they hit the surface and that the liquid striking the surface caused some formation of new foam bubbles, depending on the material and position of the surface.

The drier foams from lower foam rates or better drainage gave smaller fractions of uncondensed foam. This may have been due to less formation of new foam bubbles on the Teflon surfaces when the inlet foam was drier.

The capacities of the orifices as foam breakers appeared to be inversely proportional to the square root of the foam density, as would be expected from orifice equations. The observed capacities agree with the following:

$$q = 6000\, d^2 \quad \frac{\Delta P}{\epsilon}$$

where

q = capacity in cc/min,
d = orifice diameter in cm,
ΔP = pressure drop (from atmospheric) in cm of Hg,
ϵ = foam density in cc/cc.

This equation indicates slightly higher flows than would be calculated for gases of the same densities as the foams.

The 24-in.-Diam Column.-- The 24-in.-diam foam column (See ORNL-TM-516, November 1962 to January 1963 Quarterly) with a feed distributor of 19 tubes on a 5-in. triangular spacing was operated at higher gas rates

Table 19. Orifice Foam-Breaker Test Conditions and Results

Solution: 200 or 275 ppm Trepolate F-95and .002 to 0.010 N NaOH

Orifice		Opposing Wall		Foam Column		Pressure Drop	Foam Rate	Foam Density	Average Bubble	Fraction of Uncondensed
No.	Diam (cm)	Material	Distance	Diam (in.)	Foam Drainage Flow	(cm Hg)	(cc/min)	(mg/cc)	(diam, cm)	Foam (cc/cc)
Twelve	.015	Glass	~3	6	Horizontal	~65	1000	~3	.05	<.001
One	.100	Glass	~2	6	Horizontal	~65	5600	4.	.07	.0016
							3700	3	.06	.0005
						50	5600	4	.07	.0019
							3700	3	.06	.0011
						30	5600	4	.07	.0012
							3700	3	.06	.0010
						25	3700	3	.06	.0040
		Teflon	~2	6	Horizontal	~65	5600	4	.07	.0005
							3700	3	.06	.0006
						30	5600	4	.07	.0012
							3700	3	.06	.0014
		Teflon	~2	6	Vertical	~65	3700	12	.07	.0040
							1900	9	.06	.0016
							700	4	.05	<.0005
						50	3700	12	.07	.0040
						30	3700	12	.07	.0032
							1900	9	.06	.0021
							700	4	.05	<.0005
		Teflon	~24	6	Vertical	~65	3700	12	.07	.0016
							1900	9	.06	.0013
						30	3700	12	.07	.0027
							1900	9	.06	.0048
One	.250	Teflon	~3	24	Vertical	~60	40,000	4	.07	.0010
							32,000	3.5	.06	.0011
							16,000	1.	.05	.0005
							8000	0.5	.05	.0005

using the 0.25- and 0.31-cm-diam orifice foam breakers. The amount of channeling decreased as the gas (foam) rate was increased. With this feed distributor and 50 liters/min of foam, the flow was good, with little channeling at 5 liters/min of liquid (25 gal ft^{-2} hr^{-1}), but channeling was very bad at 13 liters/min (66 gal ft^{-2} hr^{-1}). Channeling was less, but still excessive, at 13 liters/min for 80 liters/min foam. A feed distributor, designed to give 37 feed streams on approximately 3-3/4-in. triangular spacing in a 24-in.-diam column, gave the uniform flows, low discharge velocities, and reduced channeling necessary for a larger diameter foam column. Parallel, horizontal 3/8-in.-OD tubes were spaced across the column cross section with 0.037-in.-diam metering orifices with baffles to give the low discharge velocity.

The effects of dodecylbenzenesulfonate and Na^+ concentrations on foam stability in the 24-in.-diam column with a 48-in. foam height were studied at various gas and liquid flow rates. It appears that the low-level waste foam column should have a stable foam with 25 ppm of dodecylbenzene sulfonate in the liquid, while 10 ppm in the liquid resulted in gross bubble growth and loss of over three-fourths of the surface generated.

Foam Drainage.-- A model was developed for the flow of liquid in foam for the countercurrent and drainage sections of foam separation columns. The Plateau borders are considered to be capillaries of constant pressure drops per unit length and variable diameters. Equations derived for foam densities during countercurrent foam-liquid flow and for exit foam densities after drainage with either vertical or horizontal flow of foam were confirmed by experimental results. The experimentally determined coefficients for equations for the three different flow situations are consistent and are within the range of values expected from the theoretically derived equations. The detailed results are reported in a topical report on the engineering studies.[12]

3.3.3 Pilot-Plant Design (J. M. Holmes)

Foam separation equipment is being designed for installation in the Low Level Waste Pilot Plant, Building 2528. The equipment will include a 2-ft-square by 14-ft-high countercurrent foam column for the removal of radioactivity from ORNL low-level waste, three recovery columns in series

for the removal and recycle of surfactant from the waste effluent before discharge, and two types of foam-breaking equipment (Fig. 20). The countercurrent column will have a horizontal foam-drying section for removal of liquid from the overhead foam stream just prior to its entering the centrifugal foam breaker. Liquid drained in this section will be fed back to the column alongside the main column waste feed stream. Orifice foam breakers will be used on the recovery columns. Air for the generation of foam will be distributed by spinnerets in the countercurrent column and by porous stainless steel spargers in the recovery columns. The air will be supplied by a Nash vacuum pump which will maintain a closed circulation system from the foam breakers to the foam generators. The only gas requiring cleanup will be the excess bled from the system to control the system inventory. This will be discharged to the system scrubber and the building ventilation system filters. The maximum waste feed rate for the system will be about 5 gal/min. The present Low Level Pilot Plant clarifier and filters will be used for hardness removal from the waste before it is fed to the foam columns. Solids-feeding equipment will also be installed to permit the addition of grundite clay to the clarifier for cesium removal.

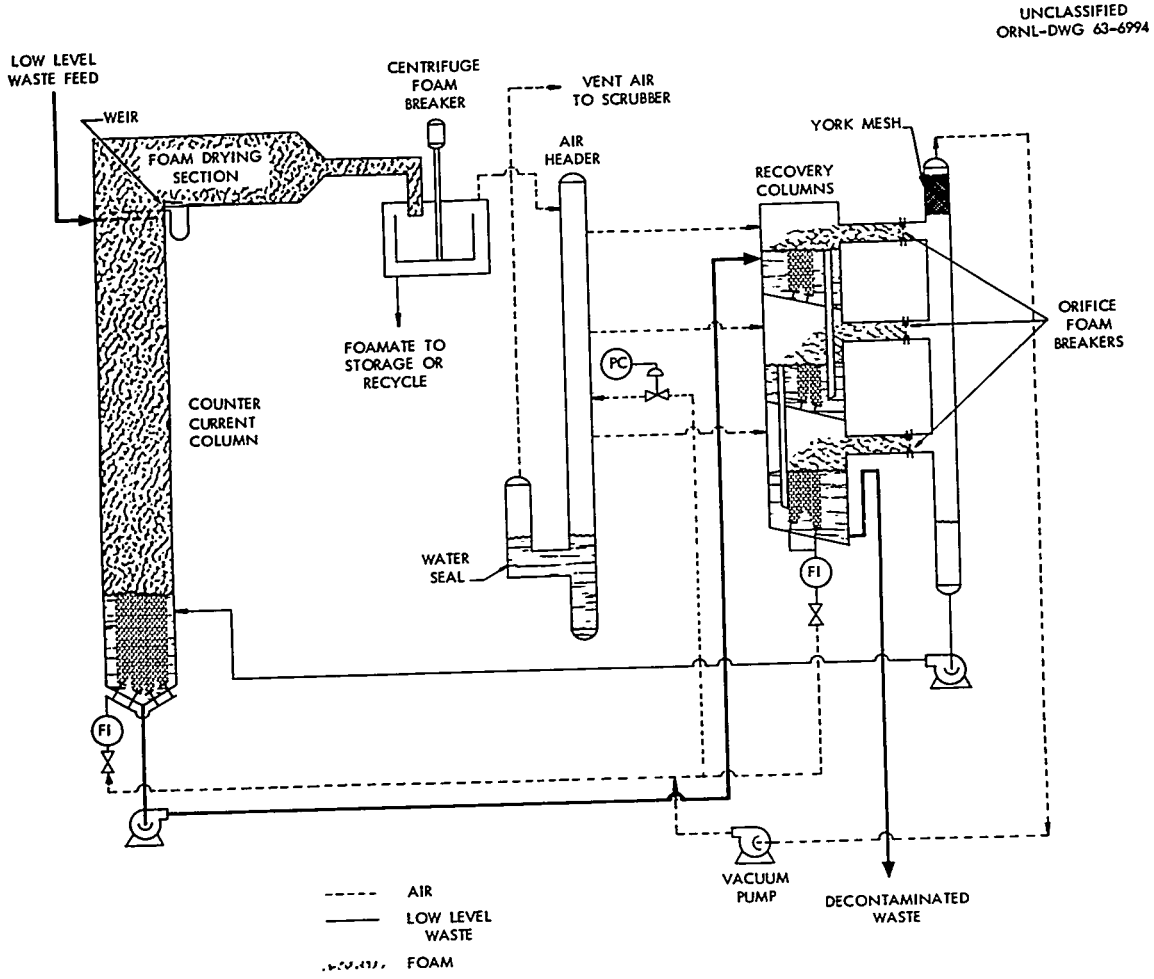

Fig. 20. Foam Separation Pilot Plant.

4. ENGINEERING, ECONOMICS, AND SAFETY EVALUATION

4.1 Engineering and Economics of Waste Management

J. J. Perona J. O. Blomeke R. L. Bradshaw

An estimate of comparative costs for final disposal of radioactive solids in concrete vaults, granite, and salt formations has been completed and published as ORNL-TM-664. Although cavities mined in salt formations are believed to offer the best possibilities for permanent disposal of these wastes, its use implies the probable need of shipping the wastes to a mine from a processing plant possibly many miles distant. Suitable deposits of granite or shale might be more accessible to a plant, and it is conceivable that high-integrity concrete vaults could be constructed at the plant site to serve the purposes of permanent containment.

Having available as a point of reference the more detailed analysis of the cost factors in the disposal of calcined wastes in salt mines,[13] a rather perfunctory analysis can show the relative costs for disposal into concrete vaults at the surface of the earth and into space excavated from granite formations. In lieu of a formal safety analysis, which may be done sometime in the future, a qualitative observation can be made that disposal in granite would at best be no safer than in salt; and concrete vaults would be less safe because of the limited period of integrity of the concrete and the proximity of the waste to the biosphere. Therefore, the costs for mining space in granite must be as low as for salt, and for vaults lower than for salt, in order for these alternative methods to be competitive.

A basic assumption is that, after the waste has been placed in storage, all accesses to the storage area are sealed to provide the maximum containment and isolation from the environment. Under these circumstances, dissipation of the radioactive decay heat will occur only by conduction through the surrounding solid medium. Better heat transfer permitting more efficient utilization of storage space could be achieved by circulation of air through the storage area and discharging it back into the atmosphere after appropriate monitoring and/or cleaning. However, this would represent a less safe situation, in that it would provide a direct

route for escape of the fission products into the environment in the event of sabotage or natural disaster.

As in previous cost studies in this series, a 6-tonne*/day plant is assumed, processing 1500 tonnes/yr of uranium converter fuel at a burnup of 10,000 Mwd/tonne and 270 tonnes/yr of thorium converter fuel at a burnup of 20,000 Mwd/tonne. This hypothetical plant would process the fuel from a 15,000 Mw_e nuclear economy, which may be in existence by 1975. Acid Purex and reacidified Thorex wastes are chosen for this study, as they possess the highest and lowest heat generation rates per unit volume, respectively.

The procedure used in this report was to calculate the relative costs for storage space and then to estimate space requirements as determined by heat transfer considerations. Handling procedures and operating costs are assumed to be identical to those used for disposal in salt.

4.1.1 Costs for Space in Vaults

This concept involves the construction of concrete rooms completely buried, with just sufficient earth cover to provide the necessary shielding. A preliminary design of a concrete vault for the storage of highly active solid wastes was done at Chalk River.[14] The gross resemblance of such a vault to tanks for storage of liquid wastes is striking, in that all are underground structures of reinforced concrete, are of about the same size and proportions, and have leak-tight metal linings over their interior surfaces (Table 20). The cost per unit of storage space for the vault was estimated at $\$10.70/ft^3$, and costs for tanks ranged from \$6 to $\$22.50/ft^3$ at Hanford, Savannah River, and Idaho Chemical Processing Plants.[15] After deductions for cooling systems and metal linings, space in these underground concrete structures costs about \$3 to $\$4/ft^3$. In comparison, salt is mined for about \$2/ton, which results in a cost for space in salt formations of about $\$0.15/ft^3$.

Since temperatures in ordinary concrete should not be allowed to exceed 400 to 500°F, the use of special high-temperature concretes (which would allow closer spacing of the cylinders) is considered. A concrete

---

*Metric ton.

Table 20. Characteristics and Costs of Vaults and Tanks for Waste Storage

Structure	Volume (ft^3)	Concrete Wall Thickness (in.)	Floor-to-Ceiling Height (ft)	Earth Cover (ft)	Lining Material	Cost ($/$ft^3$)
Vault (Chalk River)	50,000	18	12	15	Stainless Steel	10.70
Tank (Hanford)	71,200	13	18	7	Mild Steel	6.30
Tank (Hanford)	134,000	15	32.5	7	Mild Steel	6.00
Tank (Savannah River)	143,000	36	27	*	Milk Steel	11.20
Tank (ICPP)	40,000	42	21	9	Stainless Steel	22.50

*On the top, radiation shielding is provided by 3 ft 8 in. of concrete.

composed of a high-temperature cement and an aggregate of magnesium-oxide ore (dunite) can withstand temperatures exceeding 1000°F and costs about $130/yd^3$ in place, compared with about $75/yd^3$ for ordinary concrete for this type of structure. If the cost for space with ordinary concrete it taken to be $3/ft^3$, about 60% of which is for concrete, the cost for space with high-temperature concrete is about $4.30/ft^3$.

4.1.2 Space Requirements Using Vaults

The spacing between cylinders in a storage system is controlled by the need to dissipate the heat generated by radioactive decay without reaching temperatures injurious to the storage system. These limiting temperatures are 1650°F for the calcined waste, and range from 500 to 500°F for ordinary concrete to about 1000°F for special high-temperature concretes.

A minimum storage age occurs when the calcined waste and the concrete are simultaneously at their maximum allowable temperatures. For greater ages, the temperature of the concrete controls the spacing between cylinders. That is, with the concrete at its maximum allowable temperature, the waste is below its maximum allowable temperature in the case of cylinders 6 to 24 in. in diameter. Space requirements for acid Purex and reacidified Thorex wastes situated in racks in high-temperature concrete vaults and in salt rooms are shown in Figs. 21, 22, and 23 as functions of age at burial. The calculations for storage in salt rooms above the floor were reported previously.[16] From the graphs it is clear that the greatest savings in space requirements for vaults over the use of salt formations occur for storage at about 10 to 30 yr of age, and over this range of ages the space requirements differ by a constant factor. Hence, a comparison of storage costs at 30 yr of age will suffice for the purposes of this study.

4.1.3 Comparative Storage Costs Between Vaults and Salt

Using space costs of $3, $4.30, and $0.15/ft^3$ for ordinary concrete vaults, high-temperature concrete vaults, and salt, and assuming a floor-to-ceiling height of 15 ft, area costs are $45, $64.50, and $2.25/ft^2$ of

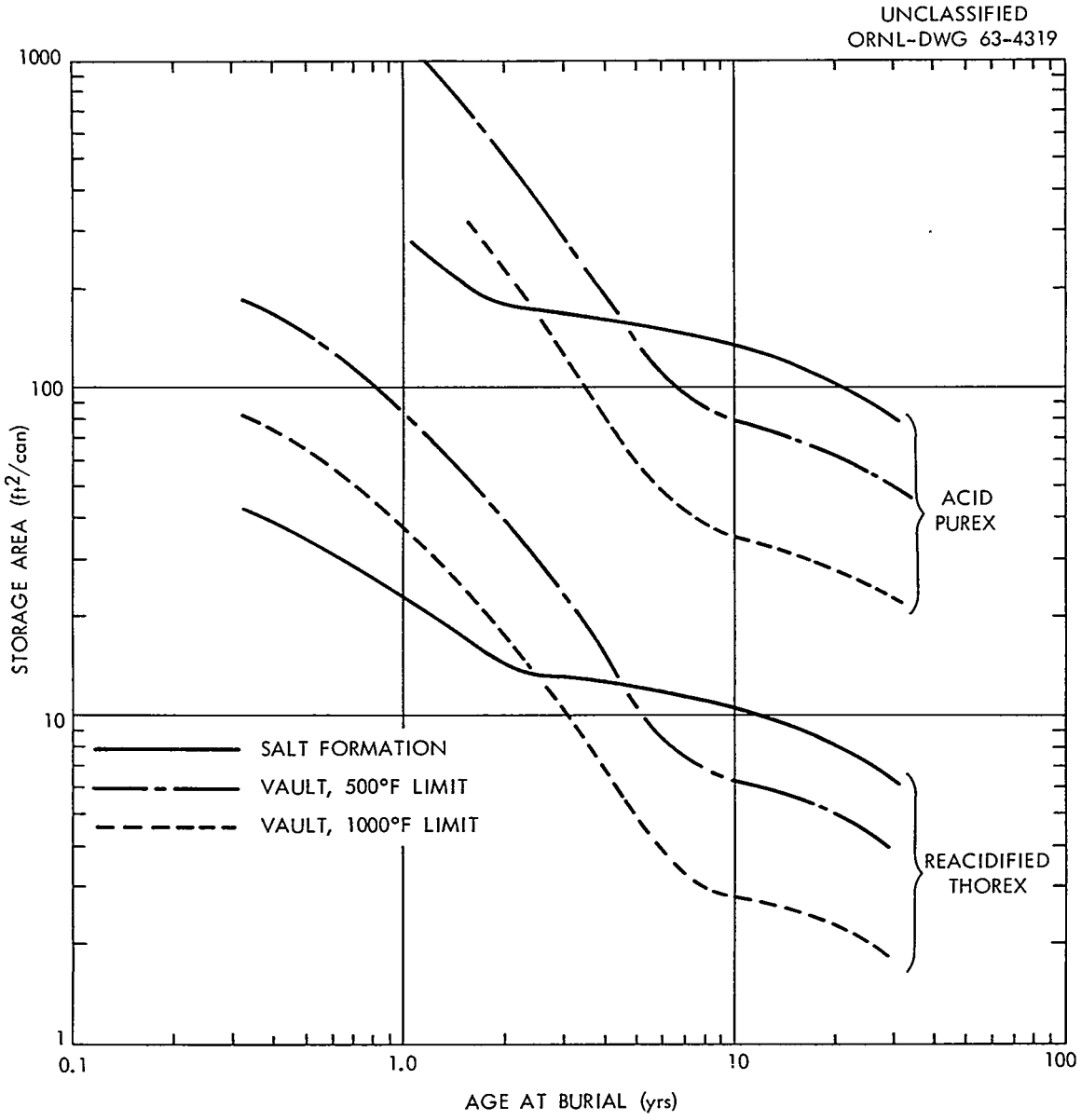

Fig. 21. Storage Areas Required for 6-in.-Diam Cylinders in Salt Formations and Concrete Vaults as Functions of Waste Age.

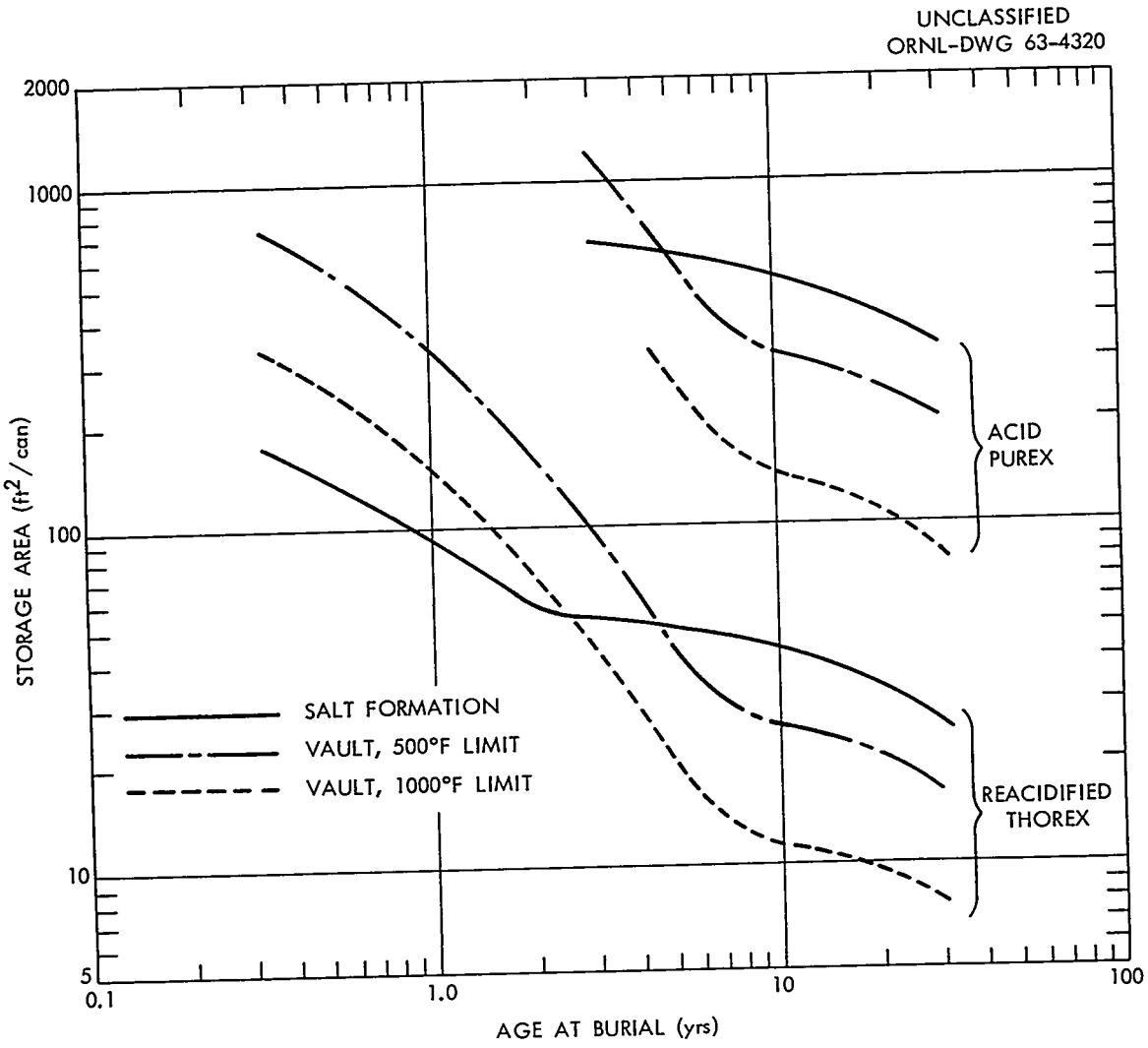

Fig. 22. Storage Areas Required for 12-in.-Diam Cylinders in Salt Formations and Concrete Vaults as Functions of Waste Age.

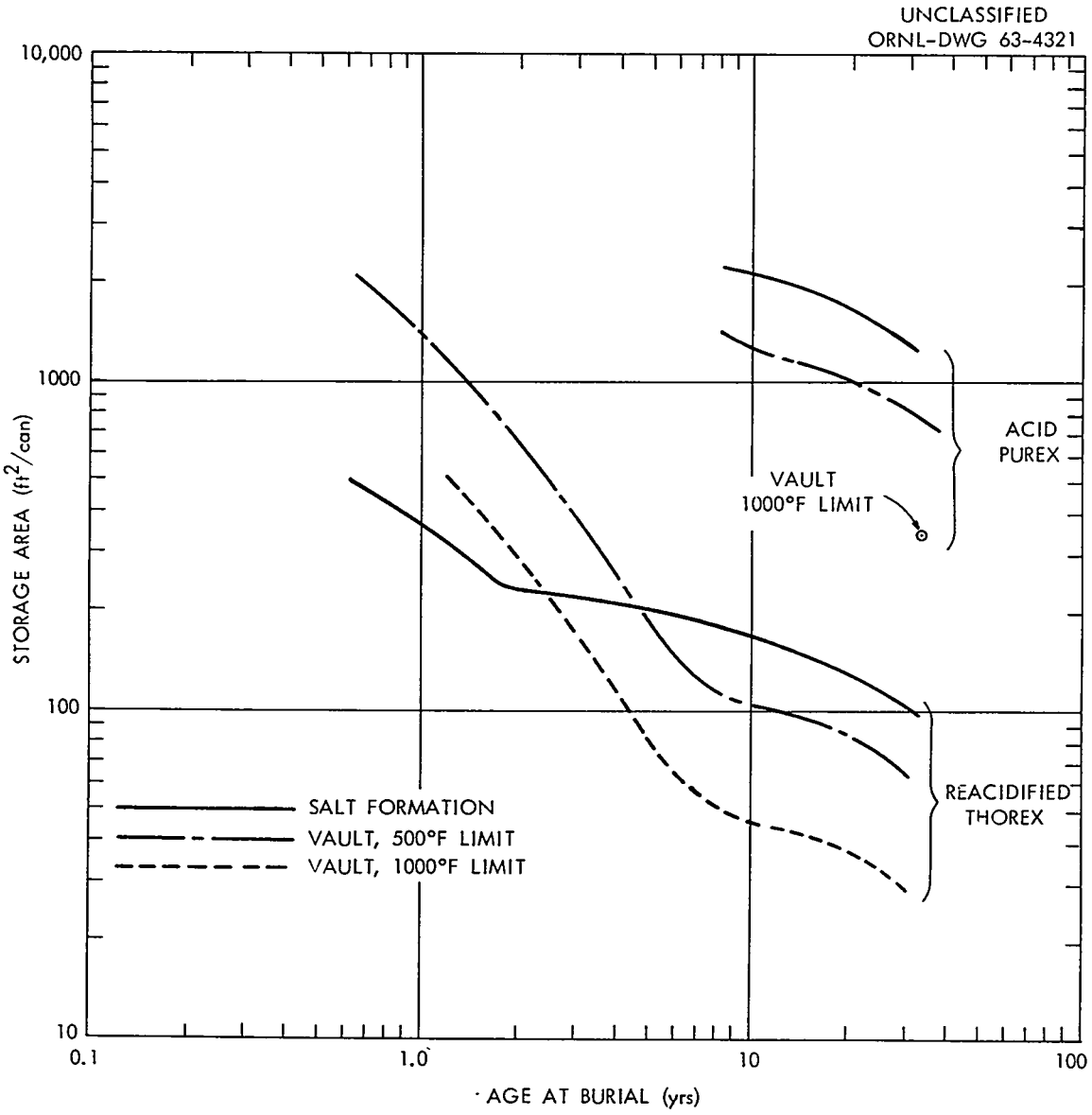

Fig. 23. Storage Areas Required for 24-in.-Diam Cylinders in Salt Formations and Concrete Vaults as Functions of Waste Age.

floor area. Costs of storage space per cylinder were obtained by multiplying these area costs by the space requirements per cylinder in Figs. 21 to 23. The results for a storage age of 30 yr (Figs. 24 and 25) show that high-temperature concrete results in lower costs than ordinary concrete but that, at best, the cost of storage space in concrete vaults is higher by a factor of 8 for both acid Purex waste and reacidified Thorex waste than the cost of storage space in salt formations. In calculating the total costs of storage in salt, 60 to 85% were for salt removal, and, since the other costs (e.g., for handling equipment and labor for storing the cans) would be about the same for all storage systems, the relative total costs would probably differ by factors of 5 to 7.

Costs for Space in Granite Formations.-- A recent estimate of $20/yd^3 has been reported for excavated space in bedrock at the Savannah River Plant.[18] Excavation costs in hard rock (granite or metamorphosed basalt) should range from $9.00 to $15.00 per yd^3, depending on the amount excavated.[17] This estimate is based on advertised bid prices of $9.00 to $12.00 per yd^3 for excavation in granite for Project Norad, an Air Force operation; on a bid price of $12.50 per yd^3 for metamorphosed basalt for a Department of Defense classified project in 1951; and on actual cost records of $9.00 to $13.00 per yd^3 for metamorphosed basalt for a second Department of Defense project in 1954-1957. The cost of shaft sinking is not included in these costs nor is the cost of roof support, if required.

In comparison, excavation costs in salt are about $4.00 per yd^3 (which is equivalent to $2/ton). Excavation costs in hard rock are higher than in salt because heavier equipment is required, drilling is more difficult and is slower, and costs of explosives are higher.

Space Requirements in Granite Formations.-- In calculating space requirements in salt formations, values for thermal conductivity and diffusivity at 300°C (572°F) were used. The thermal conductivities of salt and granite are within 10% of each other in the temperature range of 400 to over 600°F. Since heat capacities are also about the same at 0.21 Btu/lb °F, and densities are not too different, 135 lb/ft^3 for salt and a range of 125 to 187 lb/ft^3 for granite, the thermal diffusivities are nearly equal. Therefore, space requirements in salt and granite formations are about the same within the accuracy of the calculations.

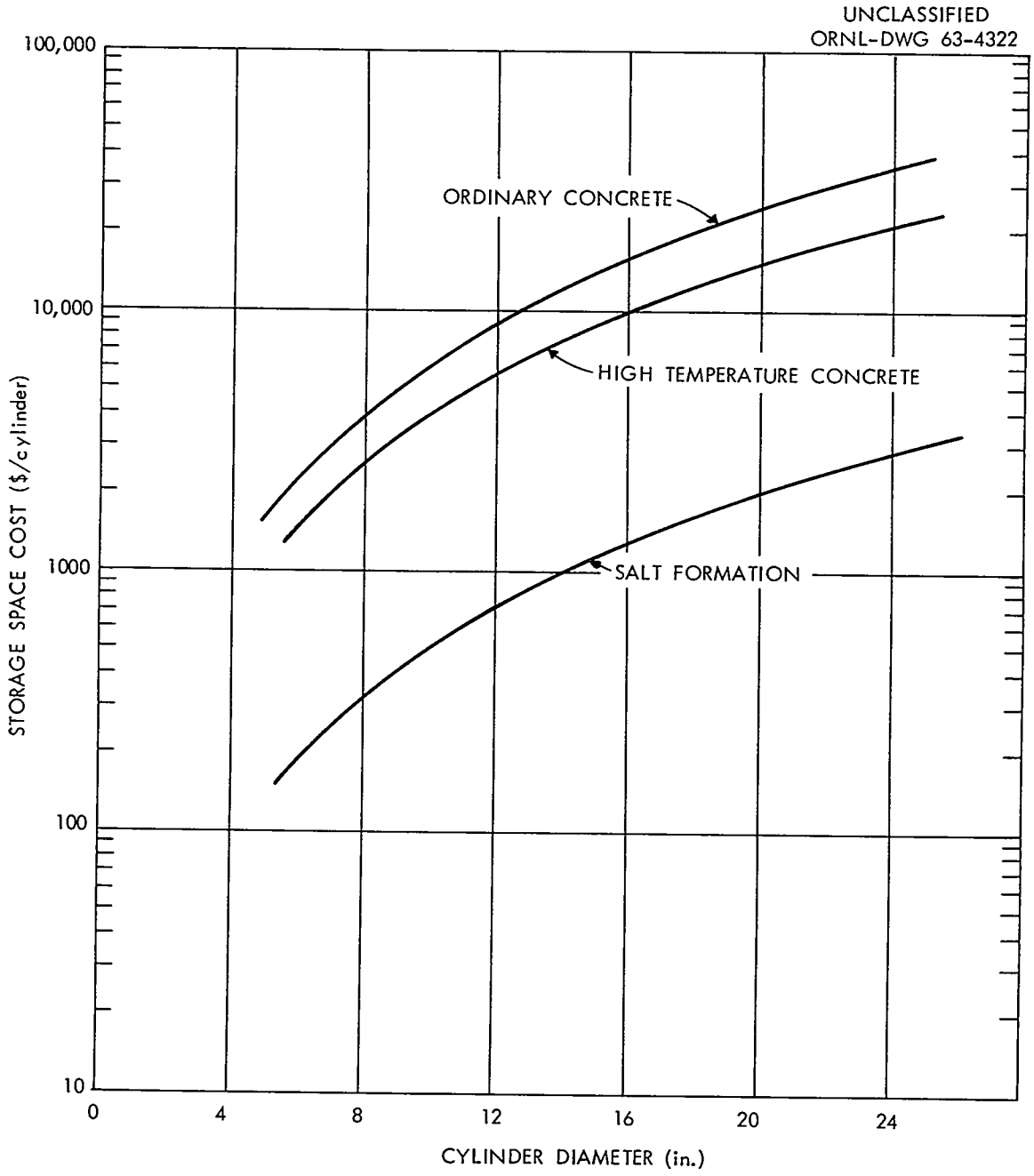

Fig. 24. Cost of Storage Space for Acid Purex Waste in Concrete Vaults and Salt Formations for Waste Aged 30 yr.

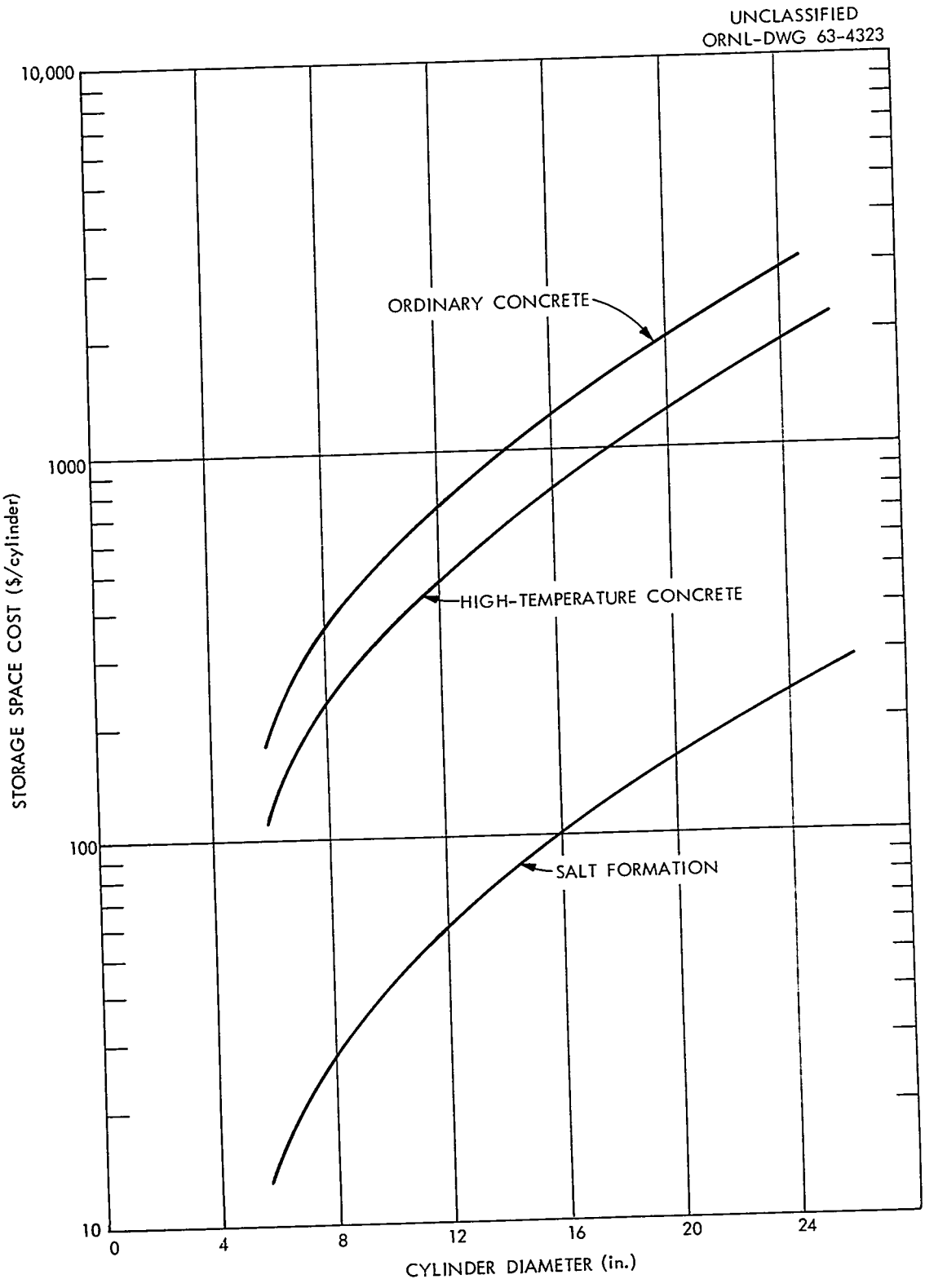

Fig. 25. Cost of Storage Space for Reacidified Thorex Waste in Concrete Vaults and Salt Formations for Waste Aged 30 yr.

Comparative Storage Costs Between Granite and Salt Formations.-- The ratio of rock volume which is mined for storage space and access tunnels to rock volume which must be left as supporting pillars is about the same in granite formations as in salt formations. Therefore, storage in granite formations would require the same amount of mined space, and unmovable capital items (such as concrete structures) would be amortized over the same time period. Assuming other costs (e.g., handling equipment and labor for storing the cans) to be the same also, storage in granite formations would cost about twice as much as storage in salt formations.

4.2 Underground Movement of Fission Products

D. G. Jacobs

One possible route of radioactive waste solutions released by tank failure would be through the geologic formation lying between the tank site and the nearest surface drainageways. A hypothetical tank site at Oak Ridge is located in Conasauga shale on a promontory, with intermittent surface streams passing to the east, south, and west of the tank site. The shale formation is quite impermeable and movement of water is restricted to flow along bedding planes, greatly limiting its velocity and direction.

Samples of the Conasauga shale were obtained below the highly weathered zone in a direct path toward the surface streams. These samples were acidified for removal of calcite, and the exchange capacities were determined by the calcium titration method of Jackson.[19] A mean value of 11 ± 1 meq/100 g was obtained. Overnight refluxing in 7 M HNO_3 at 85°C showed hydrogen ion consumption of 260 meq/100 g, which would be sufficient to cause neutralization of the entire contents of an acid waste tank within 30 ft of the tank. In the case of acid waste, it was assumed that neutralization of the acid by calcite in the formation would result in a calcium salt system. In this system, strontium was assumed to compete with calcium without selectivity of either ion, though strontium might be slightly more selectively sorbed than calcium.[20] For the sorption of strontium from neutralized wastes, and for the sorption of cesium and

ruthenium, information on the sorption properties of Conasauga shale were obtained from previous laboratory studies.[20-24]

The quality of the ground water was assumed to be similar to that of Clinch River water, which has a total cation concentration of about 0.002 meq/ml, primarily calcium and magnesium.[25] Seepage rates were assumed to be characteristic of the area surrounding Waste Pit 2, where the average seepage rate from 1953 to 1958 was 3900 gal/day through an average side-wall area of 9000 ft^2 (ref 26). This corresponds to a mean superficial velocity of 0.064 ft/day. A mean ground-water velocity of 0.67 ft/day was used, which implies approximately 10% efficiency of contact between the shale and solution. If the initial seepage rate were maintained, the daily seepage rate from the acid waste tank (filled to a height of 35 ft with 10^6 gal of waste) would be 2275 gal. The seepage from the neutralized waste tank (filled to a height of 36 ft with 1.25×10^6 gal of waste) would be 2340 gal.

Dispersion properties of solution in the formation (Fig. 26) were estimated from the results of a chloride tracer test conducted at the site.[28] These data indicate an effective plate height of 46.5, according to the notation of Glueckauf.[27]

4.2.1 Calculation of Radionuclide Movement

In addition to the assumptions outlined above, it was further assumed that the waste would move longitudinally through a zone 75 ft wide, with a height equal to the original liquid level in the waste tank, to surface water at a distance of 200 ft. No allowance was made for lateral dispersion, but the spread of the solute was assumed to occur according to Glueckauf's model for the elution of a band of solute through a linear ion exchange column. The porosity of the shale effectively contacted by solution was assumed to be 25%, with a grain density of 2.64 g/ml.

If a leak were to develop in a waste tank, the amount of solution lost to the formation would be limited by the ability of the formation to accept the solution. During percolation of the waste solution, the ground-water concentration in the zone of migration is increased, returning to normal when the waste solution is again displaced by the local ground water.

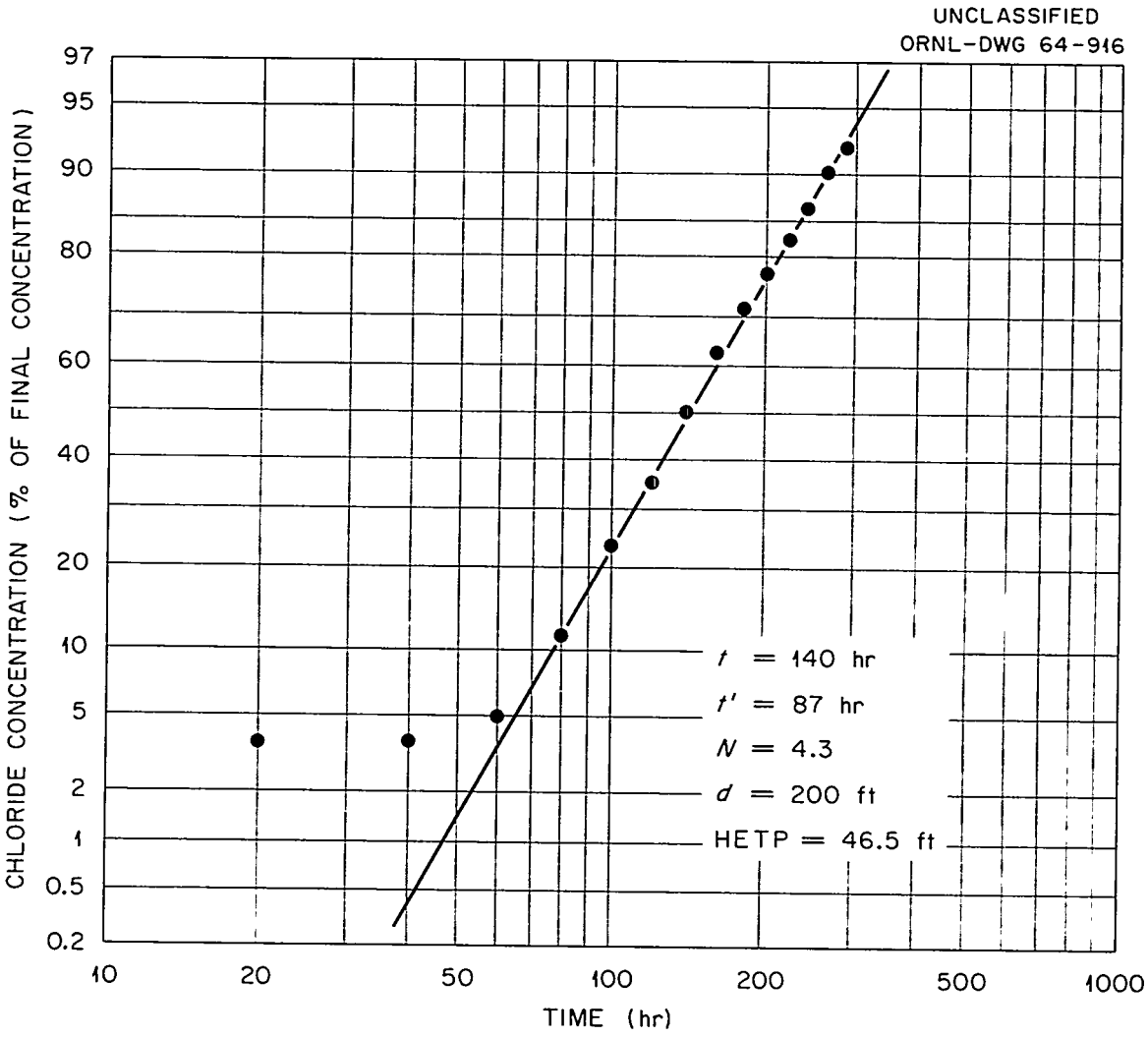

Fig. 26. Chloride Dispersion Properties of Conasauga Shale at Four-Acre Site.

Movement and dispersion of the specific radionuclides were estimated by using Glueckauf's model in order to describe the dispersion of the unsorbed anions and correcting for retention of the radionuclides by the formation, as discussed by Inoue and Kaufman.[28] However, due to the changing electrolyte concentration of ground water, the retention factor is not constant with time. In addition, radioactive decay was considered.

The results of calculations for the movement of Sr^{90} from an acid tank are shown in Fig. 27. The initial peak in Sr^{90} activity at the surface drainageway occurs at about 1 yr and is due to the relatively slight sorption of strontium by the shale in the presence of high concentrations of electrolyte. With time, these high concentrations of salt are diluted and replaced by fresh ground water, and a second concentration peak occurs after about 150 yr. The relative magnitude of these two peaks depends on the total quantity of electrolyte released to the formation. If, after a leak occurs, the waste solution is pumped from the ground, the initial rapid movement will not be observed, due to the removal of the excess electrolyte. Furthermore, in the case of Sr^{90} in an acid waste system, an appreciable fraction of the total activity could be removed (Table 21).

Table 21. Recovery of Radionuclides from the Soil After a Leak Has Developed in a Waste Tank

Isotope	Percentage Recoverable	
	Acid Waste	Neutralized Waste
Sr^{90}	88	< 1
Cs^{137}	2	< 1
Ru^{106}	18	20

For neutralized waste, the precipitation of strontium, in addition to the increased probability for ion exchange, prevents Sr^{90} from attaining any significant concentration at the surface drainageways. The high affinity of the Conasauga shale for cesium deters movement of Cs^{137} so that radioactive decay occurs before significant concentrations would be

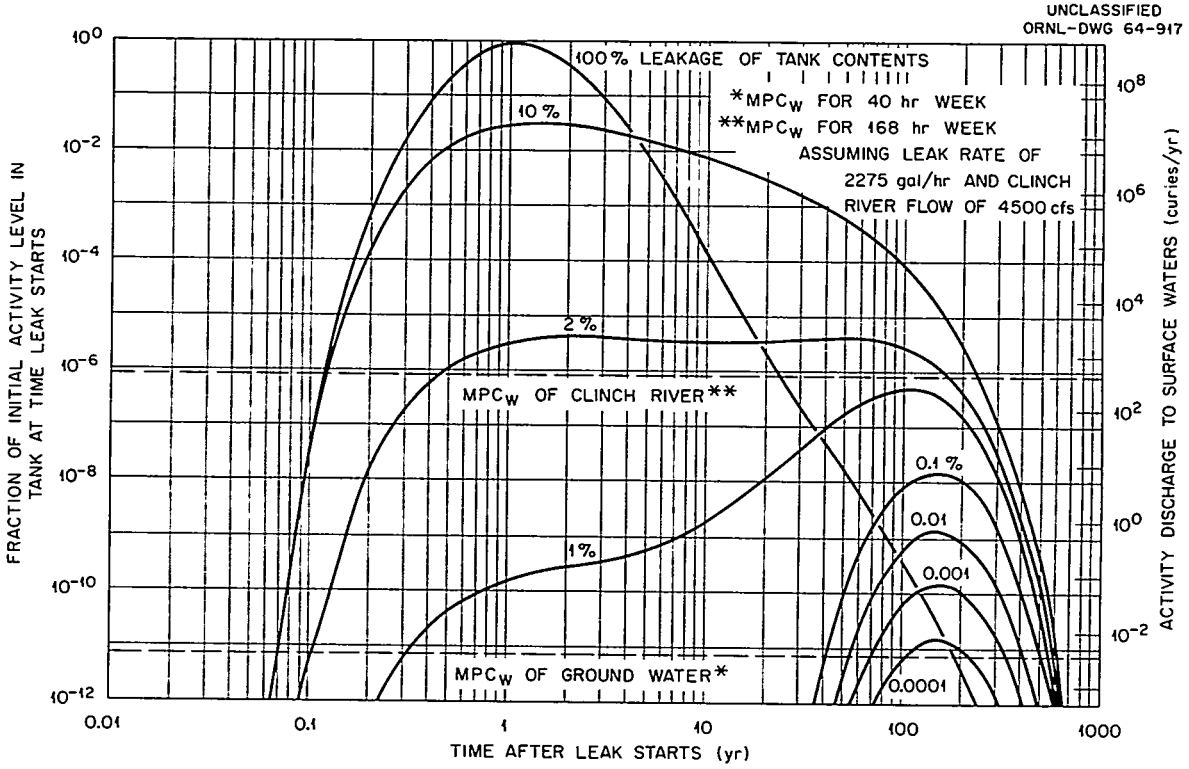

Fig. 27. Strontium-90 Activity in the Ground Water at a Plant 200 ft from a Leaking Tank of Acid Waste.

observed in either acid or neutralized waste systems. The relatively rapid decay of Ru^{106} (half-life = 1 yr) would prevent it from attaining significantly high levels at surface seeps unless a very extensive leak were to occur.

4.2.2 Distribution of Fission Products in the Soil

The distribution of fission products in the soil is important because of the thermal problems that are likely to result from high concentrations of activity in a medium that has poor heat-conducting properties. The distribution of radionuclides in the soil was estimated by using Glueckauf's expression for the build-up of activity in an ion exchange column. The distribution of cesium in the soil was further modified because of its nonlinear absorption isotherm, which gives a very sharp sorption front.[29] The results of these estimations are shown in Figs. 28 and 29. With respect to neutralized wastes, both Cs^{137} and Sr^{90} are retained close to the leaking tank, but Ru^{106} moves through the soil, causing a significant build-up of activity away from the tank. As to acid wastes, the Sr^{90} moves even faster than the ruthenium, and the entire 200-ft seepage zone is brought to a dangerously high level of contamination.

4.2.3 Conclusions

In a formation similar to Conasauga shale, the slow rate of percolation of the solution, combined with rather high sorptive properties of the formation (except for Sr^{90} in an acid waste system), would tend to prevent the rapid release of large quantities of radionuclides directly into surface waterways. However, this delay would result in the build-up of activity in the formation to levels that would probably present a serious thermal problem. The delay time afforded by the formation could be used for remedial measures, such as pumping ground water from the formation to recover the unsorbed radionuclides and for preventing further transport of the fission products.

The absolute values for radionuclide movement that have been calculated and presented in this discussion should not be considered to be precise, since the estimates were based on a rather inadequate description of the site. However, the procedure for making these estimations could be

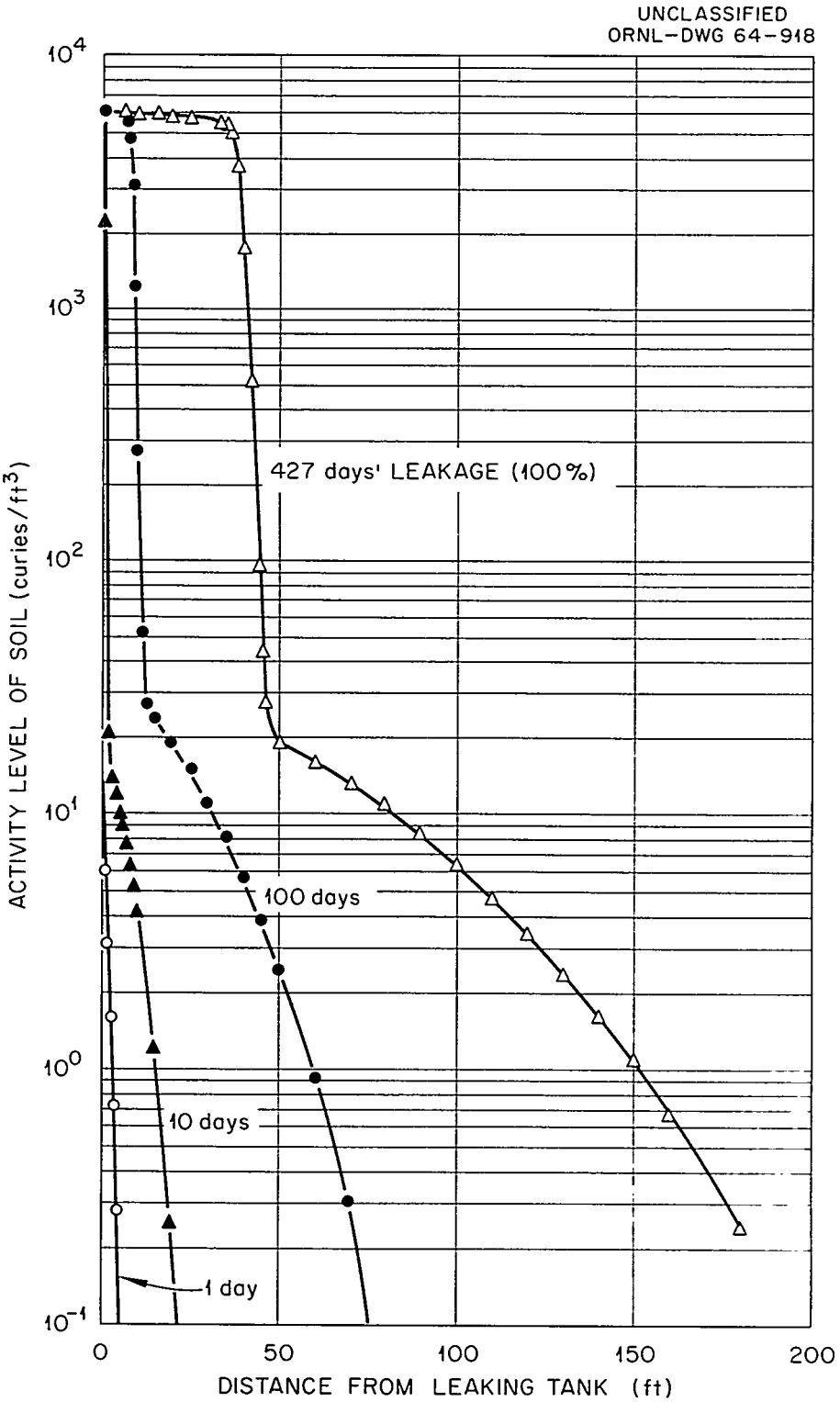

Fig. 28. Distribution of Activity in Conasauga Shale Following a Leak in a Tank of Neutralized Waste. Only cesium-137, strontium-90, and ruthenium-106 are considered.

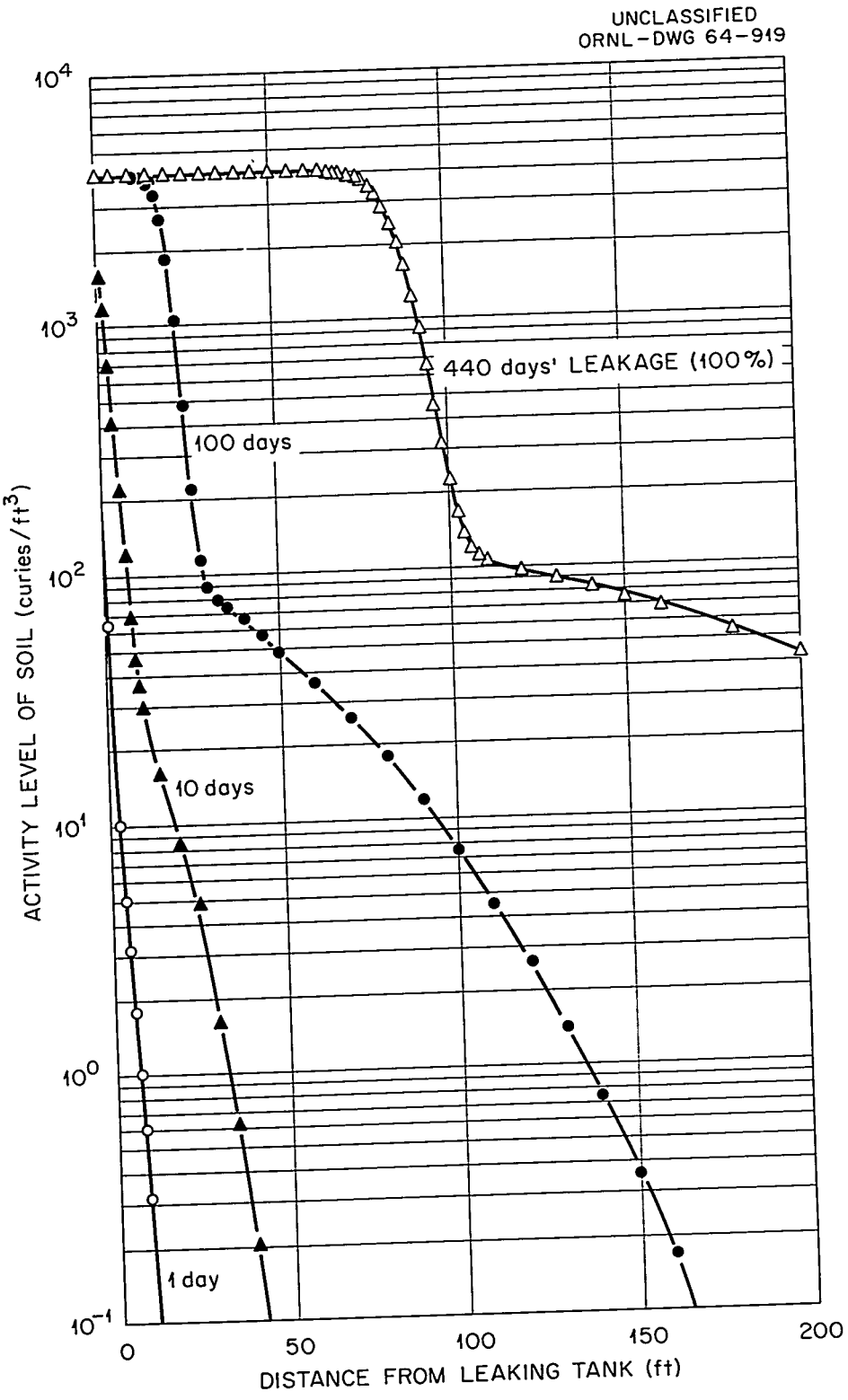

Fig. 29. Distribution of Activity in Conasauga Shale Following a Leak in a Tank of Acid Waste. Only cesium-137, strontium-90, and ruthenium-106 are considered.

applied for any proposed site. Actual tests of seepage and dispersion at a proposed site employing the layout of the tank system would provide a more adequate base for such calculations.

5. DISPOSAL IN DEEP WELLS

5.1 Disposal by Hydraulic Fracturing

5.1.1 Geology of the Hydrofracturing Pilot Plant Site (W. de Laguna)

Cores from the Joy No. 1 deep test well, located about 600 ft southwest on strike from the injection well of the hydrofracturing pilot plant (well 1), suggested that the injection well would reach the top of the Rome sandstone at about 1025 ft. The contact was in fact found at 1022 ft, showing that no structural complexities are present in the shale between these two wells. The cores also showed the average dip of the Rome and of the overlying Conasauga shale in this area to be between 10 and 15°, although, as the dip varies from 0 to 30° and is locally even vertical or overturned, the average is difficult to estimate. However, the cased observation well (well 2), located 150 ft directly updip from the injection well and which should therefore have reached the top of the Rome some 30 to 50 ft higher, found the contact at 1019 ft, only 3 ft higher. (Depths here are all referred to a common datun, the main flange on the injection well.) Marker beds found in well 1 at depths of 702, 682, 479, and 438 ft were found in well 2 at 686, 667, 465, and 421 ft, that is, from 14 to 17 ft higher. These beds are all in the gray calcareous section of the Conasauga, with the exception of the bed at 702 ft, which marks the upper contact of the red shale, that member into which the waste slurries will be injected. These differences in elevation correspond to an average dip of about 6° in the gray shale, which is abnormally low. The upper contact of the Rome is very unlikely to be horizontal.

The cased overburden monitoring well (well 3) is located about 70 ft north and 50 ft updip from well 2. It has been drilled so far only to a depth of 500 ft. The upper two key beds found in wells 1 and 2 were reached in this well at depths of 451 and 410 ft, that is, 14 and 11 ft higher than in well 2, which corresponds to a dip of about 15°.

These data warn that there may be an abnormality in the structure of the lower Conasauga between well 1 and well 2. The most probable abnormalities would be: (1) a local gentle monoclinal roll in the regional structure resulting in flatter dips in this area, (2) a high-angle thrust

fault between the two wells which would uplift well 1 stratigraphically with respect to well 2, or (3) a zone of overturned faults and folds. Possibilities (1) and (2) would have little influence on the fracturing of the rocks and hence on their use for waste disposal by hydraulic fracturing; but, a large overthrust fold, or a zone of rock containing many small folds and associated faults, might alter the fracture pattern seriously. Observations of surface exposures of the upper Rome and lower Conasauga in road cuts and outcrops show that gentle monoclinal folds, sharp overturned drag folds of a wide variety of amplitudes, and small overthrust strike faults are all common, but the data are too sparse to determine either the details of local structure or the general structural patterns.

The two most serious deficiencies in available data are: (1) the lack of oriented cores (Wells 1 and 2 were not cored.), so that dips cannot be plotted directly; and (2) the lack of any key beds in the approximately 300 ft of red shale that lies between the top of the Rome and the bottom of the "gray shales" of the Conasauga.

This red shale is the section into which the injections will be made, and it was selected because it is uniform in composition and uniformly thin-bedded. Coring and logging of closely spaced wells at the site of the second fracturing experiment failed to locate key marker beds or to define the structure in this shale because it is so uniform, and, consequently, no preliminary underground exploration was attempted as an aid in selecting the site for the hydrofracturing pilot plant. No core drilling or logging program within limits of the budget could have proved or disproved the presence of structures such as major drag folds within the red shale.

There is, however, some additional information that may be derived from the geophysical logs run in wells 1 and 2 at the pilot-plant site and, in particular, from a comparison of the gamma-ray logs, the caliper (well diameter) logs, the gamma-gamma density logs, and the neutron logs. Methods used to interpret these logs will not be described here, but the data suggested low density, enlarged diameter, and apparent high-water content in well 1 at depths of 950 and 990 ft, probably due to minor bedding-plane faults, and showed a possible fault at 1016 ft. The logs

also show low-density readings at depths of 862, 934, 960, and 975 ft, but these are associated with apparent low porosity or low hydrogen content on the neutron-gamma log, and the caliper log shows no significant enlargement of the well diameter of these depths. If these are faults, the fault zones are probably thin, and one must assume some such unusual complication, such as that the faulting had partially dehydrated the clay minerals in the fault gouge, and that the gouge is sufficiently impermeable so that the clay minerals did not readsorb the lost water. This is not a convincing hypothesis.

Low density, enlargement of the well diameter, and high porosity (hydrogen) in well 2 at depths of 1015, 1001, and 982 ft strongly suggest faults. A low rock density at 967 ft is associated with a normal well diameter and what is either a low porosity or a low hydrogen reading. Again, this could be a fault, but some other explanation is more probable. In well 2 there is also a marked peak in the gamma-neutron log at 860 ft, although the rock density and well-bore diameter are normal at this depth. There is a strong temptation to correlate the peak in the neutron-gamma log at 864 ft in well 1 with the very similar peak at 860 ft in well 2 and to attribute them not to faulting but to a bed that is for some reason either low in hydrogen or high in some element or elements that yield relatively hard gamma rays after neutron capture.

The core drilling scheduled to follow the first series of waste-mix injections may answer some of the problems raised by the logging of these two large-diameter wells. At present what is known may be summarized as follows:

1. The dip of the beds between wells 1 and 2 is low. This may be the result of either a gentle monoclinal structure which would, if anything, promote the formation of bedding-plane fractures, or it may be the result of a more complex structure, which could complicate, even seriously, the configuration of the fractures that will be formed by the waste injections. Core drilling after the first waste injections will likely answer this question.

2. There are zones of weak and probably broken rock in the approximately 50 ft of shale immediately above the Rome sandstone. These may well be bedding-plane faults parallel to the contact between the more

competent Rome and the less competent Conasauga formations. If so, they represent no problem to the proposed waste injections. They may, however, have introduced complications into the water-injection experiments described below.

3. There is a suggestion that there may be a few faults filled with tight clay gouge up to as high as 860 ft in well 1, but some alternative explanation is more probable. There is no evidence of faulting or weak rock between 860 and 710 ft; so, except for possible drag folds that would not be revealed by logging, the upper half of the 300 ft of red shale into which the waste mixtures are to be injected appears to be favorable for the operation.

5.1.2 Preliminary Water Injections (W. de Laguna)

Water-injection tests were first discussed at a meeting of the Advisory Committee on Waste Disposal on Land of the Earth Sciences Division of the NAS-NRC, held at Savannah River on December 7 and 8, 1961. The first report on the second fracturing experiment was presented to the committee at that time, and the discussion that followed centered around the committee's admonition that similar results should not be taken for granted in other areas. Indeed, it was the consensus that each site considered for disposal by hydraulic fracturing would have to be tested. This raised the question as to whether relatively inexpensive fracturing tests with water could be used, if not for a final evaluation, at least for a preliminary screening. The conclusion was that if fracturing with water required pressures substantially greater than the overburden pressure, horizontal fracturing could be presumed, though not proved; but, if fracturing pressures were less than the weight of the overburden, the fractures could not possibly be horizontal. Admittedly, there might be tests in which the pressure would be roughly equal to the overburden, so no conclusions would be possible.

An additional incentive for making water-injection tests at Oak Ridge resulted from development work on waste-cement mixtures suitable for use in the forthcoming waste injections. The immediate point of interest was that fluid-loss additives were responsible for about half the cost of the ingredients in a mix that appeared to have the most desirable properties.

However, there was no assurance that low fluid loss was desirable or even necessary. The fluid-loss additives used in the petroleum industry, and the laboratory methods employed to test the fluid loss of mixtures, are both designed for use with rocks, such as sandstones which have permeabilities four or five orders of magnitude higher than the permeability of the Conasauga shale. These considerations raised the following questions: (1) Is there fluid loss when water is injected into the lower Conasauga shale by fracturing? (2) If so, where does the fluid go? (3) Can the fluid loss be reduced by the use of conventional fluid-loss additives? The purpose in making the water-injection tests was to find answers to these three questions and to observe the results of a series of water-injection tests in an environment that earlier work had shown would probably give bedding-plane fractures.

Water Test Procedure.-- Four water injections have been made. The first three, with clear water into a slot at 986 ft in the injection well (well 1) at the pilot-plant site, used volumes of 2000, 50,000, and 23,000 gal. The fourth, with 50,000 gal of water containing fluid-loss additives, was made into a slot in the same well at a depth of 966 ft. The first test, which was terminated after four days, served primarily to establish the test procedure used in the later tests. The final phase of the second and third injections each extended over about 50 days; as to the fourth injection, the final phase is now in progress.

The test procedure consisted of five phases: (1) injecting the water (or water plus fluid-loss additive); (2) shutting in the well for 48 hr and observing the drop in pressure - designated as the "first shutin" phase; (3) opening the well for 48 hr, but limiting the flow rate to 10 gpm until the natural flow rate fell below this value, and observing the time and volume back-flowed - designated as the "first backflow" phase; (4) shutting in the well again for 24 hr and observing the pressure rise as a function of time - designated as the "second shutin" phase; and (5) reopening the well and observing the rate of flow and total cumulative volume recovered - designated as the "second backflow" phase.

Results.-- Although the results are incomplete at this writing, it is possible to draw the following conclusions:

1. First Phase. In all four tests, the fracturing pressures and injection pressures were substantially above the overburden pressure, which is strong presumptive evidence that bedding-plane fractures had been formed (Fig. 30).

2. Second Phase. In all cases, the pressure fell from some higher value almost asymptotically down to the overburden pressure, although there was a very slow continued drop after this pressure had been reached (Fig. 31). Presumably this first shutin phase represents the squeezing shut of the fracture, which at the close of the injection is held open by the water, until the fracture walls are sufficiently in contact so that the water need no longer carry the full load of the overburden. As the fracture is squeezed shut, the water must be squeezed out, either into the pores or minute fractures in the rock, or updip by a slow continuation of the fracturing. In a more permeable and more porous formation the fluid-loss additives would certainly reduce the rate of flow of water out into pores or minute fractures, but their ability to measurably reduce water loss into a far less permeable and porous shale is problematical. However, the similarity of this and the following phases of the two 50,000-gal injections, with and without the fluid-loss additives, clearly answers one of the original questions: Whatever the mechanism of fluid loss, the fluid-loss additives have little influence on its rate and are probably not required in the waste-cement mixes to be used for the waste injections.

3. Third Phase. The length of time and the volume back flowed in order that the wellhead valve could be opened fully varied considerably between the three major injections and was one of the major factors responsible for the differences in the volumes recovered during the first backflow phase of the tests (Fig. 32). The volume flowed back until the wellhead valve could be opened completely and probably represents the volume that had to be removed in each case before the fracture near the well had closed back tightly enough to limit the flow to no more than 10 gpm. This volume might be expected to vary considerably, depending on how smooth or ragged the fracture is near the well. In the first 50,000-gal injection (water only), about 7000 gal was back flowed before this point was reached. In the last injection of 50,000 gal of water containing

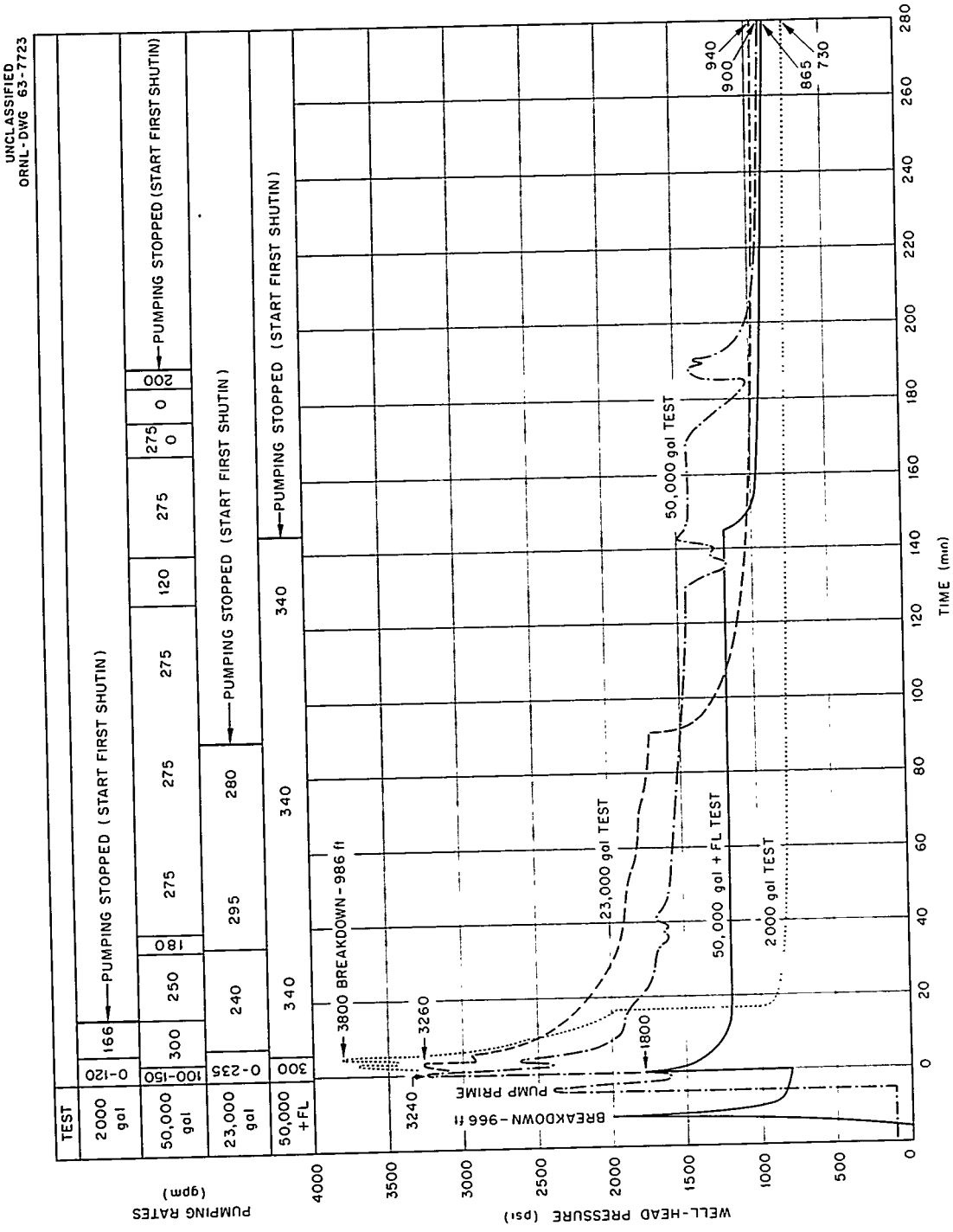

Fig. 30. Water Injection Tests Phase 1 Injection.

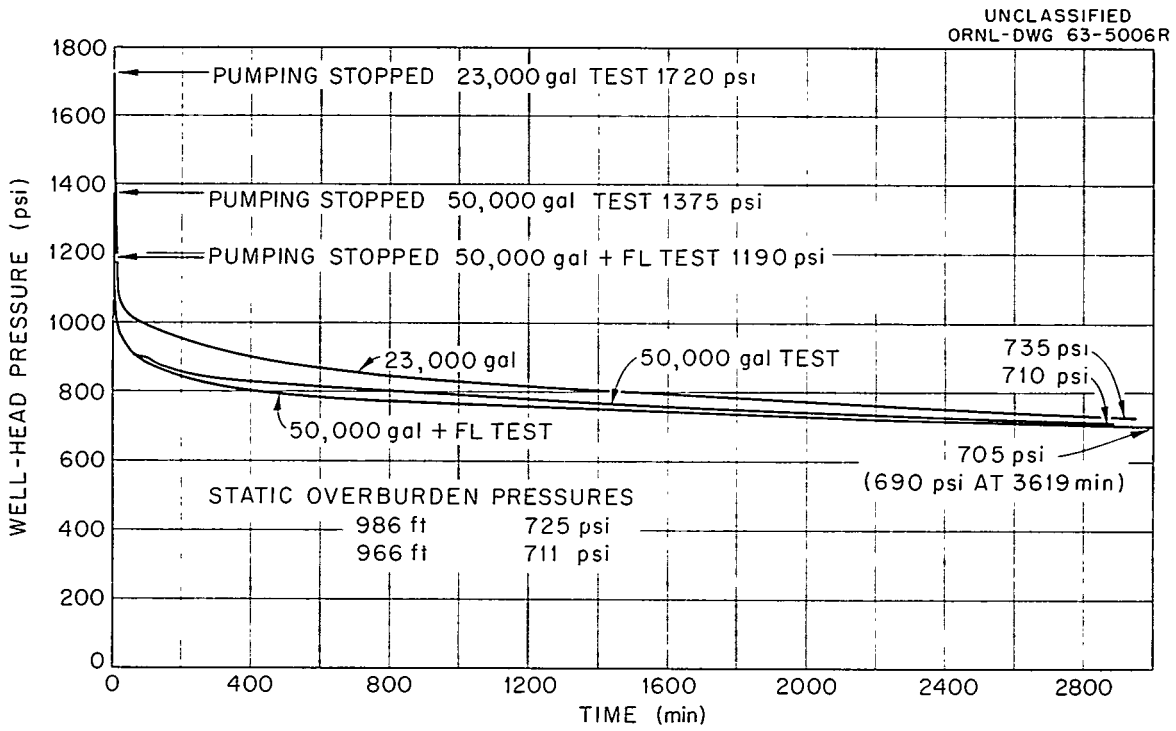

Fig. 31. Water Injection Tests Phase 2 First Shutin.

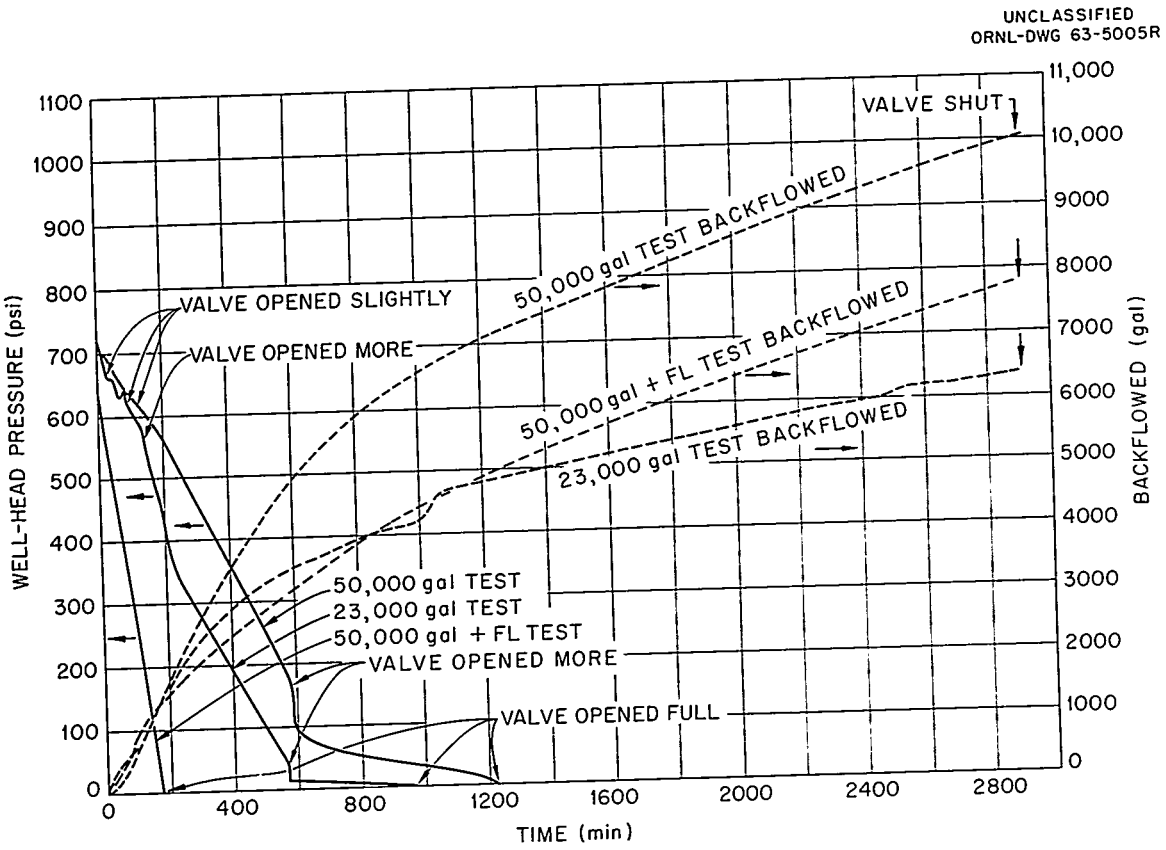

Fig. 32. Water Injection Tests Phase 3 - First Backflow.

fluid-loss additives, a backflow of only 1350 gal of water was required. The rest of the backflow curves, when plotted as volume back flowed versus time, have the same slope but are separated by a volume of 5650 (7000 to 1350) gal. The factors controlling the second and longer part of this "first back-flow" phase are therefore something other than the conditions immediately adjacent to the well and were much the same for the three major injections.

4. Fourth Phase. During the "first back-flow" the pressure of the overlying rock was forcing the liquid back to and up the well, and there must have been a pressure gradient along the fracture. When the well is shut in, the flow continues until the pressure comes to equilibrium at a value where the pressure in the liquid and the pressure of rock against rock just suffice to support the weight of the overburden (Fig. 33). The equilibrium pressure is therefore an indication of the proportion of the fracture still held open by the contained water. The time required to reach equilibrium is an indication of two things: the distances through which various volumes of water must move to establish this condition and the transmissivity of the fracture. In the two 50,000-gal injections, the equilibrium pressure had been reached after 24 hr and was almost identical for the two tests - 443 psi for the first and 450 for the second. However, the pressure increased toward the equilibrium value more rapidly in the second test. Other evidence, including the rates of flow and volumes recovered during the two back-flow phases, suggest that this fracture is not more permeable than the other, but rather that the movement of a smaller volume of water was sufficient to establish equilibrium. The near identity of the equilibrium pressures is one of the reasons for believing that the fluid-loss additives had little effect on either the fracturing or the fluid loss under the conditions of these experiments.

A total of 23,000 gal was recovered during the two flow-back phases of the first 50,000-gal water injection. If there had been no other fluid loss from the fracture, the reintroduction of 23,000 gal into the fracture should have re-established essentially the same conditions present at the close of the original injection; this is the reason why the third test consisted of pumping 23,000 gal back into this fracture. So many factors affect the injection pressure curve that the higher injection pressures

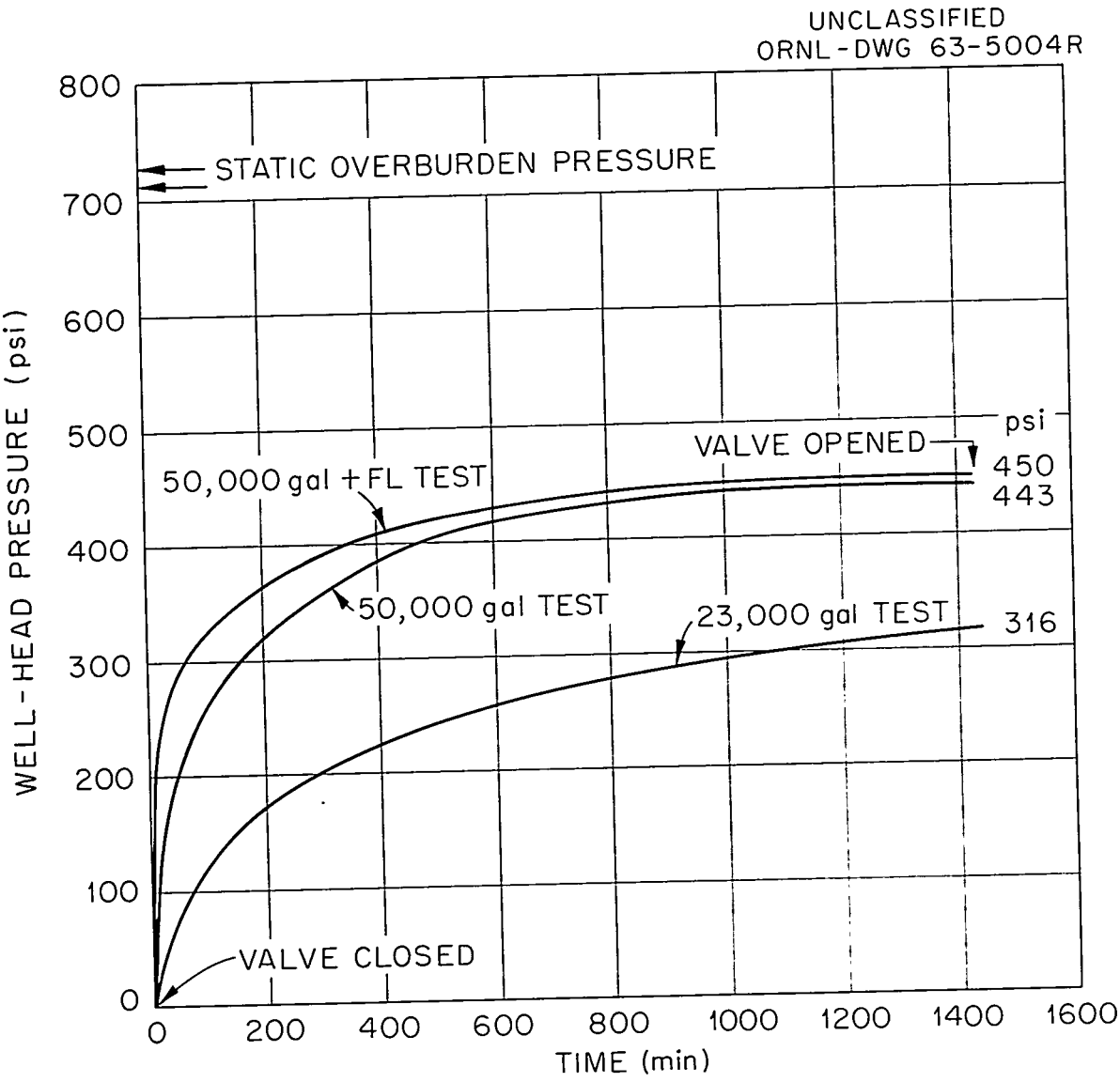

Fig. 33. Water Injection Test Phase 4 Second Shutin.

required to put back the 23,000 gal cannot be explained. Local conditions near the well, quite possibly changed by the additional fracturing or the movement of rock chips during the second injection, could have changed the first part of the first back-flow phase of the test and might even have reduced the total volume recovered during this relatively brief period. However, the time-pressure curve for the second shutin phase of the 23,000-gal test rises much less rapidly than the curve for the 50,000-gal test, and although equilibrium had not been reached at the end of 24 hr, the pressure at this time was only 316 psi, and the slope of the curve suggests that the equilibrium pressure would be between 350 and 400 psi. The difference in slope could be explained by several factors, for example, a lower transmissivity of the fracture, as suggested also by the higher pumping pressures, or by an extension of the fracture updip during the second injection. But, the lower equilibrium pressure shows that more of the overburden load was being carried by the rock, so more of the fracture must have squeezed back together. This in turn shows that the original conditions had not been re-established by the reintroduction of the 23,000 gal and suggests "fluid loss," although it does little to tell where the fluid went.

5. Fifth Phase. In the last three tests the wellhead pressure dropped to zero almost immediately, and it was possible to open the valve completely after only a few gallons had been recovered. The data recorded was the rate of flow and the volume recovered. The time-versus-rate curves for the two 50,000-gal injections were almost identical, although this part of the test runs for 50 days, and the final portion of the curve for the last test has not yet been completed (Fig. 34).

The flow rate from the 23,000-gal test fell much more rapidly with time for the first 100 hr after the final flowback was started, but then the curve flattened and after 900 hr joined and, from then on, followed the time-rate curve from the earlier test.

A plot of the volume of water remaining in the fracture, either as a function of time or as a function of the rate of flow, makes it clear that even if these curves were extrapolated to infinity, a large portion, somewhere between a half and a third of the volume injected, would remain underground. In the first 50,000-gal test, 10,000 gal was recovered in

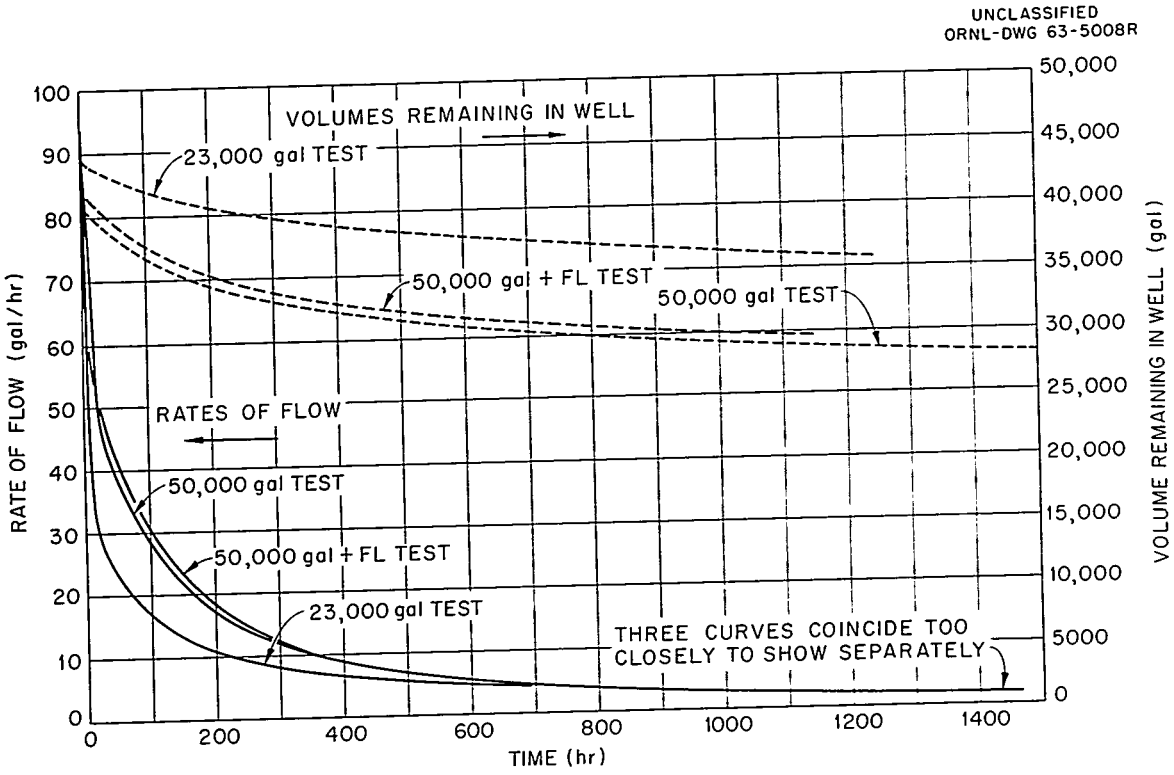

Fig. 34. Water Injection Test Phase 5 Final Backflow.

the 48-hr first back-flow and an additional 13,000 gal in the approximately 50 days of the second back-flow, at which time the rate of flow was less than 2 gpm and still declining. A total of 13,500 gal was recovered from the 23,000-gal test - 6400 in the first back-flow. The recovery from the 50,000 gal of water containing fluid-loss additives is still continuing but will total after 50 days slightly less than 23,000 gal. This final phase of the tests shows, as did the second shutin, such a striking similarity between the injections with and without fluid-loss additives that whatever the mechanism of the fluid loss, it is not affected by the additives, and, consequently, there appears to be little incentive to use them.

5.1.3 Test of Slotting Operation (W. de Laguna and H. O. Weeren)

In the course of the water injections it was necessary to slot the casing of the injection well on two separate occasions by using a high-pressure water-sand jet. Since the method was the same as that planned for use during regular operations, these preliminary injections offered a good opportunity to evaluate the slotting procedure and, if necessary, to modify it.

For the first water test, the sand-water slurry was pumped for 20 min, then the formation was fractured at a wellhead pressure of 3700 psi. For the fourth test, the slurry was again pumped for 20 min. This time, however, a pressure of 4500 psi failed to produce a fracture. It was concluded that the casing had not been penetrated; so, the slotting operation was repeated - this time for an hour. When pressure was applied again, the formation fractured at 2000 psi.

The difference that was observed between the fracturing (and injection) pressures in the two cases leads to the conclusions that for the first test the casing was perforated but not severed, and, in the initial operation of slotting for the fourth test, the casing was neither perforated nor severed. It was only after a much longer slotting operation that the casing was perforated. If this is indeed so, some modifications of the proposed operating procedure for slotting will be necessary.

5.1.4 Plant Construction (R. C. Sexton)

Construction is proceeding on the remaining portion of the injection plant. The four bulk storage tanks have been erected; the underground piping has been installed; the foundations of the cells have been poured; and construction of the cell walls has been started. Figure 35 shows the progress of construction. Shown are three of the storage tanks, the wellhead, and the lower part of the walls of the wellhead and mixer cells.

5.1.5 Mix Development (T. Tamura)

During this period considerable attention was directed toward the development of cheap mixes that would exhibit acceptable characteristics for application in the forthcoming waste injections. An economic study of hydrofracturing disposal costs showed that mix costs are a very significant part of the overall cost. Several mixes were developed, and they are pumpable, have an adequate pumping time, a low-fluid loss, and will set to form a strong, homogeneous grout. However, these mixes cost about 20 to 35¢ per gallon of waste. The objective of the work, then, has been to develop mixes whose properties, though not completely ideal in all respects, meet these principal requirements:

1. The slurry must be pumpable for long enough to complete the disposal operation.
2. The slurry must set as a homogeneous solid without phase separation.

Cement Concentration.-- If the amount of cement used with each gallon of waste is increased, the compressive strength of seven-day cured grout may be increased to at least 1000 psi. This effect is shown in Fig. 36. Also shown is the cement cost (1¢/lb) per gallon of waste for different cement concentrations. Quite obviously, if high-strength grout is desired, up to 15 lb of cement must be used per gallon, and the mix will be expensive. If a grout strength of about 100 psi can be tolerated, a mix with 4 to 5 lb of cement per gallon can be used, and the mix cost will be drastically decreased.

Suspending Agents.-- When a slurry containing only 4 to 5 lb of cement per gallon of waste is allowed to stand without stirring, a dense settled phase will form, with a lighter liquid suspension on the top. To take up

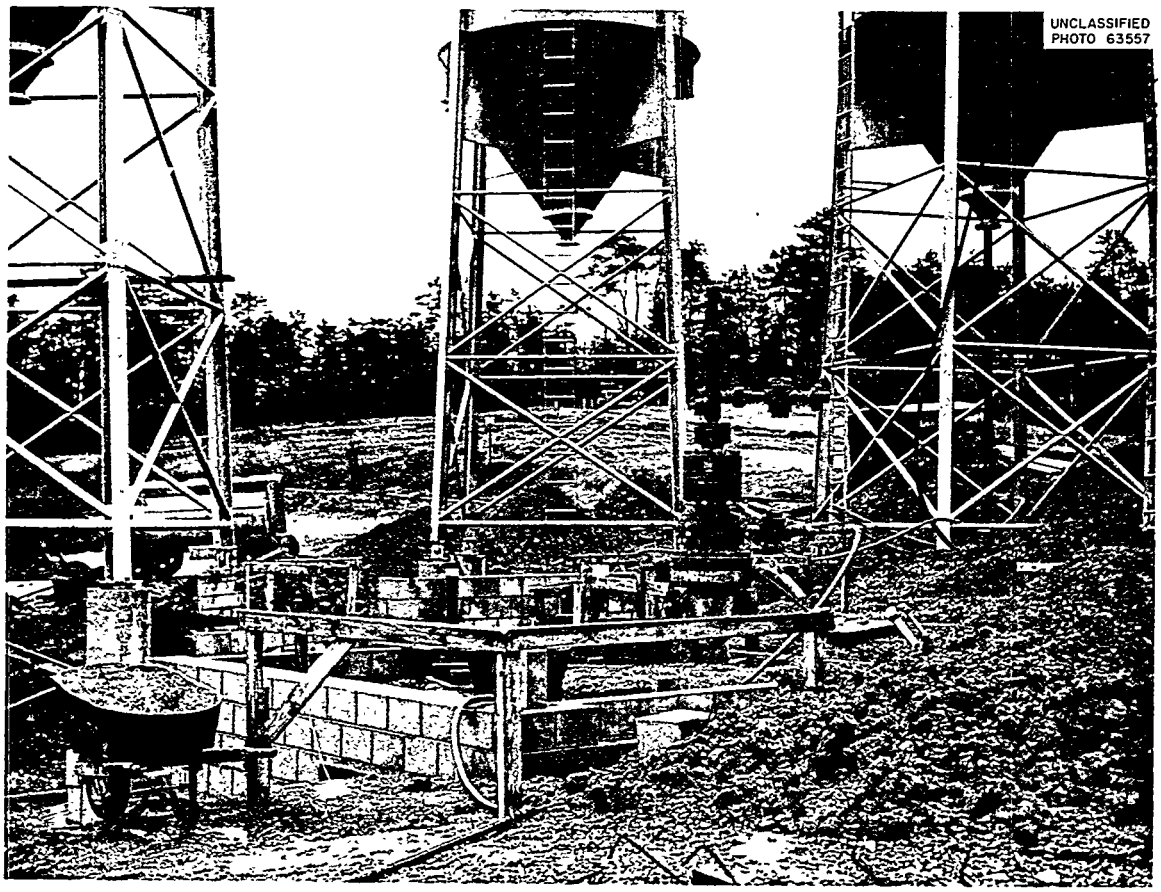

Fig. 35. Progress of Construction.

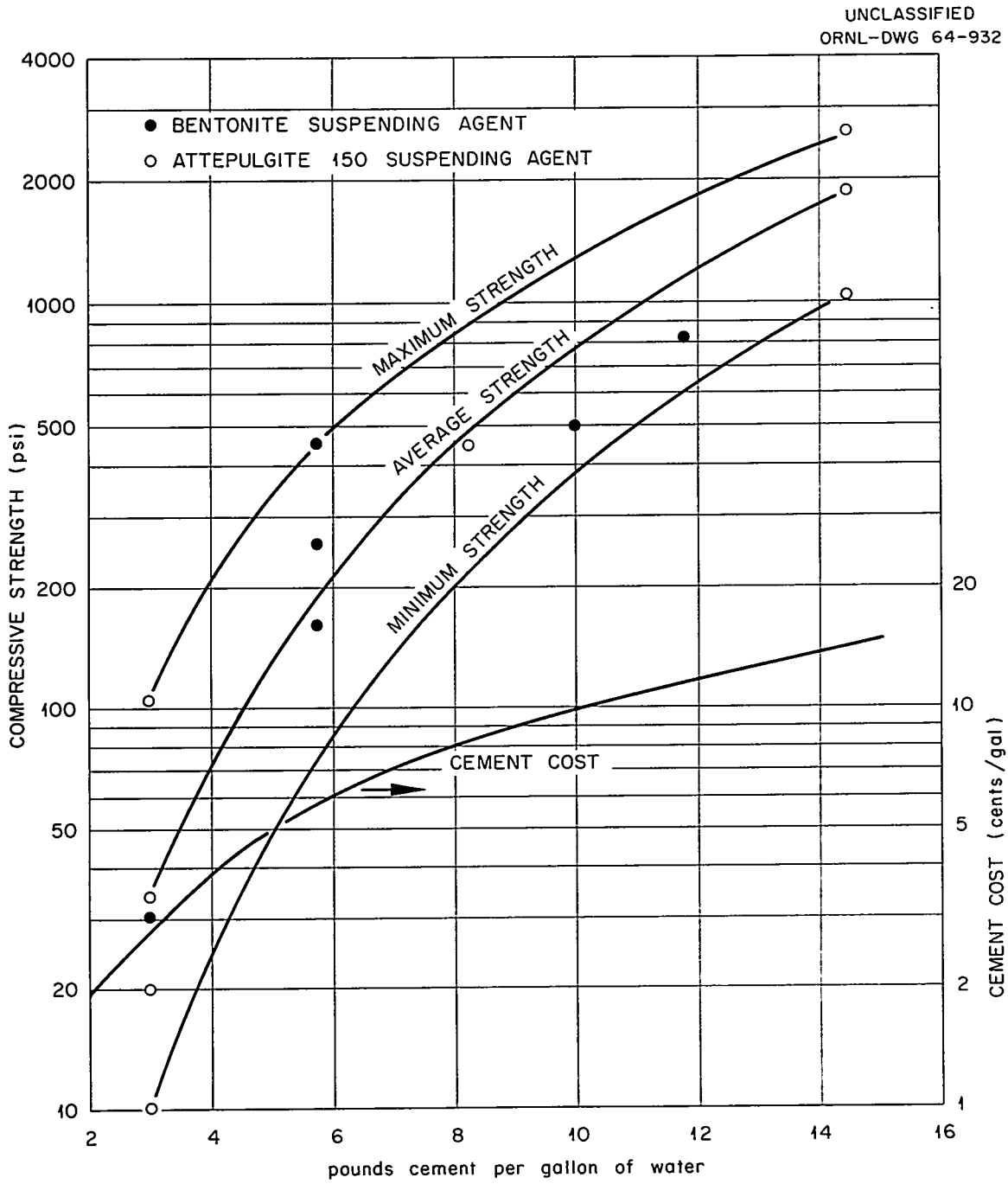

Fig. 36. Compressive Strength and Cement Cost Versus Cement Concentration in Slurry.

the excess liquid and to keep the solid phase in suspension, bentonite is generally added to such lean cement mixes. In waste solutions being considered for injection, however, the concentration of dissolved ions is extremely high - in excess of 3 M. Under these conditions bentonite flocculates and is ineffective as a suspending agent. Since attapulgite is known to be a more effective suspending agent in high-molarity salt solutions, it was tested and found to be an effective suspending agent and a good absorber of excess liquid. The most effective form of this material is attapulgite 150 or attagel 150; several other types of attapulgite (such as attapulgite RVM or LVMO were as ineffective as bentonite.

Retarders.-- For the experimental waste injections as planned, 8 hr of pumping time is considered desirable; for future injections, pumping times of 30 hr or more will be needed. If cement by itself is added to waste, the cement-waste slurry will set within 1 to 2 hr. Salt, caustic, and most suspending agents reduce this setting time further. For this reason it is necessary to add retarders to extend the pumping time.

One of the more promising retarders is calcium lignosulfonate (CLS). It is relatively cheap for the quantities required to give pumping times of approximately 30 hr. Another retarder is carboxymethyl hydroxyethyl cellulose (CMHEC). In addition to their retarding properties, both CLS and CMHEC are fluid-loss additives. The properties of several mixes prepared with low concentrations of cement are shown in Table 22. Mixes 1 through 6 contained 4 lb of cement and 6.6% attapulgite 150 per gallon; some of these mixes showed phase separation in a few cases. To remedy this, the amount of cement and attapulgite was increased to 5 lb of cement and 6.9% attapulgite 150. The higher solid content increased the setting time for the slurry and hence decreased the pumping time of the mix.

Slurry pumping times are usually measured with a consistometer. That instrument is not yet available at ORNL, and the vicat test (a measurement of the depth of penetration of a needle in a slurry) is used instead to give an indication of the slurry-pumping time. A vicat reading of 70 hr is nearly equivalent to a pumping time of 29 hr.

A more effective retarder is glucono-d-lactone (CFR-1), the solid form of gluconic acid. It is not as effective as CLS in reducing fluid loss but is a much more effective retarder. A 0.2% concentration of CFR-1

Table 22. Slurry Properties of Lean Cement-Waste Mixes

Expt. No.	Cement/Waste (lb/gal)	Suspending Agent (%)	Retarder[a] (%)	Bulk Density (g/cc)	Vicat Initial Set[b] (hr)	Fluid Loss (cc/30 min)	Cost (¢/g)
1	4	6.6 Attapulgite 150	0.8 CMHEC	---	70	82	0.095
2	4	6.6 Attapulgite 150	1.5 CLS	---	70(29)	104	0.065
3	4	6.6 Attapulgite 150	0.75 CLS	1.00	---	99	---
4	4	6.6 Bentonite	0.8 CMHEC	---	236	47	---
5	4	6.6 Bentonite	1.5 CLS	---	---	239	0.06
6	4	6.6 Bentonite	0.75 CLS	---	472	---	---
7	5	6.9 Attapulgite 150	1.5 CLS	0.9	44	78	0.08
8	5	6.9 Attapulgite RVM	1.5 CLS	---	---	124	0.08
9	5	6.9 Attapulgite 150	1.5 SLS	1.33	< 20	85	0.07
10	5	6.9 Attapulgite 150	3.0 SLS	1.25	17	90	0.08
11	5	6.9 Attapulgite 150	0.2 CFR-1	0.96	(36)	208	0.08

[a]CMHEC a carboxymethylhydroxyethyl cellulose; CLS = calcium lignosulfonate; SLS = sodium lignosulfonate; CFR-1 = glucono d lactone.

[b]Figures in parenthesis refer to consistometer pumpint time for 1000-ft schedule. A relationship between consistometer readings and vicat readings is given in run 2, where a 70-hr vicat reading was found to be equivalent to a 29-hr consistometer reading.

costs about the same as a 1.5% concentration of CLS and gives almost twice the pumping time (runs 7 and 11 in Table 22). Evaluation of this retarder is continuing.

Fluid Loss.-- The results shown in Table 22 can be interpreted as showing that CMHEC is a better fluid-loss additive when used with bentonite than when used with attapulgite 150. These results are probably misleading, however, since the low fluid-loss values are obtained in these tests because the flocculation of bentonite results in a high concentration of solids on the screen of the testing device and thus inhibits fluid loss. In an actual rock formation, fluid loss would occur from both the lower and the upper faces of the grout, and flocculation would not inhibit fluid loss. To demonstrate that it was the flocculated condition of the bentonite that was responsible for the low fluid-loss reading, attapulgite LVM (which also flocculates) was used; the fluid loss was 28 cc, compared with 47 cc for bentonite and 82 cc for attapulgite 150. It seems that the value of fluid-loss determinations as presently measured is highly questionable.

Air Entrainment.-- In many of the tests, it was noted that the bulk density of the slurry was extremely low; the cause of this low bulk density was the entrapment of air in the slurry. The experience of the cement industry has been that air entrapment is aggravated by the use of CLS; hence, slurries were prepared with sodium lignosulfonate (SLS), which has been reported to give much better results. A significant increase in the bulk density of these slurries was noted; from about 1.0 g/cc for a slurry containing CLS, the density increased to 1.3 g/cc with NLS. This bulk density is still relatively low, since the concentrated waste solution without additives has a specific gravity of 1.29. The substitution of SLS for CLS had the undesirable effect of reducing the pumping time. Air entrapment is still being investigated.

5.1.6 Proposed Experimental Waste Injections (W. de Laguna, E. G. Struxness, T. Tamura, and H. O. Weeren)

The experimental program for the first series of injections will consist of four injections in the following order, each injection to be of 40,000 gal of solution:

1. An injection of a synthetic waste solution that has the same concentration and chemical composition as the actual waste solution is expected to have in 1965, when the waste evaporator goes on stream. This solution will be mixed with 2.3 lb per gallon of attapulgite 150 (a drilling clay) to form a nonsetting slurry. This injection will not contain any radioactive materials.
2. An injection of the same synthetic waste solution mixed with about 6 lb per gallon of a cement-base mix. This mix will set with an ultimate compressive strength of between 100 and 200 psi - sufficient to fix the waste solution but probably insufficient to withstand the subsequent coring of the formation. About 30 curies of Au^{198} (2.7-day half-life) will be added so that the grout sheet can be detected at the observation well.
3. An injection of actual waste solution mixed with sufficient additional chemicals to make the chemical composition and concentration the same as for injections 1 and 2. The specific activity of this solution will be about a fifth that of normal waste. This solution will contain about 14 lb per gallon of solids, largely Portland cement. The mix will set with an ultimate compressive strength of about 1000 psi - more than sufficient to withstand coring of the formation.
4. An injection of actual intermediate-level waste solution, also mixed with about 14 lb per gallon of solids, largely cement. This mix will also set with an ultimate strength of about 1000 psi.

Injection 1 is proposed to help to determine how nonsetting mixes will perform after injection into the shale formations.

Injection 2 will help to evaluate a cheap mix for use with concentrated waste solutions and, if successful, will indicate the direction for future waste mix research.

Injection 3 will be made in order to demonstrate that concentrated waste solutions can be fixed in an underground formation. If injection 2

is completely successful, the results of injection 3 will be somewhat redundant; but, if injection 2 is less than completely successful, the results will be quite valuable.

Injection 4 will be a demonstration that actual waste solutions can be handled in the surface plant, pumped underground, and permanently confined there.

After the series of injections has been completed, the formations will be cored to obtain samples from the grout sheets and to determine the amount of leakage from the grout sheets.

5.1.7 Hazards Analysis (H. O. Weeren)

A hazards analysis of the proposed fracturing experiments was completed. It was concluded that the waste solution that would be used in the first series of injections would be so low in specific activity that no significant hazard would result. The other principal hazard involved in the experiments - that of working with high-pressure equipment - was minimized where possible by installing the equipment in cells.

The major hazard associated with the injections is the possibility that, during the course of an injection, the fittings at the wellhead may break off right at the wellhead, thereby permitting some or all of the waste grout that has been injected into the well to flow back up the well into the wellhead cell, with no way of shutting off the flow. Depending on the nature of the break at the wellhead, this flow could be up the tubing string, up the annulus between the tubing and the casing, or up both the tubing and annulus. The expected maximum flows in each case are 535 gal/min, 1010 gal/min, and 1545 gal/min, respectively. In such an accident, the grout will be washed through an 18-in. line to the nearby emergency waste trench. Here the grout can set up and be covered.

The air-borne contamination of Sr^{90} near the wellhead during such an accident has been calculated to be five times the MPC_a for a continuous 40-hr-per-week exposure. The equivalent Cs^{137} and Ru^{106} exposures are 40% and 2% of the respective MPC_a. Since any exposure would be for a very limited time, the hazard would not be serious.

A rupture of a high-pressure line at any place except at the wellhead would not constitute a major hazard. The line would be valved off or the

injection pump would be stopped after, at most, a few hundred gallons had been spilled into one of the cells. A spill of this size could be cleaned up quite readily.

This facility shares with the existing waste transfer system the risk of waste leaking into White Oak Creek from a leak in the waste transfer line that crosses the creek. Safeguards include the usual Laboratory procedure of pressurizing the line before each transfer to detect major leaks, and the monitoring of the creek a short distance downstream of the crossing.

A calculation of the hazard resulting from the leak of a considerable quantity of waste solution at a point some distance from the stream and the subsequent discharge of the waste into White Oak Lake indicated that the downstream concentration of Sr^{90} would not exceed 37% of the continuous nonoccupational MPC_w; the equivalent concentration of Cs^{137} and Ru^{106} would be 2.7% and 3.4%. This would not be a serious risk.

A power failure at the plant site would affect the waste pump, the water pump, the densometer pump, and the lights. Failure of these items would force a halt in the injection but would not cause a serious hazard. If the power failure were temporary, the wellhead could be valved off and the injection pump shut down until pumping could be resumed. Alternatively, if the power were likely to be off for a considerable time, the injection could be terminated.

5.1.8 Cost Analysis (H. O. Weeren)

An estimate was made of the probable operating cost of the shale fracturing plant if operated on a routine basis for the disposal of 400,000 gal per year of concentrated, intermediate-level, ORNL waste solution. This estimate shows that two variables are of particular significance - the cost of the mix and the life of the well. Other costs are either relatively small or fixed. The effect of these variables on the operating cost is shown in Fig. 37. It can be seen that the proportion of the total cost attributable to the well cost becomes very large if the life of the well is less than five years. The factors that limit well life are not now known with certainty; yet, it seems probable that

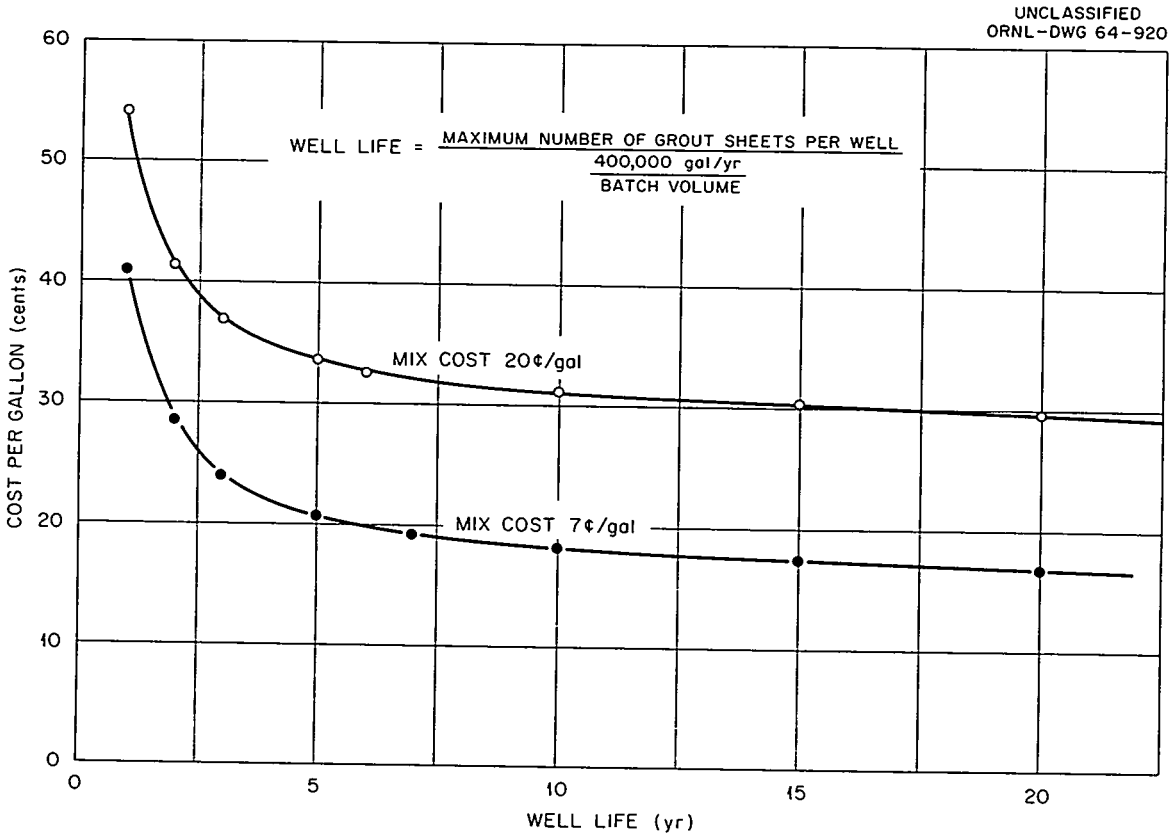

Fig. 37. Cost Estimate for Injection of ORNL Waste (400,000 gal injected per year).

vertical uplift is one such factor. If it should prove to be the controlling factor, the well life will be limited to a fixed number of grout sheets and can be extended only by injecting larger and fewer batches. If, for example, the batch size were changed from 40,000 gal to 200,000 gal, the well life would be extended by a factor of 5. It seems probable therefore that the direction of future work will be toward larger batch sizes than those now planned.

6. DISPOSAL IN NATURAL SALT FORMATIONS

6.1 Heated Model Room

W. J. Boegly, Jr. R. L. Bradshaw F. M. Empson

A rectangular room, 8 ft wide by 9 1/2 ft deep by 2 ft high, geometrically similar to a mine room, was created in the face of a large pillar in the Hutchinson, Kansas, mine of The Carey Salt Company to study the effect of temperature on mine openings. Immediately after the opening was created, electrical transducer-type strain gages, capable of operating at 200°C, were installed to measure the floor-to-ceiling convergence, the movement of the floor alone, and the convergence of the side walls.

After about 50 days of heating, the strain gages inside the cavity suddenly showed an apparent increase in the rate of convergence of the floor and ceiling. Investigation showed this to be due to bowing of the pipes supporting the strain gage anchor bracket. This bracket is located in the haulageway, outside of the cavity. Heat from the cavity is causing a vertical expansion of the haulageway floor, compressing the pipes between floor and ceiling. To correct for the bowing of the pipes, a reference-gage measuring the movement of the bracket toward the cavity was attached to the anchor bracket. The reference gage was installed after 93 days of heating. This gage indicated that movement of the bracket was somewhat erratic, and a slip joint was installed on the support pipes. This was done after 150 days of operation and appears to have corrected the difficulty. Heating of the mine room model had continued for 215 days as of October 19, 1963.

After installation of the correction gage and the slip joints, the cavity closure rates as indicated by the strain gages should be correct; but, in order to get the total cumulative closure, it was necessary to extrapolate the deformation curves from 50 days to 93 days. The corrected cumulative deformations, as indicated by the floor-to-ceiling gages at the end of 215 days of heating, are shown in Table 23. Shown in the right-hand column is the deformation rate during the period from 115 to 215 days. (The value for gage 2 is believed to be too high because of faulty gage operation.) Also shown for comparison purposes are earlier rates and the rate prior to heating. It may be noted that the closure rates are now

less than ten times higher than the closure rates before heating. The decrease in closure rate with time is still faster than it was during the background (ambient temperature) period, but it is not yet possible to ascertain whether the rate will remain above the ambient temperature closure rate, approach it asymptotically, or fall below it.

Table 23. Closure of the Cavity During Heating

Gage Number	Cumulative Deformation at 215 days (in.)	Rate of Movement in Units of 10^{-6} in. in.$^{-1}$ day^{-1}			
		Prior to Heating	During Heating		
			30 to 40 (days)	40 to 115 (days)	115 to 215 (days)
2	1.64	3.1	210	100	42
5	1.66	2.8	210	100	17
6	1.66	3.3	210	100	29
8	1.47	2.9	210	100	17
9	1.25	2.8	170	80	13

6.2 Demonstration Experiment

6.2.1 Critical Path Scheduling (W. F. Schaffer, Jr., and W. J. Boegly, Jr.)

An overall critical path schedule was prepared, based on earlier critical path schedules for the several phases of the program. Only the duration of project days required to perform each activity were estimated, and the schedule assumes that sufficient money and man power were available to begin or complete a given activity when scheduled. This assumption is probably a good one, since most of the procurement, fabrication, and installation will be done outside the Laboratory and will not be delayed by local priority jobs or work stoppages, except perhaps for prototype equipment. Based on the best available sequencing and activity duration, the critical path schedule is through the mine renovations and preparation of the experimental area and shows a project completion date of March 22,

1965. If additional funds are available in fiscal year 1964, additional underground work can be done during this period and will result in improving the schedule by over two months. Additional funds by midyear would secure and increase the reliability of the schedule with respect to much of the equipment required for handling the radioactive materials, such as the shipping carrier, fuel canisters, hole liners, and handling tools, which currently are delayed by lack of funds. If procurement is delayed until fiscal year 1965, man-power limitations might be serious.

6.2.2 Renovation of Lyons Mine (W. J. Boegly, Jr., and F. M. Empson)

The Stearns-Roger Corporation was employed to survey the present Lyons, Kansas, salt mine facilities and to design new equipment required to increase the hoisting capacity from 3000 lb to 7 tons. A new headframe, shaft collar, and man and equipment cages would be required to handle 7-ton loads. They also recommended a general renovation of the hoist motor, electrical circuits, and safety devices. A competitive-bid contract was awarded to the L. R. Foy Construction Company of Hutchinson, Kansas, for the construction and installation of the new headframe, shaft collar, and cages. The bid price was $56,703, and the estimated time to complete the job was 120 days. Excavation for the shaft collar and headframe foundations started on November 7, 1963. No access to the underground workings is now available. It is planned to again obtain access to the underground workings during February 1964, although the topside work will not be 100% complete.

The balance of the topside work at the present shaft is also in progress. To date, new hoisting cables and main shaft power cable have been purchased and are at the site; new electrical switchgear is in order; and the area around the shaft has been graded. A contract was let for the installation of a security fence around the main shaft area. Specifications are being developed for the installation of a concrete floor in the hoist house to meet safety requirements.

Below-ground renovations and the design of the experiment are being detailed. Used mining equipment for the below-ground excavation was purchased for delivery in January 1964.

Study of the critical path schedule for the underground cleanup and mining of the experimental area indicated that both jobs must be carried out at the same time. A time interval must be allowed before mining starts so that the remainder of the plastic flow gages can be installed. To complete the mine preparation on schedule, drilling of the array holes and thermocouple holes will also have to be started as soon as each room in the new area is completed.

The diameter of the waste-charging shaft was fixed at 18 to 20 in. cased inside diameter. A shaft this size can handle calciner pots, hole liners, and also will serve as another exit from the mine if access to the main hoisting facilities is not possible.

6.2.3 Engineering Design (W. F. Schaffer, Jr.)

Waste Disposal Carrier.-- Specifications for a waste disposal carrier for underground service and invitations to bid were sent to the leading fabricators of heavy industrial road equipment. It was concluded that the overall tractor-trailer design should be given to a contractor experienced in this field in order that the tractor and trailer be compatible and capable of performing the service required. The radiation shield is being designed at the Laboratory. Compatibility of the shield and trailer designs will be assured. The size and weight of the components of the tractor, trailer, and shield were limited to allow transfer to the mine for final assembly. The bid was awarded to the Stowers Machinery Company, Knoxville, Tennessee, representing the Caterpillar Tractor Company and Athey Products Corporation, a builder experienced in the design of special trailers.

The prime mover recommended and purchased is a two-wheel rubber-tired tractor, Caterpillar model 619C. The trailer design is completed, and detailed engineering design for fabrication is scheduled to start in the latter part of November.

The detailed shield design is complete and ready for bid. The shield consists of a vertical cylindrical body with two-piece horizontally operating doors at both the top and bottom. Nominal overall dimensions are: 3 ft in diameter and 11 ft in height. The body shielding consists of removable chevron-shaped rings of uncased lead between inner and outer steel

cylindrical members. Each door is separately powered by a hydraulic motor, which drives a worm screw through a chain and connection. The shield is equivalent to about 10 in. of lead and is capable of handling waste calcination pots nearly 12 in. in diameter and 9 ft long, as well as the fuel element canisters required for the demonstration.

Safety features include mechanical and electrical interlocks which prevent accidental or careless operation of the doors during movement of the transporter through the mine. The trailer will be locked automatically in position at the time the door control mechanism is activated. The shield can be moved within a 3-ft-diam circle to align it over the waste disposal hole. The shield will move vertically from the center position a distance of 1 ft in either direction.

The shield positioning, the door operating mechanism, and the winch can be remotely operated from an extension control panel. The doors and winch will normally be remotely operated because of the difficulty of preventing radiation streaming between the shield and the salt without the use of shadow or floor and roof recess shields.

A unique safety feature to prevent upset or collision damage in case of a tire blowout employs a metal wheel with a solid rubber tire within each tubeless tire. The size is chosen so that normal tire flexures are permitted without touching the inner wheel, but the inner wheel is of sufficient size when in contact with the floor to prevent instability of the vehicle.

The vehicle was designed to withstand a 10-g impact without destroying the structural integrity of the transporter or shield. The forces applied to the shield under a 10-g collision will be reduced to 3 g's by hydraulic shock absorbing cylinders.

Completion of the vehicle is scheduled for May 1964.

Shipping Cask.-- Design drawings are almost complete for the conversion of the SRE shipping cask for handling ETR fuel. The modifications include one new short body section to replace an existing longer section, the addition of a charging door in the front bulkhead of the cask, the filling with lead of a spacer ring used in the SRE modification, the addition of external cast steel shielding in the central section of the cask, and a new water-cooled magazine for holding the seven fuel canisters.

The magazine presented the most difficult design problem because of the space limitations imposed by the internal cavity of the cask and the required diameter of the canister shield plug. The modified cask will have the equivalent of 10 in. of lead shielding and will weigh about 35 tons.

Final drawings will be released after completion of the stress analysis of the cask and approval of the cask in accordance with the proposed Federal Shipping Regulations (Title 10, Code of Federal Regulations, Part 72). Hazards evaluations of the shipment of the fuel to the mine are well advanced. The hazards report is scheduled for completion in December 1963.

Fuel Element Canister.-- The design of the fuel element canister is complete, and the fabrication of two prototype units for test and evaluation is in progress. Delivery of the two prototypes is scheduled for early December 1963.

The design of the canister has been radically changed from the first concept. The canister employs a uranium shield plug to reduce the radiation "shine" from the storage hole to permissible levels. Four thermocouples brazed together in a flat ribbon measure temperatures at the center regions of both elements.

The center closure design was replaced by an end closure. The primary seal is welding of the joint, and a copper seal ring is used as a secondary hermetic seal. Remote assembly methods were simplified by redesign of the thermocouple and closure. Both elements can now be inserted from one end of the canister on internal track guides. Preliminary review of the drawings by the Phillips Petroleum operating personnel at Idaho indicate that no difficulty should be encountered in remotely loading the canisters.

Hole Liner.-- The design of the hole liner is nearing completion. Considerable improvement has been made in the present design over the earlier concepts. The liner now consists of two main assemblies to permit removal of the lower section for replacement of heaters and thermocouples during the course of the demonstration. The new design also permits removal of the lower liner and fuel element canister as a unit, in the event that an unforeseen incident prevents removal of the canister alone from the liner. The earlier design, based on estimated salt pressures

on the liner of 3500 to 5000 psi, required a heavy-wall tube, which reduced the radiation to the salt. The main feature of the new design is an air annulus around the lower section to avoid the salt pressure and corrosion problems on the liner, heaters, and thermocouples.

The movement of the salt toward the liner will be measured. At a designated closure, the lower liner can be withdrawn, the hole reamed to a larger size, and the liner replaced. This method permits the use of a light liner of relatively inexpensive construction using standard materials of construction for the liner, heaters, and thermocouples. Special sheath material for the heaters alone would have been very expensive. The upper section of the liner will be standard, high-strength, oil-well casing. Standard junction boxes will be provided for thermocouples and heater connections. (See Fig. 38 for a diagrammatic sketch of the hole liner installation.) One prototype unit is scheduled for fabrication during December 1963.

6.2.4 Experimental Design (W. J. Boegly, Jr., and R. L. Bradshaw)

It is anticipated that about 450 thermocouples will be installed around the three arrays and the heated pillar. Two 144-point data loggers will routinely record temperatures from the experimental area. Critical temperatures (such as those on the fuel assemblies) will be printed on 12-point recorders. Some of the thermocouples in the salt will not be connected to recording equipment but will be read in place. The metal-sheathed thermocouples will be inserted in plastic or Teflon tubes in the salt. The tubes will allow easier changeout of thermocouples should a unit fail, and, since the sheath of the thermocouple will not be in contact with the salt, a less expensive metallic sheath can be used.

One of the most important aspects of the demonstration experiment is to determine the effect of heat and radiation on the plastic flow of salt and the resulting effect on the stability of the mine. In order to obtain background information on room closure in the Lyons mine for safety purposes, and also to obtain pre-excavation flow rates, a number of plastic-flow measuring stations were installed. The majority of the gages now installed are around the shaft bottom and along the access corridor. Since the hoist will be out of operation during the time that the headframe is

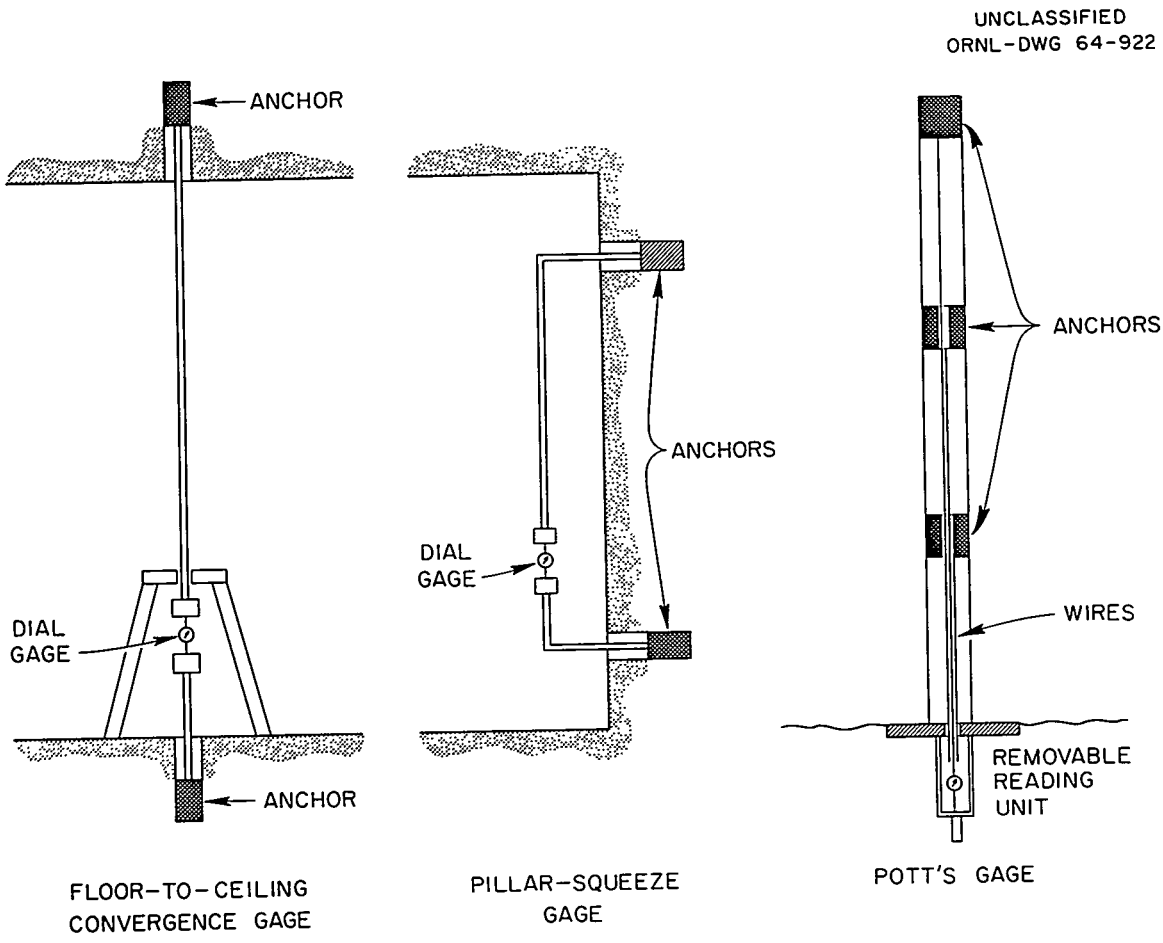

Fig. 39. Types of Strain-Measuring Gages to be Used in Lyons Mine.

stress distribution around an isolated rectangular opening with rounded corners,[30] but, for multiple openings, stress distributions are known only from photoelastic and photostress model tests. Since stress causes strain, but is itself altered by strain, both stress and strain will be intimately related in any theoretical solution of the creep and load-transfer problem. At this time it does not seem possible to obtain a theoretical solution. It is thus pertinent to examine the available experimental information on salt to determine if it is possible to arrive at an empirical solution.

Very little has been published on the effects of stress and temperature on the creep of rock salt. The three most useful sources are the Serata,[31] the LeComte thesis data,[32] and the Corps of Engineers' report.[33] Unfortunately, none of the investigators used the same test conditions, and there were few samples tested at elevated temperatures. Serata used cubes of rock salt and tested under uniaxial conditions, both with and without friction reducers on the ends of the samples. He presented data for only one test at an elevated temperature. LeComte used samples prepared by compressing granular salt. Only three of the elevated temperature triaxial tests run by LeComte could be compared with control tests at ambient temperature. Only three of the Corps of Engineers' tests at elevated temperatures were not subject to question, and these three were all at the same temperature. Their tests were run on drilled cores taken from the Tatum salt dome.

LeComte ran five samples under the same conditions to test reproducibility. From his results, plus the results of the other investigators, it must be concluded that creep rate variations of less than a factor of 2 from one set of conditions to another may not be significant.

Due to the varied testing conditions and the variability of the samples, it was concluded that only an approximate analysis of the stress and temperature effects on creep could be made. This can best be done by taking the ratios of the creep rates at various stresses to that under the same test conditions at some reference stress and by taking ratios of creep rates at various temperatures to that at ambient temperature.

The effect of axial stress on creep rates at ambient temperature is shown in Fig. 40. It should be pointed out that there is some uncertainty

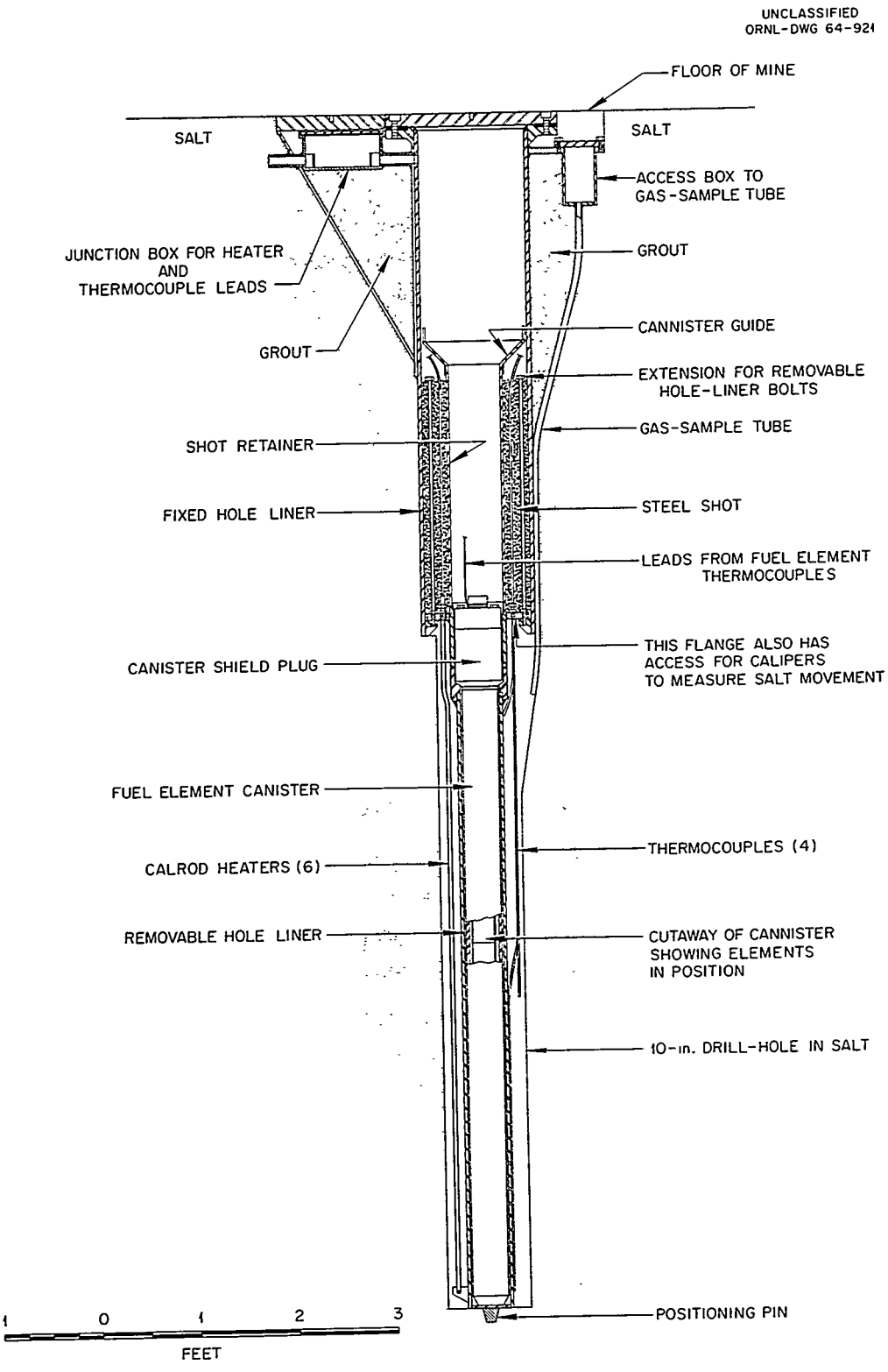

Fig. 38. Sketch of the Hole-Liner Installation.

replaced, the rest of the gages will be installed early next year. It is anticipated that all gages will be installed by the time mining starts on the experimental area.

Three basic types of gages will be used for strain measurements in these studies. The first gage (Fig. 39) is used to measure the convergence between the floor and the ceiling, or between columns. The ends of the gage are located a sufficient distance into the salt to eliminate erroneous readings due to surface spalling. Readings are taken by inserting a dial gage between the reading cups. The second type of gage is used to measure the floor-to-ceiling squeeze in the pillars. The ends of the gage are mounted in the columns in horizontal planes, and readings are obtained in the same fashion as for the floor-to-ceiling convergence gages (Fig. 39). The third type of gage (Fig. 39) was developed and furnished to us by Professor Potts of the University of Newcastle-Upon-Tyne, England, and allows a number of strain measurements to be made in a single borehole. This type of gage is used to make strain measurements into the salt at depths up to 120 ft. Basically, the gage consists of wires or tapes connected to anchors set at various distances into the salt and to a metal reference plate fastened to the surface of the salt. To measure the strain, a special reading device is fastened to this plate, and each tape or wire is preloaded to a known tension and the flowage determined.

At various locations in the mine, stress changes produced by excavation and heating will be monitored by "stressmeters" developed by Professor Potts. This information, plus the strain measurements should provide sufficient information to describe what is happening in the mine before the experiment is started, and what effect the heating has on the stability of the mine.

6.3 Prediction of Effects of Stress and Temperature On Creep in Salt Mines

R. L. Bradshaw

At present there exists no general solution for creep of salt in even the simplest configurations. For multiple rectangular openings, such as found in a mine, theoretical solutions do not even exist for stress distributions assuming elastic behavior. There is a solution to the elastic

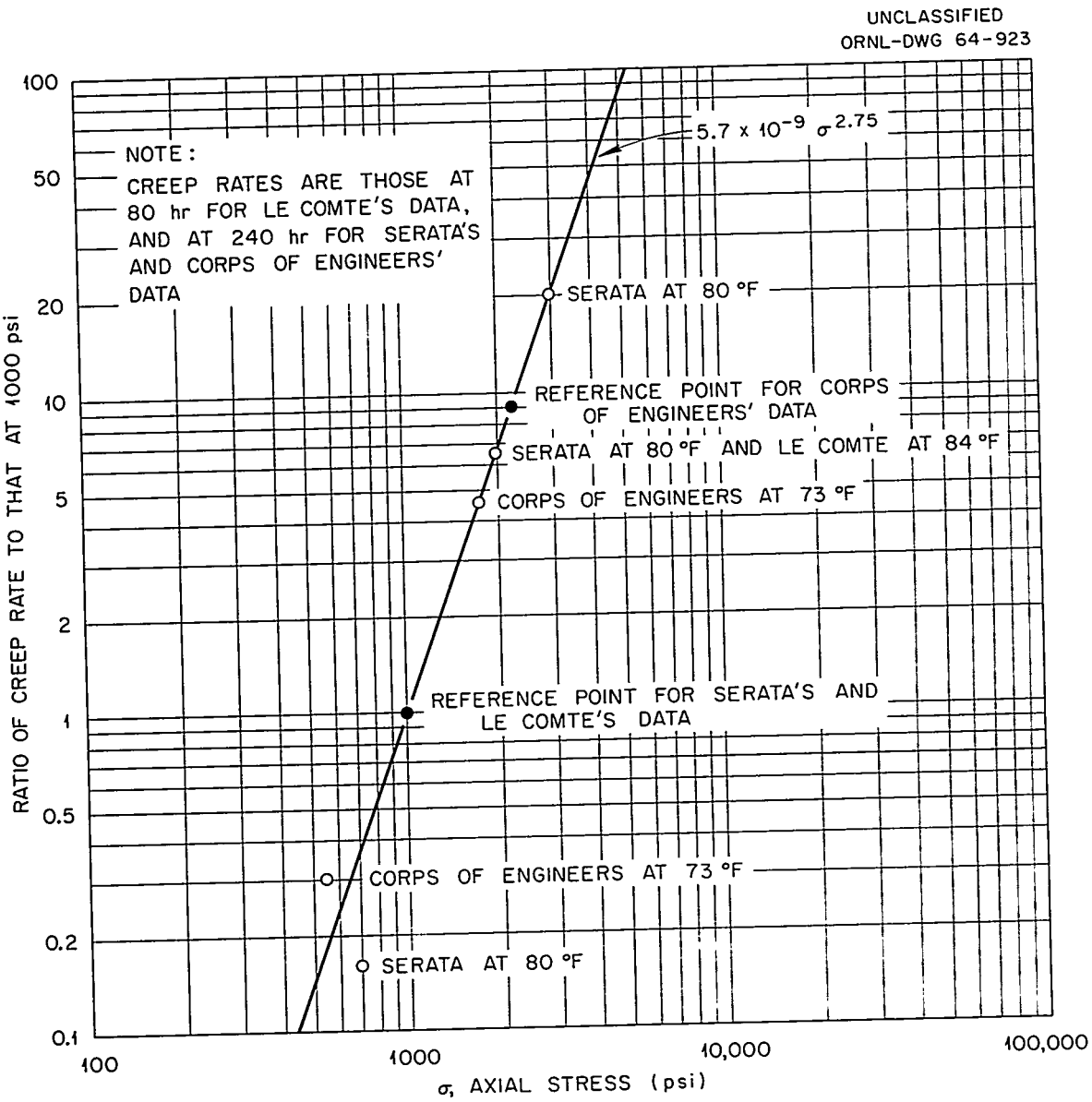

Fig. 40. Effect of Axial Stress on Creep Rates at Ambient Temperature.

in some of the points shown on the curve and the fact that five of the seven points fall on the curve is apt to be misleading. It should also be mentioned, however, that there is other evidence that supports the existence of a power function relationship between axial stress and creep rate.

Figure 41 shows the effect of temperature on creep rates. The two points taken from the LeComte data at 104°C indicate that increasing the confining pressure decreases the creep rate. Although the two creep rates differ by only a factor of 2, there is reason to believe that this difference is real. Serata's point at 410°C is believed to be too low because this was a test with a friction reducer on the ends of the sample. Serata's data show that at ambient temperatures a friction reducer increases the creep rate considerably, but it is believed that friction reduction will be less important at 410°C; thus, the creep-rate ratios with friction reducers would be low when compared with the ratios for samples without reducers.

Handin and Hager (Shell Development Company, 1958)[34] measured the ultimate strength and yield stress of artificially grown crystals, under 2000 bars confining pressure, at 24, 150, and 300°C. These crystals had approximately the same dimensions as the samples tested by LeComte, and, thus, their behavior might be similar to the behavior of the LeComte samples. Figure 42 is adapted from Handin and Hager, the ultimate strength curve being constructed from the average of the tabulated values for the two samples tested at each temperature. The yield strength values were not tabulated, so points were obtained from the curve in their report. It may be noted from Fig. 42 that the ultimate strength falls sharply with increasing temperature, approaching the yield strength somewhere around 300 to 400°C. The yield strength drops about 40% between 24 and 300°C.

A possible hypothesis to explain the effects of stress and temperature on creep rates is that the relationship between creep rate and axial stress always follows the same power law, with the curve (Fig. 40) merely being shifted along the stress axis as the ultimate strength of the salt changes due to temperature. If this hypothesis were found to be true, then it seems likely that the same relationship would hold for salt of different origins having different ultimate strengths at the same temperature.

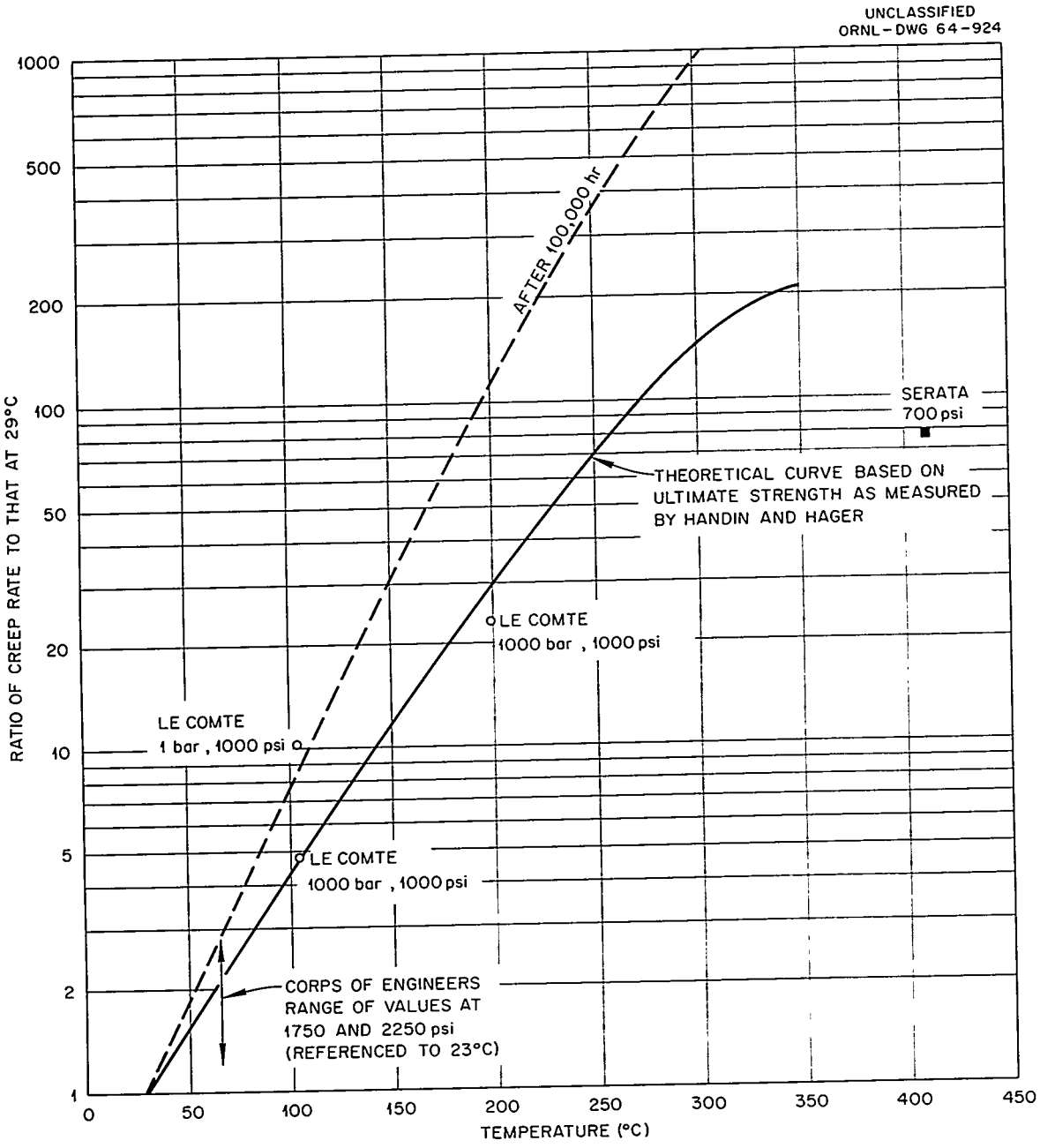

Fig. 41. Effect of Temperature on Creep Rates.

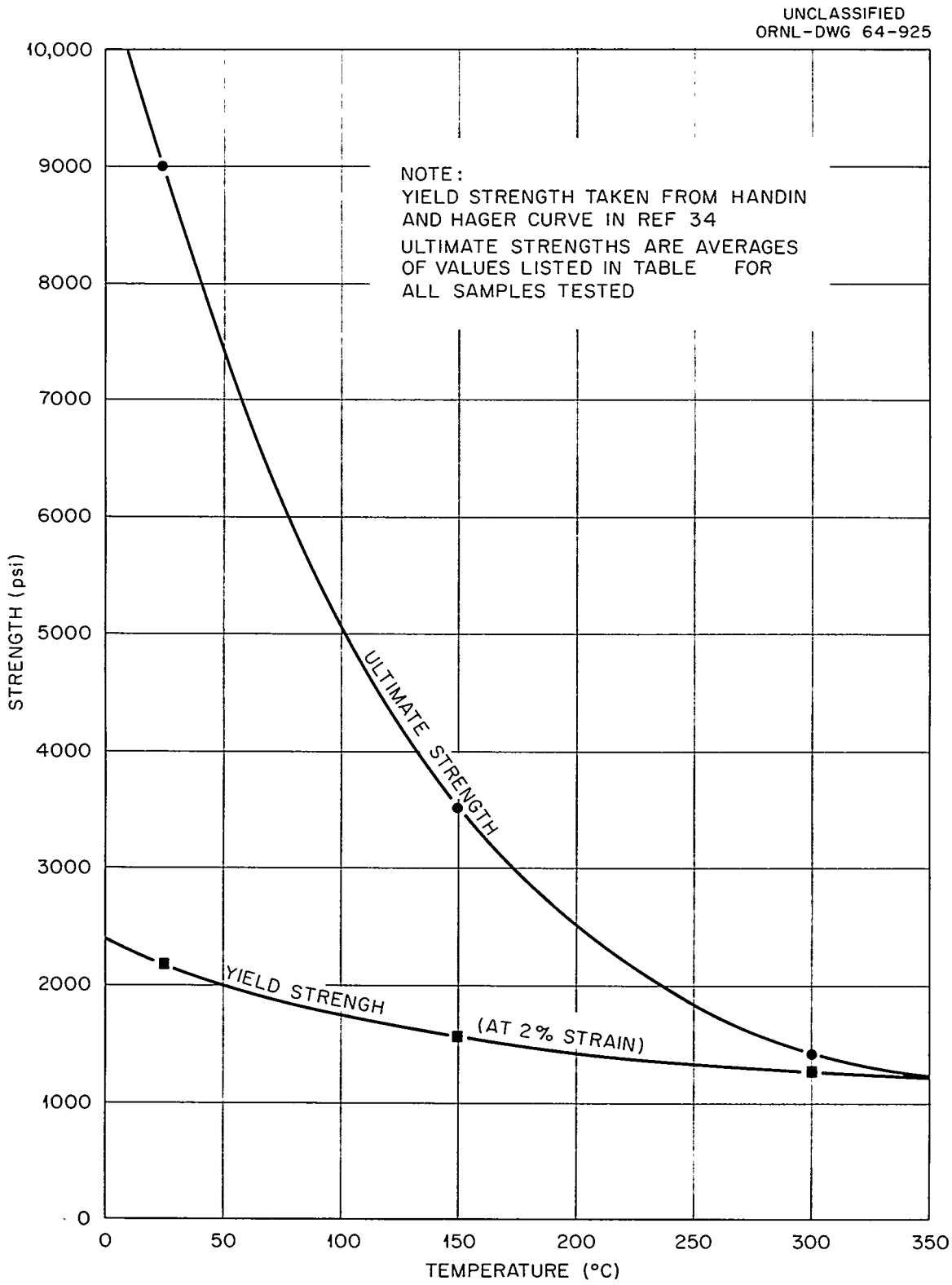

Fig. 42. Ultimate Compressive Strength of Single NaCl Crystals at 2000 Bar Confining Pressure - Adapted from Handin and Hager.

In order to test this hypothesis, the curves of Figs. 40 and 42 were used to derive the theoretical curve, shown as a solid line in Fig. 41. This curve appears to give a reasonable fit to the experimental data and thus tends to support the hypothesis.

The theoretical curve in Fig. 41 should apply to salt under triaxial conditions, that is, with confining pressure; moreover, it is known that pillars in a mine behave in a manner similar to that of triaxially compressed samples. For example, pillars in mines, where the salt has a uniaxial compressive strength of 3000 to 4000 psi in a conventional test of a cubical sample, actually support loads of up to 8000 psi. Thus, it is believed that the curve of Fig. 41 will give approximate values for creep of mine pillars if the creep rate at ambient is known. The hypothesis is such that the creep-rate ratio, as a function of temperature, is independent of the axial stress, and, thus, the curve of Fig. 41 should theoretically apply for any axial stress which is below the ultimate strength of the salt at the temperature in question. For example, elevating the temperature of a mine pillar, stressed at 1000 psi, to 100°C would increase the creep rate about fourfold. Elevating a pillar which was stressed to 2000 psi would also produce a fourfold increase in creep rate; however, the 2000-psi stressed pillar would have a creep rate at ambient about 6-1/2 times as great as that of the 1000-psi pillar at ambient. This stress independence is because the curve of Fig. 41 is assumed to hold up to the ultimate strength of the salt. That this is a reasonable assumption is supported by unpublished data of Serata[35] and L. Obert[36] on laboratory tests of scale-models of mine openings.

The creep rates represented by the data points in Figs. 40 and 41 were measured at times of 10 days or less. Serata showed that it is possible to predict creep rates in mine pillars at ambient temperature by extrapolation of creep rates of scale models. He found that the creep rate can be expressed by:

$$\dot{\epsilon} = Ct^{-n} \quad ,$$

where

C = a constant for a particular salt,

t = time,

n = a constant.

Thus it is seen that the creep rate will plot a straight line of slope n on log-log paper. The term "n" has been found to range from about 1 to 0.8, tending toward the lower value as the pillar load approaches the ultimate strength of the salt. It would thus be expected that the slope of the curve in Fig. 40, and thus the curve in Fig. 41, would become steeper with time. The dashed curve in Fig. 41 shows the temperature effect which would be expected in a mine pillar if it were to be heated after the opening had been created for 100,000 hr (11.4 yr).

As an example of the application of the foregoing, take the area in the south end of the Hutchinson mine where gage station 3 is located. The floor-to-ceiling convergence rate is about 0.17 in. per year, 10 years after the opening was created. The calculated pillar stress in this area is 2600 psi (75% extraction). If the creep rate were to remain fixed (presumably, it is still decreasing with time), the rooms would close in about 700 years. If the temperature of the pillars were to be elevated to 100°C, the rooms would close in less than 100 years, based on the theoretical temperature effect at 100,000 hr, as indicated by the dashed curve in Fig. 41. At 150°C, closure would take place in less than 25 years. At 200°C the pillar load of 2600 psi exceeds the ultimate strength (Fig. 42), and the area would be expected to close by rapid plastic flow as the temperature approached 200°C. As another example, assume a mine at a depth of 3000 ft with an extraction of 50% (pillar load 6000 psi). In this case, the temperature could not be allowed to exceed about 75°C without causing pillar failure.

The fact that the pillars will flow and that the rooms will eventually close is not, in itself, of any particular concern in the operation of a facility for the burial of solid radioactive wastes. In fact, complete closure of the salt around the wastes is desirable from the standpoint of long-term safety. The only concern is that the rooms do not close so rapidly that operations are disrupted before an area has been completely utilized, and, that in flowing, the pillars do not transfer a significant part of their load to other parts of the mine through beam action of the roof. Excessive load transfer could result in failure of other, as yet unheated, pillars.

It is concluded that it is possible to make empirical predictions of the effects of stress and temperature on creep in salt-mine pillars. It appears that sufficient laboratory data can be obtained by testing scale-model pillars at several different stresses at each of several different temperatures, including ambient. (The tests should be run for a minimum of 10 days in order to permit the extrapolation of creep rates out to several years.) It will still be necessary, however, to continue to make in situ measurements in the mines in order to verify predictions based on laboratory models and in order to clarify some uncertainties as to creep behavior in openings that are several decades old.

It should be pointed out that the foregoing section assumes a relatively homogeneous salt, such as is found in salt domes. If there are shale bands of appreciable thickness in the pillars or in the formation just below the floor or above the roof, other factors will modify these conclusions. It should also be pointed out that being able to predict creep rate as a function of temperature and pressure does not necessarily imply the ability to predict the effect of the creep rate on the overall stability of a mine. Specifically, the question of load transfer, due to the flow of the pillars, cannot be answered by means of the model tests referred to above.

6.4 Radiolytic Production of Chlorine in Salt

H. Kubota

During the course of the radiolysis studies, finely ground salt was found to produce more oxidizing agent per unit weight than unground salt. Since the grinding could have introduced strains and flaws to the crystals, the powder was annealed at 250 and 500°C for 25 hr before irradiation. The annealed and irradiated powders still showed greater production of oxidizing agent (Table 24). This indicated that the oxidizing agent produced in a crystal is partially a surface effect. In order to test this hypothesis, large crystals of sodium chloride were grown in the laboratory and irradiated. These relatively strain-free crystals showed the same degree of oxidizing power as the original reagent-grade material. It is tentatively concluded that the amount of oxidizing power created within

salt is independent of the size and surface area of the crystals per unit weight, but stresses and strains imparted to salt increase the total oxidizing power. Thermal annealing of ground powder for 25 hr was not sufficient to remove all the damage caused by the grinding.

Table 24. G Values for the Production of Oxidizing Agent

Dose (rads)	C.P. Crystals	< 100 Mesh (ground)	< 100 Mesh (annealed[a])	Synthetic Large Crystal
3.2×10^6	4.7×10^{-2}	0.147		
10^7	6.8×10^{-3}	3.7×10^{-2}		
3.8×10^8	2×10^{-3}		6×10^{-3}	2.1×10^{-3}
10^9	1.1×10^{-3}	4.5×10^{-3}		

[a]Annealed 24 hr at 500°C.

6.5 Thermal Stability of Salt

H. Kubota

Salt samples from France and England were heated to see whether they would shatter at elevated temperatures, similar to most of the bedded salt found in this country. The sample from France shattered at 237°C, while the English sample shattered at 252°C. Since only one sample was used in either case, it is not conclusive that European salt has a significantly lower shattering temperature than most of the American salt (260 to 300°C). It does show, however, that occluded water is found in most salt beds.

7. CLINCH RIVER STUDY

7.1 Dispersion Due to Power Releases

P. H. Carrigan, Jr.* B. J. Frederick* F. L. Parker

During the recent summer months a series of tracer tests were conducted to study the effects that the peaking power releases of water from Melton Hill Reservoir will have on the dispersion in the Clinch River of radioactive releases originating from White Oak Lake. The electric-generating equipment is not yet fully installed at Melton Hill Dam, and, as a consequence, the variation in flow for the tests was simulated by releases through the spillway gates at the dam.

The first tracer test with steady releases from Melton Hill Dam was preliminary in order to determine the quantity of tracer needed in succeeding tests and to assess the reliability of instruments under field conditions. Subsequent tests were run with the typical pattern of summer water releases. The discharge hydrograph for a week of such releases is shown in Fig. 43.

The regulated flow through the gates of Melton Hill Dam was obtained through the co-operation of A. J. Cooper and M. A. Churchill of the Tennessee Valley Authority.

The three tests made under summer power release conditions differed largely in the procedure of injecting the tracer. In the first of three tests, the fluorescent dye tracer, "Rhodamine B," was injected instantaneously in a line across the Clinch River at the mouth of White Oak Creek. In the second test, the dye was injected continuously for 24 hr into the nappe at White Oak Dam. In the third test, the dye was injected continuously for 1 week into the nappe at White Oak Dam.

The dispersion with time which occurred in the Clinch River during the latter two tests was very similar to the expected dispersion of radioactive wastes from White Oak Creek when power generation begins at Melton Hill Dam. At the time that flow suddenly began in the river, a rapid rise

---

*On loan from Water Resources Division, U.S. Geological Survey.

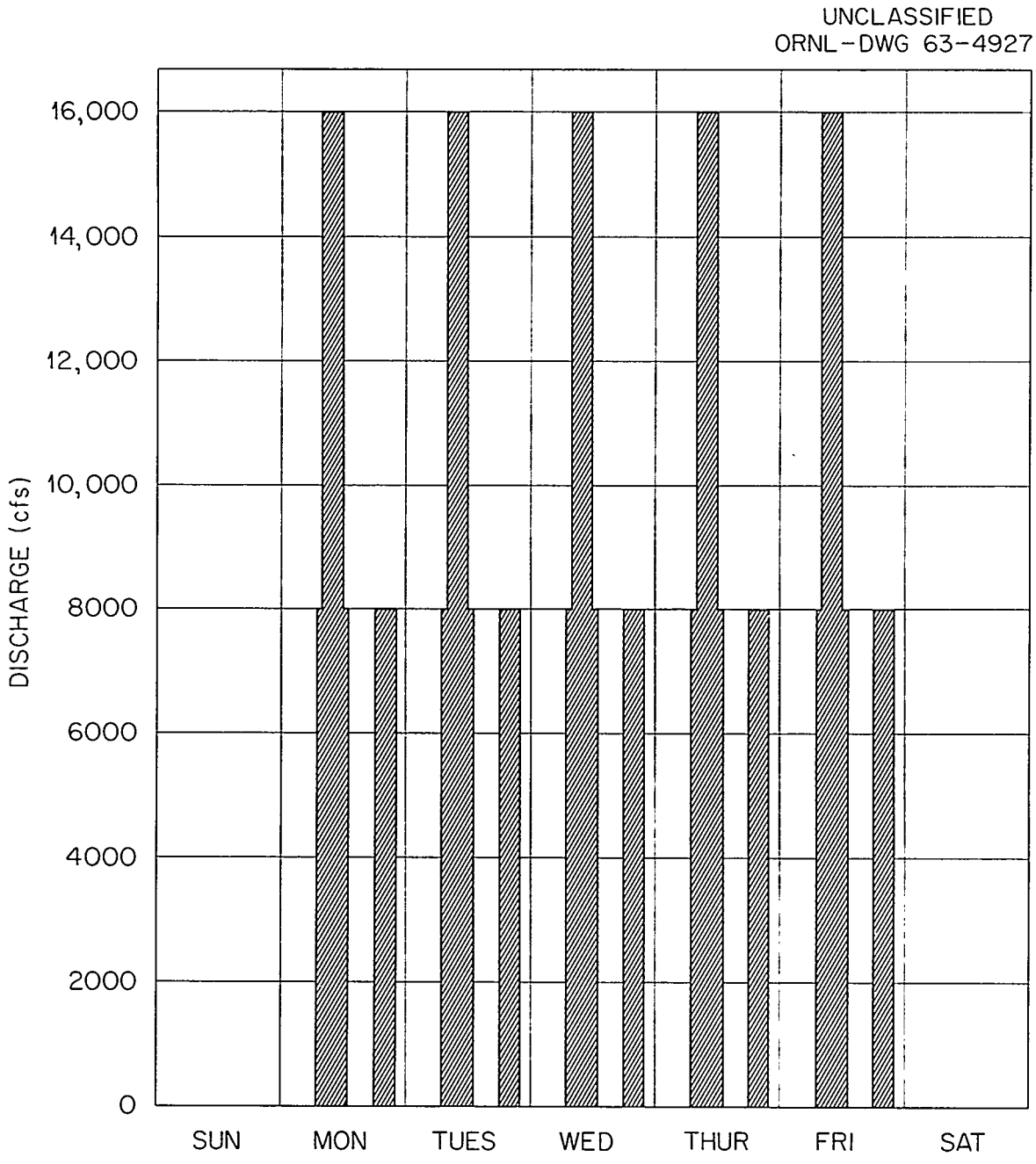

Fig. 43. Estimated Summer Discharge Pattern for Melton Hill Dam.

in river water level occurred at the mouth of White Oak Creek. As a result of the increased water level at the creek mouth, an adverse hydraulic gradient was created in the creek from its mouth to White Oak Dam; and an upstream flow occurred. For a considerable part of the time that water was being released through Melton Hill Dam, there was little flow from the creek into the river. At the cessation of the release, the water level in the river suddenly dropped, and a sudden rush of water from White Oak Creek embayment took place. A discrete pulse of dye accompanied this rush of water from the creek. Because there was no flow in the river, the dye mass remained close to the mouth of the creek.

The progressive spreading of the dye pulse in the stilled river was observed by means of aerial photography. In Fig. 44 the extent of visible dye after the cessation of water release is shown.

At the beginning of the next water release, the slug of dye in the river was swept downstream as a reasonably intact mass, and flow up White Oak Creek again occurred.

Two pulses of dye were injected into the river each weekday. For at least their first 6.4 miles of travel downstream from the mouth of White Oak Creek, the individual pulses of dye could be identified.

The ebb and flow of water in White Oak Creek embayment due to the power releases is much the same as flow in a tidal estuary. With techniques of tidal flow analysis, it was possible to compute the maximum magnitude of concentration of the dye pulse at downstream sections in the river and to determine the travel time of the pulse to these sections. A comparison of predicted and actual times of arrival are shown in Fig. 45.

The last test of the series, in which dye was released for 168 hr, began at 0100 hr on August 21. At 2100 hr on Friday, the week-end shutdown of water releases occurred. The shutdown, with no flow in the river, continued for 58 hr until 0700 hr on the following Monday. Flow of water and dye from the creek into the stilled river commenced soon after the shutdown began. The release of dye continued until startup of flow on Monday morning. On Sunday afternoon, at about 1500 hr, aerial observation of dye spreading was made. It was observed that a continuous mass of dye extended from CRM (Clinch River Mile) 20.0 to CRM 22.5; the mouth of White Oak Creek is at mile 20.8. It was also observed that another discrete

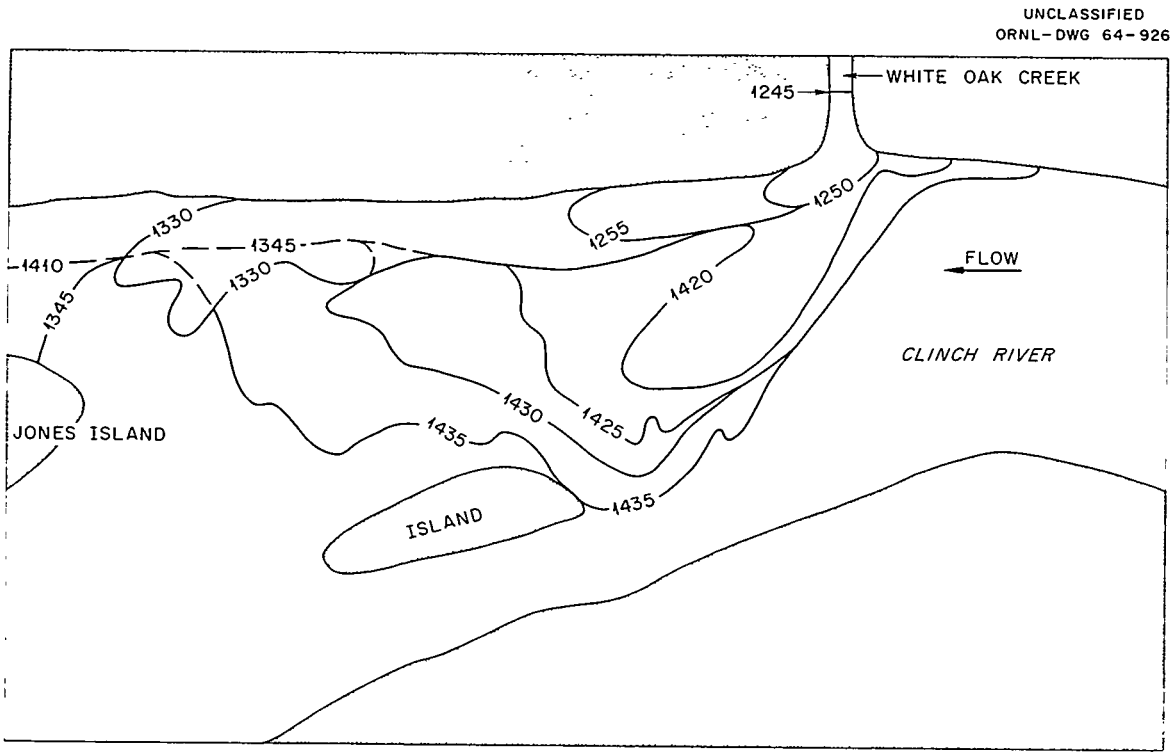

Fig. 44. Sketch of Time Development of Dye Front At and After the End of a 16,000-cfs Release in Clinch River at Mouth of White Oak Creek.

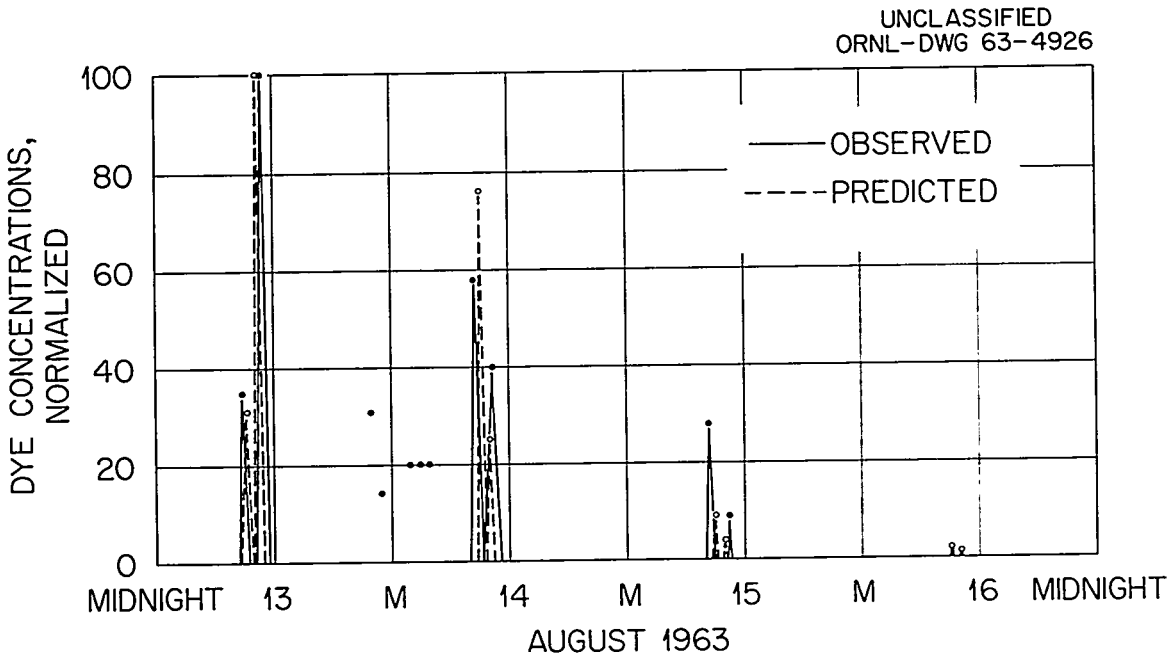

Fig. 45. Dye Concentrations at Clinch River Mile 16.2.

mass of dye was centered about mile 18.5. The mass at mile 18.5 was the pulse created by the first release of water on Friday.

As a result of the large-scale release of dye on the week end, considerably greater concentrations were observed on Monday of the second week at an observation section at Gallaher Bridge sampling site, 6.4 miles downstream from the mouth of White Oak Creek. The variation in dye concentration with time at this sampling site for the test period is shown in Fig. 46.

The twice-daily pulses of dye from the creek occurred on several weekdays during the test period of about 1000 and 1145 hr at the Gallaher Bridge observation station. Increased concentrations began at this station on Sunday afternoon. When there is no release from Melton Hill Reservoir, upstream flows could occur because of river control operations in the Tennessee River, re-establishment of thermal stratification in the Clinch River, or as a result of a combination of both processes. These upstream flows, though minor, could move a mass of dye short distances. It is believed that the mass of dye that passed the section at Gallaher Bridge at 1145 hr on Friday of the first week was slowly moved upstream during the week end and remained almost stagnated at the sampling site, beginning on Sunday afternoon. During the second week of the test, the mass of dye passing the site at 1145 hr stagnated about 2 miles downstream because of cessation of release from Melton Hill Reservoir.

The peak concentration that occurred on Monday of the second week of the test represents the critical condition in so far as dispersion of radioactive wastes are concerned. On the basis of the concentration of tracer injected at White Oak Dam and the peak concentration observed on Monday, the effective dilution at the Gallaher Bridge sampling site is computed to be 50. The median dilution of White Oak Creek releases by Clinch River water for the period of 1950 to 1960 has been 570 (ref 37). At the Gallaher Bridge station the radionuclide concentration in river water during the last few years has been less than 1% of the maximum permissible occupational concentration. On the basis of the dye tracer test, the dilution due to power release will be decreased by a factor of 11. It is thus tentatively concluded that the radionuclide concentrations at Gallaher Bridge would remain below MPC_w during the summer months when power releases from Melton Hill Reservoir are begun.

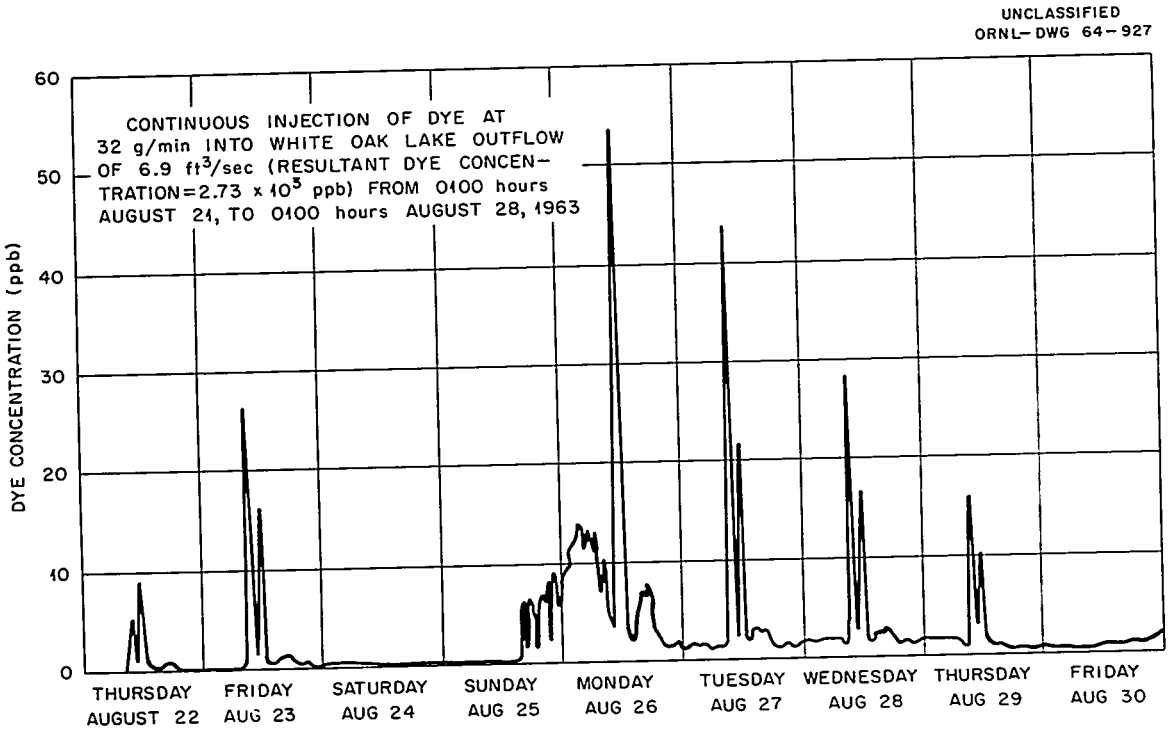

Fig. 46. Variation in Rhodamine B Concentration with Time During Period August 22-30, 1963, at Clinch River Mile 14.4.

7.2 Analysis of Clinch-River-Bottom Sediment Cores Collected in 1962

R. J. Pickering* P. H. Carrigan, Jr.*

Scanning of Clinch-River-bottom sediment cores collected during June, July, and August, 1962, for gross-gamma radioactivity was completed. The scans demonstrate that the greatest thicknesses of radioactive sediments occur in the lower reaches of the river, downstream from CRM 14. The single core showing the greatest thickness of radioactive sediment, 8.7 ft, was obtained at CRM 7.5. Sampler penetration, core recovery, and variations in gross-gamma radioactivity with depth at that cross section are shown in Fig. 47.

It can be seen from Fig. 47 that most of the radioactive sediment has been deposited on the more gently sloping side of the stream channel (note the vertical exaggeration). A recurring general pattern of variation of radioactivity with depth can be observed in several of the cores from CRM 7.5. The same general pattern is exhibited by a number of cores from other cross sections in the lower portion of the river. It is believed that certain features of this general pattern may be correlated with past events in waste-disposal operations at the Laboratory. However, additional data on the distribution of individual radionuclides with depth in the sediments are needed before such correlations can be established positively.

The radioactive portion of each core, as determined from the gross-gamma scans, will be mixed and sampled for radionuclide analysis to determine the total content of each of the major radionuclides in Clinch River bottom sediments.

Spectra of each 2-in. increment of the radioactive portion of selected cores will be obtained to determine the distribution with depth of the gamma-emitting radionuclides in the bottom sediment and to provide information on which to base correlations of their distribution in the cores with past events in waste-disposal operations.

---

*On loan from the Water Resources Division, U.S. Geological Survey.

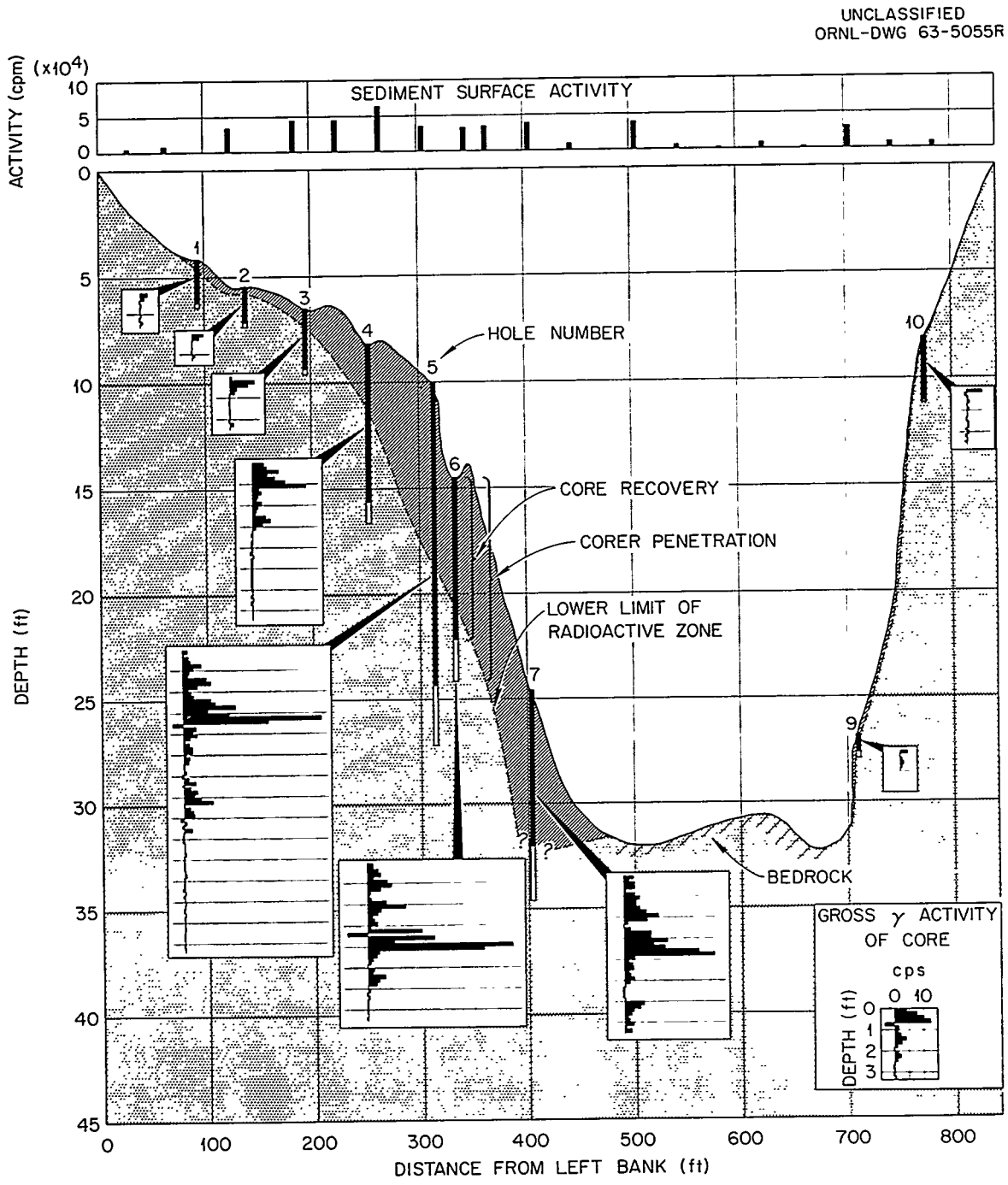

Fig. 47. Shape of Section and Radiation Levels at Clinch River Mile 7.5.

The primary purpose of the geochemical study of the cores is to determine the chemical forms in which the radionuclides exist and, thereby, the mechanisms by which they are incorporated in the bottom sediments.

The particle-size distribution, mineralogy, and cation-exchange capacities of the samples will also be measured. The interstitial water contained in the sediments will be extracted, and the distribution of stable and radioactive chemical constituents between the liquid and solid phases will be determined.

A diagrammatic representation of core-processing plans is shown in Fig. 48.

7.3 Radionuclide Desorption from Clinch River Sediments

T. Tamura W. P. Bonner

To understand the behavior and the mode of retention of radionuclides associated with sediments in the Clinch River, desorption studies were made with naturally contaminated, as well as artificially contaminated, sediments. The results of desorption tests of sediment from the mouth of White Oak Creek (CRM 20.8) were reported earlier for the radionuclides of cobalt, cesium, and ruthenium.[38] Desorption results for Sr^{90} on aliquots from the same sample have been obtained, and the results are shown in Table 25. The sediment contained 2400 dis/min/50 g, based on the oven-dried weight of Sr^{90}.

As shown in Table 25, 11.0% of the strontium was removed by tap water; this corresponds to a K_d of 65, which may be compared with K_d's ranging from 62 to 145 for sediment samples from different sections of the Clinch River. Of the solutions used, the most effective desorbing agent is tap water acidified to pH 2 with HNO_3 or HCl; the acid solution is even more effective than 1 M $CaCl_2$, KCl, or NaCl at near neutral pH. It should be pointed out that removal of 30 to 75% of the strontium by the different salt solutions is higher than the removals observed for Co^{60}, Cs^{137}, and Ru^{106} by these same solutions. It is also apparent from the data that pH has a very important influence on the desorption of strontium; the more acid solutions remove more strontium both in highly salted solutions and in tap water systems than do less acid solutions.

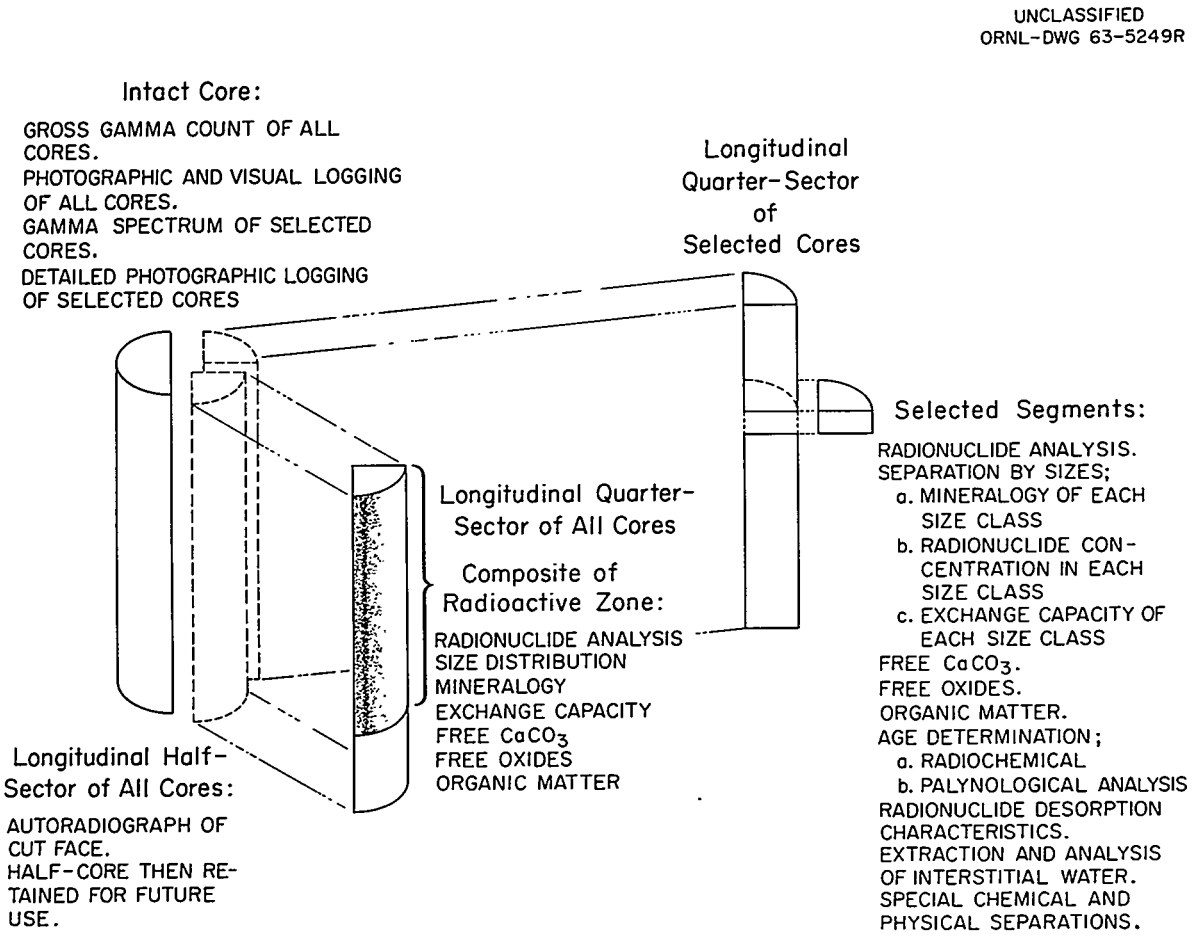

Fig. 48. Diagram of Plan for Analysis of Cores Taken from Clinch River Bottom Sediment During 1962.

Table 25. Removal of Strontium from Clinch River Sediment By Various Solutions Prepared from Tap Water

50 g (oven dried) CRM 20.8
400 ml solution
24-hr contact

Reagent	Concentration	pH	Percentage Strontium Removed
Tap water		6 (HNO_3)	21.3
Tap water		2 (HNO_3)	80.9
Tap water		6 (HCl)	19.4
Tap water		2 (HCl)	89.9
Tap water		7.7 (Natural pH)	11.0
$NaHSO_3$	0.1 M	6	37.7
$K_2Cr_2O_7$	0.1 M	5.9	73.1
$CaCl_2$	0.1 M	7	58.6
$CaCl_2$	1.0 M	7	76.9
NaCl	0.1 M	6	39.2
NaCl	0.1 M	8	30.1
NaCl	1.0 M	6	63.1
NaCl	1.0 M	8	56.0
KCl	0.1 M	6.2	53.0
KCl	1.0 M	6.2	68.7
NaOH		8	6.0
NaOH		12	4.9
NH_4OH		8	20.0
NH_4OH		11.8	3.5
Ethyl alcohol			< 1.0

7.3.1 Strontium Desorption from Artificially Contaminated Sediment

To better understand the nature of the retention of strontium by sediments, desorption studies were made by contaminating sediments artificially in the laboratory. A sample from CRM 15.3 was first contaminated with Sr^{85} in tap water at pH 8. About 46% of the strontium was sorbed; this gives a K_d of 85, a reasonable approximation of the K_d of Sr^{90} on the naturally contaminated sediment. The sample was leached with the solutions listed in Table 26. The desorption characteristics of the strontium sorbed at pH 8 is similar to the behavior observed with the naturally contaminated sediment; a slight difference is the greater effectiveness

Table 26. Equilibrium Sorption and 45-hr Desorption of 1.0 g of CRM 15.3 Sediment in 100 ml of Tap Water at Indicated pH

	Sorption pH			
	8	10.8	10.2[a]	10.1[b]
Sorption (%)	46.2	93.2	94.1	68.4
Desorption (%)				
Tap H_2O; pH 2 (HNO_3)	96.3	95.3	100	89.3
Tap H_2O; pH 12 (NaOH)	14.7	5.1	3.6	
1 M $CaCl_2$, pH 7	97.8	68.8	61.2	5.8
1 M NaCl, pH 8	90.2	83.0	100	85.3

[a] 95 ml tap water + 5 ml simulated waste + Sr^{85}.

[b] 95 ml tap water + 5 ml simulated waste + Sr^{85} (no sediment added).

of $CaCl_2$ over pH-2 tap water in removing strontium from the artificially contaminated material.

Sorption from a tap water system at pH 10.8 revealed that a much larger percentage of the strontium was sorbed (93%). The K_d for strontium at this pH is about 1300, compared with a K_d of about 220 or about 155 for the naturally contaminated system at pH 12, using the data for either NH_4OH or NaOH presented in Table 25. This suggests that another mechanism

is likely operative at this pH for removing strontium; and from observations and considerations of the system, it is apparent that $CaCO_3$ was being formed and was responsible for the much higher removals. The removal may be illustrated by the following equation:

$$Ca(HCO_3)_2 + 2\ OH^- \rightarrow CaCO_3 + 2\ H_2O + CO_3^{=} .$$

In desorption tests for strontium, $CaCl_2$ was not as effective as pH-2 tap water and even 1 M NaCl solution (Table 26).

Almost identical sorption and desorption responses were noted for the sediment when placed in a simulated waste solution containing dissolved ions normally found in intermediate-activity wastes.

Data on the removal of strontium simply from diluting simulated waste with tap water is shown in Table 26. No sediment is present and the pH is 10.1. The removal of strontium by the fine colloidal precipitate averaged 68.4%. Calcium chloride is an ineffective desorbing agent for this precipitate. An explanation of the different behavior of strontium sorbed at pH 8 and 10 from tap water systems may be given by considering the following reactions:

$$Ca^{2+} + \text{Sr-Clay} \rightleftarrows Sr^{2+} + \text{Ca-Clay} , \qquad (1)$$

$$\text{Sr-}CaCO_3 \rightleftarrows Sr^{2+} + Ca^{2+} + CO_3^{2-} . \qquad (2)$$

Since the pH of the tap water was about 8, sorption of the strontium by the sediment was primarily by ion exchange since the $Ca(HCO_3)_2$ is not affected and no $CaCO_3$ is expected at this pH. When calcium or other cations are introduced to the Sr-clay system, the exchange of ions occurs and the sorbed strontium is desorbed, as shown in reaction (1). At the same molarity concentrations, calcium would be expected to be more effective than sodium, as evidenced by the response shown in Table 26, column 1.

When sorption of strontium occurred at pH 10, strontium was sorbed not only by the clay but on the precipitate of calcium carbonate. When $CaCl_2$ salt solution at neutral pH was added, the strontium on the ion-exchange complex was displaced (reaction 1); but the strontium on the precipitate was not. The ineffectiveness of the $CaCl_2$ can be explained

by reaction (2), whereby release of strontium is associated with the dissolution of $CaCO_3$. The dissolution of $CaCO_3$ is repressed by the high Ca^{2+} concentration from the $CaCl_2$, which drives reaction (2) to the left, even though the pH had been decreased from 10 to 7. However, with sodium chloride solution, it would not repress the solubility by the common ion effect; and the reduction in pH would be expected to result in the redissolution of $CaCO_3$.

The use of these desorbing agents may provide a basis for identifying strontium sorbed on $CaCO_3$ and on clay exchange sites in sediments. Thus the results shown in Table 25 suggest that a portion of the strontium is associated with $CaCO_3$ in the naturally contaminated sediment. This tentative conclusion is reached, since less strontium was removed by $CaCl_2$ than by pH-2 tap water when the naturally contaminated sediment was tested. If all the strontium had been in ion exchange sites, more of the strontium would have been removed by the $CaCl_2$.

7.4 Hazards Analyses

K. E. Cowser

The discharge of radioactive solutions to the Clinch River may result in exposure of man to ionizing radiation. Calculations have been made of likely dose received due to exposure pathways deemed to be most important.[39,40] This report includes additional calculations of the internal and external exposure due to consumption of contaminated fish and exposure to the buildup of radionuclides in Clinch River water systems.

7.4.1 Contaminated Fish

Fish that feed in the Clinch River and Tennessee River downstream from White Oak Creek assimulate some of the radionuclides released to the river system. Since fish is a dietary staple, radionuclides in the fish will contribute to the total dose received. Parker showed that a catastrophic release of radionuclides from the biota of the Clinch River system is quite unlikely; the total inventory of radionuclides in the biota is estimated to be less than 1 curie.[41]

The data on radionuclide concentration in fish, used to estimate the dose that man may receive, was developed by the Subcommittee on Aquatic Biology, Clinch River Study Steering Committee.[42-47] Fish were collected during various seasons for the period, 1960 to 1962, and were processed to approximate, in so far as possible, normal human utilization.[43,47] Bottom feeders (carp, carpsucker, and buffalo) were processed either by grinding the flesh and bones together (total analyses) or by removing the flesh after cooking (flesh analyses). Sight feeders (white crappie, bluegill, white bass, largemouth bass, sauger, drum, and catfish) were processes by removing the flesh after cooking. For this analysis, catfish are included with the sight feeders, since only the flesh of the catfish was processed. Another fish sampling program was completed May 1963, but analytical results were not available for inclusion in this report.

Not all species of bottom feeders and sight feeders were collected with each sampling program; the number of a particular species collected varied. Therefore, for this analysis, all bottom feeders are assumed to be a single sample collected at one time; sight feeders were handled similarly. This assumption precludes any differences in fish due to the time of collection. That is, information on seasonal variation of such factors as feeding rates and water content of the flesh and their effect on radionuclide concentrations is unavailable and cannot be considered in the calculations.

Results of analyses of fish collected from the Clinch and Tennessee rivers are listed in Tables 27 and 28, respectively. Average values are given for the four principal nuclides detected (Sr^{90}, Cs^{137}, Ru^{106}, and Co^{60}); variation of the averages is indicated by the standard error of the mean. Standard errors do not appear where fish were composited before analyses. Bottom feeders are listed by species, since information is available on the quantities of these fish harvested commercially from Watts Bar Reservoir and from East Tennessee (Table 29). Information on sight feeders harvested is meager in comparison and does not warrant analyses by species. Only sport fishing routinely takes place on the Clinch River.

Table 27. Concentration of Radionuclides in Clinch River Fish
($\mu\mu$c/kg, fresh weight)

Fish Species	Sr^{90}		Cs^{137}		Ru^{106}		Co^{60}	
	Flesh	Total[a]	Flesh	Total[a]	Flesh	Total[a]	Flesh	Total
Carp	(17)[b] 500 ± 140	(40) 5100 ± 1700	(71) 510 ± 57	(39) 560 ± 79	(69) 170 ± 18	(39) 290 ± 78	(67) 66 ± 6.1	(39) 49 ± 9.9
Carpsucker	(18) 540 ± 190	(39) 940 ± 120 (39) 4800[d]	(122) 1200 ± 460	(37) 640 ± 67	(22) 120 ± 30	(37) 56 ± 16	(22) 120 ± 19	(37) 32 ± 6.8
Buffalo	(3) 240 ± 89	(30) 830 ± 110	(5) 480 ± 94	(30) 590 ± 92	(5) 110 ± 32	(30) 150 ± 38	(5) 78 ± 21	(30) 32 ± 6.8
Sight feeders[c]	(109) 180 ± 83		(126) 680 ± 120		(127) 120 ± 32		(127) 22 ± 11	

[a]Total fish consists of flesh and bone.

[b]Parenthetical values are numbers of fish analyzed.

[c]Sight feeders include white crappie, bluegill, white bass, largemouth bass, sauger, and drum; catfish also included.

[d]Includes four carpsuckers (composited) collected at CRM 19.6.

Table 28. Concentration of Radionuclides in Flesh of Tennessee River Fish (μμc/kg, fresh weight)

Fish Species	Sr^{90}	Cs^{137}	Ru^{106}	Co^{60}
Carp	(13)[a] 120 ± 33	(14) 180 ± 55	(14) 80 ± 27	(14) 71 ± 17
Carpsucker	(10) 99 ± 28	(10) 130 ± 27	(10) 69 ± 23	(10) 62 ± 18
Sight feeders[b]	(24) 250	(24) 170	(24) 48	(24) 66

[a]Parenthetical values are number of fish analyzed.

[b]Sight feeders include white crappie, bluegill, white bass, large-mouth bass, sauger, and drum; catfish also included.

Table 29. Commercial Fish Harvest from Watts Bar Reservoir and East Tennessee

(pounds, fresh weight)

Location	Carpsucker	Carp	Smallmouth Buffalo
Watts Bar Reservoir	15,600	23,700	161,000
East Tennessee	61,700	135,000	327,000
Fish dilution factor[a]	3.95	5.70	2.03

[a]Fish dilution factor = $\frac{\text{pounds of East Tennessee fish}}{\text{pounds of Watts Bar fish}}$.

Average values are observed to vary by factors ranging from about 2 to 5 between fish types from the same river; similar variations occur between fish of the same type but from the two rivers. A peculiar difference is noted in Sr^{90} concentrations in sight feeders; the average concentration in Tennessee River fish is about 50% larger than Clinch River fish. At present there is no explanation for these differences. Four carpsuckers, collected at CRM 19.6, contained sufficient radionuclides to audioradiograph. This is typical of fish that have spent considerable time in White Oak Creek (or White Oak Lake).[48] Inclusion of these fish in the analysis can be seen to increase significantly the average concentration of radionuclides.

An estimate is made of man's intake of radionuclides by assuming an annual rate of fish consumption of 37 lb.[49] This rate of fish consumption applies to commercial fishermen and, as a result, would estimate the intake of an admittedly high-exposure group. Data on the quantity of specific types of fish consumed and method of preparation is not available. Thus calculations made are based on the annual consumption of 37 lb of bottom feeders, considering both the total fish and the flesh, and consumption of 37 lb of sight feeders, considering only the flesh. The fraction of the various species of bottom feeders caught is assumed to be distributed according to commercial harvests from Watts Bar Reservoir. Estimates of the annual intake of specific radionuclides by consuming Clinch River or Tennessee River fish are given in Tables 30 and 31, respectively. A very noticeable increase in Sr^{90} intake is observed when consumption of bottom feeders (total fish) is considered. This significantly larger intake is due to the concentration of Sr^{90} by the bones of the fish, all of which are assumed to be eaten. Consumption of 37 lb of "fishburgers" each year is certainly an overestimate and unnecessarily conservative. However, without better data of fish consumption, it is impossible to arrive at a more reasonable value of intake.

Radionuclide intake by the general population is likely to be influenced by all fish harvested in East Tennessee, in addition to the differences in radionuclide content among species of bottom feeders. Applying the fish dilution factor (bottom feeders) for East Tennessee fish (Table 29), annual intakes were recalculated, and results are given in Tables 30 and

Table 30. Estimated Annual Intake of Radionuclides by Assumed Consumption of Clinch River Fish (10^{-3} μc/year)

	Sr^{90}		Cs^{137}		Ru^{106}		Co^{60}	
	Flesh	Total[a]	Flesh	Total[a]	Flesh	Total[a]	Flesh	Total[a]
Bottom feeders[b]	4.9 ± 1.3	23 ± 3.7 (28)[e]	9.0 ± 1.4	10 ± 1.3	2.0 ± 0.44	2.7 ± 0.54	1.3 ± 0.28	0.58 ± 0.094
Bottom feeders[c]	1.9 ± 0.60	7.6 ± 0.83 (8.9)	3.7 ± 0.64	4.4 ± 0.19	0.81 ± 0.21	1.1 ± 0.25	0.58 ± 0.044	0.24 ± 0.061
Sight feeders[d]	3.0 ± 1.4		11 ± 2.6		2.0 ± 0.54		0.38 ± 0.19	

[a]Total fish consists of flesh and bone.

[b]Bottom feeders include carp, carpsucker, and buffalo.

[c]Intake adjusted by fish dilution factor, Table 29

[d]Sight feeders include white crappie, bluegill, white bass, largemouth bass, sauger, and drum; catfish also included.

[e]Parenthetical values include four carpsuckers (composited) collected at CRM 19.6.

34% of the MPI may be attained as a result of consuming bottom feeders (total fish) from the Clinch River. Strontium-90 is responsible for almost the entire bone dose.

Table 33. Estimated Percentage of Maximum Permissible Intake That Man May Attain by Consuming Flesh of Tennessee River Fish

Fish Species	Critical Organ			
	Bone	Total Body	GI Tract	Thyroid
Bottom feeders[a]	7.2 ± 1.4	6.2 ± 1.2	0.11 ± 0.014	0.55 ± 0.084
Bottom feeders[b]	1.5 ± 0.28	1.3 ± 0.24	0.021 ± 0.0026	0.11 ± 0.017
Sight feeders[c]	16	14	0.11	0.83

[a]Bottom feeders include carp and carpsucker.

[b]Intake adjusted by fish dilution factor, Table 29.

[c]Sight feeders include white crappie, bluegill, white bass, largemouth bass, sauger, and drum; catfish also included.

Considerably more information would be required to estimate the dose received due to past events. For example, desired information would include at least: (1) rate of transfer of radionuclides from water to fish (flesh and bone) as a function of radionuclide and stable element concentration, fish age, and season of the year; (2) rate of transfer of radionuclide from bone to flesh while cooking; and (3) type and quantity of fish consumed, method of fish preparation, and dietary habits of individuals as a function of age. Current research suggests that the concentration of Sr^{90} in the flesh of white crappie reaches equilibrium rapidly with the water.[51] Such information lends itself to answering in part the questions raised by (1) above and extension of these studies will enhance the ability to estimate doses to man due to past events.

An interesting calculation is made based on the Sr^{90} content of the four carpsuckers previously mentioned. The combined weight of flesh and

whole fish (flesh and bone) for the four carpsuckers was 0.51 kg and 0.83 kg, respectively; the Sr^{90} concentration of flesh was 500 μμc/kg and of whole fish was 43,000 μμc/kg. An individual eating the four fish could have attained 0.3% of the MPI (bone) from the flesh and 44% of the MPI (bone) from the whole fish. Although such an event is unlikely, it seems appropriate to reduce further the probability of its occurrence. Such reduction is possible by preventing fish from leaving the controlled area of White Oak Lake and preventing fish from feeding in the stretch of White Oak Creek extending from White Oak Dam to the Clinch River.

7.4.2 Radionuclide Concentration in Water Systems

The presence of radionuclides in the raw water entering a water treatment plant may create, through processes of concentration, an external or internal dose problem. Three water systems that use Clinch River water as a source of supply were investigated. The Oak Ridge Water Plant has its raw water intake at CRM 41.5, well above the confluence of White Oak Creek and the Clinch River. The other two water treatment plants - the Sanitary Water Plant serving the Oak Ridge Gaseous Diffusion Plant (ORGDP) and that serving the Kingston Steam Plant - have water intakes at CRM 14 and on the Emory River near CRM 4.4, respectively. The water treatment plants are basically similar, differing only in design details. Treatment processes include: prechlorination for algae control; coagulation with alum, soda ash (as dictated by raw-water alkalinity), and occasionally coagulant aids, for turbidity removal; settling; filtration (either sand or anthracite); and postchlorination for disinfection. Activated carbon is used when undesirable taste and other problems occur. Water used in boilers is treated further by zeolite softeners.

The investigation consisted of external radiation surveys, with a scintillation-type survey meter (calibrated with radium), and collection of samples of sludge from settling basins, condensers, hot water heaters, boilers, air conditioners, and an elevated tank; samples of sediment from filters and cores of filter media; and samples of zeolite softener regenerant and the softener media. Results of the analyses are incomplete and will be reported later.

31. A significant reduction in radionuclide intake is observed, ranging from factors of about 2 to 4.

Table 31. Estimated Annual Intake of Radionuclides by Assumed Consumption of Flesh of Tennessee River Fish
(10^{-3} μc/year)

Fish Species	Sr^{90}	Cs^{137}	Ru^{106}	Co^{60}
Bottom feeders[a]	1.9 ± 0.38	2.7 ± 0.59	1.3 ± 0.31	1.1 ± 0.21
Bottom feeders[b]	0.39 ± 0.075	0.53 ± 0.11	0.26 ± 0.062	0.23 ± 0.043
Sight feeders[c]	4.3	2.8	0.81	1.1

[a]Bottom feeders include carp and carpsucker.

[b]Intake adjusted by fish dilution factor, Table 29.

[c]Sight feeders include white crappie, bluegill, white bass, large-mouth bass, sauger, and drum; catfish also included.

A maximum permissible intake (MPI) is calculated by assuming a daily intake of 2.2 liters of water containing the maximum permissible concentration (MPC) of the radionuclide of interest. Values used for MPC are discussed at length elsewhere.[50] All MPC_w values used for data relating to the Clinch River are taken as one-tenth of the occupational MPC_w values for continuous exposure recommended by ICRP and NCRP. To obtain MPC_w values relating to the Tennessee River, the MPC_w for continuous occupational exposure has been reduced by a factor of one-hundredth for whole body as critical organ and by one-thirtieth with thyroid, bone, and gastrointestinal tract as the critical organs. Using the estimated intakes (Tables 30 and 31), it is possible to calculate the fraction of MPI attained for the various critical organs as a result of eating contaminated fish (Tables 32 and 33). Estimates indicate that bone of the postulated high-exposure group may receive the largest dose; on the average, 28 to

Table 32. Estimated Percentage of Maximum Permissible Intake That Man May Attain by Consuming Clinch River Fish

Fish Species	Critical Organ			
	Bone	Total Body	GI Tract	Thyroid
Bottom feeders[a] (flesh)	6.1 ± 1.6	1.5 ± 0.39	0.072 ± 0.0081	0.38 ± 0.072
Bottom feeders[a] (total)	28 ± 4.5 (34)[e]	7.1 ± 1.2 (8.6)	0.14 ± 0.014 (0.15)	1.4 ± 0.19 (1.6)
Bottom feeders[c] (flesh)	2.4 ± 0.75	0.61 ± 0.19	0.03 ± 0.0039	0.16 ± 0.034
Bottom feeders[c] (total)	9.5 ± 1.1 (12)	2.4 ± 0.33 (2.9)	0.053 ± 0.0047 (0.0058)	0.48 ± 0.051 (0.57)
Sight feeders[d] (flesh)	3.8 ± 1.7	1.0 ± 0.44	0.071 ± 0.012	0.31 ± 0.080

[a]Bottom feeders include carp, carpsucker, and buffalo.

[b]Total fish consist of flesh and bone.

[c]Intake adjusted by fish dilution factor, Table 29.

[d]Sight feeders include white crappie, bluegill, white bass, largemouth bass, sauger, and drum; catfish also included.

[e]Parenthetical values include four carpsuckers (composited) collected at CRM 19.6.

At the time of the surveys, various amounts of water had been treated since the settling basins had last been cleaned or filters backwashed (Table 34). Thus, there was variation in the amount of sludge accumulated in the settling basins or sediment accumulated on the filters. Results of the external radiation survey are summarized in Table 35. Generally, there was little difference noted in dose rates at different units of the plants. Any increase in dose rate above background levels (referenced to the Oak Ridge Water Treatment Plant) was, with one exception, undetectable. At a distance of 2 in. above a partially drained filter at the Kingston Steam Plant supply, a dose rate of 0.021 mr/hr was detected. The dose rate remained the same after the filter was backwashed. It is likely that the anthracite filter is to some extent concentration radionuclides by ion exchange; this is currently being investigated by laboratory studies. The dose rate above the filters (0.015 mr/hr) of this supply is also influenced by the natural radioactivity present in the shale block used for construction of the building walls.

Table 34. Operational Data of Water Treatment Plants

System	Volume Through[a] Flocculator and Settling Basin (gal)	Volume Through[a] Filter (gal)	Sludge in Settling Basin (ft^3)	Plant Capacity (gal/day)
Oak Ridge water plant	1.1×10^9	1.8×10^6	2×10^4	22×10^6
ORGDP	5.4×10^8	4.5×10^6	6×10^3	4×10^6
Kingston steam plant	1.9×10^6	3.7×10^5	----	5.7×10^5

[a]Volume through flocculator, settling basin, and filter since last cleaned.

Table 35. Measurements of Ionizing Radiation In Water Treatment Plants (mr/hr)[a]

System	Ground Surface	Flocculator	Settling Basin	6 in. Above Water in Settling Basin	Filter
Oak Ridge water plant	0.016	0.013	0.012	0.0097	0.0095
ORGDP	0.017	0.011	0.012	0.0092	0.0092
Kingston steam plant	0.015	0.0083	0.0087	----	0.015

[a]All measurements (except as noted) were made 3 ft above the walking surface of the particular component of the treatment plant.

8. FUNDAMENTAL STUDIES OF MINERALS

T. Tamura

8.1 Desorption of Trace Amounts of Cesium from Minerals

Desorption tests performed on naturally contaminated sediments and reported in the previous quarterly[52] showed that cesium is resistant to most leaching agents, including concentrated salt solutions and concentrated acids. To determine which mineral might be responsible for the strong retention of cesium, desorption tests were carried out on minerals that had been contaminated in a manner similar to the sediment; hence, the minerals were contacted with tap water containing only trace level of Cs^{137}. After seven days' contact, the minerals were washed and air dried. A 0.1-g sample was then treated with 1 M sodium acetate for 24 hr and the desorption determined; the sodium acetate was decanted, and 1 M HNO_3 was added and the desorption determined for the acid treatment.

The results of these desorption tests are shown in Table 36. Three relatively distinct group responses are observed. Both kaolin and montmorillonite release their cesium to sodium acetate; in 24 hr, kaolin released 83.4%, and montmorillonite released 90.3%. The lower percentage release in the acid medium for these minerals is due to the prior removal in the sodium acetate treatment. These two minerals also show another interesting difference from the other minerals: The percentage desorbed after 24 hr with sodium acetate is higher than after only 1 hr of contact, whereas, with the other minerals, a marked decrease is noted in the amount of cesium released with the longer contact time.

Both vermiculite and biotite show similar response, particularly in the 1 M HNO_3. In 1 M HNO_3 vermiculite released 87.6%, and biotite released 98.0%. The nearly complete removal of cesium by the acid treatment of these two minerals is a reflection of their instability in acids. Both vermiculite and biotite are trioctahedral micas, which corresponds to three ions in the octahedral layer, and they contain appreciable ferrous iron in their structure. The iron is attacked by the acid and is released by the mineral; essentially, then, this is a decomposition process, and release of cesium is to be expected. The four minerals that show a decrease

Table 36. Desorption of Cesium from Several Minerals

	Illite	Vermiculite	Kaolinite	Montmorillonite	Muscovite	Biotite
Initial activity[a]	528,380	499,380	286,550	442,440	454,330	492,610
Desorbed with 1 M NaOAc, %						
1 hr	12.5	36.5	75.1	85.8	35.4	25.5
24 hr	6.39	24.0	83.4	90.3	20.0	6.91
Desorbed with 1 M HNO_3, %						
1 hr	25.0	51.6	5.44	5.92	26.6	75.4
4 hr	27.0	77.5	9.61	12.4	22.9	86.6
24 hr	25.4	87.6	11.0	15.0	17.8	98.0
Total desorbed, %	31.8	111.6	94.4	105.3	37.8	104.9

[a]Initial activity given in counts min^{-1} 0.1 g^{-1}.

in the cesium released in 1 M sodium acetate with the longer contact time have one structural feature in common. These minerals all possess a c-axis spacing of 10 A. (Vermiculite is 14 A, but 50% of the material is a 10-A mica.) It appears then that when the cesium was sorbed from a tap-water system, a portion of the cesium was held in the more readily exchangeable sites which on contact with 1 M sodium acetate were released. With longer contact, however, a portion of the released cesium moves into a more selective and retentive site. This type of site has been previously described as an "edge site" by the author and has led to some confusion. These edge sites are believed to be located in the clay but at the periphery of the crystallite; these sites are a part of the sites referred to as interlayer sites. The accessibility of the interlayer sites depends on the interlayer spacing. If the interlayer spacing is large (14-A c spacing minus 9.3-A silicate layer = 4.7-A interlayer spacing) such as with montmorillonite, the ions located in the center of the crystallite and at the edges of the crystallites are all readily exchangeable. If the interlayer spacing is small (10 A minus 9.3 A = 0.7 A), the ions located in the center and the edges are difficult to remove; the sites at the edges do prefer cesium, and cations located there enter into exchange reaction with cesium. In addition to the interlayer sites, attraction for ions exist on the external surface due to "broken bonds" such as with the mineral kaolinite; these sites are generally readily exchangeable, and, though they prefer cesium ions, they do not show extremely high selectivities. Evidence exists that if the c spacing of kaolinite can be increased from 7.2 A to 10 A, selectivity for cesium is greatly enhanced.[53]

The third group of minerals in these experiments is the illite-muscovite group. These two minerals resist acid attack, and the total cesium released by the sodium acetate and nitric acid treatments is 31.8% for illite and 37.8% for muscovite. These two minerals differ from biotite and vermiculite in atomic arrangement in the octahedral layer. Illite and muscovite are dioctahedral; that is, they contain two aluminum ions in the octahedral layer.

The measurement of over 100% desorption in several cases reflect errors in the method of testing. The possible cause of the error is the difference in efficiency of counting 0.1 g of solid and 1 ml of solution; the counts were used to calculate the desorption percentage.

These experiments are being continued in order to establish the influence of longer contact time during sorption. It is believed that with longer contact time, more of the cesium will diffuse from the edge sites deeper into the interlayer sites of the 10 A minerals; and desorption tests should reveal a lower removal of cesium from these minerals.

8.2 Ion Exchange Behavior of Vermiculite with Cesium

Vermiculite is often suspected to be the "fixer" of cesium ions, since the well-known potassium fixation reactions are associated with this mineral. Investigations here showed that the same potassium fixation mechanism can be demonstrated with respect to cesium. The response observed in this type of fixation is shown in Fig. 49 (natural material). The increasing K_d (increasing sorption) with increasing cesium ion concentration reflects the change in the lattice of vermiculite as more cesium is sorbed. The initial decrease in the K_d is due to the high sodium concentration of the solution (0.1 M NaCl), which requires a minimum cesium concentration in the solution to overcome the influence of the sodium ions.

If the vermiculite is treated with sufficient potassium ions to induce the lattice change ascribed above to cesium, then the K_d is not expected to show an increase with increasing cesium concentration, since the factor responsible for this mode of fixation is inoperative. In this case the K_d decreases, as shown in the curve of Fig. 49, labeled "potassium saturated." The increased K_d for this potassium-saturated vermiculite in the low cesium concentrations is due to the formation of the favorable structure with potassium, which exchanges with the cesium. This mechanism is to be contrasted with the natural material, which is sorbing cesium directly during the formation of the collapsed structure.

The curve labeled "cesium saturated" not only illustrates the reduced sorption of cesium but illustrates the case for a relatively constant K_d over a range of cesium concentration. These curves were shown earlier for different minerals; however this is the first demonstration of the three types of curve by a single material. The "potassium saturated" curve is similar to those obtained for heated montmorillonite, illite, and micas; the "cesium saturated" curve was also shown by kaolinite and montmorillonite.

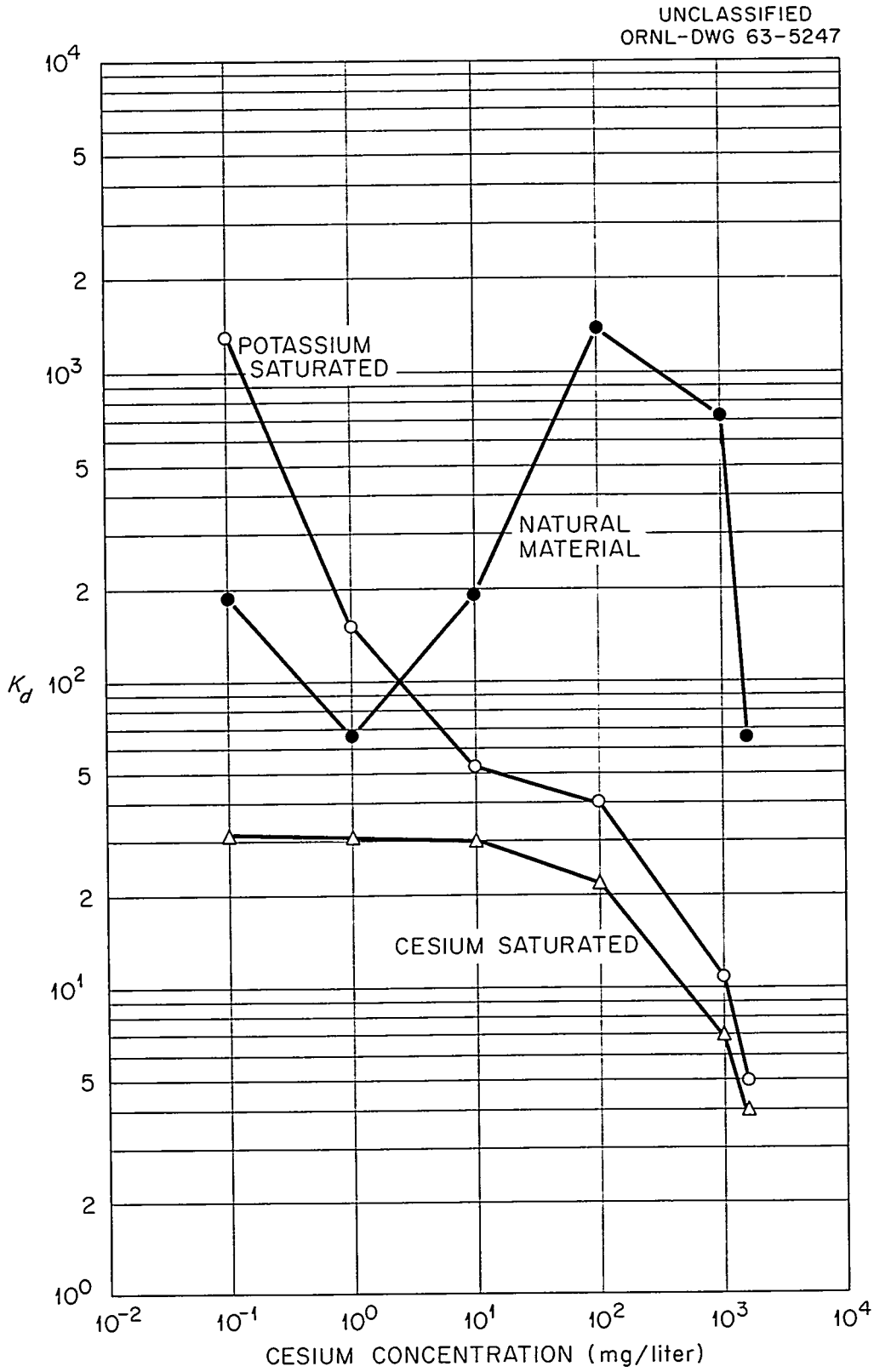

Fig. 49. Sorption of Cesium by Hydrobiotite.

9. WHITE OAK CREEK BASIN STUDY*

9.1 Evaluation of Fission-Product Distribution and Movement In and Around Chemical Waste Seepage Pits 2 and 3

T. F. Lomenick

9.1.1 General

The area in and around the million-gallon chemical waste seepage pits 2 and 3 contains an estimated 180,000 curies of Cs^{137}, 40,000 curies of Sr^{90}, about 10,000 curies of Ru^{106}, and lesser amounts of the rare earths, Ru^{103}, Sr^{89}, Co^{60}, Cs^{134}, and $Zr\text{-}Nb^{95}$. Previous investigations described the movement of ruthenium in and around the site;[54] however, little is known about the behavior of cesium and strontium in the pit area, except that it is apparently concentrated relatively close to the pit walls, since such small amounts have been found in the monitoring wells about the area. The recent abandonment and subsequent filling of the pits provided an opportunity to investigate, in much greater detail, the nature and extent of fission-product migration from the pits, especially of Sr^{90} and Cs^{137}. The study of migration was not possible earlier because of the high-radiation field in the area. The primary objectives of this study are (1) to determine the quantity and distribution of the various radionuclides within the area, (2) to determine the degree of fixation of the activity on the shale that underlies the site and in the sludge and precipitates within the pits, and (3) to predict the future effects of ground water on the waste.

At ORNL, intermediate-level liquid waste is disposed of through a system of seepage pits dug in the Conasauga shale formation. This method of disposal allows the waste solution to seep slowly through the ground, while most of the radioactive materials are retained by the shale. The

---

*This project, entitled, "Environmental Radiation Studies: Evaluation of Fission Product Distribution and Movement in White Oak Creek Drainage Basin " (AEC Activity 060501), is supported by the U. S. Atomic Energy Commission"s Division of Biology and Medicine. All other projects covered in this report are supported by the Division of Reactor Development (AEC Activity 04640011).

discharge of large quantities of contaminated waste water to seepage pits began in 1952 with the construction of waste pit 2. Three years later waste pit 3 was put into operation, and eventually four additional ones were opened. Pits 2 and 3 formerly had the shape of a frustum of an inverted rectangular pyramid, with dimensions of 200 ft by 100 ft by 15 ft in depth. To prevent animals from getting to the waste water, the pits were covered with a galvanized iron screen. In addition to the several million gallons of liquid waste pumped to these pits, large quantities of sludge or precipitate of illitic clay and calcium carbonate from the low-level waste treatment plant were routinely dumped into pit 3 and to a lesser extent into pit 2.

With construction of covered seepage pits 5, 6, and 7, waste pits 2 and 3 were abandoned and subsequently filled in 1962. Weathered shale containing many thin limestone lenses was the principal fill material. However, a few hundred steel barrels of solid waste were dumped into each pit, and, in addition, the galvanized iron screen that covered the pits and their supporting posts were pushed into the holes. During filling of the pits, it was observed that the soft sludges and precipitates in the bottom of the pits were not being covered by the fill, but were being squeezed into the still uncovered portion of the pit. It was necessary to use wooden siding and other debris to cover the sludge and thus prevent its upward movement.

9.1.2 Quantity and Distribution of Radionuclides in the Area

Due to the nature of the waste pit environment, some unique problems were encountered in obtaining representative samples of the contaminated materials. The metal drums, wire mesh nets and their supporting posts, lumber, and other miscellaneous fill debris in the pits pose special drilling problems. It is also difficult to obtain cores with a single sampling device from the weathered and unweathered portions of the Conasaugs shale, as well as from the loose, fill material in the pits, sludge from the low-level waste water treatment plant, and accumulated precipitates from the waste water. The high degree of contamination of the sludge and weathered shale further complicates the sampling.

A preliminary series of cores was taken in and around the two waste pits to determine the effectiveness of conventional sampling equipment and methods for obtaining representative samples of the various types of rock and fill materials. In addition, a sufficient number of cores were taken and analyzed to grossly delineate radioactivity concentrations on the soil and materials in and around the pits. A sketch map of a portion of the waste pit area, showing the sample locations, is presented in Fig. 50. Due principally to the still relatively high radiation field in the vicinity of waste pit 2, which reduced considerably the allowable working time, fewer samples were taken in that area. The depth of sampling at the various locations varied from 6 to 32 ft. Split-barrel assemblies were used to recover samples of the fill material and weathered shale, while thin-wall tubes were used to sample the soft sludges and precipitates. A series "m" core barrel with diamond bit, with water as a drilling fluid, was used for coring the deeper unweathered shale. Some difficulty was experienced with collapse of the side walls of the holes in the fill material and soft sludges, but the greatest disadvantage to this method of sampling was the very poor core recovery obtained by the series "m" core barrel in zones of alternating hard and soft shale.

Radiochemical analyses of sections of the cores indicate that apparently most of the activity which is largely cesium and strontium is associated with the soft sludges and precipitates and the first few inches of weathered shale on the side walls and bottoms on the pits. Also, the sludges and precipitates are not evenly distributed over the bottoms of the pits but have accumulated in irregular shaped pockets. A cross sectional view of waste pit 2, showing the areas of high activity concentrations and the distribution of sludge within the pit, is presented in Fig. 51. It is noted in well 3 that the sludge is about 10 ft thick and is within 4 ft of the ground surface, while no sludge was found in hole 11 in the center of the pit. This is due to the highly mobile state of the sludge, which allowed it to be pushed ahead of the fill material until it was confined by timbers and eventually covered. On a dry-weight basis, concentrations of Cs^{137} and Sr^{90} were as high as 96 μc/g and 17 μc/g, respectively, in the sludge, and 3 μc/g and 0.2 μc/g in the weathered shale on the side walls and bottoms of the pits. There appears to be little difference in the

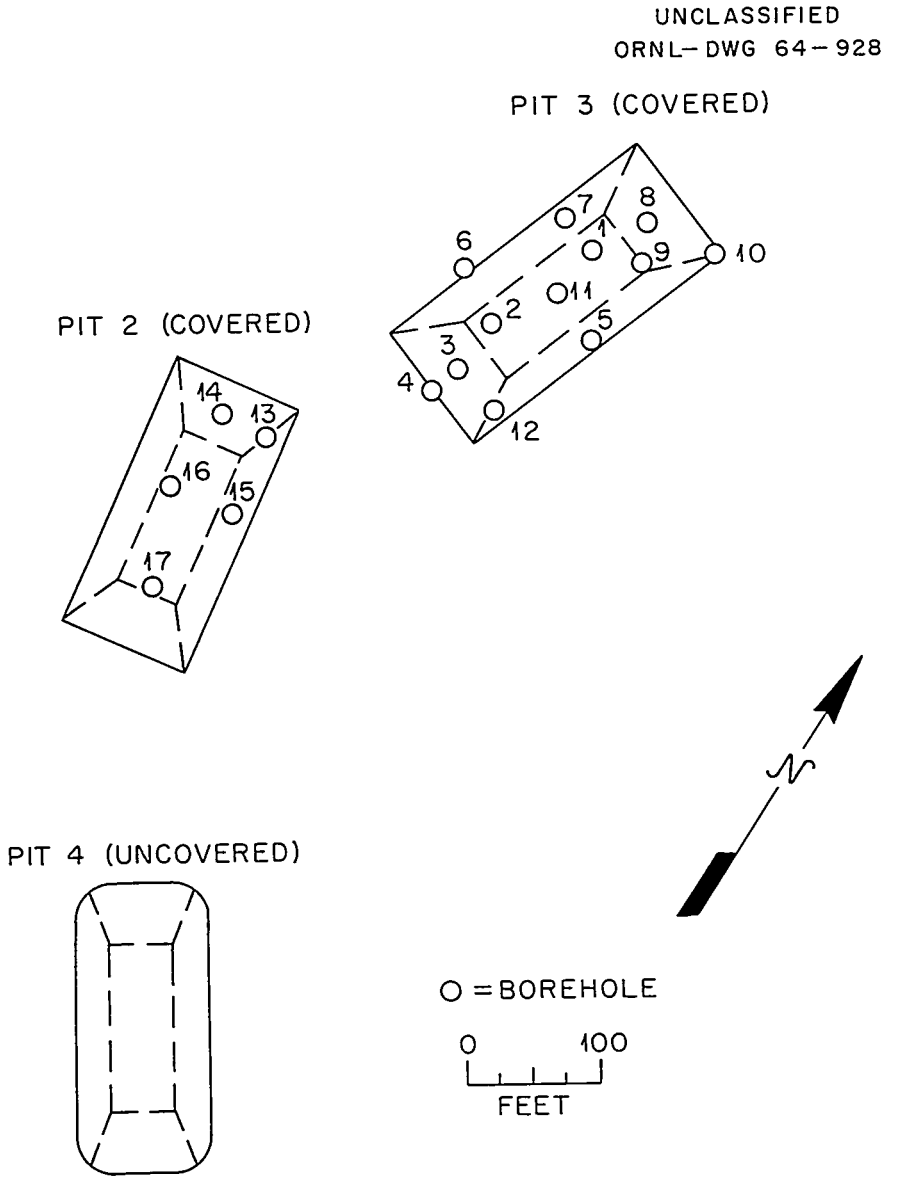

Fig. 50. Sketch Map of a Portion of the Waste-Pit Area, Showing Locations of the Preliminary Series of Boreholes.

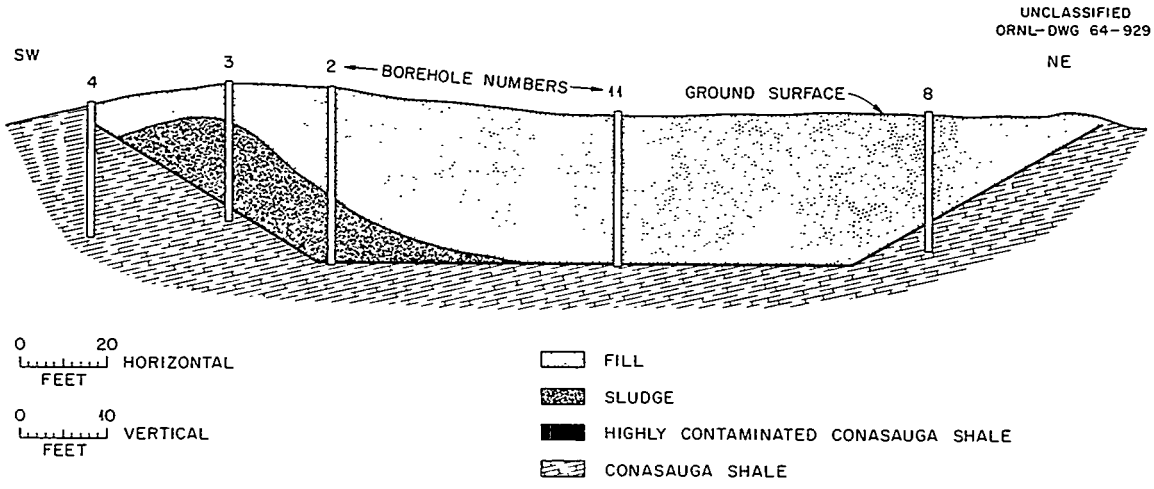

Fig. 51. Longitudinal Cross Section Through Waste Pit 3.

concentrations of activity found on the sludge and weathered shale in the two pits, although the quantity of sludge in waste pit 2 is considerably less than that in pit 3.

The alternating hard and soft shale sequence immediately below the bottom of the pits could not be cored satisfactorily with the drilling equipment used, and, as a consequence, incomplete data was obtained on the quantity and distribution of activity beneath the pits. However, some information on the downward migration of the radionuclides was obtained from boreholes that penetrated the softer and more easily sampled side walls of the pits. For boreholes 10 and 14 it was found that the concentrations of cesium and strontium on the shale were about 100 times greater at the former surface of the wall than at distances of 2 ft below the former surface of the wall.

9.2 Hydrology of White Oak Creek Basin

W. M. McMaster * R. M. Richardson*

A series of water samples was collected from White Oak Creek and from sources contributing radioactive contaminants directly to the stream on September 19, 1963, in order to measure gains or losses in specific radionuclide load as a labeled mass of water moved downstream. The sampling was done during a period of low base-flow conditions.

A mass of White Oak Creek water was labeled for identification by pouring a quantity of dye directly into the stream about 200 ft above the outfall of the effluent from the Process Waste Water Treatment Plant (PWWTP). This procedure was repeated at each source on the accompanying map (Fig. 52) and at other downstream points as the mass of dyed water passed.

As shown in Fig. 53, the stream load of each radionuclide changed considerably as the water moved, increasing downstream to the old intermediate-pond dike, then decreasing by the time it reached sampling point 7. At point 8, water content of total rare earths, Sr^{90}, and Co^{60} increased significantly. This increase is probably due to seepage into White Oak

---

*On loan from Water Resources Division, U. S. Geological Survey.

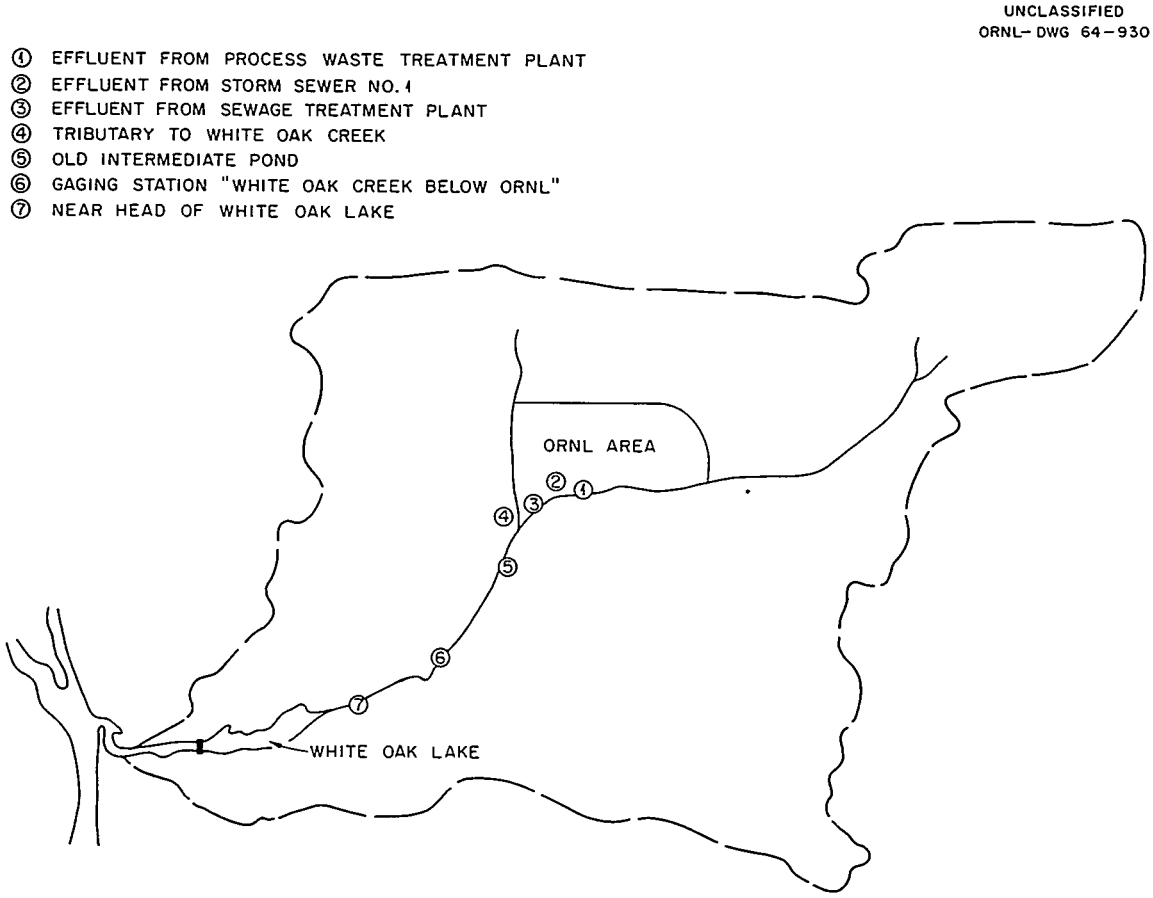

Fig. 52. Map of White Oak Creek Basin, Showing Sources of Contamination Samples and Stream Sampling Sites, September 19, 1963.

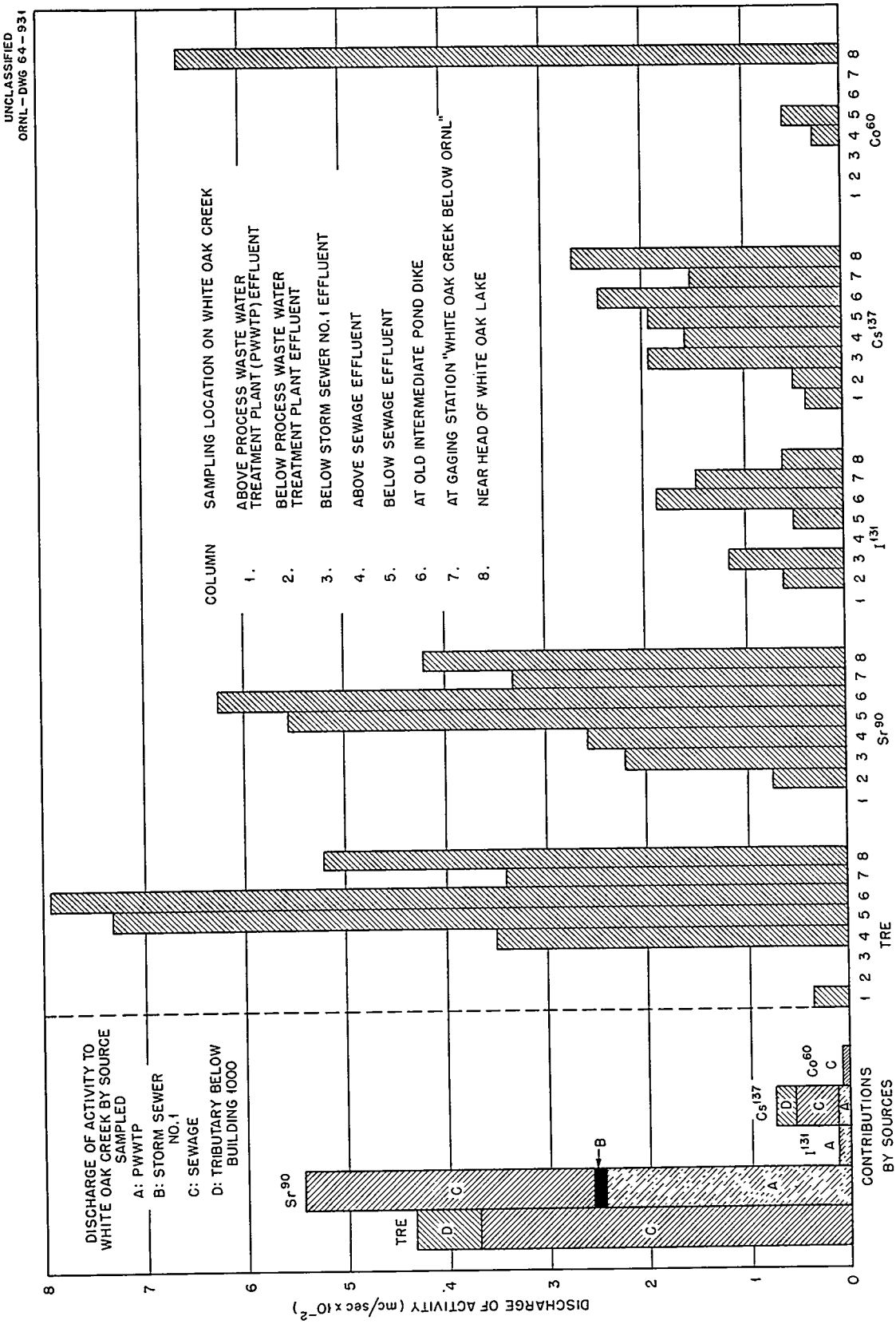

Fig. 53. Discharge of Activity to White Oak Creek According to Sources Sampled.

Creek of contaminated ground water originating at the east drainage stream of the chemical waste pits.[55]

Results of analyses of the samples collected from the PWWTP effluent and from the sewage treatment plant effluent showed that the sewage effluent was contributing more Sr^{90} than the process waste water effluent. On the basis of a discharge of 100,000 gal per day, the sewage effluent would have contributed a total of 542 μc/day, whereas the PWWTP, on the same basis, would have contributed 460 μc/day. Lomenick[56] found during an eight-month study in 1961 that the mean concentration of Sr^{90} in the sewage treatment plant effluent was 1.7×10^{-6} μc/cc, slightly higher than the concentration sampled September 1963.

Prior to the test, an attempt was made to measure small increments of discharge in White Oak Creek for the purpose of accurately computing radionuclide loads at points in the stream. The dilution method was used with Rhodamine B dye as a tracer. The dye was injected into the stream at a constant rate at a point about 200 ft upstream from the PWWTP effluent for a total of 3.5 hr, in order to allow a plateau of dye concentration to become established throughout the stream. Near the end of the injection period, water samples were collected at several points along the channel; dye concentration was then read by fluorometer, and the discharge was computed for each sampling site by the dilution formula. Discharge values obtained from samples collected between the injection point and the sewage effluent were acceptable, but below the sewage effluent computed discharge values became increasingly too large with distance. Later, a short experiment showed that Rhodamine is extremely sensitive to free chlorine. It is thought that sufficient free chlorine enters White Oak Creek in the sewage effluent because of decomposition of part of the dye, precluding the use of dyes in the stream for quantitative measurements. The discharges on which the radionuclide loads were based were interpolated between points of known discharge in the stream.

During the week of October 21, water-level measurements were made in the wells in White Oak Creek Basin, during the period of lowest water surface for the 1963 water year, for the purpose of constructing a low-water-surface map of White Oak Creek Basin.

REFERENCES

1. A. M. Platt, Hanford Atomic Products Operation, private communication.

2. R. E. Blanco, F. L. Parker, Waste Treatment and Disposal Quarterly Progress Report for February-April 1963, ORNL-TM-603 (Dec. 16, 1963).

3. Letter, I. R. Higgins to R. E. Blanco, January 1963.

4. R. E. Blanco, F. L. Parker, Waste Treatment and Disposal Quarterly Progress Report for November-December 1962 and January 1963, ORNL-TM-516 (June 12, 1963).

5. R. R. Holcomb, Low-Radioactivity-Level Waste Treatment, Part 1 - Laboratory Development of a Scavenging-Precipitation Ion-Exchange Process for Decontamination of Process Water Wastes, ORNL-3322 (June 25, 1963).

6. R. E. Brooksbank et al., Low-Radioactivity-Level Waste Treatment Part II - Pilot Plant Demonstration of the Removal of Activity from Low-Level Process Wastes by a Scavenging-Precipitation Ion-Exchange Process, ORNL-3349 (May 13, 1963).

7. G. B. Hatch and O. Rice, "Surface Active Properties of Hexametaphosphate," Ind. Eng. Chem. 31, p 51 (1939).

8. E. Schonfeld, Effect of Some Impurities on the Precipitation of Calcium and Magnesium from Process Waste Water, ORNL-TM-505 (April 25, 1963).

9. Chemical Technology Division Annual Progress Report for Period Ending May 31, 1963, ORNL-3452.

10. R. E. Blanco, F. L. Parker, Waste Treatment and Disposal Quarterly Progress Report for February-April 1963, ORNL-TM-603 (Dec. 16, 1963).

11. R. M. G. Boucher and A. L. Weiner, "Sonic Defoaming - Its Present Status," Food Processing (October 1962).

12. P. A. Haas, Engineering Development of a Foam Column for Countercurrent Surface-Liquid Extraction of Surface Active Solutes, ORNL-3527 (in preparation).

13. R. E. Blanco, E. G. Struxness, Waste Treatment and Disposal Progress Report for February and March 1962, ORNL-TM-252, pp 39-43 (Sept. 10, 1962).

14. L. C. Watson, H. K. Rae, R. W. Durham, E. J. Evans, and D. H. Charlesworth, Methods of Storage of Solids Containing Fission Products, CRCE-736 (June 1958).

15. E. Doud, Design of Underground Storage Tanks for Radioactive Wastes, HW-57282 (March 1959).

16. R. E. Blanco, E. G. Struxness, Waste Treatment and Disposal Progress Report for October and November 1961, ORNL-TM-133, pp 33-39 (Mar. 13, 1962).

17. Paul L. Russell, Bureau of Mines, U. S. Dept. of the Interior, personal communication, May 16, 1963.

18. Bedrock Waste Storage Concept and Cost Appraisal, du Pont Company Report, DPE-2210 (May 1962).

19. M. L. Jackson, Soil Chemical Analysis, Prentice-Hall, Englewood Cliffs, New York., 1958.

20. D. G. Jacobs, "Ion Exchange in the Deep Well Disposal of Radioactive Wastes," International Colloquium on Retention and Migration of Radioactive Ions in Soils, Centre d'Etudes Nucleaires de Saclay, France, October 16, 17, and 18, 1962, pp 43-35 (1963).

21. R. L. Blanchard, B. Kahn, and G. G. Robeck, Laboratory Studies on the Ground Disposal of ORNL Intermediate-Level Liquid Radioactive Wastes, ORNL-2475 (Mar. 15, 1958).

22. W. J. Lacy, Radioactive Waste Disposal Report on Seepage Pit Liquid Waste-Shale Column Experiment, ORNL-2415 (Nov. 1, 1957).

23. D. G. Jacobs and T. Tamura, Proc. 7th Int. Conf. Soil Sci. 2, 206 (1960).

24. D. G. Jacobs, Health Physics 4, 157 (1960).

25. R. J. Morton (ed.), Status Report No. 3 on Clinch River Study, ORNL-3370 (Nov. 21, 1962).

26. K. E. Cowser, W. de Laguna, and F. L. Parker, Soil Disposal of Radioactive Wastes at ORNL (to be published as an ORNL-TM report).

27. E. Glueckauf, Trans. Far. Soc. 51, 34 (1955).

28. Y. Inoue and W. J. Kaufman, Ground Disposal of Radioactive Wastes, TID-7628, p 303 (1962).

29. E. Glueckauf, Ion Exchange and Its Applications, p 34, Society of Chemical Industry, London (1955).

30. G. N. Savin, Stress Concentration Around Holes, Pergamon Press, New York, 1961.

31. S. Serata, Development of Design Principles for Disposal of Reactor Fuel Waste Into Underground Salt Cavities, Technical Report of University of Texas to Atomic Energy Commission (Jan. 1, 1959).

32. P. LeComte, Creep and Internal Friction in Rock Salt, doctoral dissertation, Division of Geological Sciences, Harvard University, Cambridge, Mass. (May 1960).

33. Corps of Engineers, Project Dribble Petrographic Examination and Physical Tests of Cores, Tatum Salt Dome, Mississippi, Technical Report No. 6-614, U.S. Army Engineer Waterways Experiment Station, Vicksburg, Miss. (Jan. 1963).

34. J. Handin and R. V. Hager, Jr., "Experimental Deformation of Sedimentary Rocks Under Confining Pressure: Tests at High Temperature," Bulletin of The American Association of Petroleum Geologists 42(12), pp 2892-2934 (Dec. 1958).

35. S. Serata, Michigan State University, personal communication.

36. L. Obert, Applied Physics Laboratory, U. S. Bureau of Mines, personal communication.

37. R. J. Morton (ed.), Status Report No. 3 on Clinch River Study, ORNL-3370, p 106 (Nov. 21, 1962).

38. R. E. Blanco and F. L. Parker, Waste Treatment and Disposal Progress Report for February-April 1963, ORNL-TM-603 (Dec. 16, 1963).

39. K. E. Cowser, W. S. Snyder, and M. J. Cook, "Preliminary Safety Analysis of Radionuclide Release to the Clinch River," Proceedings of Conference on Transport of Radionuclides in Fresh Water, January 30, 31, and February 1, 1963, Austin, Texas, U. S. Atomic Energy Commission, Washington, D. C., p 17-39, TID-7664 (July 1963).

40. K. E. Cowser, "Clinch River Study: Hazards Analyses," Waste Treatment and Disposal Progress Report for February-April 1963, ORNL-TM-603 (Dec. 16, 1963).

41. F. L. Parker, "Clinch River Studies," Proceedings of Conference on Transport of Radionuclides in Fresh Water, January 30, 31, and February 1, 1963, Austin, Texas, U. S. Atomic Energy Commission, Washington, D. C., p 161-181, TID-7664 (July 1963).

42. A. G. Friend et al., Fate of Radionuclides in Fresh Water Environments: Progress Report No. 2, Clinch and Tennessee Rivers, February 9-15, 1960, interim report to Clinch River Study Steering Committee, Sept. 1960 (multilithed, 1962).

43. A. G. Friend et al., Fate of Radionuclides in Fresh Water Environments: Progress Report No. 5, Clinch and Tennessee Rivers, May 15-30, 1960, interim report to Clinch River Study Steering Committee, Oct. 1961 (multilithed, 1962).

44. A. G. Friend et al., Fate of Radionuclides in Fresh Water Environments: Progress Report No. 6, Clinch and Tennessee Rivers, September 19-30, 1960, interim report to Clinch River Study Steering Committee, Oct. 1961 (multilithed, 1962).

45. D. B. Porcella, Data on Fish Collected in June and December 1961 and March 1962 (personal communication, May 8, 1963).

46. S. I. Auerbach, Chairman, et al., Progress Report No. 1, Subcommittee on Aquatic Biology, copies submitted to Clinch River Study Steering Committee, April 26, 1962 (unpublished).

47. S. I. Auerbach, Chairman, et al., Progress Report No. 2, Subcommittee on Aquatic Biology, copies submitted to Clinch River Study Steering Committee, Feb. 6, 1963 (unpublished).

48. R. E. Martin, S. I. Auerbach, and D. J. Nelson, Growth and Movement of Smallmouth Buffalo, Ictiobus Bubalus (Rafinesque), in Watts Bar Reservoir, Tennessee (ORNL report in press).

49. P. Bryan and C. E. White, "An Economic Evaluation of the Commercial Fishing in the T.V.A. Lakes of Alabama During 1956," Proceedings of the Twelfth Annual Conference Southeastern Association of Game and Fish Commissioners, 128-132 (1958).

50. C. P. McCammon, Chairman, et al., Progress Report No. 2, Subcommittee on Safety Evaluation, copies submitted to Clinch River Steering Committee, Feb. 6, 1963 (unpublished).

51. R. J. Morton (ed.), Status Report No. 4 on Clinch River Study, Clinch River Study Steering Committee, ORNL-3409 (Sept. 11, 1963).

52. R. E. Blanco and F. L. Parker, Waste Treatment and Disposal Progress Report for February-April 1963, ORNL-TM-603 (Dec. 16, 1963).

53. J. S. Wahlberg and M. J. Fishman, Adsorption of Cesium on Clay Minerals, Geological Survey Bulletin 1140-A, U.S. Government Printing Office, 1962.

54. K. E. Cowser, W. de Laguna, and F. L. Parker, Soil Disposal of Radioactive Liquid Wastes at ORNL, ORNL-2996 (in press).

55. T. F. Lomenick, "Movement of Ruthenium in the Bed of White Oak Lake," Health Physics 9, 835-845 (1963).

56. T. F. Lomenick, "Accumulation and Movement of Radionuclides in White Oak Creek Basin" in Status Report No. 4 on Clinch River Study, ORNL-3409, pp 15-32 (Sept. 11, 1963).

INTERNAL DISTRIBUTION

1. ORNL - Y-12 Technical Library Document Reference Section
2-4. Central Research Library
5-14. Laboratory Records Department
15. Laboratory Records, ORNL-RC
16-17. R. E. Blanco
18. J. O. Blomeke
19. W. J. Boegly, Jr.
20. R. L. Bradshaw
21. J. C. Bresee
22. R. E. Brooksbank
23. F. N. Browder
24. K. B. Brown
25. P. H. Carrigan, Jr.
26. W. E. Clark
27. K. E. Cowser
28. F. L. Culler
29. W. Davis, Jr.
30. W. de Laguna
31. F. M. Empson
32. D. E. Ferguson
33. E. J. Frederick
34. H. W. Godbee
35. H. E. Goeller
36. J. M. Googin
37. P. A. Haas
38. C. W. Hancher
39. C. E. Haynes
40. R. F. Hibbs
41. R. R. Holcomb
42. J. M. Holmes
43. D. G. Jacobs
44. W. H. Jordan
45. L. J. King
46. H. Kubota
47. T. F. Lomenick
48. K. Z. Morgan
49. R. J. Morton
50. E. L. Nicholson
51-52. F. L. Parker
53. J. J. Perona
54. R. M. Richardson
55. J. T. Roberts
56-57. E. G. Struxness
58. J. C. Suddath
59. J. A. Swartout
60. T. Tamura
61. J. W. Ullmann
62. H. O. Weeren
63. M. E. Whatley

EXTERNAL DISTRIBUTION

64. E. L. Anderson, AEC, Washington, D. C.
65. W. G. Belter, AEC, Washington, D. C.
66. H. Bernard, AEC, Washington, D. C.
67. Arnold B. Joseph, AEC, Washington, D. C.
68. J. A. Lieberman, AEC, Washington, D. C.
69. W. H. Regan, AEC, Washington, D. C.
70. Robert F. Reitemeier, AEC, Washington, D. C.
71. John N. Wolfe, AEC, Washington, D. C.
72. H. M. Roth, AEC, ORO
73. C. S. Shoup, AEC, ORO
74. J. R. Horan, AEC, Idaho
75. K. K. Kennedy, AEC, Idaho
76. J. A. Buckham, Phillips Petroleum Company
77. J. A. McBride, Phillips Petroleum Company
78. C. M. Slansky, Phillips Petroleum Company
79. H. J. Carey, Jr., The Carey Salt Company, Hutchinson, Kansas
80. C. W. Christenson, Los Alamos Scientific Laboratory
81. J. C. Frye, State Geological Survey, Div., Urbana, Ill.
82. W. B. Heroy, Sr., Geotechnical Corp., Dallas, Texas

83. H. Gladys Swope, University of Wisconsin, Madison
84. Rolf Eliassen, Stanford University, Stanford, California
85. Gene Simpson, University of Arizona, Tucson
86. E. F. Gloyna, University of Texas, Austin
87. W. J. Kaufman, University of California, Berkeley
88. Sue Derby, University Library, University of California, La Jolla
89. L. Silverman, Harvard Graduate School of Public Health
90. G. M. Fair, Harvard University, Pierce Hall
91. H. A. Thomas, Jr., Harvard University, Pierce Hall
92. John Geyer, Johns Hopkins University
93. C. R. Naeser, George Washington University
94. W. A. Patrick, Johns Hopkins University
95. H. C. Thomas, University of North Carolina
96. L. P. Hatch, Brookhaven National Laboratory
97. H. H. Hess, Princeton University
98. Abel Wolman, Johns Hopkins University
99. O. F. Hill, Hanford
100. C. R. Cooley, Hanford
101. E. R. Irish, Hanford
102. A. M. Platt, Hanford
103. W. H. Reas, Hanford
104. G. Rey, Hanford
105. R. L. Moore, Hanford
106. W. H. Swift, Hanford
107. J. H. Horton, Savannah River
108. R. M. Girdler, Savannah River
109. Harvey Groh, Savannah River
110. C. H. Ice, Savannah River
111. J. W. Morris, du Pont, Savannah River
112. C. M. Patterson, du Pont, Savannah River
113. W. B. Scott, Savannah River
114. E. B. Sheldon, Savannah River
115. D. S. Webster, Savannah River
116. V. R. Thayer, du Pont, Wilmington
117. A. A. Jonke, Argonne National Laboratory
118. S. Lawroski, Argonne National Laboratory
119. W. A. Rodgers, W. R. Grace and Company, Naperville, Ill.
120. J. J. Weinstock, RAI
121. J. F. Honstead, IAEA, Vienna
122. D. W. Pearce, IAEA, Vienna
123. R. L. Nace, USGS, Washington, D. C.
124. P. H. Jones, USGS, Washington, D. C.
125. Stanley J. Reno, Environmental Health Service, Topeka, Kansas
126. C. P. Straub, U. S. Public Health Service, Cincinnati, Ohio
127. Dade Moeller, U. S. Public Health Service, Winchester, Massachusetts
128. W. J. Lacy, Office of Civil Defense, Washington, D. C.
129. J. E. Crawford, U. S. Bureau of Mines, Washington, D. C.
130. J. W. Watkins, U. S. Bureau of Mines, Washington, D. C.
131. L. C. Watson, AECL, Chalk River, Canada
132. John Woolston, AECL, Chalk River, Canada
133. AECL, Chalk River, Canada, Attn: C. A. Mawson, I. L. Ophel
134. AEC, Sidney, Australia, Attn: R. C. Cairns, L. Keher

135. AERE, Harwell, England, Attn: H. J. Dunster
136. AERE, Harwell, England, Attn: R. H. Burns, K.D.B. Johnson
137. CEA, Grenoble, France, Attn: G. Wormser
138. CEA, Saclay, France, Attn: F. Duhamel, A. Menoux, C. Gailledreau
139. Peter a Krenkel, Vanderbilt University, Nashville, Tennessee
140. Yehuda Feige, Ministry of Defense, Atomic Energy Commission, Rehovoth, Israel
141. CEA, Fontenay-aux-Roses, Attn: P. Regnaut, P. Faugeras, and M. Bourgeois
142. Centre d'Etude Nucleaire, Mol, Belgium, Attn: L. Baetsle
143. Centre d'Etude Nucleaire, Mol, Belgium, Attn: P. de Jonghe
144. Euratom (ISPRA), Casella Postale No. 1, Attn: M. Lindner
145. Eurochemic, Mol, Belgium, Attn: R. Rometsch, T. J. Barendregt, and F. Marcus
146. Jitender D. Sehgal, Bombay, India
147-160. DTIE